Institute of Neurobiology
Prof. Dr. Harald Wolf
Ulm University

Inhibition shapes vulnerability to Traumatic Brain Injury: pharmacological, toxicological and chemogenetic investigation

Cumulative dissertation submitted in partial fulfilment of the requirements for the degree of Dr. rer. Nat of the Faculty of Natural Sciences, Ulm University

Submitted by

Akila Chandrasekar
Bangalore, India

Ulm, 2019

Dean of the Faculty of Natural Sciences: Prof. Dr. Peter Dürre

1. Reviewer: Prof. Dr. Harald Wolf

2. Reviewer: Prof. Dr. Jan Tuckermann

Date of submission of thesis: 27.01.2019

Day doctorate awarded: 25.06.2019

Results gained from my thesis have been previously published in the following publications:

- **Chandrasekar, A.,** Heuvel, F.O., Palmer, A., Linkus, B., Ludolph, A.C., Boeckers, T.M., Relja, B., Huber-Lang, M., Roselli, F., 2017 Oct. Acute ethanol administration results in a protective cytokine and neuroinflammatory profile in traumatic brain injury. Int. Immunopharmacol. 51, 66–75.
- **Chandrasekar. A.,*** Aksan, B.,* Heuvel, F.O., Förstner, P., Sinske, D., Rehman, R., Palmer, A., Ludolph, A., Huber-Lang, M., Böckers, T., Mauceri, D., Knöll, B., Roselli, F. (2018) Neuroprotective effect of acute ethanol intoxication in TBI is associated to the hierarchical modulation of early transcriptional responses. Exp Neurol. 302:34-45.
- **Chandrasekar, A.,** Heuvel, F.O., Welper, M., Rehman, R., Palmer, A., Catanese, A., Linkus, B., Ludolph, A., Boeckers, T., Huber-Lang, M., Radermacher, P., Roselli, F. (2018) The Neuroprotective Effect of Ethanol Intoxication in Traumatic Brain Injury Is Associated with the Suppression of ErbB Signaling in Parvalbumin-Positive Interneurons. J Neurotrauma. 35:22, 2718-2735.
- **Chandrasekar, A.,** Heuvel, F.O., Tar, L., Hagenston, A.M., Palmer, P., Linkus, B., Ludolph, A., Huber-Lang, M., Boeckers, T., Bading, H., Roselli, F. (2018). Parvalbumin Interneurons Shape Neuronal Vulnerability in Blunt TBI. Cereb Cortex. https://doi.org/10.1093/cercor/bhy139. 1–15

Table of contents

1 Statutory declaration

I hereby declare that I wrote this thesis titled:

“Inhibition shapes vulnerability to Traumatic Brain Injury: pharmacological, toxicological and chemogenetic investigation”

independently and without any aids other than those cited. Sources for identical or paraphrased text passages from other publications have been identified. All people involved in the generation and/ or analysis of the presented manuscript in this work are clearly mentioned in the list of authors or the acknowledgements.
I further declare that I have carried out my scientific work according to the principles of the current “Satzung der Universität Ulm zur Sicherung gutter wissenschaftlicher Praxis”.

Ulm,

(Akila Chandrasekar)

2 List of abbreviations

A

AAV: Adeno Associated Virus

AD: Alzheimer's disease

ATF-3: Activating Transcription Factor 3

ATP: Adenosine Tri-Phosphate

B

BAC: Blood Alcohol Concentration

BAL: Blood Alcohol Level

BBB: Blood Brain Barrier

BDNF: Brain Derived Neurotrophic Factor

C

Ca^{2+}: Calcium

CCI: Controlled Cortical Impact

CNS: Central Nervous System

CT: Computed Tomography

D

DAMP: Danger Associated Molecular Patterns

DAPI: 4',6-diamidino-2-phenylindole

DPI: Days Post Injury

DREADDs: Designer Receptors Exclusively Activated by Designer Drug

E

EI: Ethanol Intoxication

EGFR: Epidermal Growth Factor Receptor

EGR3: Early Growth Response Protein 3

Eph-A: Ephrin A

Eph B: Ephrin B

ErbB:

ERK: Extracellular signal-regulated kinases

EtOH: Ethanol

F

FDA: Food and Drug Association

FGFR: Fibroblast Growth Factor Receptor

FPI: Fluid Percussion Injury

G

GABAR: Gamma Amino-Butyric Acid Receptor

GCS: Glasgow Coma Scale

GSK: Glycogen Synthase Kinase

GM-CSF: Granulocyte-Macrophage Colony-Stimulating Factor

I

ICP: Intracranial Pressure

IEG: Immediate Early Genes

Il-1β: Interleukin 1 beta

IL-13: Interleukin 13

M

MAPK: Microtubule Associated Protein Kinase

MCP-1: Monocyte Chemoattractant Protein 1

M-CSF: Macrophage Colony-Stimulating Factor

N

NG2: Neural/Glial Antigen 2

NMDAR: N-Methyl D-Aspartate receptor

NSS: Neurological Severity Score

NPAS4: Neuronal PAS domain protein 4

P

PBBI: Penetrating Ballistic-like Blast Injury

PSAM: Pharmacologically Selective Activation Module

PV: Parvalbumin

PV-NLS: Parvalbumin nuclear localization sequence

Q

Q-PCR: Quantitative Polymerase Chain Reaction

R

RTK: Receptor Tyrosine Kinase

T

TBI: Traumatic Brain Injury

TGF-β1: Transforming Growth Factor beta 1

TNF-α: Tumor Necrosis Factor alpha

Trk: Tyrosine kinase

W

WHO: World Health Organisation

3 Summary

Traumatic brain injury (TBI) is a worldwide public health problem typically caused by contact and inertial forces acting on the brain with a broad spectrum of symptoms and disabilities. The molecular mechanism underlying the primary and secondary injuries after trauma have not been well investigated. Excess excitation has been hypothesized to be a significant part of the damage after traumatic brain injury. On the other hand, reduced neuronal excitability and a disturbed excitation/inhibition balance have also been detected post TBI. Clinical data show that ethanol intoxication is a potential modifier of TBI outcome. Here, we aimed at understanding the impact of ethanol intoxication on TBI-associated neurological deficits, signaling pathways and pathogenic cascades unfolding after TBI to identify new modifiers of TBI pathophysiology. We also Pharmacologically Selective Activation Module (PSAM) and Pharmacologically Selective Effector Module (PSEM) control of PV-Cre^{+} neurons and the Designer Receptors Exclusively Activated by Designer Drug (DREADD) control of principal neurons in a blunt model of TBI to explore the role of inhibition in shaping neuronal vulnerability to TBI. We also elucidated that the protective effect of PV inactivation was suppressed during the expression of the nuclear calcium buffer, PV nuclear localization sequence (PV-NLS), thus implying an activity-dependent neuroprotection. Thus, we give an insight into the neuroinflammatory and IEG pathways unfolding after TBI. We identify, for the first time, phosphorylation of ErbB2/ErbB3 in the excitatory synapses of the injured cortex and that ErbB2 inhibitors were able to recapitulate, to a significant effect, the neuroprotective effect of trauma. Finally, we were able to show that sustaining neuronal excitation in the early phase of TBI is neuroprotective by increasing activity dependent survival.

4 Introduction

4.1 Traumatic Brain Injury

Traumatic brain injury (TBI) is a type of injury caused when the brain is acted upon by external forces and can result in long last cognitive motor deficits (Carron et al 2016, Lu and Xia et al 2015, Faul et al 2010). It is a major health problem worldwide and is responsible for the injury of 108-332 per 10,000 of the world population (Johnstone et al 2013, Bruns et al 2003). In the United States alone it is a leading cause of death and affects people belonging to different age groups, race, ethnicity and incomes. In a study conducted between the years 2002 and 2006 it was identified that 1.7 million people in the US are affected by TBI annually out of which approximately 10 percent are due to sports and recreational activities. Of these 1.4 million are treated for TBI, 275,000 people are hospitalized, and 52,000 people die. More than one-third of all the injury related deaths are because of TBI (Coronado et al 2011, Kaur et al 2017, Leo et al 2016, Sahler et al 2012, Lu and Xia et al 2015, Prins et al 2013). In Europe health care costs for such types of injuries exceed 33 billion Euros. After TBI many individuals are left with physical and mental impairment years after the incidence of TBI impeding the quality of life of these patients (Reis et al 2015, Zaloshnja et al 2005). TBI occurrence peaks both in young adults below the age of 44 and in the elderly and males (59%) are more prone to TBI than females (9%). Fall, motor vehicle accidents and a hit on the head by an object are the leading causes for TBI in the US population. WHO predicts that TBI will be the leading cause of death and disability by the year 2020 (Lu and Xia et al 2015, Johnstone et al 2013, Bruns et al 2003, Coronado et al 2011).

The biggest advance in identifying the prognosis of TBI was made in the 1970's by two scientists named Thomas Langfitt and Brian Jennett. Although little progress had been made in the field since the early 1900s, they applied the knowledge of pathophysiology to understand the patient prognosis and used the available therapeutic advances such as resuscitation, respiratory and circulatory support and intracranial pressure (ICP) monitoring. Cranial CTs also improved the survival of patients by rapid diagnosis of intracranial hematomas (Stein et al 2010). Introduction of the Glasgow Coma Scale (GCS) in 1976 by Graham Teasdale and Brian Jennet helped associate loss of consciousness with TBI and significantly helped to assess possible brain pathologies by measuring spontaneous and stimulated verbal, motor or eye opening responses (Reis et al, 2015, Grote et al 2011, Bruns et al 2003). The GCS also helped classify TBI as mild (GCS 13-15) moderate (GCS 9-12) or severe (GCS 3-8) (Reis et al 2015, Lu and Xia et al 2015, Grote et al 2011, Joseph et al 2015, Bruns et al 2003).

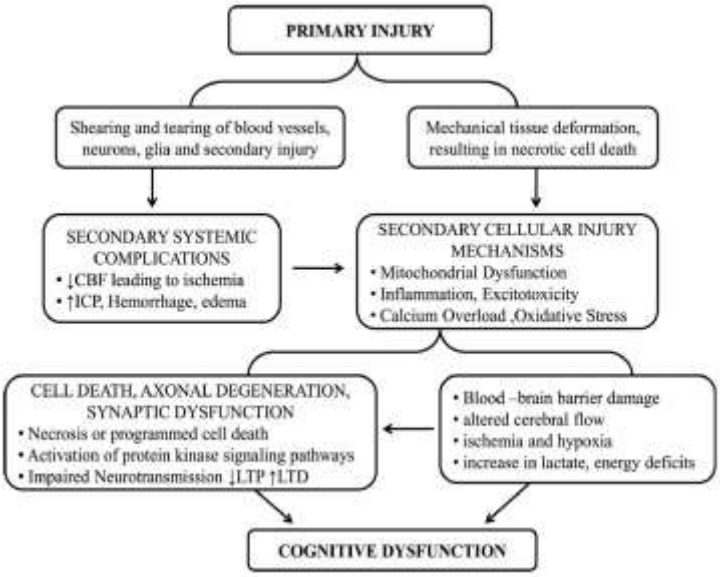

Fig 1: Pathophysiology of primary brain injury. Kaur and Sharma et al 2017

The neurological damage from TBI does not only occur due to the primary injury but also involves the secondary injury ensuing over the next hours, days and weeks (figure 1, Yu et al 2015). Primary injury is the first collision which causes the brain to be knocked into the skull. It is the focal (intracranial hematomas, skull fractures, coup-countercoup lacerations) and diffuses the mechanical harm imposed on the brain. It is the phase in which there is shearing of blood vessels and axons due to the injury. This primary insult leads further to the swelling of

the brain, ischemia, and infection, changes in cerebral blood flow and intracranial pressure, and cellular damage which comprises the secondary injury (Yu et al 2015, Kaur and Sharma et al 2017). This combination of the primary and secondary injuries following TBI, makes it a complex to understand and treat.

TBI is a single dynamic process which includes a multitude of cascades of pathological cellular pathways. The multidimensional cascade following TBI and its varied symptomatic presentation with differences in individuals, injury type, injury severity, age and gender make it challenging to diagnose understand and treat TBI (Kaur and Sharma et al 2017, Prins et al 2013). Many interventions can be done after TBI to reduce intracranial pressure and excitotoxicity, manage hyperventilation, and recover oxygenation. However, it is important to keep in mind that the multiple foci of physiological disruptions generated by TBI require a multi-targeted approach. Increasing understanding of the pathophysiology following TBI provides a great promise for different therapies in the future.

4.2 Animal models for TBI

TBI is a neurological event which can be defined as an alteration in brain function, or other evidence of brain pathology, caused by an external force (Wojnarowicz et al 2017, Menon et al 2010). Thus, TBI is a diagnostic formulation that hints at a sudden onset of tissue pathology due to the external insult. This makes TBI a medical event and not a disease per se (Wojnarowicz et al 2017). There is a pathophysiological heterogeneity observed in human patients with TBI. There are many reasons why this might arise which include but are not limited to the location, nature and severity of the primary injury and preexisting conditions. Further heterogeneity is introduced by factors such as age, health, gender, medication, alcohol and drug use, and genetics. Therefore it is easier to conceptualize TBI as a dynamic neurological process and focus the clinical attention on evaluation of a potentially fluctuating course rather than diagnosis of a static condition (Xiong et al 2013).

This diverse nature of human TBI highlights the challenges in developing clinically relevant animal models. This lead to a consensus that no one model is sufficient to cover this diversity. In light of this, animal models in TBI are available to cover a large number of brain injuries. In human patients TBI is very heterogeneous. Animal models of injury are designed to produce a relatively homogenous type of injury and therefore any one animal model might not be able to recapitulate all secondary injury developments observed in humans (Xiong et al 2013, Johnson et al 2016).

The purpose of experimental models of traumatic brain injury is to replicate certain pathological components or phases of clinical trauma in experimental animals aiming to address pathology and/or treatment. Regardless of the goal of the research, a TBI model should satisfy specific criteria: 1) the mechanical force should be controlled, reproducible and quantifiable, 2) the

injury should be reproducible and bear some resemblance to human conditions, 3) should be possible to measure the injury outcome using morphological, physiological, biochemical and behavior parameters and these should be related to the mechanical injury inflicted, and 4) the intensity of the mechanical force used to inflict the injury should be able to predict the severity of the outcome (Cernak et al 2005). Keeping these criteria in mind, though larger animals might be closer in size and physiology to humans, it is widely accepted by investigators to use rodents in TBI research mostly due to their modest cost, small size and easy handling among many reasons (Xiong et al 2013, Cernak et al 2005). Among the many models available the most widely used TBI models in research are: fluid percussion injury (FPI), controlled cortical impact (CCI), weight drop injury, and blast injury (figure 2).

- *Fluid percussion model*

Fluid percussion model is a helps replicate moderate to severe forms of TBI. In this model, the injury is inflicted by a fluid pressure pulse to the dura (through a craniotomy) using a pendulum which strikes the piston of a reservoir of fluid. The craniotomy is either performed centrally around the midline or laterally over the parietal bone between the bregma and the lambda (Alder et al 2011, Kabadi et al 2013, Xioang et al 2013). The percussion provides a displacement and deformation of brain tissue and the severity of the injury is controlled by the strength of the pressure pulse. Although there is no skull fracture in this model, which is usually seen in moderate to severe TBI in humans, this model helps replicates intracranial hemorrhage, brain swelling and progressive gray matter damage.

- *Controlled cortical impact*

The controlled cortical impact (CCI) model is the most commonly used model of TBI. It is mechanical model of TBI which uses a pneumatic or electromagnetic impact device to drive a rigid impactor onto the exposed intact dura following a craniotomy (Xiong et al 2013, Romine

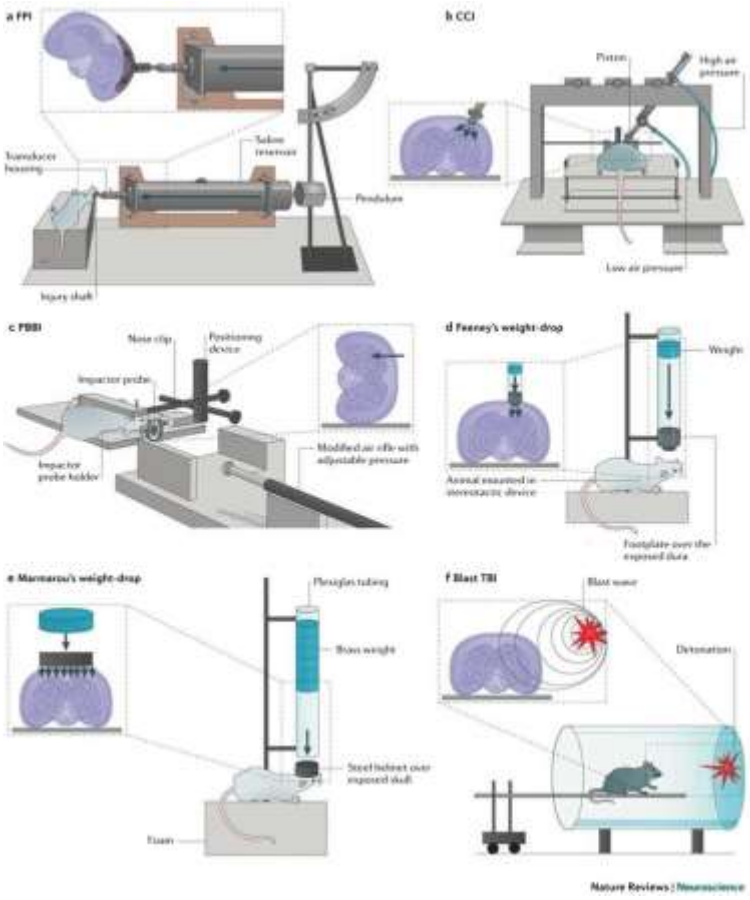

Fig. 2: Experimental animal models of traumatic brain injury. Xiong et al 2013.

et al 2014, Osier and Dixon et al 2016(b)). CCI models mild to moderate TBI. This model was used to mimic biomechanical deformities after TBI, for example after automotive crashes. They are also used now to study the morphological and behavioral changes after TBI (Osier and Dixon et al 2016 (a)). The advantage of this model over other models is the ease with which mechanical factors such as time, velocity and depth of impact can be controlled. An additional advantage of this method is that unlike the weight drop models of TBI, there is no rebound injury (Xiong et al 2013).

– *Penetrating ballistic-like brain injury*

Penetrating ballistic-like brain injury (PBBI) has been established as a military-relevant model of TBI (Shear et al 2011). It is caused by transmission of projectiles with a high energy penetrator and a shock wave which release a high amount of kinetic energy that is transferred into the brain. This kinetic energy produces a temporary intracranial cavity in the brain which is a major contributor to the wound damage. The model can be controlled by controlling the anatomical path of the projectile and the degree of energy transfer (Xiong et al 2013, Williams et al 2006). It is highly relevant to study moderate to severe TBI and for a mechanistic evaluation of the injury.

- Weight drop models

In weight drop models of TBI, the skull is exposed (with or without craniotomy) to a free falling guided object. The injury severity is controlled by controlling the weight of the object falling and the height from which it falls. The different weight drop models available are: a) Feeney's weight drop model in which the weight is delivered to the exposed dura. This leads to intracranial hemorrhage and cavity formation (Feeney et al 1981), b) Sohami's closed head injury model in which a weight impact is delivered on one side of the unprotected skull. This model was further standardized and a neurological severity score was performed to evaluate the neurological impairment in the mice (Chen et al 1996, Flierl et al 2009), and c) Marmarou model of diffused axonal injury (DAI) to mimic diffused TBI in human caused by falls or motor vehicle accidents. This is also a closed head injury model in which a brass weight free falls onto a stainless steel disc which is mounted on the exposed skull between the bregma and the lambda (Marmarou et al 1994). This model causes extensive damage of neurons, axons dendrites and the microvasculature. A disadvantage of the weight drop models of TBI is the high variability of the location and severity of the injury (Xiong et al 2013). However, it is inexpensive and the TBI closely mimics a closed head concussive injury seen in humans.

Animal models give us insight into the dynamic neurological processes following TBI, there are some limitations to the currently available animal models. Although there is a similarity between the rodent and human brains, there are still physiological differences in terms of brain structure and function which exist that may lead to substantially different responses to trauma. Another drawback is the measurement of the injury severity. The assessment of the severity is key for diagnosis, management and prognosis of TBI. However, similar to the GCS in humans there is no common scoring system, which is widely accepted, to measure the severity of the injury in rodents. The current animal models mimic some types of brain injury but to get a

breakthrough in TBI we require development of more clinically relevant TBI models combined with innovative clinical trials.

4.3 Ethanol intoxication and TBI

Alcohol intoxication is a well-known risk factor of trauma and more specifically TBI. 43% of patients involved in car accident have positive blood alcohol concentrations (BAC, Savola et al 2005) and up to 55% patients admitted for TBI in particular have positive BAC, a majority of the patients displaying a binge drinking pattern (i.e., not chronic alcoholics, Leo et al 2016, Cummings et al 2006). These statistics show that positive blood alcohol levels (BAL) is a clinically relevant variable affecting the pathophysiology and the clinical management of TBI.

The effect of blood alcohol concentration on the outcome of TBI is controversial. Surprisingly positive BAL had been associated with a better outcome of TBI compared to undetectable BAL in several clinical studies (Brennan et al., 2015; Raj et al., 2015; Raj et al., 2016; Berry et al., 2011; Salim et al., 2009; Cho et al., 2016, Tien et al 2006) and experimental studies (Kelly et al 1997, Janis et al 1998, Wang et al 2013). However, there are some studies which also dispute this notion (Joseph et al., 2015; Pandit et al., 2014, Wu et al 2014, Vaagenes et al 2015). In particular, BAL> 230 mg/dL has been suggested to provide the largest decrease in mortality (Salim et al., 2009; Berry et al., 2011) in moderate-to-severe TBI.

Patients with positive BAL showed a faster recovery of neurocognitive functions (Lange et al 2008), although other studies found either a detrimental or no effect of positive BAL (Schutte et al 2010, Kaplan et al 1992). Likewise, Interaction between ethanol intoxication and TBI has been investigated in experimental models utilizing different TBI models and different schedules of ethanol administration. Ethanol administration before a fluid percussion injury (Wu et al 2014), or three-dose ethanol administration before and after controlled cortical impact (in rats, Vaagenes et al 2015) worsened sensorimotor recovery, whereas a single-dose ethanol administration soon after blunt TBI (Wang et al 2013) or before blunt TBI, (Chandrasekar et al

2017), contusive TBI (Kelly et al 1997), or controlled cortical injury (Janis et al 1998) lead to faster recovery after Injury.

Despite being the most common comorbidity of TBI, the clinical relevance and interaction of BAL on the TBI pathophysiology is only partially understood from a molecular and cellular point of view. Ethanol Intoxication (EI) at the instance of trauma modulates the neuroinflammatory profile, reducing production of proinflammatory cytokines and enhancing secretion of interleukin (IL)-13 (Goodman et al 2013) although it is also reported to increase brain edema (Katada et al 2012). Nevertheless, the pharmacological spectrum of ethanol activities include antagonistic effects on N-methyl-D-aspartate receptor (NMDAR, Criswell et al 2004), and agonistic effects on gamma-aminobutyric acid (GABA) receptor (Kumar et al 2009), suggesting that ethanol intoxication may affect multiple, distinct sets of biological functions in neurons, astrocytes, and immune cells (such as synaptic plasticity, proliferation, and inflammation) at once.

In particular, a beneficial or detrimental effect of ethanol on TBI, and the boundaries of the parametric space of such an effect (in terms of doses and of timing of administration), remains unclear and the molecular mechanisms of EtOH interaction on TBI, and their consequences, are largely unknown.

4.4 Pathways unfolding after TBI

4.4.1 Inflammation

The pathogenic cascade set in motion after TBI has a strong neuro-inflammatory profile. Neuroinflammation follows the primary injury and may persist up to 17 years after TBI (Giunta et al 2012) and has been long considered to contribute to the damage sustained following brain injury (Kumar et al 2012). Neuroinflammation is one of the major causes of neural death post-TBI as it interferes with the endogenous repair mechanisms through immune cells, microglia, astrocytes, cytokines, chemokines and other inflammatory molecules. Although the inflammatory response to TBI is initially protective to prevent the invasion of pathogens, these molecules eventually cross the blood brain barrier (BBB) and release prostaglandins and pro inflammatory cytokines which eventually prevents the efficient repair of the damaged tissue (Schimmel et al 2017). The inflammatory response to TBI is also characterized by an elevated level of ATP released upon injury. ATP activates the purinergic pathway in the inflammatory cells and thus plays an important role in migration, proliferation, phagocytosis and apoptotic signaling (Garg et al 2018).

Danger associated molecular patterns (DAMPs) are recruited minutes after the injury followed by a set of cytokines and chemokines (Gyoneva et al 2015, Morganti Kossmann et al 2001). This is further followed by the arrival of neutrophils (Soares et al 1995) and 2-3 days later multiple subpopulations of neuroinflammatory cells including lymphocytes, monocytes and NK cells to name a few (figure 3, Goodman et al 2013, Gyoneva et al 2015, Hsieh et al 2013, Holmin et al 1995). Neuroinflammation after TBI occurs both in the primary and secondary phases following TBI (Chiu et al 2016, Woodcock and Morganti-Kossmann 2013, Lozano et al

2015) and the polarization of the immune response taking place within the damaged cerebral tissue may contribute to the net consequences of the neuro-inflammatory response (Gyoneva et al 2015, Mckee et al 2016).

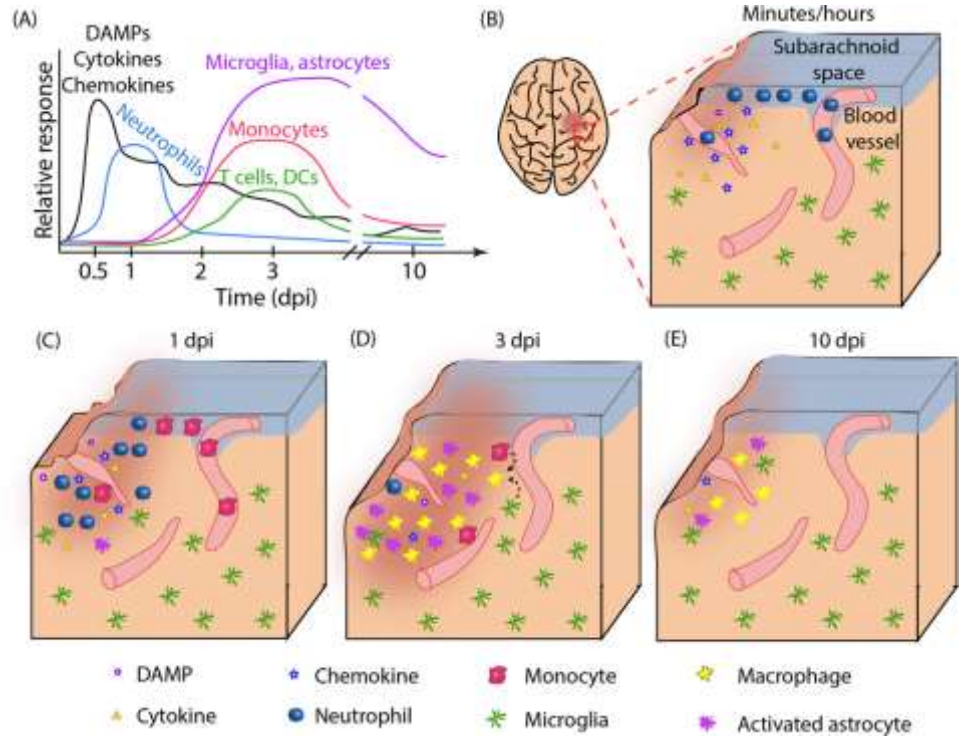

Fig. 3: Inflammatory response to TBI. The figure shows a time course of the molecular and cellular mediators after TBI and the histological representation of the inflammatory reaction. Gyoneva et al 2015.

Gliosis is a widespread phenomenon occurring widely after an insult on the brain and includes astrocytes, NG2 glia and microglia recruitment mediating both beneficial and detrimental effects after TBI (Sirko et al 2015, Dimou et al 2015). In a healthy brain microglia have a ramified morphology and are termed as ‘resting microglia’. Upon an external disturbance, the cells rapidly change and form an amoeboid becoming ‘active microglia’ (Faerber et al 2004, Folkersma). In the injured brain, microglia forms the first line of defense and initially benefit the brain post injury by separating the healthy and injured tissues to limit the damage (Xiong et al 2018, Schimmel et al 2017). They are protective by producing anti-inflammatory mediators, scavenger cellular debris and orchestrate neurorestorative processes to promote neurological

recovery after TBI. However, microglia also produce proinflammatory mediators that exacerbate brain damage, hinder brain repair and neurological functional recovery (Xiong et al 2018, Schimmel et al 2017, Kabadi et al 2014, Hernandez-Ontiveros et al 2013).

Astrocytes are also involved in the injury sites along with microglia. They work with neurotrophic factors by upregulating neurotrophic factors which in turn aid in axonal repair, increasing cell proliferation, aid in neuronal survival and inhibit programmed cell death. Along with this they also reduce glutamate excitotoxicity by regulating the glutamate levels (Schimmel et al 2017). Contrary to the beneficial effects, astrocytes are also detrimental due to the formation of glial scars, which is a physical barrier surrounding the injury site preventing efficient repair of the damaged tissue (Schimmel et al 2017, Kumar et al 2012). Astrocytes derived cytokines are also released at the site of the injury where cytokines such as IL-1β and TNF-α promote neurotoxicity whereas TGF- β1 is considered to be neuroprotective (Chiu et al 2016).

This close association between TBI and neuroinflammation, helps neuroinflammation emerge as an important target for the amelioration of TBI. Modulation of the inflammatory pathways provide an extended time window for therapeutic interventions to prevent the development of secondary pathology and promote neuronal recovery. Ethanol intoxication before trauma could provide important insights into the status of the pro-survival signaling pathways post-TBI. Ethanol and trauma induced inflammation has been studies on a systemic level, where ethanol has demonstrated significant immunosuppressive abilities (Wagner et al 2016, Relja et al 2016a), reducing cytokine levels and inflammation induced damage (Relja et al 2015, Relja et al 2016b). The effect of ethanol on the neuroinflammatory response after TBI shows both enhanced (Teng et al 2014) and reduced responses (Goodmann et al 2013). This makes it interesting to use ethanol intoxication to study the inflammatory signaling pathways following TBI and the histological evaluation of microglia.

4.4.2 Receptor Tyrosine Kinases

Receptor tyrosine kinases (RTKs) are essential components of signal transduction pathways that mediate cell to cell communication (Hubbard and Miller et al 2008). These transmembrane receptors which bind to mainly growth factors, play key roles in processes such as cellular grown differentiation, metabolism and motility. Due to their roles as growth factor receptors, RTKs have been implicated in the onset or progression of various cancers either through mutations of receptor/ligand overexpression (Hubbard and Miller et al 2008, Blume-Jensen et al 2001). Among the many protein kinases involved in cellular signaling, some important ones are mitogen-activated protein kinases (MAPKs), protein kinase B (figure 4, also known as Akt), and glycogen synthase kinase (GSK). Emerging evidence shows that these three signaling cascades respond to TBI and are of particular interest because of their involvement in the regulation of cell fate, repair, plasticity, memory and motor skills (Neary et al 2005).

Clinical data suggests that ethanol intoxication is a potential modifier of TBI outcome showing surprisingly that patients with positive BAL survive TBI better (Brennan et al 2015, Raj et al 2015, Raj et al 2016, and Berry et al 2011). Thus, acute ethanol intoxication prior to TBI may produce context-dependent beneficial effects after TBI offering an entry point to understand targets of intervention. Mechanistic understanding of influence of ethanol on TBI is limited. However, the pharmacological spectrum of ethanol include antagonistic activities of NMDAR (Criswell et al 2004) and agonistic effects of GABA receptor (Kumar et al 2009) suggesting that ethanol affects multiple distinct set of biological functions in different cell types such as neurons, astrocytes and immune cells thus modulating synaptic plasticity, proliferation and inflammation at once.

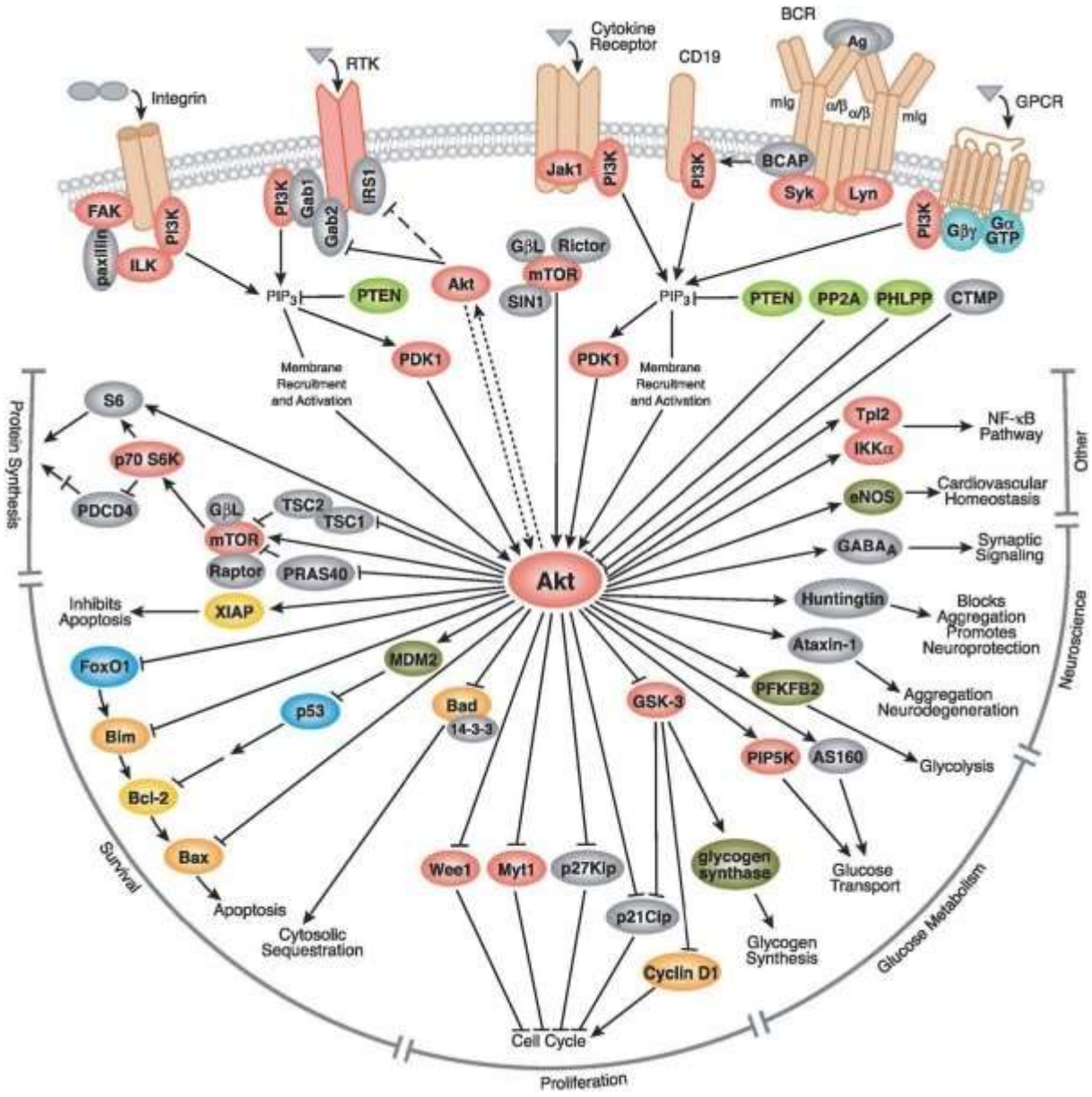

Fig. 4: The AKT signaling pathway. AKT is activated by PI3K which is itself activated by several upstream signaling pathways such as insulin receptors, receptor tyrosine kinases, G coupled receptors and cytokine receptors to name a few. The molecules in this pathway are involved in cell proliferation,glucose metabolism, cell survival, cell cycle, protein synthesis and neuronal morphology and plasticity. Pathway diagram reproduced from Cell Signalling Technology, Inc. (www.cellsignal.com). Emamian et al 2012

These effects of ethanol could be studied at a molecular level by studying the effect of TBI and ethanol on a set of RTKs including, among many, the ErbB family and Trk family receptors (involved in synaptic plasticity and astrocyte proliferation, Sun et al 2016, Mei et al 2014, Gupta et al 2013), Axl/Dtk/Metk receptors (affecting microglia physiology, Fourgeaud et al 2016), and

EphA and EphB family receptors (modulating astrocyte responses, Sheffler-Collins et al 2012). Because distinct sets of RTKs control different biological responses and structures (synaptic plasticity, astroglial responses, and neurovascular unit, Mei et al 2014, Sheffler.Collins et al 2012, Guillemot et al 2011, Su et al 2015, Gurnik et al 2016), monitoring the activation status of such receptors make it possible to probe the ongoing cellular responses elicited by TBI and the combination of EI and TBI. In particular, activation of the ErbB family RTKs provides an entry point to the excitation/inhibition balance in the affected cortex. In fact, ErbB family members, including ErbB2, ErbB3 and ErbB4, are expressed on inhibitory interneurons (Bean et al 2014, Fazzari et al 2010, Neddens et al 2011), where they control the strength of excitatory synapses (Vullhorst et al 2015, Sun et al 2016). Among the inhibitory interneurons, ErbB receptors are prominent regulators of parvalbumin-positive (PV) Interneurons (Wen et al 2010, Yin et al 2013) and thus provide an entry point to the effects of EI and TBI on perisomatic inhibition and cortical excitability (Atallah et al 2012).

4.4.3 Immediate Early genes

Immediate early genes are genes which are activated rapidly and transiently to cellular stress or immune responses. Trauma also induces alterations in the transcription of immediate early genes and subsequently has a role in either restoration of function and progression of cell loss (Marciano et al 2002, Whitfield et al 2000). Specifically, the induction of prototypical immediate-early genes (IEG), such as c-Fos and Atf3, have been detected in rodents and in human tissue (Dutcher et al., 1999; Giza et al., 2002; Czigner et al., 2004; Wang et al., 2014; Natale et al., 2003; Zhang et al., 2014). Transcriptome data suggest that c-Fos is among the master regulators of the transcriptional response to TBI (Samal et al., 2015).

The acute phase of concussive and contusive Traumatic Brain Injury (TBI) is characterized by pathogenic cascades linked to the physical damage of neurons and their uncontrolled excitation. Excitation-dependent IEG transcription is associated with enhanced neuronal integrity and survival after insults to the central (Zhang et al., 2002; Zhang et al., 2009; Zhang et al., 2011; Ahlgren et al., 2014; Rawat et al., 2016) and peripheral nervous system (Gey et al., 2016). The transcription modulates a wider set of biological responses in the CNS, such as learning and memory (Ramanan et al., 2005; Mellström et al., 2014; Li et al., 2007), neuroinflammation (Nomaru et al., 2014; Wang et al., 2012), and structural/functional circuitry remodelling (Hu et al., 2004; Lösing et al., 2017; Renaudineau et al., 2009). Pathological conditions such as downregulation of axonal sprouting (Lösing et al., 2017), expression patterns in Alzheimer's disease (AD, Corbett et al., 2017) and epilepsy (Honkaniemi and Sharp, 1999; Morris et al., 2000; Yutsudo et al., 2013) are also modulated by immediate early genes. Ethanol is known to have both GABA-enhancing and NMDAR-antagonist properties (Criswell et al., 2003, 2004) which makes it well suited to affect the excitation-dependent transcriptional response to TBI, which has a strong NMDAR component (Wang et al., 2014). This points in the direction that ethanol can be used as an entry point to understand how to TBI affects not only neuronal survival but also synaptic plasticity and neuronal inflammation.

4.5 Inhibition of PV interneurons after TBI

The pathogenic cascade following concussive and contusive TBI is strongly driven by excitation triggered cascades. Studies have revealed a strong and rapid increase of extracellular glutamate in both experimental models and patients (Folkersma et al 2011, Chamoun et al 2010) after TBI. Physical forces of trauma trigger axonal stretching, membrane damage and neuronal depolarization which not only cause excess glutamate release but can also cause a failure in glutamate re-uptake (Kaur and Sharma 2017). The rise of glutamate and the suprophysiological activation of excitatory glutamate receptors is thought to contribute critically to Ca^{2+} dysregulation via NMDA receptor signaling (Weber et al., 2001, Weber, 2012, Hardingham et al., 2002, Pohl et al., 1999, Wroge et al., 2012, Hinzman et al., 2015, Samson et al., 2016) and may lead to death of neurons due to excitotoxicity (Hardingham and Bading, 2010). The extrasynaptic Ca^{2+} overload is followed by a loss of structural integrity, mitochondrial dysfunction and metabolic disturbances, culminating in bioenergetics failure and neuronal loss (Weber, 2012; Hinzman et al., 2015; Sun et al., 2017; Bading, 2017).

Excitotoxicity plays an important role in the development of the secondary injuries that occur after the initial insult and contributes significantly to the expansion of the total volume of the injury (Yi and Hazell et al 2006, Fujikawa et al 2015, Guerriero et al 2016). Despite this, there is ample evidence suggesting that reduced excitation may play a role in the pathophysiology of acute TBI shifting the excitation/inhibition balance more towards increased inhibition (Sawant-Pokam et al., 2017). Neuronal responses to synaptic stimulation and sensory inputs are suppressed for several days after TBI (Johnstone et al., 2013; Johnstone et al., 2014; Allitt et al., 2016) and neuronal metabolism is decreased in the affected cortex (Dietrich et al., 1994).Surprisingly, glutamatergic antagonists are protective only in the very early phases of

TBI (Pohl et al 1999) which makes it interesting to study the effect of excitation-dependent signaling on neuronal vulnerability to TBI.

The net neuronal firing is determined not only by intrinsic properties, but is strongly influenced by the activity of glutamatergic synapses (together with the activation of non-synaptic glutamatergic receptors), as well as by the inhibitory inputs (Isaacson and Scanziani, 2011). Indeed, neuronal activity has been shown to increase resistance to oxidative stress and reduce vulnerability to apoptosis (Papadia et al., 2008; Zhang et al., 2007; 2009; Leveille et al., 2010; Hardingham and Bading, 2010). Thus, both excessive glutamatergic drive (excitotoxicity) and insufficient neuronal excitation may modulate the sensitivity of neurons to TBI-associated pathogenic cascades (as in other neurodegenerative conditions; Roselli and Caroni, 2015). GABAergic interneurons provide a homeostatic regulation of firing of excitatory neurons and shape the propagation of excitation in space and time (Wilent and Contreras, 2005; Haider et al., 2013). Although selective loss of GABAergic subpopulations has been shown to take place in the chronic phase of TBI (Cantu et al., 2015), the functional role of inhibitory interneurons in acute TBI is yet to be fully elucidated.

Parvalbumin-positive (PV) interneurons constitute a subset of the cortical GABAergic population integrated in the local microcircuitry and providing perisomatic inhibition both in feedback and feed-forward architectures (Hu et al., 2014). PV interneurons regulate the overall output of the principal neurons (Defelipe et al., 1999; Cardin et al., 2009; Donato et al., 2013; Donato et al., 2015) and a strong activation of PV interneurons is sufficient to shut-down the firing of principal neurons (Atallah et al., 2012, Khoshkoo et al., 2017). Although PV interneurons appear to be affected by TBI (Vascak et al., 2017) and their derangement may contribute to the delayed-onset of post-traumatic hyperexcitability (Hsieh et al., 2017), their role in the acute phase after TBI remain unexplored.

5 Aim of thesis

Traumatic brain injury is an open or closed head injury caused by an external force. Depending on the etiology, TBI can be closed head or penetrating and occur as a single event or in a repetitive fashion. The primary injury is always closely followed by a series of secondary events which are usually the reason for the complexity of the injury. Multiple pathways are simultaneously affected by the primary injury including the inflammatory cascade and the receptor tyrosine kinase pathway suggesting a multiple target approach to find a therapeutic intervention after injury. Apart from its effect on the cellular and molecular level, TBI also affects the cortical microcircuitry. Excitotoxicity is an important drawback in the pathophysiology of TBI leading to neuronal loss and apoptosis. This leads us to believe that controlling the neuronal activity could be a useful approach to understand the pathophysiology of TBI. Acute ethanol intoxication provides an entry point leading to a therapeutic intervention due to its role in the in targeting multiple signaling cascades, RTK signaling, modulation of the neuroinflammatory profile post injury, and controlling the activity and plasticity of inhibitory interneurons.

The aim of the present study is to establish the effect of ethanol intoxication and understand some of the signaling cascades which unfold upon injury and further if this could lead to therapeutic intervention. To this end I used acute ethanol administration in vivo to study the effect of ethanol intoxication on injury. I used behavior studies to characterize the sensory and motor impairments post injury and to elucidate the effect of ethanol intoxication. I further used protein microarrays to find specific targets affected by TBI and modulated by ethanol and identified the specific cell type which contributed to the therapeutic intervention post-TBI. I further exploited a set of viral tools including engineered ion channels with orthogonal

pharmacology (Pharmacologically Selective Activation Module [PSAM]) and Designer Receptors Exclusively Activated by Designer Drug (DREADDs) to control PV interneuron and principal neuron firing within discrete time windows before and after TBI. Using these methods I was able to study neuronal vulnerability to TBI.

6 Results

6.1 Acute ethanol administration results in a protective cytokine and neuroinflammatory profile in traumatic brain injury

Akila Chandrasekar[a], Florian olde Heuvel[a], Annette Palmer[b], Birgit Linkus[a], Albert C. Ludolph[a], Tobias M. Boeckers[c], Borna Relja[d], Markus Huber-Lang[b], Francesco Roselli[a]

a) Dept. of Neurology, University of Ulm, School of Medicine, Germany

b) Institute of Clinical and Experimental Trauma Immunology, University Ulm, Ulm, Germany

c) Dept. of Anatomy and Cell Biology, Ulm University, School of Medicine, Germany

d) Dept. of General and Visceral Surgery, Goethe University, Frankfurt, Germany

Accepted: 7 August 2017

Published in: International immunopharmacology. October 2017. 51: 66-75

doi: https://doi.org/10.1016/j.intimp.2017.08.002

International Immunopharmacology 51 (2017) 66–75

Contents lists available at ScienceDirect

International Immunopharmacology

journal homepage: www.elsevier.com/locate/intimp

Acute ethanol administration results in a protective cytokine and neuroinflammatory profile in traumatic brain injury

Akila Chandrasekar[a], Florian olde Heuvel[a], Annette Palmer[b], Birgit Linkus[a], Albert C. Ludolph[a], Tobias M. Boeckers[c], Borna Relja[d], Markus Huber-Lang[b], Francesco Roselli[a,*]

[a] Dept. of Neurology, University of Ulm, School of Medicine, Germany
[b] Institute of Clinical and Experimental Trauma Immunology, University Ulm, Ulm, Germany
[c] Dept. of Anatomy and Cell Biology, Ulm University, School of Medicine, Germany
[d] Dept. of General and Visceral Surgery, Goethe University, Frankfurt, Germany

ARTICLE INFO

Keywords:
Traumatic brain injury
Ethanol
Cytokines
Microglia

ABSTRACT

Ethanol intoxication is a common comorbidity in traumatic brain injury. To date, the effect of ethanol on TBI pathogenic cascades and resulting outcomes remains debated. A closed blunt weight-drop murine TBI model has been implemented to investigate behavioral (by sensorimotor and neurological tests), and neuro-immunological (by tissue cytokine arrays and immuno-histology) effects of ethanol intoxication on TBI. The effect of the occurrence of traumatic intracerebral hemorrhage was also studied. The results indicate that ethanol pretreatment results in a faster and better recovery after TBI with reduced infiltration of leukocytes and reduced microglia activation. These outcomes correspond to reduced parenchymal levels of GM-CSF, IL-6 and IL-3 and to the transient upregulation of IL-13 and VEGF, indicating an early shift in the cytokine profile towards reduced inflammation. A significant difference in the cytokine profile was still observed 24 h post injury in the ethanol pretreated mice, as shown by the delayed peak in IL-6 and by the suppression of GM-CSF, IFN-γ, and IL-3. Seven days post-injury, ethanol-pretreated mice displayed a significant decrease both in CD45 + cells infiltration and in microglial activation. On the other hand, in the case of traumatic intracerebral hemorrhage, the cytokine profile was dominated by KC, CCL5, M-CSF and several interleukins and ethanol pretreatment did not produce any modification. We can thus conclude that ethanol intoxication suppresses the acute neuro-inflammatory response to TBI, an effect which is correlated with a faster and complete neurological recovery, whereas, the presence of traumatic intracerebral hemorrhage overrides the effects of ethanol.

1. Introduction

Traumatic brain injury (TBI) is a significant source of morbidity and mortality, with 576.8/100,000 cases occurring every year in the US alone, leading to 17.6/100,000 deaths per year [1,2]; 3.2–5.3 million patients surviving severe TBI suffer from life-long disabilities [3].

Alcohol intoxication is a highly prevalent comorbidity of TBI and 43% of car accidents involve alcohol as a risk factor [4]. Up to 55% of patients admitted for TBI show positive Blood Alcohol Levels (BAL) [2,5], the majority of them being binge-drinkers. Positive BAL is therefore a relevant clinical variable, potentially affecting the pathophysiology and the clinical management of TBI.

Surprisingly, positive BAL has been associated with a better outcome of TBI in several clinical [6–12] and experimental studies [13–15], but not in others [16–19]. The mechanism for the purported beneficial effects and the causes of the variable outcomes of the clinical studies are still not clear.

Pathogenic cascades set in motion by TBI have a strong neuro-inflammatory component: after injury, danger-associated molecular patterns (DAMPs) may act within minutes, engaging the corresponding receptors on astrocytes and microglia, which in turn release cytokines and chemokines [20]. TBI-associated immune response evolves with the recruitment of neutrophils [21] and, within 2–5 days, with the arrival of multiple subpopulations of immune cells including lymphocytes, NK cells and monocytes [22–23]. The polarization of the immune response taking place within the damaged cerebral tissue may contribute to the net consequences of the neuro-inflammatory response [20,24].

Despite the clinical relevance, the interplay of ethanol intoxication

* Corresponding author at: Dept. of Neurology, Ulm University, School of Medicine, Center for Biomedical Research (ZBF), Helmholtzstrasse 8/2 (R1.44), 89081 Ulm, Germany.
E-mail addresses: akila.chandrasekar@uni-ulm.de (A. Chandrasekar), annette.palmer@uniklinik-ulm.de (A. Palmer), birgit.linkus@uni-ulm.de (B. Linkus), albert.ludolph@rku.de (A.C. Ludolph), tobias.boeckers@uni-ulm.de (T.M. Boeckers), info@bornarelja.com (B. Relja), markus.huber-lang@uniklinik-ulm.de (M. Huber-Lang), francesco.roselli@uni-ulm.de (F. Roselli).

http://dx.doi.org/10.1016/j.intimp.2017.08.002
Received 19 June 2017; Received in revised form 2 August 2017; Accepted 7 August 2017
Available online 12 August 2017

and the neuro-immune response to TBI is poorly understood. The effect of ethanol on the neuro-inflammatory response after TBI has been debated: both enhanced [25] and reduced [26] responses have been reported.

On the other hand, the interaction of ethanol and trauma-induced inflammation has been studied at a systemic level, where ethanol has demonstrated significant immunosuppressive abilities [27–28], reducing cytokine levels and containing inflammation-induced damage [29,30].

In this study, the effects of ethanol on sensorimotor recovery and on the polarization of the neuro-immune response after TBI were investigated by monitoring the intraparenchymal cytokines fingerprint in the acute stage of TBI and the status of pro-survival signaling pathways, together with the sensorimotor performance and the histological evaluation of microglial activation.

2. Materials and methods

2.1. Animals, ethanol, and traumatic brain injury model

We used a blunt moderate-severity TBI model that was previously reported [31]. A summary of the timeline of pharmacological treatments and procedures is provided in Fig. 1. B6-SJL WT male mice aged 80–90 days were administered, by oral gavage, 400 μl of ethanol solution (5 g/kg as previously reported [29] corresponding to 32% v/v in saline) or saline 30 min before the procedure. Animals were premedicated with Buprenorphine (0.1 mg/kg by intraperitoneal injection) and put under sevoflurane anesthesia (5% in 95% O_2). According to established procedures [31], the scalp skin was shaved and incised on the midline (8–10 mm) and gently pushed sideway (5 mm) to expose only the right parietal bone. Scalp skin incision did not involve the manipulation of major vessels or sensory structures and did not result in macroscopic blood loss. In order to avoid damage to the cornea, ocular gel (Bepanthen, Bayer Leverkusen Germany) was placed on the corneal surfaces before the procedure. Animals were then manually positioned in the weight-drop apparatus as previously described [31], with the impactor site localized in the center of the right parietal bone. A 333 g impactor from a 3 cm height was used to deliver the TBI. Soon after the experimental TBI, animals were administered 100% O_2 and were monitored for apnea time. After spontaneous breathing was restored, the scalp skin of the anesthetized mice was stitched with Prolene 6.0 surgical thread and the animals were transferred to a recovery cage (single-housed) containing a warmed pad and ad libitum access to food and water. Additional doses of buprenorphine were administered every 12 h for the following 48 h post-injury. To avoid unnecessary suffering of the mice, their general health was checked regularly using a score sheet developed for TBI, determining fixed termination criterions. Effort was made to minimize animal suffering and reduce the number of animals required.

2.2. Behavioral and neurological score assessment

The overall neurological impairment was evaluated post injury using the composite Neurological Severity Score [31] at 3 h, 24 h, 2 dpi, 3 dpi and 7 dpi. Briefly, the assessment included motor (muscle status, abnormal movement), sensory (visual, tactile, proprioceptive), reflex, and balance tests. Mice were awarded one point for failure to perform a task, so that scores ranged from 0 to 10, increasing with the severity of dysfunction. The Arena Escape test, part of NSS evaluation, was performed by placing the mice in a circular, brightly-lit area whose wall included a narrow opening leading to a dark compartment. The time required by the mice to enter the dark compartment was measured and averaged over three attempts. The Beam walk test was performed [31] by allowing the mice walk over a suspended wooden beam, from an open platform to a dark compartment. The time required by the mice for the completion of the test was measured. All tests were recorded with an overhanging digital camera and scored off-line. In all the tests, the performance of a cohort (n = 3) of mice never administered with any drug and never exposed to any procedure (defined "drug-naïve") was measured as a comparison to sham mice. To maintain homogeneity within the cohort, the reported behavioral data have been obtained from mice which did not display, at post-mortem examination 7 dpi, macroscopic signs of traumatic hemorrhage (defined as the presence of intracerebral hematoma or hematoma on the meningeal surface). Therefore, experimenters were blind to the presence of hematoma during the period of behavioral testing.

2.3. Tissue sampling, cytokine and Akt array

For the evaluation of cytokines and signaling profiles, mice were euthanized at 3, 6 or 24 h post-injury and the brain was rapidly dissected out and cooled in ice-cold PBS. Brain samples were visually evaluated for the presence of macroscopic hematomas. In hematoma-free brains, cortical samples, 1.5 mm in diameter, centered on the TBI site, were dissected and snap frozen. In samples showing hematoma formation, the brain was immersed in a large volume of ice-cold PBS and the clot was removed using two 20G sterile needles under visual guidance with a 4× magnification lens. Using the tip of a sterile scalpel, additional cortical tissue was removed until no macroscopic residue of blood could be seen. The size of the hematoma was in no case larger than 0.5 mm and did not disrupt the gross architecture of the brain. After clot removal, a cortical sample was obtained with a

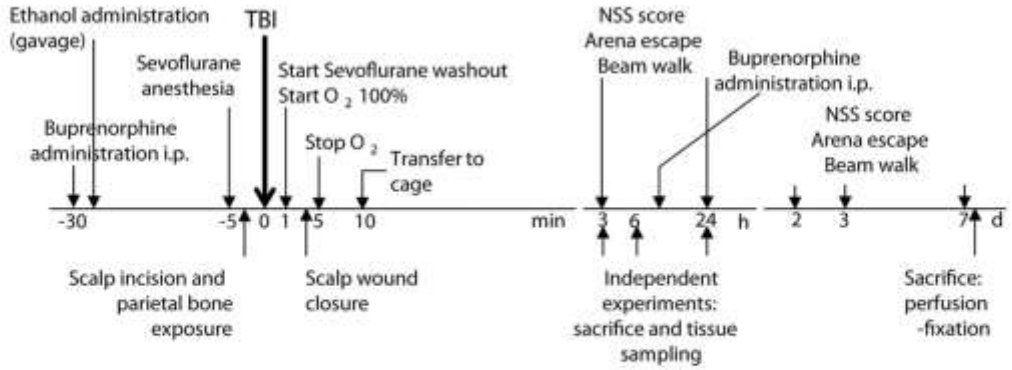

Fig. 1. Timeline of the experimental design depicting the timing for the administration of ethanol, buprenorphine and for behavioral tests, tissue sampling for cytokines, biochemistry and histology.

diameter of 1.5 mm, centered on the lesion. The clot removal procedure, performed in ice-cold PBS, did not last longer than 10 min.

Tissue samples were then suspended in Lysis Buffer (1 × Lysis Buffer; CST; 20 mM Tris-HCl (pH 7.5), 150 mM NaCl, 1 mM Na_2EDTA, 1 mM EGTA, 1% Triton, 2.5 mM sodium pyrophosphate, 1 mM b-glycerophosphate, 1 mM Na_3VO_4, 1 μg/ml leupeptin) in which freshly prepared Phosphatase (1 tablet per 10 ml lysis buffer) and Protease (1 tablet per 50 ml lysis buffer) inhibitors (Roche cOmplete tablets, Sigma-Aldrich, Taufkirchen, Germany) cocktail were added and homogenized with 20 strokes of Dounce homogenizer. Tissue homogenates were then cleared by centrifugation (10.000 g, 10 min) and assayed for protein concentration with the Bradford Protein Assay.

Cytokine array assay (Mouse Cytokine Array GS1, Raybiotech, Norcross GA, US) was performed in line with the manufacturer's instructions. Briefly, arrays were equilibrated at RT for 15 min before blocking each sub-array in Blocking Buffer (provided by the manufacturer) for 30 min. Tissue lysates were diluted in blocking buffer to a concentration of 0.5 mg/ml and 100 μl of lysate from each tissue sample was incubated in each sub-array for 18 h at 4 °C on an orbital shaker. The sub-arrays were then washed 5 × 5 min in Washing Buffer I (as provided by the manufacturer) and 2 × 5 min in Washing Buffer II (provided by the manufacturer). The antibody array was incubated for 2 h at RT with 70 μl of Biotin-conjugated Anti-Cytokine Antibody mix (provided by the manufacturer) in each sub-array. The Antibody array was then washed 5 × 10 min in Washing Buffer I and 2 × 10 min in Washing Buffer II before being incubated for 2 h at RT with Streptavidin-Alexa 488 conjugate (diluted 1:1000 in blocking buffer). After further washing steps (as above), the array was air-dried and scanned in a fluorescent scanner (Genepix 4000B microarray scanner, Molecular Devices Gmbh, Biberach, Germany).

The phospho-Akt array (Cell Signaling Technologies Europe, Leiden, The Netherlands) was performed according to the manufacturer's instructions. Briefly, the antibody array was blocked for 2 h with 100 μl of Array Blocking Buffer (provided by the manufacturer) in each sub-array. After discarding the blocking buffer, 75 μl of tissue lysate (diluted in blocking buffer to a concentration of 1 μg/μl) was added to each sub-array and incubated for 18 h at 4 °C on an orbital shaker. Tissue lysate was discarded and each sub-array was washed 4 × 5 min with 100 μl of Array Wash Buffer (provided by the manufacturer); after which, 75 μl of the Detection Antibody cocktail (provided by the manufacturer) was added to each sub-array and incubated for 1 h at RT. Arrays were then washed 4 × 5 min with Wash Array Buffer, before being incubated with Streptavidin-Alexa488 conjugate (1:1000) for 30 min at RT on an orbital shaker. After 30 min the arrays were washed 4 × 5 min in Array Wash buffer, the array slide was rinsed briefly in distilled water, air-dried, and scanned in a fluorescent slide scanner (Genepix 4000B microarray scanner, Molecular Devices Gmbh, Biberach, Germany).

2.4. Array image analysis

Array images were scanned as 16-bits images and fluorescence intensity was quantified using ImageJ software. Briefly, a fixed-size circular region of interest was positioned on each spot in the array and the median fluorescence intensity value was logged. The median values for four (cytokine array) or two (Akt array) replicated spots were averaged, after excluding the spots showing artifacts (dust grains, crystals, damaged spot area). Local background was assessed for each spot and subtracted. All arrays contained a homogeneous arrangement of saline-sham, ethanol-sham, saline-TBI and ethanol-TBI samples. The fluorescence intensity value was expressed as percentage of the average value of the corresponding analyte in the saline-sham samples.

2.5. Immunostaining and confocal imaging

For the evaluation of microglial activation and leukocytes infiltration, mice were euthanized at 7 dpi by transcardial perfusion (50 ml ice-cold PBS followed by 50 ml 4% PFA in PBS). This was performed by subjecting the mice to anesthesia using ketamine/xylazine (100 mg/kg and 16 mg/kg). After the animal was deeply anesthetized (checked by loss of tail pinch reflex), a lateral thoracotomy was performed and a gauge22 needle, connected to the perfusion apparatus, was positioned in the left ventricle. Upon activation of the perfusion pump, the right atrium was surgically opened (to allow the outflow of the perfusion fluid). Perfusion of PBS or of 4% PFA was performed with a rotary peristaltic perfusion pump (Ismatec) imposing a flow of 8.5 ml/min (monitored during the procedure). Perfusion of ice-cold PBS required approximately 6 min and quickly achieved the cooling of the mouse body to the temperature of the ice-cooled solution and washed away the residual blood. 4% PFA perfusion was performed at the same perfusion rate and it was completed in 6 min. During the procedure, macroscopic changes in liver, lung and muscle stiffness were monitored for quality control and this was achieved 3 min after perfusion with 4% PFA. Thereafter, the brain was dissected and post-fixed for 18 h in 4% PFA at 4 °C, then washed in PBS and cryoprotected in 30% sucrose in PBS for 48 h. 40 μm cryosections, spanning the parietal cortex (subject to TBI), were subjected to the antigen-retrieval procedure (60 min incubation at 70 °C in 10 mM Sodium Citrate buffer, pH 8.5) and thereafter blocked in Bovine Serum Albumin 3%/Triton 0.3% in PBS for 2 h. Then, the sections were incubated in rat anti-CD45 (1:50, BD Biosciences), rabbit anti-Iba1 (1:250, Wako), diluted in blocking buffer, for 48 h at 4 °C on an orbital shaker. The brain sections were then washed in PBS (3 × 30 min) and incubated with the secondary antibodies (Alexa-594-conjugated donkey anti rat, Alexa-647-conjugated donkey anti rabbit), diluted 1:500 in blocking buffer for 2 h at 24 °C. The sections were thereafter washed in PBS (3 × 30 min) and mounted using Prolong Gold Antifade (ThermoFisher) mounting medium.

Overview images were acquired with a Zeiss Axioscope equipped with a 10 × air objective; high-resolution images were acquired with a Zeiss LSM 710 confocal microscope (both microscopes from Zeiss, Oberkochen, Germany) equipped with a 40 × oil-immersion objective. All images were acquired as 12-bit and z-stack of 20–40 optical sections, with acquisition parameters set to avoid saturation of the detectors. Image analysis was performed using the ImageJ software suite. For microglial density analysis, confocal stacks of 3–5 optical sections were collapsed in maximum-intensity projection, thresholded and the surface occupied by Iba1-positive structures was computed. For CD45 + cell counts, cells with identifiable nucleus and cytoplasm immunostained for CD45 were manually counted.

2.6. Statistical analysis

Statistical analysis was performed with the GraphPad Prism software. All behavioral experiments were performed using 4–5 mice per group and the cytokine and Akt array experiments were performed using 3–6 independent biological replicates per group. For the analysis of the behavioral performance, non-parametric rank-based Kruskall-Wallis test was applied, with Dunn correction for multiple comparisons. Since NSS score was consistently 0 in saline-sham mice, the variance was significantly different in sham vs TBI mice. Although behavioral data have been analyzed using non-parametric tests (and the values for statistical significance are reported accordingly), in order to improve the readability of the time courses, we have chosen to display the results as mean ± SEM. For the analysis of cytokine and Akt arrays, one-way ANOVA with Tuckey correction for multiple comparisons was applied to each time point independently. Data are displayed as mean ± SD; to avoid graph overcrowding, statistical significance has been depicted only for sal-TBI vs eth-TBI comparisons. Statistical significance was set at $p < 0.05$.

3. Results

3.1. Ethanol intoxication results in improved sensorimotor recovery after severe TBI

The sensorimotor and overall neurological impairment due to severe closed TBI (3 cm) [31] in mice pre-treated with either saline or ethanol (5 g/kg) were assessed using the NSS scoring system and quantitatively scoring the arena escape test and the beam walk test. Mice were assessed post hoc (at 7 dpi or as soon as euthanization criteria were reached) for the presence of intracerebral hematoma; in order to obtain a homogeneous cohort, only mice which did not display any hematoma were included in the present analysis (5 animals displaying hematoma, 3 pretreated with saline and 2 with ethanol, were excluded). Saline-pretreated mice subjected to TBI (henceforth sal-TBI) displayed a significant acute neurological impairment (measured at 3 h) compared to saline-sham mice (henceforth sal-S; NSS = 0 in sal-S mice and 5.75 ± 1.0 in sal-TBI mice, $p < 0.01$) and ethanol-sham mice (henceforth eth-S; NSS = 1.0 ± 0.5 for eth-S); NSS score improved over time and decreased to 4.0 ± 1.0 at 24 h post-injury, 3.0 ± 1.0 at 2 dpi, 2.5 ± 0.75 at 3 dpi and 1.5 ± 0.75 at 7 dpi (all time points $p < 0.001$ vs sal-S and eth-S mice; Fig. 2A). Ethanol-pretreated mice (henceforth eth-TBI) displayed a trend towards lower NSS scores already at 3 h and 24 h post-injury (4.0 ± 1.25 and 3.0 ± 1.25) which became statistically significant at 2, 3 and 7 dpi (1.5 ± 0.75, 1.25 ± 0.5 and 0.5 ± 0.5, respectively; $p < 0.05$ vs sal-TBI; Fig. 2A), indicating a faster and better recovery of eth-TBI mice. The quantitative assessment of sensorimotor performance in the beam walk assay revealed that sal-TBI mice were significantly slower in the test at 3 h post-injury (32.5 ± 7.5 s vs 7.0 ± 3.5 s in sal-S, $p < 0.0001$); their performance improved over time, with completion times of 27.6 ± 8.4 s, 26.1 ± 9.4 s, 18.5 ± 7.4 s and 14.3 ± 4.4 s after 24 h post-injury, 2, 3 or 7 dpi ($p < 0.005$ vs sal-S and eth-S; Fig. 2B). Eth-TBI mice, on the other hand, performed significantly better after 24 h post-injury and 2 dpi (17.2 ± 6.4 and 13.8 ± 5.5 s, respectively; $p < 0.05$ vs sal-TBI), resulting in a significantly improved recovery at 7 dpi (8.1 ± 2.2 s; $p < 0.05$ vs sal-TBI; Fig. 1B). Likewise, the arena escape test revealed that sal-TBI mice were significantly slower in entering the dark compartment than sal-S or eth-S mice after trauma (at 3 h post-injury, 111.4 ± 30.2 s, $p < 0.001$ vs sal-S or eth-S) and did not display a statistically-significant improvement over time, with escape time at 7 dpi comparable to that at 3 h post-injury (102.2 ± 28.3 s; $p > 0.05$ vs 3 h post-injury time point). Eth-TBI mice performed significantly better than sal-TBI mice in the arena escape at 2 and 3 dpi (43.4 ± 18.1 s and 46.3 ± 18.5 s, respectively; $p < 0.05$ vs sal-TBI) and displayed a better recovery at 7 dpi (40.4 ± 17.3 s, $p < 0.05$ vs sal-TBI). Of note, in all tests sal-S and eth-S mice performed comparably to drug-naïve mice, implying that ethanol per se is not the cause of improved motor performance. Based on accepted ethanol catabolic rate (500–600 mg/kg/h), [32,33,34] complete clearance of ethanol would take place within 24 h from the administration, and therefore the performance at 2, 3 and 7 days is not directly affected by ethanol. Taken together, these data support the view that positive BAL at the time of TBI may deliver neuroprotective effects.

3.2. Ethanol administration causes a distinct early tissue cytokine pattern after TBI

In order to investigate the mechanisms linking ethanol intoxication to improved neurological performance, we focused on the effect of ethanol on the neuro-inflammatory response caused by TBI. We sampled primary somatosensory cortex from the impact side, 3, 6 and 24 h post-injury, in order to investigate the earliest phases and to adequately cover the time in which brain tissue may be exposed to ethanol itself or its metabolites, based on known pharmacokinetic parameters [32].

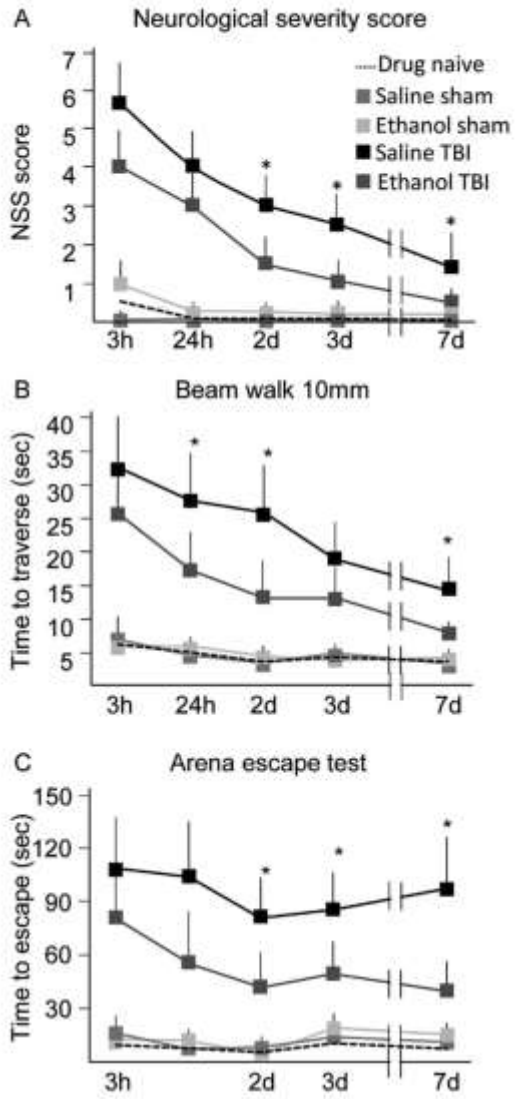

Fig. 2. Ethanol pretreatment improves acute neurological impairment and accelerates recovery. All mice included in this analysis did not show signs of traumatic hematoma when brains were examined, post-hoc, at 7 dpi. A) Ethanol-pretreated mice display a significantly lower NSS score than saline-pretreated mice at 2, 3 and 7 dpi (1.5 ± 0.75, 1.25 ± 0.5 and 0.5 ± 0.5 for eth-TBI vs 3.0 ± 1.0 at 2 dpi, 2.5 ± 0.75 at 3 dpi and 1.5 ± 0.75 for sal-TBI at 2, 3 and 7 dpi, respectively; $p < 0.05$ for all three time points after correction for multiple comparisons). Sham mice performed comparably to drug-naïve mice. B) Ethanol-pretreated TBI mice display a better performance (faster traverse) in the Beam Walk test at several time points after injury (for eth-TBI 17.2 ± 6.4, 13.8 ± 5.5 s, 8.1 ± 2.2 at 24 h post-injury, 2 dpi and 7 dpi, respectively, as compared to 27.6 ± 8.4 s, 26.1 ± 9.4 s, 18.5 ± 7.4 s and 14.3 ± 4.4 in sal-TBI; $p < 0.05$ for all three time points). Sham mice performed comparably to drug-naïve mice. C) Ethanol pretreated TBI mice show a faster escape from open arena than saline-pretreated mice (42.4 ± 18.1 s, 46.3 ± 18.5 s and 40.4 ± 17.3 s at 2, 3, and 7 dpi, respectively, as compared to 91.4 ± 24.5, 95.2 ± 31.2 and 102.2 ± 28.3 s in saline-pretreated mice). Sham mice performed comparably to drug-naïve mice. Statistical analysis was performed with the non-parametric Kruskall-Wallis test; for clarity, values are depicted as mean ± SEM of n = 4–6 mice *$p < 0.05$.

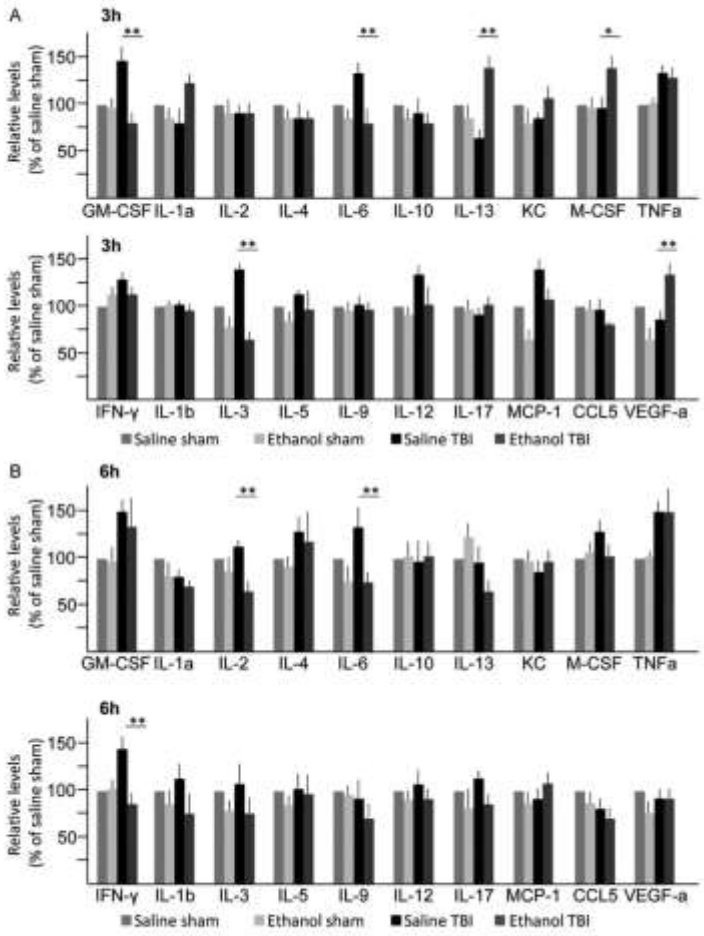

Fig. 3. Parenchymal cytokine pattern in cerebral cortex after TBI is modified by ethanol pretreatment. A) Cortical samples obtained at 3 h post-injury from saline-treated mice show a statistically significant increase in the levels GM-CSF, IL-6, TNF-α, IFN-γ, IL-3 and MCP-1; IL-13 levels are reduced. Ethanol-pretreated mice display a decrease in the levels of MCP-1 and VEGF, as well as of GM-CSF, IL-6 and IL-3; levels of IL-13, M-CSF and VEGF are increased. B) Cortical samples obtained at 6 h post-injury shows the upregulation GM-CSF, TNF-α and IFN-γ levels, and a smaller increase in IL-4 and IL-6 levels. In ethanol-pretreated animals, cortical samples show the downregulation of IL-2, IL-6 and IFN-γ as well as IL-13 whereas GM-CSF and TNF-α levels were comparable in the two groups. Values are mean ± SD of n = 3–6 mice *p < 0.05.

Semi-quantitative values for twenty cytokines in whole-tissue protein extract were determined by solid-state antibody array and the values were expressed as fold-changes of the saline-sham control.

In sal-TBI samples, significant elevation in the levels of several cytokines was observed at 3 h post-injury: among the 20 cytokines analyzed, levels of GM-CSF (147.8 ± 10.1% of baseline, $p < 0.01$ vs saline-sham), IL-6 (132.5 ± 7.9%; $p < 0.01$), TNF-α (129.7 ± 6.8%; $p < 0.05$ vs saline-sham), IFN-γ (125.4 ± 7.7%; $p < 0.05$), IL-3 (136.4 ± 9.9%, $p < 0.05$) and MCP-1 (141.4 ± 9.7%, $p < 0.01$) were significantly higher than in sal-S controls (Fig. 3A). Only IL-13 levels were reduced in the sal-TBI compared to the sham groups (65.4 ± 10.5% of saline-sham), with all other cytokines showing deviations which were not statistically significant when compared to sal-S. Whereas ethanol per se, caused a small decrease in the levels of MCP-1 and VEGF (67.4 ± 10.2 and 70.2 ± 11.3% of baseline respectively, $p < 0.05$), the interaction of ethanol and TBI in eth-TBI mice generated a distinct cytokine pattern only partially overlapping the sal-TBI. In the eth-TBI group, GM-CSF (75.6 ± 7.9% of baseline, $p < 0.01$ vs sal-TBI), IL-6 (79.8 ± 11.3% of baseline, $p < 0.01$ vs sal-TBI) and IL-3 (67.8 ± 9.8% of baseline, $p < 0.01$ vs sal-TBI) levels were significantly decreased. Notably, the eth-TBI group displayed a remarkable increase in IL-13 (139.7 ± 5.5% of baseline, $p < 0.01$ vs sal-TBI) M-CSF (133.4 ± 13.2% of baseline, $p < 0.05$ vs sal-TBI) and VEGF levels (132.2 ± 10.1% of baseline, $p < 0.05$ vs sal-TBI).

In order to investigate the evolution of these distinct cytokine patterns in sal-TBI and eth-TBI, we analyzed tissue cytokine levels, 6 h and 24 h after the trauma. At the 6 h time point the sal-TBI still displayed an elevation of the GM-CSF (149.4 ± 7.7%, $p < 0.01$ vs baseline), TNF-α (149.3 ± 8.8% of sal-S, $p < 0.01$) and IFN-γ (143.4 ± 9.8% of sal-S; $p < 0.01$) levels, and a less evident increase in IL-4 and IL-6 (129.4 ± 8.8% and 133.4 ± 17.2%, $p < 0.05$ vs sal-S) levels (Fig. 1B). The eth-TBI group displayed a largely divergent cytokine pattern: IL-2 (65.5 ± 11.2% of saline sham; $p < 0.01$ vs sal-TBI), IL-6 (75.5 ± 6.5% of sal-S; $p < 0.01$ vs sal-TBI) and IFN-γ (82.4 ± 15.4% of sal-S; $p < 0.01$ vs sal-TBI) as well as IL-13 (65.5 ± 10.2% of sal-S; $p < 0.01$ vs sal-TBI) were significantly decreased compared to sham or sal-TBI, whereas GM-CSF (133.5 ± 20.2% of sal-S; $p > 0.05$ vs sal-TBI) and TNF-α (151.2 ± 20.4%, $p > 0.05$ vs sal-TBI) levels were comparable in sal-TBI and eth-TBI (Fig. 3B).

At 24 h post-injury, the sal-TBI and eth-TBI groups still displayed different tissue cytokine patterns: whereas in sal-TBI the upregulation of GM-CSF (147.8 ± 8.8% of saline sham; $p < 0.01$), IL-6 (135.5 ± 8.1%, $p < 0.05$ vs saline sham), IL-13 (154.5 ± 8.3%; $p < 0.01$ vs sal-S), IL-3 (142.4 ± 7.7%, $p < 0.01$ vs sal-S) and CCL5 (135.5 ± 9.4% of sal-S, $p < 0.01$) was maintained, the eth-TBI group displayed a significant downregulation of IL-13 (64.4 ± 10.8% of sal-S, $p < 0.01$), KC (52.4 ± 18.2% of sal-S, $p < 0.01$), IFN-γ (101.4 ± 6.4%, $p < 0.05$ vs sal-TBI) and IL-3 (75.5 ± 8.3% of sal-S,

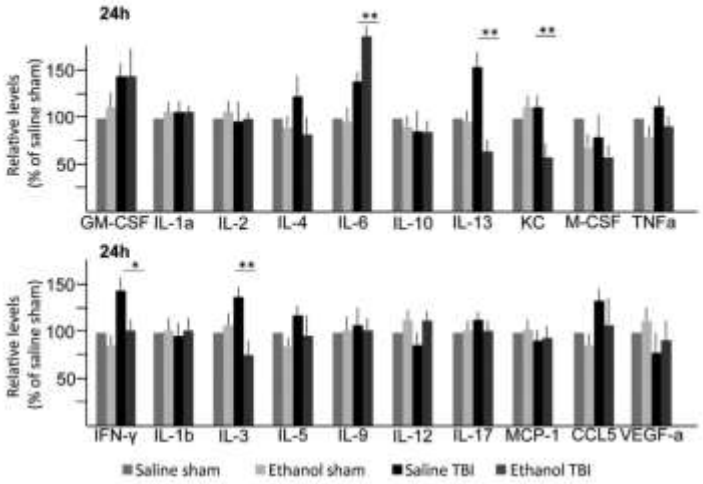

Fig. 4. Cortical samples from saline-pretreated mice subject to TBI show the upregulation of GM-CSF, IL-6, IL-13, IL-3 and CCL5, whereas in ethanol-pretreated mice a significant downregulation of IL-13, KC, IFN-γ and IL-3 is detected; ethanol-pretreated mice show an enhanced expression of IL-6. Values are mean ± SD of n = 3–5 mice *p < 0.05.

p < 0.01 vs sal-TBI) but a stronger expression of IL-6 (183.4 ± 17.1% of sal-S; p < 0.05 vs sal-TBI; Fig. 4).

Taken together, the cytokine patterns highlight a major effect of ethanol intoxication at the moment of the trauma, which carries over 24 h to produce a significant divergence in the immune response associated with TBI.

3.3. Effect of ethanol in TBI-activated signaling landscape

In order to explore the relationship between the cytokine patterns and the overall tissue response to TBI, we analyzed the activation of several signaling pathways (including mTOR, Akt, and Erk) which correlate with cell survival and protein synthesis. At 3 h post-injury (Fig. 5A), cortical tissues, subject to TBI, displayed a decreased level of Akt (S473) phosphorylation (73.4 ± 15.5% of sal-S, p < 0.05) and a significant suppression of protein synthesis pathway, as shown by the decrease in the phosphorylation of the ribosomal protein S6 (51.4 ± 12.5%, p < 0.01 vs sal-S) and in the elevation in phosphorylation of PRAS-40 (127.7 ± 10.6%; p < 0.05 vs sal-S). Notably, activation of the Erk pathway was also significantly decreased (51.6 ± 14.7%; p < 0.05 vs sal-S). Some of these effects were significantly reversed by ethanol pretreatment, with Akt (S473) (115.6 ± 24.8% of sal-S; p < 0.05 vs sal-TBI) and Erk (81 ± 9.8% of saline sham; p < 0.05 vs sal-TBI) levels increased in eth-TBI mice compared to sal-TBI and PRAS-40 levels restored to baseline (98.5 ± 15.3%; p < 0.05 vs sal-TBI). Notably, the overall impact of ethanol on pS6 levels was negligible (53.7 ± 16.7% of sal-S; p > 0.05 vs sal-TBI). Phosphorylation levels of AMPK, RSK1, PTEN, and PDK1 were not altered by TBI or ethanol (not shown).

This distinct effect of ethanol pretreatment on the signaling profile of the cortical tissue observed at 3 h post-injury persisted at 24 h post-injury (Fig. 5B). While pS6 phosphorylation levels were still reduced in sal-TBI (55.4 ± 13.5% vs sal-S; p < 0.05), they were significantly increased in eth-TBI (79.4 ± 18.3 of sal-S; p < 0.05 vs sal-TBI); likewise, at this time point, eth-TBI mice displayed significantly higher phosphorylation levels of mTOR (78.4 ± 6.7% in sal-TBI vs 93.4 ± 10.4% in eth-TBI, p < 0.05) and Erk (52.9 ± 7.9% in sal-TBI vs 87.8 ± 19.4% in eth-TBI, p < 0.05) than sal-TBI mice, although

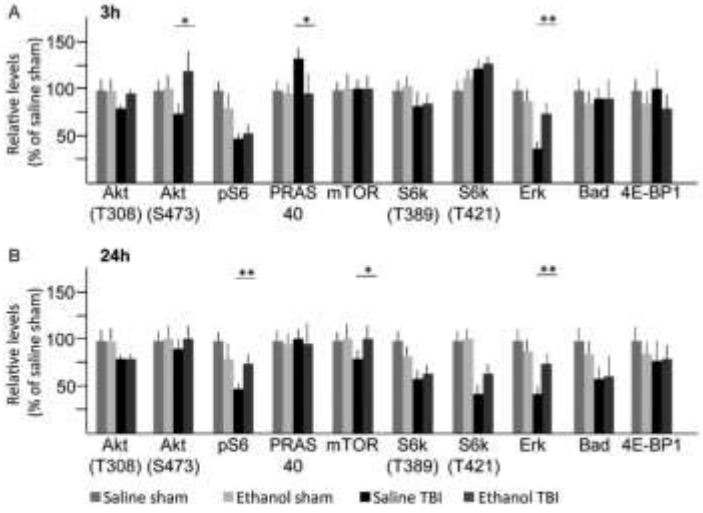

Fig. 5. Distinct signaling profile in saline and ethanol-pretreated mice after TBI. A) At 3 h post-injury, whole cortical lysates from saline-pretreated mice show decreased level of Akt (S473) phosphorylation as well as decreased phosphorylation of the ribosomal protein S6 and increased in phosphorylation of PRAS-40. Erk phosphorylation is also significantly decreased. In samples from ethanol-pretreated mice, levels of Akt (S473) and Erk are increased and PRAS-40 levels are restored to baseline. B) At 24 h post-injury, pS6 levels are still decreased in saline-pretreated TBI mice but they are significantly higher in ethanol-pretreated mice. Ethanol-pretreated TBI mice also display significantly higher levels of mTOR and Erk phosphorylation. Values are mean ± SD of n = 3–5 mice *p < 0.05.

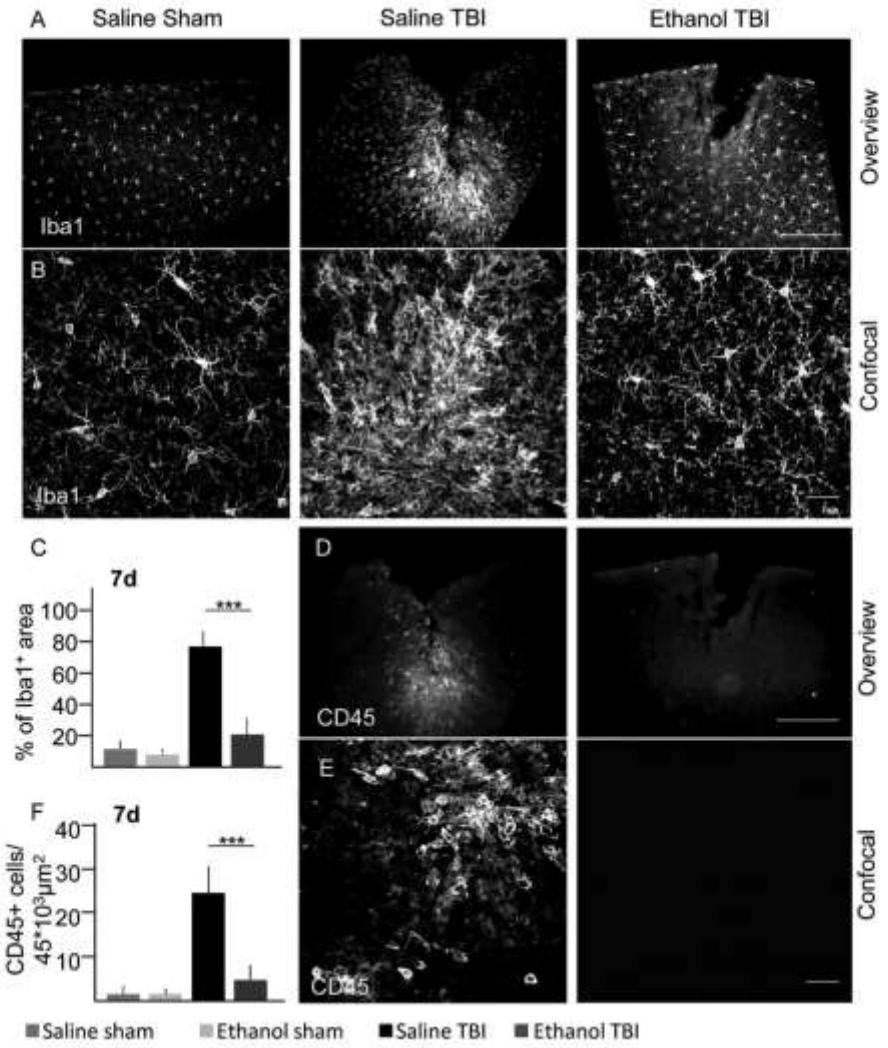

Fig. 6. Reduced neuro-inflammation at 7 dpi in ethanol-pretreated mice. A–C) Brain sections obtained at 7 dpi from eth-TBI and sal-TBI mice (and respective controls) were immunostained for the neuronal marker Neu-N, the microglial marker Iba1 and the leukocytes marker CD45. Whereas sal-TBI mice show massive microglial activation with amoeboid morphology (quantified in C), eth-TBI mice show a dystrophic microglia phenotype with modest increase in overall microglia density. D–F) Leukocyte infiltrate the injury site of sal-TBI mice at 7 dpi, whereas ethanol intoxication at the injury time results in the suppression of leukocytes infiltration (quantified in F). Scalebar for overview images, 200 µm; scalebar for confocal images, 25 µm. Values are mean ± SD of n = 3-4 mice *p < 0.05.

phosphorylation levels of Bad (63.5 ± 8.9% in sal-TBI vs 67.5 ± 9.6% in eth-TBI; p > 0.05) were similar in the two groups.

3.4. Ethanol intoxication decreases microglial activation and leukocytes infiltration

The different cytokine patterns observed at early time points were then evaluated for their impact on the level of the microglial response in the subacute phase. To this aim, mice treated with either saline or ethanol before the TBI were sacrificed at 7 dpi and the cortical sections spanning the injury site were immunostained for the microglia marker Iba1 and the leukocyte marker CD45. All samples (sal-TBI and eth-TBI) included an identifiable injury site, corresponding to the disruption of the gross cortical architecture (Fig. 6A). As expected, at 7 dpi in sal-TBI mice, the density of microglia was increased (77.0 ± 11.1 in sal-TBI, vs 11.1 ± 4.2 in saline sham; $p < 0.05$) at the injury site, with microglial cells assuming a distinctively amoeboid morphology (Fig. 6B, C), whereas in eth-TBI mice, microglia density was significantly decreased compared to sal-TBI (18.7 ± 2.2, $p < 0.05$ vs sal-TBI) and displayed a branched-dystrophic appearance (Fig. 6B, C). Likewise, a strong infiltration of CD45+ cells were detected in sal-TBI mice (25.5 ± 7.4 cells/$45 * 10^3$ µm^2 vs 0.5 ± 0.5 in sham; Fig. 6D–F). This population was largely missing in eth-TBI mice (1.2 ± 0.5 cells/$45 * 10^3$ µm^2; Fig. 6D–F). Taken together, these data suggest that the early divergence in cytokine pattern caused by ethanol intoxication results in distinct neuro-inflammatory profiles in the subacute phase.

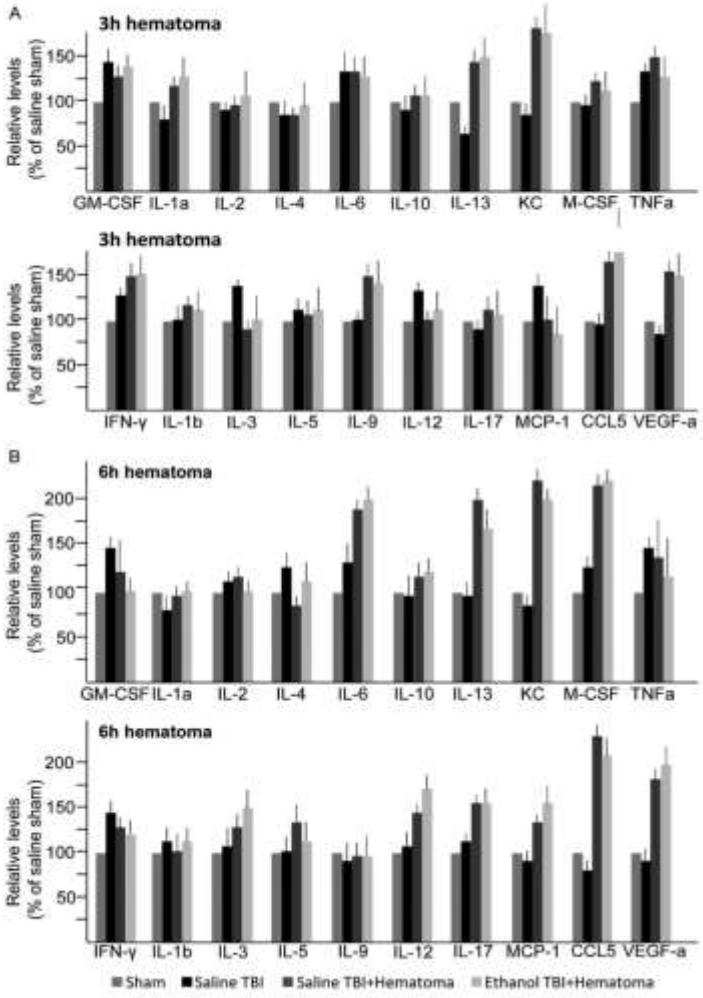

Fig. 7. Hematoma influences the cytokine profile and the sensitivity to ethanol in TBI. A) At 3 h post-injury, cortical samples from TBI displaying macroscopic hematomas show, compared to samples with no hematoma, strong elevation in KC, VEGF, IL-9 and CCL5. No cytokine was significantly affected by ethanol pretreatment. Values are mean ± SD of n = 3–4 mice $^{*}p < 0.05$.
B) At the 6 h time point, samples from mice with TBI-hematoma samples show a massive upregulation of KC, IL-6, M-CSF, IL-13 and CCL5 and significant increases in VEGF, IL-12 and IL-17 compared to TBI without hematoma. Notably, ethanol pretreatment does not modify any of the investigated cytokines. Values are mean ± SD of n = 3-4 mice $^{*}p < 0.05$.

3.5. Loss of ethanol effects on cytokine patterns in TBI with hematoma

Vascular damage with associated blood extravasation and hematoma formation is not uncommon in TBI [33]. Since the clinicopathological details of TBI patients are often not used to stratify epidemiological studies on risk factors, we tried to ascertain if the brain tissue cytokine patterns observed in TBI with hematoma formation was comparable to the one in concussive TBI and how ethanol might modify the contusive TBI response. To this aim, cortical tissue was sampled from mice which underwent experimental TBI and upon brain dissection displayed a macroscopic hematoma on visual examination. The blood clot was removed and the cortical samples were processed as the concussive TBI samples. Both at 3 and 6 h the cytokine patterns of TBI samples with or without hematoma were strongly different: the former displayed a strong elevation in KC (177.8 ± 8.6% of sal-S; $p < 0.001$ vs sal-TBI-no hematoma) VEGF (155.4 ± 11.7% of sal-S; $p < 0.01$ vs sal-TBI-no hematoma), IL-9 (151.3 ± 8.6% of sal-S; $p < 0.01$ vs sal-TBI-no hematoma) and CCL5 (167.5 ± 11.6% of sal-S; $p < 0.001$ vs sal-TBI-no hematoma) levels when compared to concussive TBI at 3 h (Fig. 7A).

At the 6 h time point, sal-TBI-hematoma samples showed a massive upregulation of KC (220.4 ± 14.4% of sal-S; $p < 0.001$ vs sal-TBI-no hematoma), IL-6 (182.3 ± 13.4% of sal-S, $p < 0.01$ vs sal-TBI-no hematoma), M-CSF (212.6 ± 14.4% of sal-S; $p < 0.01$ vs sal-TBI-no hematoma), IL-13 (202.6 ± 14.8% of sal-S; $p < 0.01$ vs sal-TBI-no hematoma) and CCL5 (227.5 ± 18.4% vs sal-S; $p < 0.001$ vs sal-TBI-no hematoma) and significant increases in VEGF (182.4 ± 16.2%, $p < 0.01$ vs sal-TBI-no hematoma), IL-12 (155.4 ± 12.6% of sal-S; $p < 0.01$ vs sal-TBI-no hematoma) and IL-17 (150.9 ± 11.4% of sal-S; $p < 0.01$ vs sal-TBI-no hematoma) levels compared to TBI without hematoma (Fig. 7B). Thus, the influence in blood-derived products can be detected as a significantly different cytokine activation profile in the two types of TBI.

Notably, in contrast to what is seen for TBI without intracerebral hematoma, ethanol did not influence significantly the cytokine pattern in TBI-hematoma: at 3 h post-injury in eth-TBI-hematoma samples, levels of KC (174.3 ± 18.8% of sal-S; $p > 0.05$ vs sal-TBI-hematoma), IL-9 (147.4 ± 14.5% of saline sham; $p > 0.05$ vs sal-TBI-hematoma), CCL5 (218.3 ± 24.3%, $p > 0.05$ vs sal-TBI-hematoma) and VEGF (153.6 ± 19.6% of sal-S; $p < 0.05$ vs sal-TBI-hematoma) were comparable to the saline-pretreated TBI-hematoma samples (Fig. 7A). Likewise, at 6 h post-injury levels of IL-13 (182.4 ± 23.9% of sal-S;

$p > 0.05$ vs sal-TBI-hematoma), KC (202.9 ± 19.8% of sal-S; $p > 0.05$ vs sal-TBI-hematoma), M-CSF (2016.5 ± 22.8% of sal-S; $p > 0.05$ vs sal-TBI-hematoma), IL-17 (157.9 ± 14.4% of sal-S; $p > 0.05$ vs sal-TBI-hematoma), CCL5 (214.7 ± 20.4% of sal-S; $p > 0.05$ vs sal-TBI-hematoma) and VEGF (198.4 ± 23.4% of sal-S; $p > 0.05$ vs sal-TBI-hematoma) and all other upregulated cytokines were comparable in sal-TBI-hematoma and eth-TBI-hematoma (Fig. 7B).

4. Discussion

Our data supports the view that a positive BAL may represent a protective factor in TBI outcome and suggest that modulation of the neuro-inflammatory response, as detected by the shift in cytokine patterns, may be one of the mechanisms of ethanol-induced neuroprotection. Interestingly, our findings also suggest that the cytokine profiles and ethanol effects are profoundly affected by additional pathological features, such as traumatic intracerebral hemorrhage.

Overall, ethanol appears to suppress the earliest phases of TBI-induced neuro-inflammation, and this correlates both with the improved neurological score and recovery with higher levels of Akt and Erk phosphorylation and loss of protein synthesis suppression. These findings are in line with the immunosuppressive effects of ethanol observed in experimental trauma models and in trauma patients, where ethanol pre-administration results in lower blood IL-6 and leukocyte counts in human patients [36,27,28] and in decreased KC release after inflammatory challenge in cell lines [29,30]. This correlates well with previous findings [26]. It is important to note, however, that cytokine milieu is only one of the factors regulating the neuro-immune response to trauma [20] and that the analysis of cytokine patterns provide only a partial view of this very complex response.

Nevertheless, by considering a larger panel of cytokines, we have shown that ethanol exerts a suppressive effect on several, but not all (see e.g. TNF-α), inflammation-related cytokines, such as IL-6, MCP-1, and GM-CSF (in agreement with what has been previously reported [26]) while, at the same time, enhancing intraparenchymal levels of IL-13 and M-CSF. The acute overall suppression of inflammatory cytokine levels (with reduced levels of KC and IFN-γ) suggest a stable decrease in the inflammatory response, which corresponds both to the improved neurological condition in ethanol-pretreated mice, and to the higher level of Akt signaling and protein synthesis (as shown by behavioral and biochemical assays). Although the overall effect of cytokine patterns is most likely attributable to the interaction of multiple players (with roles that remain to be ascertained), IL-13 emerges as a strikingly dynamic cytokine in TBI and subject to strong ethanol modulation. In fact, ethanol can enhance IL-13 release under reactive conditions [37,38] raising the possibility that the observed peak in IL-13 may originate in the periphery or in the brain. Irrespective of the source, IL-13 is a critical factor in inducing a protective/reparative phenotype in macrophages [39] and together with IL-4, is a key factor in inducing alternative polarization of microglia [40–42]. Furthermore, IL-13 can induce apoptosis in activated microglia [43–44] and can have direct protective effects by inducing the secretion of BDNF in astrocytes [45]. Although the direct effect on VEGF levels may depend on cell- and tissue-specific mechanisms [46–47], IL-13-dependent VEGF upregulation has been described [48], suggesting that the IL-13 and VEGF peaks observed in eth-TBI mice may be correlated. Thus, the early peak in IL-13 may be a critical instructive signal reducing early inflammation and therefore allowing for reduced neurological deterioration. These data suggest that the translational study of IL-13 in TBI is warranted.

Likewise, ethanol causes a remarkable change in the time course of IL-6 levels in cerebral parenchyma suppressing it in the early phase but enabling a significant increase at 24 h post-injury. Interestingly, IL-6 has been considered a detrimental factor in acute TBI, and neutralization of IL-6 in TBI (when associated with hypoxia) is sufficient to decrease the extent of neuronal damage [49]. Conversely, increased levels of astrocytic IL-6 increases acute neuro-inflammation, but upon prolonged secretion, results in a complete recovery [50]. Therefore, both the initial suppression and the later increase of IL-6 may contribute to the beneficial effect of ethanol, by suppressing early inflammatory cascades activation but enhancing astrocyte recruitment and repair mechanisms.

Despite the short half-life of ethanol [32], the effects on cytokine patterns are long lasting and affect the extent of immune cells infiltration and microglial activation at 7 dpi, in agreement with the improvement in neurological function. Since ethanol is cleared within < 24 h, these long-lasting effects may be of consequence in early events of TBI neuro-inflammation that play a critical "priming" role in orienting the cascades that unfold in time. This priming effect may be contributed by the systemic suppression of inflammatory mediators caused by ethanol, such as the blunting of the hepatic IL-6 response [27–30]. The earliest response to TBI is thought to be orchestrated by local release of chemokines and by neutrophil infiltration [51]; notably, neutrophil depletion has been shown to be protective in TBI [52] and, since ethanol pretreatment results in decreased levels of the neutrophil chemoattractant KC, interference with early neutrophil recruitment is an additional mechanism, together with the direct modulation of microglia, through which acute ethanol exposure may modulate the TBI-associated neuro-inflammatory response and the behavioral outcome.

Most notably, the brain tissue exposed to macroscopic traumatic intracerebral hemorrhage displays a radically different cytokine pattern, dominated by KC, IFN-γ, and CCL-2, implying a much stronger, and qualitatively different, immune response. In these conditions, ethanol produces no discernible effect on the cytokine pattern. Thus, any beneficial effect brought about by ethanol immunomodulatory effects may be absent when a significant traumatic intracerebral hemorrhage takes place.

As limitations of the present study, it must be noted that the experimental conditions (including the pre-administration of buprenorphine) which are ethically and legally mandated in animal experimentation may not closely reproduce the variability of TBI in human patients (a limitation shared by virtually all experimental TBI investigations); in addition, only one dose of ethanol, comparable to what is previously reported [53], was investigated. However, it is possible that a beneficial or detrimental outcome may result as a function of the dose of ethanol and of its metabolism, as suggested by clinical observations [9,10]. We are unable to provide data for low-dose ethanol, because in the 3 cm- weight drop model (sal-TBI mice) a pre-specified aggregated rejection rate (mortality and hemorrhage mice) was > 20% and therefore it was judged not to be ethical to test with a low dose of ethanol. However, our data in a lower-severity drop-weight model (2 cm weight drop) showed that high-dose (5 g/kg) ethanol produced a significant improvement in performance whereas the low-dose (1 g/kg) produced only a minor effect (that was non-statistically significant for all but one timepoint) in behavioral improvement (Supplementary Fig. 1).

The divergent pattern suggests that the presence of hemorrhage should be factored in as stratification criterion in clinical studies investigating ethanol effects in human patients, since ethanol may not produce any effect in these patients. Broadly speaking, immunomodulatory therapies for TBI may need to be tailored for specific subgroups of patients displaying homogeneous neuro-immune response profiles, since treatment strategies aimed at a specific cytokine pattern may have different efficacies depending on the underlying polarization of the neuro-immune response.

Supplementary data to this article can be found online at http://dx.doi.org/10.1016/j.intimp.2017.08.002.

Acknowledgement

This work has been supported by the DFG (SFB1149-B05) "Danger

response, disturbance factors and regenerative potential after acute trauma"-subproject B05. FR is also supported by the ERANET-NEURON initiative "European Research Projects on External Insults to the Nervous System" as part of the MICRONET consortium, and by the Ulm University-Medical Faculty Baustein Program.

Competing interests

The authors declare to have no financial or otherwise competing interest which may affect the design, the execution or the interpretation of the present paper.

References

[1] J. Bruns Jr., W.A. Hauser, The epidemiology of traumatic brain injury: a review, Epilepsia 44 (Suppl. 10) (2003) 2–10.
[2] P. Leo, M. McCrea, Epidemiology, in: D. Laskowitz, G. Grant (Eds.), Translational Research in Traumatic Brain Injury, CRC Press/Taylor and Francis Group, Boca Raton (Fl.), 2016(Chapter 1).
[3] E. Zaloshnja, T. Miller, J.A. Langlois, A.W. Selassie, Prevalence of long-term disability from traumatic brain injury in the civilian population of the United States, 2005, J. Head Trauma Rehabil. 23 (2008) 394–400.
[4] O. Savola, O. Niemelä, M. Hillbom, Alcohol intake and the pattern of trauma in young adults and working aged people admitted after trauma, Alcohol Alcohol. 40 (2005) 269–273.
[5] P. Cummings, F.P. Rivara, C.M. Olson, K.M. Smith, Changes in traffic crash mortality rates attributed to use of alcohol, or lack of a seat belt, air bag, motorcycle helmet, or bicycle helmet, United States, 1982–2001, Inj. Prev. 12 (2006) 148–154.
[6] J.H. Brennan, S. Bernard, P.A. Cameron, J.V. Rosenfeld, et al., Ethanol and isolated traumatic brain injury, J. Clin. Neurosci. 22 (2015) 1375–1381.
[7] R. Raj, M.R. Skrifvars, R. Kivisaari, et al., Acute alcohol intoxication and long-term outcome in patients with traumatic brain injury, J. Neurotrauma 32 (2015) 95–100.
[8] R. Raj, E.D. Mikkonen, J. Siironen, et al., Alcohol and mortality after moderate to severe traumatic brain injury: a meta-analysis of observational studies, J. Neurosurg. 124 (2016) 1684–1692.
[9] C. Berry, E.J. Ley, D.R. Margulies, et al., Correlating the blood alcohol concentration with outcome after traumatic brain injury: too much is not a bad thing, Am. Surg. 77 (2011) 1416–1419.
[10] A. Salim, P. Teixeira, E.J. Ley, et al., Serum ethanol levels: predictor of survival after severe traumatic brain injury, J. Trauma 67 (2009) 697–703.
[11] J.S. Cho, S.D. Shin, K.J. Lee, et al., Alcohol intake and reduced mortality in patients with traumatic brain injury, Alcohol. Clin. Exp. Res. 40 (2016) 1290–1294.
[12] H.C. Tien, L.N. Tremblay, S.B. Rizoli, et al., Association between alcohol and mortality in patients with severe traumatic head injury, Arch. Surg. 141 (2006) 1185–1191.
[13] D.F. Kelly, S.M. Lee, P.A. Pinanong, D.A. Horda, Paradoxical effects of acute ethanolism in experimental brain injury, J. Neurosurg. 86 (1997) 876–882.
[14] L.S. Jana, M.R. Hoane, D. Conde, et al., Acute ethanol administration reduces the cognitive deficits associated with traumatic brain injury in rats, J. Neurotrauma 15 (1998) 105–115.
[15] T. Wang, D.Y. Chou, J.Y. Ding, et al., Reduction of brain edema and expression of aquaporins with acute ethanol treatment after traumatic brain injury, J. Neurosurg. 118 (2013) 390–396.
[16] B. Joseph, M. Khalil, V. Pandit, et al., Adverse effects of admission blood alcohol on long-term cognitive function in patients with traumatic brain injury, J. Trauma Acute Care Surg. 78 (2015) 403–408.
[17] V. Pandit, N. Patel, P. Rhee, et al., Effect of alcohol in traumatic brain injury: is it really protective? J. Surg. Res. 190 (2014) 634–639.
[18] W. Wu, R. Tian, S. Hao, et al., A pre-injury high ethanol intake in rats promotes brain edema following traumatic brain injury, Br. J. Neurosurg. 28 (2014) 739–745.
[19] I.C. Vazgeses, S.Y. Tsai, S.T. Tsu, et al., Binge ethanol prior to traumatic brain injury worsens sensorimotor functional recovery in rats, PLoS One 10 (2015) e0120356.
[20] S. Gyonova, B.M. Ramsoboff, Inflammatory reaction after traumatic brain injury: therapeutic potential of targeting cell-cell communication by chemokines, Trends Pharmacol. Sci. 36 (2015) 471–480.
[21] H.D. Soares, R.R. Hicks, D. Smith, T.K. McIntosh, Inflammatory leukocytic recruitment and diffuse neuronal degeneration are separate pathological processes resulting from traumatic brain injury, J. Neurosci. 15 (1995) 8223–8233.
[22] C.L. Hsieh, C.C. Kim, B.E. Ryba, et al., Traumatic brain injury induces macrophage subsets in the brain, Eur. J. Immunol. 43 (2013) 2010–2022.
[23] S. Holmin, T. Mathiesen, J. Shetye, P. Biberfeld, Intracerebral inflammatory response to experimental brain contusion, Acta Neurochir. 132 (1995) 110–119.
[24] C.A. McKee, J.R. Lukens, Emerging roles for the immune system in traumatic brain injury, Front. Immunol. 7 (2016) 556.
[25] S.X. Teng, P.E. Molina, Acute alcohol intoxication prolongs neuroinflammation without exacerbating neurobehavioral dysfunction following mild traumatic brain injury, J. Neurotrauma 31 (2014) 378–388.
[26] M.D. Goodman, A.T. Makley, E.M. Campion, et al., Preinjury alcohol exposure attenuates the neuroinflammatory response to traumatic brain injury, J. Surg. Res. 184 (2013) 1053–1058.
[27] N. Wagner, A. Akbarpour, K. Mörs, et al., Alcohol intoxication reduces systemic interleukin-6 levels and leukocyte counts after severe TBI compared with not intoxicated TBI patients, Shock 46 (2016) 261–269.
[28] B. Relja, J. Meske, N. Wagner, et al., Effects of positive blood alcohol concentration on outcome and systemic interleukin-6 in major trauma patients, Injury 47 (2016) 640–645.
[29] B. Relja, N. Omid, A. Schaible, et al., Pre- or post-treatment with ethanol and ethyl pyruvate results in distinct anti-inflammatory responses of human lung epithelial cells triggered by interleukin-6, Mol. Med. Rep. 12 (2015) 2991–2998.
[30] B. Relja, N. Omid, N. Wagner, et al., Ethanol, ethyl and sodium pyruvate decrease the inflammatory responses of human lung epithelial cells via Akt and NF-κB in vitro but have a low impact on hepatocellular cells, Int. J. Mol. Med. 37 (2016) 517–525.
[31] M.A. Flierl, P.F. Stahel, K.M. Beauchamp, et al., Mouse closed head injury model induced by a weight-drop device, Nat. Protoc. 4 (2009) 1328–1337.
[32] P.K. Wilkinson, Pharmacokinetics of ethanol: a review, Alcohol. Clin. Exp. Res. 4 (1980) 5–21.
[33] T.P. Faulkner, S.B. Cantleberry, V.J. Watts, A.S. Hussain, Comparative pharmacokinetics of ethanol in inbred strains of mice using doses based on total body water, Alcohol. Clin. Exp. Res. 14 (1) (Feb 1990) 82–86.
[34] D.J. Livy, S.E. Parnell, J.R. West, Blood ethanol concentration profiles: a comparison between rats and mice, Alcohol 29 (3) (Apr 2003) 165–171.
[36] P. Greiffenstein, K.W. Mathis, C.V. Stouwe, P.E. Molina, Alcohol binge before trauma/hemorrhage impairs integrity of host defense mechanisms during recovery, Alcohol. Clin. Exp. Res. 31 (2007) 704–715.
[37] J.C. Bouchard, J. Kim, D.R. Beal, et al., Acute oral ethanol exposure triggers asthma in cockroach allergen-sensitized mice, Am. J. Pathol. 181 (2012) 845–857.
[38] M. Alonso, J. Gomez-Rial, F. Gude, et al., Influence of experimental alcohol administration on serum immunoglobulin levels: contrasting effects on IgE and other immunoglobulin classes, Int. J. Immunopathol. Pharmacol. 25 (2012) 645–655.
[39] **L. Bosurgi, Y.G. Cao, M. Cabeza-Cabrerizo, et al., Macrophage function in tissue repair and remodeling requires IL-4 or IL-13 with apoptotic cells, Science (2017),** http://dx.doi.org/10.1126/science.aai8132 **(pii: eaai8132, Epub ahead of print).**
[40] N. Kiguchi, H. Sakaguchi, Y. Kadowaki, et al., Peripheral administration of interleukin-13 reverses inflammatory macrophage and tactile allodynia in mice with partial sciatic nerve ligation, J. Pharmacol. Sci. 133 (2017) 53–56.
[41] S. Mori, P. Maher, B. Conti, Neuroimmunology of the Interleukins 13 and 4, Brain Sci. 6 (2016) (pii: E18).
[42] D. Dooley, E. Lemmens, T. Vangansewinkel, et al., Cell-based delivery of interleukin-13 directs alternative activation of macrophages resulting in improved functional outcome after spinal cord injury, Stem Cell Rep. 7 (2016) 1099–1115.
[43] M.S. Yang, E.J. Park, S. Sohn, et al., Interleukin-13 and -4 induce death of activated microglia, Glia 38 (2002) 273–280.
[44] S.Y. Won, S.R. Kim, S. Maeng, B.K. Jin, Interleukin-13/interleukin-4-induced oxidative stress contributes to death of prothrombinkringle-2 (pKr-2)-activated microglia, J. Neuroimmunol. 265 (2013) 36–42.
[45] Y.M. Brombacher, J.K. Nono, K.S. De Gouveia, et al., IL-13-mediated regulation of learning and memory, J. Immunol. 198 (2017) 2681–2688.
[46] K.A. Radek, A.M. Matthies, A.L. Burns, et al., Acute ethanol exposure impairs angiogenesis and the proliferative phase of wound healing, Am. J. Physiol. Heart Circ. Physiol. 289 (2005) H1084–90.
[47] J.W. Gu, J. Elam, A. Sartin, et al., Moderate levels of ethanol induce expression of vascular endothelial growth factor and stimulate angiogenesis, Am. J. Phys. Regul. Integr. Comp. Phys. 281 (2001) R365–72.
[48] J. Corne, G. Chupp, C.G. Lee, et al., IL-13 stimulates vascular endothelial cell growth factor and protects against hyperoxic acute lung injury, J. Clin. Invest. 106 (2000) 783–791.
[49] S.H. Yang, M. Gangidine, T.A. Pritts, et al., Interleukin 6 mediates neuroinflammation and motor coordination deficits after mild traumatic brain injury and brief hypoxia in mice, Shock 40 (2013) 471–475.
[50] M. Penkowa, M. Giralt, N. Lago, et al., Astrocyte-targeted expression of IL-6 protects the CNS against a focal brain injury, Exp. Neurol. 181 (2003) 130–148.
[51] K.N. Gorps, T.L. Roth, D.B. McGavern, Inflammation and neuroprotection in traumatic brain injury, JAMA Neurol. 72 (3) (Mar 2015) 355–362.
[52] E. Kenne, A. Erlandsson, L. Lindbom, L. Hillered, P. Clausen, Neutrophil depletion reduces edema formation and tissue loss following traumatic brain injury in mice, J. Neuroinflammation 9 (Jan 23 2012) 17.
[53] B. Relja, D. Henrich, G. Wetzel, et al., Effects of acute ethanol gavage on intestinal integrity after hemorrhage/resuscitation, Scand. J. Gastroenterol. 48 (2013) 448–458.

6.2 Neuroprotective effect of an acute ethanol intoxication in TBI is associated to the hierarchical modulation of early transcriptional responses

Akila Chandrasekar[a,*], Bahar Aksan[b,*], Florian olde Heuvel[a], Philip Förstner[c], Daniela Sinske[c], Rida Rehman[a], Annette Palmer[d], Albert C. Ludolph[a], Markus Huber-Lang[d], Tobias M. Boeckers[e], Daniela Mauceri[b,#], Bernd Knöll[c,#], Francesco Roselli[a,#]

a) Dept. of Neurology, Ulm University, Germany

b) Dept. of Neurobiology, IZN, University of Heidelberg, Germany

c) Institute of Physiological Chemistry, Ulm University, Germany

d) Institute of Clinical and Experimental Trauma-Immunology, Ulm University, Germany

e) Dept. of Anatomy and Cell Biology, Ulm University, Germany

*These authors contributed equally to this work. # Co-senior authors.

Accepted: 30 December 2017

Published in: Experimental Neurology. April 2018. 302: 34-45

doi: https://doi.org/10.1016/j.expneurol.2017.12.017

Experimental Neurology 302 (2018) 34–45

Contents lists available at ScienceDirect

Experimental Neurology

journal homepage: www.elsevier.com/locate/yexnr

Research Paper

Neuroprotective effect of acute ethanol intoxication in TBI is associated to the hierarchical modulation of early transcriptional responses

Akila Chandrasekar[a,1], Bahar Aksan[b,1], Florian olde Heuvel[a], Philip Förstner[c], Daniela Sinske[c], Rida Rehman[a], Annette Palmer[d], Albert Ludolph[a], Markus Huber-Lang[d], Tobias Böckers[e], Daniela Mauceri[b,2], Bernd Knöll[c,2], Francesco Roselli[a,*,2]

[a] Dept. of Neurology, Ulm University, Germany
[b] Dept. of Neurobiology, IZN, University of Heidelberg, Germany
[c] Institute of Physiological Chemistry, Ulm University, Germany
[d] Institute of Clinical and Experimental Trauma-Immunology, Ulm University, Germany
[e] Dept. of Anatomy and Cell Biology, Ulm University, Germany

ARTICLE INFO

Keywords:
Traumatic brain injury
Ethanol intoxication
Immediate early genes
Transcription
Neuroprotection
c-Fos

ABSTRACT

Ethanol intoxication is a risk factor for traumatic brain injury (TBI) but clinical evidence suggests that it may actually improve the prognosis of intoxicated TBI patients.

We have employed a closed, weight-drop TBI model of different severity (2 cm or 3 cm falling height), preceded (−30 min) or followed (+20 min) by ethanol administration (5 g/Kg). This protocol allows us to study the interaction of binge ethanol intoxication in TBI, monitoring behavioral changes, histological responses and the transcriptional regulation of a series of activity-regulated genes (immediate early genes, IEGs). We demonstrate that ethanol pretreatment before moderate TBI (2 cm) significantly reduces neurological impairment and accelerates recovery. In addition, better preservation of neuronal numbers and cFos + cells was observed 7 days after TBI. At transcriptional level, ethanol reduced the upregulation of a subset of IEGs encoding for transcription factors such as *Atf3*, *c-Fos*, *FosB*, *Egr1*, *Egr3* and *Npas4* but did not affect the upregulation of others (e.g. *Gadd45b* and *Gadd45c*). While a subset of IEGs encoding for effector proteins (such as *Bdnf*, *Inhba and Dusp5*) were downregulated by ethanol, others (such as *Il-6*) were unaffected. Notably, the majority of genes were sensitive to ethanol only when administered before TBI and not afterwards (the exceptions being *c-Fos*, *Egr1* and *Dusp5*). Furthermore, while severe TBI (3 cm) induced a qualitatively similar (but quantitatively larger) transcriptional response to moderate TBI, it was no longer sensitive to ethanol pretreatment. Thus, we have shown that a subset of the TBI-induced transcriptional responses were sensitive to ethanol intoxication at the instance of trauma (ultimately resulting in beneficial outcomes) and that the effect of ethanol was restricted to a certain time window (pre TBI treatment) and to TBI severity (moderate). This information could be critical for the translational value of ethanol in TBI and for the design of clinical studies aimed at disentangling the role of ethanol intoxication in TBI.

1. Introduction

Ethanol (EtOH) intoxication is a common comorbidity of trauma and in particular of traumatic brain injury (TBI). Up to 43% of car crashes involve patients testing positive for blood alcohol level (BAL; Cummings et al., 2006) and up to 55% of patients hospitalized due to TBI show a positive BAL (Savola et al., 2005). However, patients with positive BAL may actually have a better prognosis than patients with undetectable BAL (Brennan et al., 2015; Raj et al., 2015; Raj et al., 2016; Berry et al., 2011; Salim et al., 2009; Cho et al., 2016, although some studies dispute this notion: Joseph et al., 2015; Pandit et al., 2014). In particular, BAL > 230 mg/dL has been suggested to provide the largest decrease in mortality (Salim et al., 2009; Berry et al., 2011) in moderate-to-severe TBI. Despite being among the most common comorbidities of TBI, the clinical relevance and the impact of BAL on the multifaceted TBI pathophysiology remains only partially

* Corresponding author at: Dept. of Neurology-Ulm University, Center for Biomedical Research (ZBF), Helmholtzstrasse 8/2(R1.44)-89081, Ulm-DE, Germany.
E-mail address: francesco.roselli@uni-ulm.de (F. Roselli).
[1] These authors equally contributed to this work.
[2] Co-senior authors.

https://doi.org/10.1016/j.expneurol.2017.12.017
Received 18 October 2017; Received in revised form 8 December 2017; Accepted 30 December 2017
Available online 04 January 2018

understood particularly from a molecular and cellular point of view. In particular, a beneficial or detrimental effect of EtOH on TBI, and the boundaries of the parametric space of such an effect (in terms of doses and of timing of administration), remains unclear and the molecular mechanisms of EtOH interaction on TBI, and their consequences, are largely unknown.

The neuronal response to TBI is strongly driven by excitation-triggered cascades. Micro dialysis studies have revealed strong and rapid increases in extracellular glutamate both in experimental models (Folkersma et al., 2011) and in patients (although with different kinetics; Chamoun et al., 2010). Both the shock wave of acute trauma and increased levels of excitatory amino acids have been linked to the onset of the spreading depolarization waves (Sato et al., 2014; Hinzman et al., 2016). Initial release of glutamate is followed by secondary enhancement of excitatory amino acid levels through the dysfunction of the glial uptake systems (for review see Dorsett et al., 2017). The rise of glutamate and the activation of excitatory glutamate receptors is thought to contribute critically to Ca^{2+} dysregulation (Weber et al., 2001; Weber, 2012) and may lead to death of neurons due to excitotoxicity (Hardingham and Bading, 2010). Moreover, excitation-dependent transcriptional programs are activated in TBI. Specifically, the induction of prototypical immediate-early genes (IEG), such as *c-Fos* and *Atf3*, have been detected in rodents and in human tissue (Dutcher et al., 1999; Giza et al., 2002; Czigner et al., 2004; Wang et al., 2014; Natale et al., 2003; Zhang et al., 2014). Transcriptome data suggest that c-Fos is among the master regulators of the transcriptional response to TBI (Samal et al., 2015).

Although excitation-dependent IEG transcription is associated with enhanced neuronal integrity and survival after insults to the central (Zhang et al., 2002; Zhang et al., 2009; Zhang et al., 2011; Ahlgren et al., 2014; Rawat et al., 2016) as well as to the peripheral nervous system (Gey et al., 2016), it modulates a wider set of biological responses in the CNS, such as learning and memory (Ramanan et al., 2005; Mellström et al., 2014; Li et al., 2007), neuroinflammation (Nomaru et al., 2014; Wang et al., 2012), and structural/functional circuitry remodelling (Hu et al., 2004; Lösing et al., 2017; Renaudineau et al., 2009). IEGs have been implicated in adaptive as well as maladaptive changes in pathological conditions such as downregulation of axonal sprouting (Lösing et al., 2017), expression patterns in Alzheimer's disease (Corbett et al., 2017) and epilepsy (Honkaniemi and Sharp, 1999; Morris et al., 2000; Yutsudo et al., 2013).

Because of the combined GABA-enhancing and NMDAR-antagonist properties (Criswell et al., 2003, 2004), it could be hypothesized that EtOH would be well-suited to affect the excitation-dependent transcriptional response in TBI, which has been shown to have a strong NMDAR component (Wang et al., 2014). These effects impinge not only on neuronal survival but also on synaptic plasticity and neuroinflammation. However, the actual effect of EtOH on TBI-induced transcriptional regulation, and on the resulting outcome, has not been explored before.

Here we show that high doses of EtOH show neuroprotective effects (at behavioral and histological level) through the partial inhibition of neuronal injury response, which involves the significant decrease of the induction of a subset of IEGs. Furthermore, we demonstrate that EtOH is effective only when taken/administered before TBI and these effects are limited to moderate but not to severe TBI. By analyzing a number of IEGs encoding transcription factors or effector genes and by administering EtOH before or after TBI, we show that there is a hierarchy on the activation of transcription factors upon TBI with differential sensitivity to EtOH.

2. Materials and methods

2.1. Experimental animals, EtOH administration and traumatic brain injury model

All experiments were approved by the local veterinary and animal experimentation committee under the license number 1222. Four experimental groups were employed: Saline-sham (mice administered with saline and undergoing only sham surgery; henceforth sal-S), EtOH-sham (EtOH administration, sham surgery; eth-S), saline TBI (sal-TBI) and EtOH TBI (eth-TBI). When treatment was administered after TBI (both EtOH and saline), additional sham mice (saline and EtOH-administered after the TBI procedure) were analyzed. The group size for each experimental group is provided in Supplementary Table 1. Administration of saline or EtOH and delivery of TBI or sham surgery was randomized and the evaluation of gene transcription, histology and behavior was performed by experimenters blind to the treatment group. Independent animal groups, together with the corresponding controls, were included for each timepoint of tissue sampling and for different schedules of administration. Sham mice underwent all the procedures (gas anesthesia, O_2 administration, opening and closing of the scalp skin, handling and positioning in the TBI apparatus, treatment with buprenorphine; see below) but were not subjected to the trauma itself.

B6-SJL male mice aged 80–90 days were subject to closed weight-drop TBI (Flierl et al., 2009) after being administered by oral gavage either 5 g/kg or 1 g/kg of EtOH solution in 400 μl (32% v/v or 6.4% v/v, respectively, in saline) or saline 30 min before or, in separate experiments, 20 min after TBI. Both doses and administration routes were in agreement with previously published protocols (Wagner et al., 2017; Karelina et al., 2017; Relja et al., 2013). Buprenorphine (0.1 mg/kg by subcutaneously injection) was administered before anesthetizing the mice with sevoflurane (4% in 96% O_2). The skull surface was exposed by incision of the scalp skin on the midline, before positioning the animal in the weight-drop apparatus as previously described (Flierl et al., 2009). The impact was directed to the center of the right parietal bone, with TBI produced by a 333 g impactor free-falling from a 2 cm or a 3 cm distance. Apnea time was monitored. The overall time of exposure of the mice to sevoflurane, in 96% O_2, never exceeded 10 min. After the restoration of regular breathing, the skin was sutured with Prolene 6.0 surgical thread and the animals were transferred to a recovery cage (single-housed) with warmed pad at 35 °C and ad libitum access to food and water. Additional doses of buprenorphine were administered every 12 h for the following 24 h. To avoid unnecessary suffering of the mice, their general state was checked regularly using a score sheet developed for TBI determining fixed termination criterions. Effort was made to minimize the suffering of animals and reduce the number of animals used.

2.2. Behavioral assessment

The overall neurological impairment was evaluated using the composite Neurological Severity Score, as described by Flierl et al. (2009). At 3 h post-injury, 24 h post-injury, 2 dpi, 3 dpi and 7 dpi the assessment of motor (muscle status, abnormal movement), sensory (visual, tactile, proprioceptive) reflex, and balance abilities were tested. Animals were awarded one point for failure to perform a task, such that increasing scores ranged from 0 to 10 indicate stronger severity of dysfunction. The Arena Escape test, part of NSS evaluation, was performed by placing the animals into a circular, brightly-lit area whose wall included a narrow opening leading to the dark compartment. The time required by the animal to enter the dark compartment was measured and averaged over three attempts. The Beam walk test was performed as previously reported (Luong et al., 2011). Mice were habituated to walking over a suspended wooden beam (11 mm in diameter) from an open platform to a dark compartment and the test was then repeated at 2 dpi and 7 dpi. The time required to reach the dark box

was measured. The tests were recorded with an overhanging digital camera and scored off-line.

The Open Field test was performed as previously reported (Zimprich et al., 2014). Briefly, the animals were placed into a squared (45.5 × 45.5 × 39.5 cm) arena, illuminated with 200 lx in the center, and monitored with an overhanging monochrome camera for 20 min. The movement of the mouse and speed parameters was analyzed off-line by the EthoVision system (Version 3.1.16, Noldus Information Technology, The Netherlands; 12.5 Hz; Activity settings: minimum distance moved: 1 cm).

2.3. Tissue sampling for molecular biology

Independent cohorts of mice were sacrificed by cervical dislocation 1 h or 3 h after trauma. Mice were decapitated, the brain was extracted after opening of the parietal and occipital bones and quickly deposited in ice-cold PBS. Left and right hippocampi were identified by gross morphology, dissected out manually under 4 × magnification and snap-frozen.

2.4. Quantitative RT-PCR

Total RNA was extracted from ipsilateral and contralateral hippocampi from mice subjected to TBI using the RNeasy Mini Kit (Qiagen, Hilden, Germany) with additional on-column DNase I digestion to eliminate genomic DNA contamination according to the manufacturer's instructions (Qiagen). 2.4 μg of extracted RNA was reverse transcribed into first strand cDNA using the High Capacity cDNA Reverse Transcription Kit (Applied Biosystems, Foster City, CA). For the screening of activity-dependent transcription factors, mRNA levels in moderate and severe TBI samples (Figs. 2A, B, 5A, 6A, Suppl. Fig. 1 and Suppl. Fig. 2), quantitative reverse transcriptase PCR (QRT-PCR) was performed with the StepOnePlus™ Real-Time PCR System, TaqMan Gene Expression Master Mix and FAM dye-labeled probe sets designed by Applied Biosystems (validated in previous studies; Mauceri et al., 2011). The expression levels of target genes were normalized to the expression of *Gapdh*.

For the quantification of effector molecules (Figs. 3A–C, 5A[Dusp5 and Dusp6], 6B) qPCR was performed on a Roche LightCycler® 480 with the SYBR Premix Ex Taq (Tli RNase H Plus) PCR Master Mix (TaKaRa). *Gapdh* RNA levels served as internal standard for normalization. The two approaches were used because for each gene, the set of primers and the corresponding qPCR method, which was already pre-tested and established was used. Primer sequences are provided upon request.

2.5. Western blot

Protein lysates were prepared with the ISOLATE II RNA/DNA/protein kit (Bioline) according to manufacturer's instructions. Phosphatase inhibitors (1 × PhosStop (Roche)) were added to the protein lysates. Samples were resolved on 8–10% SDS-PAGE, followed by transfer on PVDF membranes (Amersham). After 1 h of blocking, the membranes were incubated with the primary antibodies overnight at 4 °C: anti-Egr1 (rabbit 1:500; Santa Cruz) and mouse anti-tubulin (1:1000; Acris). Detection of the primary antibodies involved horseradish-peroxidase conjugated secondary antibodies (1:2000; Santa Cruz) and the ECL Western Blotting Substrate (Pierce or Millipore). For the quantification of the antibodies, images were imported in ImageJ and ROI were traced on the significant bands. The optical density value was obtained and corrected for local background.

2.6. Perfusion fixation and histology

For histological evaluation of the neuronal density and c-Fos expression in hippocampus, the cohort of mice undergoing behavioral testing was sacrificed at 7 dpi. For cFos expression at 3 h, an independent cohort of mice was used. Anesthesia and perfusion were performed as previously reported (Chandrasekar et al., 2017). Briefly, mice were terminally anesthetized with ketamine/xylazine (100 mg/kg and 16 mg/kg) and intra-cardially perfused with 50 mL ice-cold PBS followed by 50 mL of 4% PFA in PBS. The brain was then extracted and postfixed in 4% PFA for 18 h at 4 °C, washed in PBS and cryoprotected in 30% sucrose in PBS. Brains were thereafter embedded in OCT on dry ice and sectioned in 40 μm-thick coronal sections in a cryostat (Leica CM 1950). Floating sections corresponding to the dorsal hippocampus were processed for immunostaining. Briefly, sections were blocked in 3%BSA/3%Donkey serum/0.3%Triton in PBS for 2 h at 24 °C and then incubated with the appropriate primary antibody (mouse anti-NeuN, 1:100, Millipore; rabbit anti-c-Fos, 1:500, Santa Cruz) for 48 h at 4 °C; sections were thereafter washed 3X30min in PBS and incubated in the appropriate secondary antibody mix (Donkey anti mouse 568, invitrogen; Donkey anti rabbit 488, Invitrogen) for 2 h at 24 °C, together with DAPI (1:1000) for nuclear counterstain, washed again (3 × 30 min in PBS), and finally mounted in Fluorogold-Prolong Antifade (Invitrogen).

2.7. Confocal imaging and image analysis

Confocal images were acquired using an LSM-700 (Carl Zeiss AG) inverted microscope, fitted with a 20 × air objective. All images were acquired in 12-bit format. Imaging parameters were set in order to obtain signal for the immunostained antigen > 150 (arbitrary fluorescence intensity/grey value scale in 12 bits images, ranging 0–4095) while avoiding saturation in high-intensity neurons. In order to avoid fluorescence cross-bleed, all fluorescent channels were acquired independently. For each mouse, 3–4 brain sections obtained at 200–300 μm distance, encompassing the dorsal hippocampus, were imaged focusing on the upper blade of dentate gyrus (DG) and on the apex of the CA1 profile. For neuronal counting, optical stacks composed of 20 1-μm-thick optical sections were imported in ImageJ and collapsed separately in maximum-intensity-projection mode for each channel. A fixed-area (10^5 μm^2 in size) was manually positioned at the apex of the CA1 profile or on the upper blade of the DG. An intensity-threshold was applied to bin the image into positive and negative cells; the value of the threshold was kept constant across images and replicated. $NeuN^+$ and $cFos^+$ cells were then visually identified and counted by an experimenter blind to the treatment groups.

2.8. Blood ethanol level measurement

Whole blood drawn by puncture of the right ventricle (in sterile plasma EDTA microtubes; Kabe Labortechnik, Nuembrecht-Elsenroth, Germany) was centrifuged at 800g for 10 min at 4 °C. The supernatant was further centrifuged at 13000g for 2 min at 4 °C. The resulting supernatant was collected and stored at − 80 °C. Ethanol levels were measured using the Abcam Ethanol Assay Kit (ab65343; Abcam plc, Cambridge, UK) according to the manufacturer's instructions. Briefly, 50 μl of diluted sample (1:500 for eth-S and eth-TBI; sal-S and sal-TBI samples were diluted 1:10) were added to each well of a 96-well plate, together with 50 μl of reaction mix (46 μl Ethanol Assay buffer, 2 μl Ethanol Probe and 2 μl Ethanol Enzyme Mix). After brief mixing, the plate was incubated for 30 min at room temperature. Absorbance was measured with OD 570 (Fluostar Optima plate scanner, BMG LABTECH).

2.9. Statistical analysis

Statistical analysis was performed with the GraphPad Prism software suit. Statistical analysis of behavioral data (NSS, Arena Escape and Open Field) was performed using two-way ANOVA for repeated measures with Turckey post-hoc multiple-comparisons test. For the

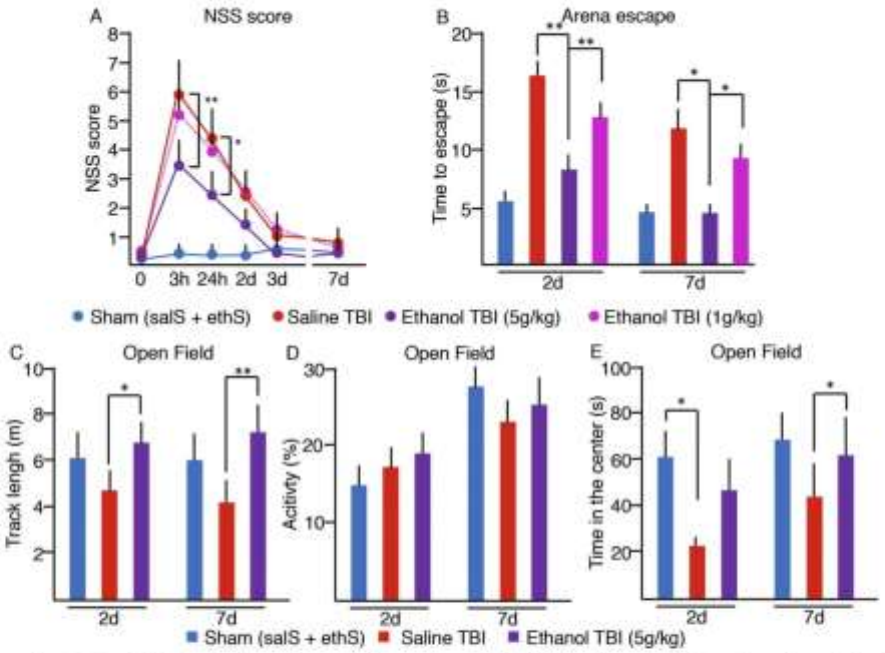

Fig. 1. High-dose but not low-dose Ethanol administration enhanced neurological recovery after TBI. In all behavioral tests sal-S and eth-S performed comparably and were displayed (for graphical simplicity) as a unified "sham" group.

A) At 3 h after injury, the NSS score were comparable in sal-TBI and low-dose eth-TBI but were significantly reduced in high-dose eth-TBI mice (3.50 ± 0.75). Whereas low-dose eth-TBI mice were never different from sal-TBI mice, at 24 h high-dose eth-TBI still displayed a lower NSS score than sal-TBI mice.

B) Sal-TBI mice required significantly longer time to exit arena than sham controls (at 2 dpi). Low-dose eth-TBI mice were not statistically different from sal-TBI, whereas high-dose eth-TBI was significantly faster at 2 dpi and became comparable to sham mice in the next timepoints.

C) In the comparison of Open Field track-length of sham, sal-TBI and eth-TBI, sal-TBI displayed a trend toward reduced track-length at 2 dpi and a significantly decreased track-length at 7 dpi. Eth-TBI was comparable to sham both at 2 and 7 dpi.

D) Overall activity fraction (the percentage of time spent in movement) was comparable in sham, sal-TBI and eth-TBI mice both at 2 dpi and at 7 dpi.

E) The time spent in the central quadrant (a measure of anxiety) was significantly shorter after injury in sal-TBI mice compared to eth-TBI whereas eth-TBI mice were comparable to sham mice. A similar trend was detectable at 7 dpi. Behavioral data are displayed as average ± SEM. (* ≤ 0.05, ** ≤ 0.01, *** ≤ 0.001).

comparison of cell counts (NeuN + density, cFos + density), one-way ANOVA with Holm-Sidak post-hoc multiple comparisons test was used. The analysis of Western blot was performed with non-parametric Kruskall-Wallis ANOVA with Dunn's multiple-comparisons test. For the analysis of the gene expression, non-parametric ANOVA was performed using the rank-based Kruskall-Wallis test, with Dunn correction for multiple comparisons. Statistical significance was set at $p < 0.05$.

3. Results

High-dose EtOH pretreatment enhances neurological recovery after moderate TBI.

First, we inspected the impact of EtOH on overall TBI survival. Neither high-dose nor low-dose EtOH had a negative effect on overall TBI survival. For the moderate TBI (2 cm falling height), survival rate was 32/35 (91%) for sal-TBI and 30/34 (88%) for eth-TBI (high-dose) and 5/5 (100% survival) for low-dose eth-TBI. In order to establish the overall effect of EtOH intoxication on the neurological outcome of moderate TBI, we administered mice with either 1 g/Kg (low-dose) or 5 g/Kg (high-dose) of EtOH 30 min before the experimental TBI procedure. As control, mice were injected with saline solution. The performance of the mice was assessed by the Neurological Severity Score (NSS) and by their performance in the Arena Escape (AE) test (Flierl et al., 2009). The performance of eth-S and sal-S mice was indistinguishable in NSS and AE tests. Therefore, for graphical simplicity, the two groups were merged and a single "sham" group (sal-S + eth-S) is displayed in Fig. 1A–E.

The performance of the mice in different groups was significantly different across treatment groups ($F_{(3,15)} = 45.6$, $p < 0.0001$) and time points ($F_{(5,75)} = 54.9$, $p < 0.0001$) with a significant interaction between treatment and time ($F_{(15,75)} = 8.8$, $p < 0.0001$). Post-hoc analysis revealed that 3 h after injury, all mice subject to TBI displayed an increase in NSS score, underscoring their acute neurological impairment. Whereas NSS scores were comparable in sal-TBI and low-dose eth-TBI mice (6.0 ± 1.25 in sal-TBI vs 5.25 ± 1.50, $p > 0.05$; Fig. 1A), mice administered with the high-dose EtOH had a significantly better (lower) NSS score (3.50 ± 0.75; $p < 0.01$ vs sal-TBI; Fig. 1A). The beneficial effect of high-dose EtOH administration was still detectable at 24 h, when high-dose eth-TBI still displayed a lower NSS score (2.75 ± 0.5) than sal-TBI mice (4.25 ± 1.25, $p < 0.05$), whereas low-dose eth-TBI were never different from sal-TBI (Fig. 1A).

The effect of EtOH on the acute neurological impairment and recovery was further investigated in the Arena Escape test. A significant effect of treatment ($F_{(3,27)} = 32.7$, $p < 0.001$) and time point ($F_{(1,27)} = 16.4$, $p = 0.0004$) was identified but no interaction between treatment and time ($F_{(3,27)} = 1.9$, $p = 0.149$). Post-hoc analysis revealed that sal-TBI mice required significantly longer to exit the arena than sham controls (at 2 dpi, 16.8 ± 4.1 s vs 5.7 ± 1.4 s, respectively; $p < 0.01$; Fig. 1B). Low dose eth-TBI mice were not statistically different from sal-TBI, whereas high-dose eth-TBI were significantly faster at 2 dpi (9.1 ± 2.2 s; $p < 0.01$ vs sal-TBI, $p > 0.05$ vs sham) and become comparable to sham mice afterward (Fig. 1B). Statistically

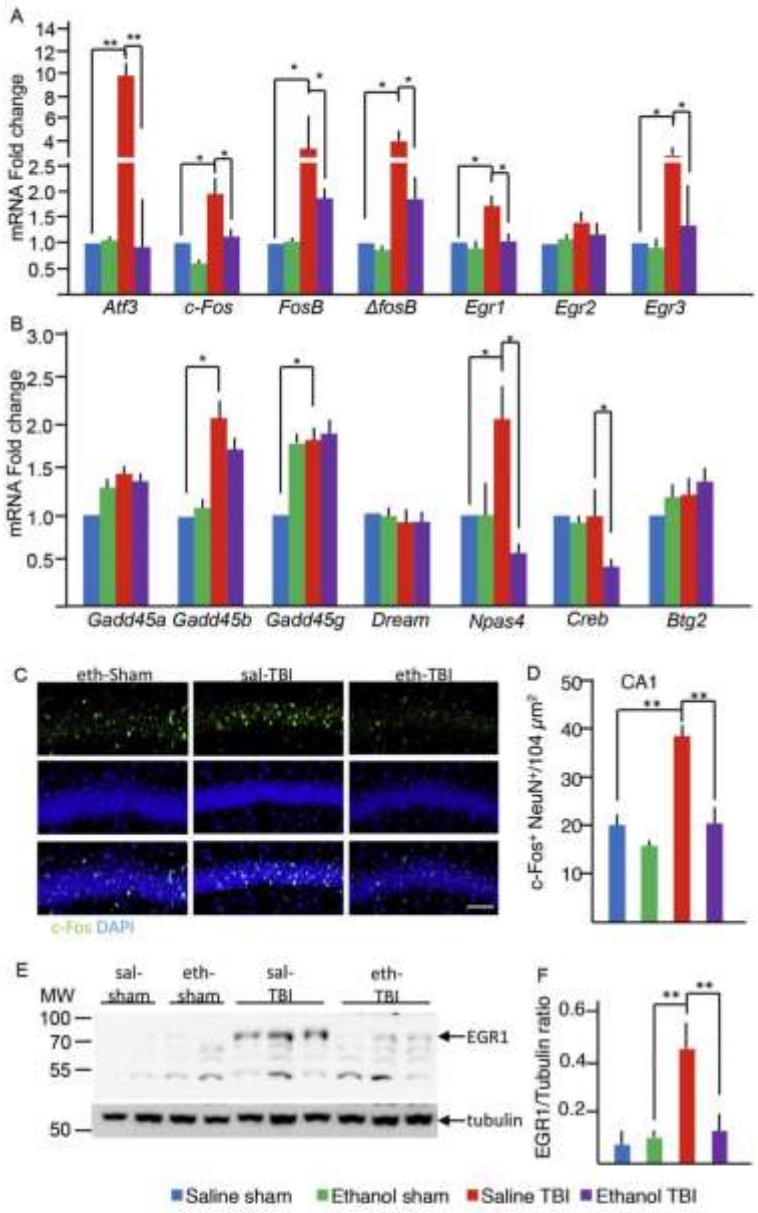

Fig. 2. TBI-induced transcriptional response was decreased by acute ethanol administration.

A) sal-TBI mice displayed a significant upregulation of *Atf3*, *c-Fos*, *FosB*, *Δ-FosB*, *Egr1*, *Egr3* but not *Egr2*. In ethanol-pretreated TBI mice, the induction of *Atf3* and of all the genes of the Fos family were significantly reduced. This effect was also observed for *Egr1* and *Egr3*.

B) In sal-TBI mice, levels of mRNA for *Npas4*, *Gadd45b* and *Gadd45g* were upregulated, but not those of *Gadd45a*, *Btg2*, *Dream* and *Creb*. Ethanol administration prevented the up-regulation of *Npas4* but did not affect the induction of *Gadd45b* and *Gadd45g* mRNA. Notably, although not affected by TBI or ethanol alone, *Creb* mRNA was reduced in eth-TBI samples. ($^{*} \leq 0.05$, $^{**} \leq 0.01$, $^{***} \leq 0.001$).

C, D) Hippocampal sections (3 h) were immunostained for DAPI and cFos. The number of cFos + neurons were significantly higher in sal-TBI than in sal- sham (not shown) and eth-sham mice but were significantly reduced by the pretreatment with ethanol. Scalebar 50 μm.

E, F) Western Blot of total hippocampal lysate showed the upregulation of Egr1 protein level at the 3 h timepoint in the sal-TBI but not in the eth-TBI samples. Data displayed as average ± SEM. ($^{*} \leq 0.05$, $^{**} \leq 0.01$, $^{***} \leq 0.001$).

significant differences between sal-TBI and eth-TBI persisted at 7 dpi ($p < 0.01$; Fig. 1B).

Thus, any beneficial effect of EtOH intoxication on the neurological outcome of TBI is limited to high-dose administration. We further investigated this dose in an independent cohort of mice which were tested in the Open Field test for the evaluation of spontaneous ambulation and anxiety. As before, the performance of sal-S and eth-S mice was comparable and the two groups were merged (and are displayed as "Sham" in Fig. 1D–F). When the track-length of sham, sal-TBI and eth-TBI were compared, a statistically significant effect of treatment ($F_{(2,25)} = 7.6$, $p = 0.0026$) but not of time point ($F_{(1,25)} = 0.02$, $p = 0.88$) was identified. Post-hoc analysis showed that sal-TBI mice displayed a trend toward reduced track-length at 2 dpi ($p < 0.05$) as well as at 7 dpi ($p < 0.01$) compared to eth-TBI mice whereas eth-TBI was comparable to sham both at 2 and 7 dpi (6.03 ± 1.41 m, 4.62 ± 1.21 m and 6.67 ± 1.2 m at 2 dpi for S, sal-TBI and eth-TBI, respectively; $p > 0.05$; 6.03 ± 1.12 m, 4.21 ± 1.08 m and 7.22 ± 1.11 m at 7 dpi for sham, sal-TBI and eth-TBI, $p < 0.05$ for sal-TBI vs eth-TBI; Fig. 1D). Furthermore, the overall activity fraction (the percentage of time spent in movement) was comparable across treatment groups ($F_{(3,25)} = 0.2$, $p = 0.8$), but a significant effect of time was detected ($F_{(1,25)} = 18.6$, $p = 0.002$; Fig. 1E). When the time spent in the center

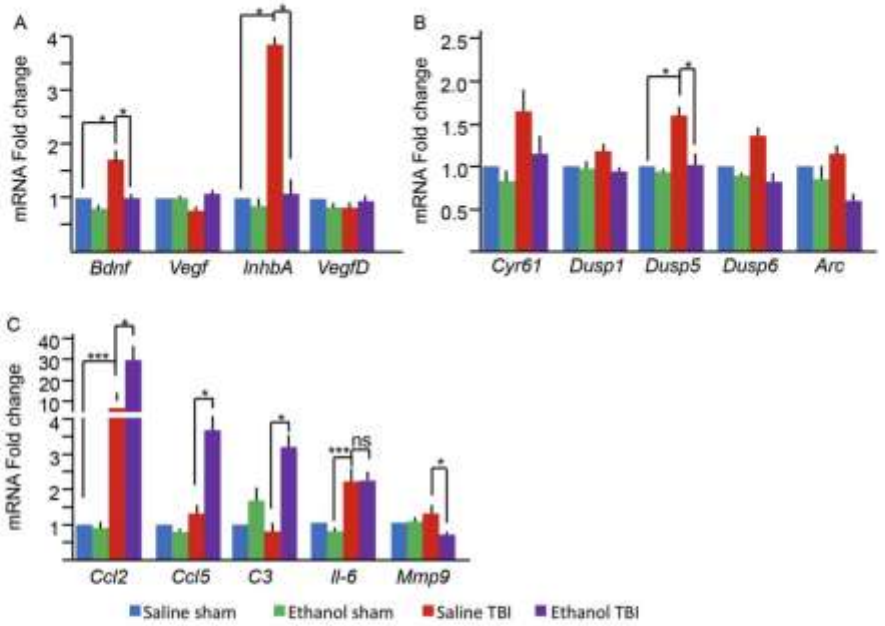

Fig. 3. Activity-dependent effector genes are modulated by ethanol.
A) The activity-dependent genes *Bdnf* and *InhbA* are significantly increased in sal-TBI but repressed by ethanol administration, whereas *Vegf* and *VegfD* are not affected by TBI or ethanol. B) The Erk phosphatase *Dusp5* is significantly upregulated in sal-TBI whereas *Arc*, *Dusp1* and *Dusp6* are not and *Cyr61* displays only a trend toward increased levels. Ethanol pretreatment leads to the downregulation of *Dusp5* induction.
C) TBI causes the marked upregulation of *Ccl2* and *Il6*, but not of *Ccl5*, *C3* or *Mmp9*. In eth-TBI samples, mRNA for *Ccl2*, *Ccl5* and *C3* are increased compared to sal-TBI whereas *Il6* expression is unchanged ($p > 0.05$ vs sal-TBI) and levels of *Mmp9* are actually reduced ($p < 0.05$). Data displayed as average ± SEM. (* ≤ 0.05, ** ≤ 0.01, *** ≤ 0.001).

of the quadrant (a measure of anxiety) was assessed, a significant effect of treatment was found ($F_{(2,21)} = 11.2$, $p = 0.0005$) but not of the timepoint ($F_{(1,21)} = 0.9$, $p = 0.3$). Post-hoc analysis showed that at 2 dpi sal-TBI mice spent significantly less time than sham mice in the central quadrant ($p < 0.001$) whereas eth-TBI were once again comparable to sham mice (60.8 ± 13.3 s, 20.2 ± 4.5 s and 47.0 ± 17.9 s at 2 dpi for sham, sal-TBI and eth-TBI, respectively; $p < 0.05$; Fig. 1F); at 7 dpi, sal-TBI spent significantly less time in the center quadrant than eth-TBI ($p < 0.05$; Fig. 1F). Taken together, these data suggest that EtOH intoxication at the instance of trauma leads to a faster and better behavioral recovery after TBI.

3.1. EtOH reduces a subset of excitation-dependent transcriptional responses induced by moderate TBI

We set out to investigate the effect of EtOH intoxication on the TBI-induced transcriptional profile in hippocampus, focusing on a set of 14 transcription factors genes known to be regulated in an activity-dependent manner (Lösing et al., 2017). Mice were administered either EtOH (5 g/Kg) or saline by oral gavage 30 min before closed moderate TBI (2 cm-weight drop). As control, we employed EtOH or saline treated animals with a sham surgery (sal-S or eth-S). EtOH administration resulted in a blood EtOH level (BAL) of 205.0 ± 105.3 mg/dL in sham-operated and of 375.9 ± 132.2 mg/dL in TBI mice ($p < 0.05$). These values correspond to BAL measured typically measured in TBI patients (Raj et al., 2016). Apnea time was comparable in EtOH-pretreated or saline-pretreated mice (6.8 ± 1.1 s vs 7.1 ± 1.4 s; $p > 0.05$). We sampled hippocampi at 3 h post-injury in order to simulate a clinically-relevant time point of observation. Saline-treated TBI mice displayed a significant upregulation of mRNA encoding for *Atf3* (9.6 ± 7.6 of sal-S, $p < 0.01$; Fig. 2A), *c-Fos* (1.74 ± 0.51 of sal-S, $p < 0.05$; Fig. 2A), *FosB* (5.31 ± 1.96 of sal-S, $p < 0.05$; Fig. 2A), *ΔFosB* (4.63 ± 1.95 of sal-S, $p < 0.05$; Fig. 2B), *Egr1* (1.78 ± 0.31 of sal-S, $p < 0.05$; Fig. 2A), *Egr3* (3.81 ± 1.92 of sal-S, $p < 0.05$; Fig. 2A) but not *Egr2* (1.3 ± 0.4, $p > 0.05$; Fig. 2A). Likewise, levels of mRNA for *Npas4* (2.05 ± 0.23 of sal-S, $p < 0.05$; Fig. 2B), *Gadd45b* (fold change 2.03 ± 0.82 of sal-S, $p < 0.05$) and *Gadd45g* (1.82 ± 0.56 vs sal-S, $p < 0.05$) were upregulated (Fig. 2B), but not those of *Gadd45a* (1.42 ± 0.31 of sal-S, $p > 0.05$; Fig. 2B). On the other hand, the mRNA for the genes *Btg2*, *Dream* and *Creb* were unaffected by TBI (1.33 ± 0.54, 0.87 ± 0.32 and 0.91 ± 0.26 of sal-S, respectively; $p > 0.05$; Fig. 2B).

Next, we wondered to which extent EtOH administration modulates TBI mediated gene induction. EtOH administration per se did not result in a major change in the transcriptional profile of the 15 genes under study. However, in EtOH-pretreated TBI mice (eth-TBI), the induction of *Atf3* and of all genes of the Fos family was significantly reduced (3.2 ± 2.1, 0.99 ± 0.22, 1.88 ± 1.49, 1.75 ± 1.72 of sal-S, for *Atf3*; $p < 0.01$, *c-Fos*, *FosB*, *ΔFosB*, respectively, $p < 0.05$ vs sal-TBI; Fig. 2A). The effect of EtOH was also observed on *Egr1* (1.13 ± 0.19, in eth-TBI vs sal-S, $p < 0.05$ vs sal-TBI), *Egr3* (1.44 ± 1.13 in eth-TBI vs sal-S, $p < 0.05$ vs sal-TBI; Fig. 2A) and *Npas4* (0.73 ± 0.21 in eth-TBI vs sal-S, $p < 0.05$ vs sal-TBI; Fig. 2B). Notably, although not affected by TBI or EtOH alone, *Creb* mRNA levels appeared to be reduced in eth-TBI samples (0.67 ± 0.12 of sal-S; $p < 0.05$; Fig. 2A). On the other hand, induction of *Gadd45b* and *Gadd45g* mRNA was not affected by EtOH pretreatment (1.51 ± 0.39 and 1.84 ± 0.39 of sal-S, respectively; $p > 0.05$ vs sal-TBI; Fig. 1A).

We confirmed the effects observed at mRNA level by evaluating the number of c-Fos$^+$ cells in the CA1 region of immunostained hippocampal sections. There a significant difference across treatment groups ($F_{(2,7)} = 21.2$, $p = 0.001$). Post-hoc analysis (Holm-Sidak) showed that the number of cFos + cells in CA1 was significantly increased 3 h after TBI when compared to sal-S (38.5 ± 0.7 cFos + neurons/10^4 μm^2 vs

20.0 ± 2.4 cFos + neurons/10^4 μm^2, $p < 0.01$; Fig. 2C, D). Whereas administration of EtOH per se decreased slightly the number of c-Fos + cells compared to sal-S (18.5 ± 0.5 cFos + neurons/10^4 μm^2), eth-TBI mice displayed a marked decrease in the number of c-Fos + cells compared to sal-TBI (22.7 ± 2.1 cFos + neurons/10^4 μm^2, $p < 0.01$ vs sal-TBI; Fig. 2C, D). Furthermore, we assessed Egr-1 protein level by Western Blot in whole-hippocampus (at 3 h) protein extract. We confirmed the upregulation of Egr-1 in sal-TBI samples (0.53 ± 0.05 Egr-1/β-tubulin ratio in sal-TBI mice vs 0.09 ± 0.04 and 0.11 ± 0.05 in sal-S and eth-S, respectively; Fig. 2E, F), which was significantly decreased by EtOH pretreatment (0.16 ± 0.05 Egr-1/β-tubulin ratio; Fig. 2E, F) in accordance with data observed for c-Fos on protein level.

As acute secondary damage has been reported to spread in neuronal networks (Hinzman et al., 2016), we analyzed the expression of a subset of IEGs in the contralateral hippocampus. The transcriptional response in the contralateral hippocampus, coherent with the distance from the impact site, showed similarities, but the increase of mRNA levels were significantly blunted compared with ipsilateral one. Only *FosB* (3.4 ± 2.7 of sal-S, $p < 0.05$; Supplementary Fig. 1A) and *Gadd45g* (1.7 ± 0.3 of sal-S, $p < 0.05$; Supplementary Fig. 1A) mRNA levels were upregulated compared to sal-S. In agreement with the effect observed in the ipsilateral hippocampus, in the contralateral hippocampus, too, EtOH pretreatment resulted in the significant decrease in *Fos8* (1.6 ± 1.3 of sal-S, $p < 0.05$ vs sal-TBI; Supplementary Fig. 1A) but not of *Gadd45g* (1.8 ± 0.5 of sal-S, $p > 0.05$ vs sal-TBI; Supplementary Fig. 1A).

In summary, EtOH administration interferes with TBI associated induction of a large set of activity-dependent genes.

3.2. EtOH pretreatment extensively affect TBI-associated transcriptional response

We further extended the analysis of the impact of EtOH pretreatment to TBI-induced transcriptional responses considering a set of effector genes regulated by activity-dependent transcription factors (Lösing et al., 2017). These genes encode for proteins involved in the regulation of neuronal survival and structural integrity (*Bdnf*, *Vegf*, *InhibinA*, *VegfD;* Mauceri et al., 2011; Zhang et al., 2009), signaling (*Arc*, *Cyr61*, Dual Specificity Phosphatase [*Dusp*] 1, *Dusp5* and *Dusp6*, which inhibit MAP kinase signaling by dephosphorylating ERK; Lösing et al., 2017) and neuroinflammation (*Ccl2*, *Ccl5*, Complement *C3* factor, *Il-6* and *Mmp9*).

Whereas *Vegf* and *VegfD* were not induced by TBI (0.63 ± 0.31 and 0.87 ± 0.07, respectively, fold change vs sal-S, $p > 0.05$) *Bdnf* and *InhbA* were significantly increased (1.75 ± 0.45 and 3.81 ± 0.96 of sal-S, $p < 0.05$; Fig. 3A). These data are consistent with previous data showing that increased neuronal activity does not increase *VegfD* levels while triggering expression of *Bdnf* and *InhbA* (Mauceri et al., 2011; Zhang et al., 2009). The TBI-induced upregulation of *Bdnf* and *InhbA* was markedly decreased by EtOH pretreatment (1.07 ± 0.54 and 1.11 ± 0.70, $p < 0.05$ vs sal-TBI; Fig. 3A).

Notably, mRNA levels of *Dusp5* were significantly upregulated (1.61 ± 0.33 of sal-S, $p < 0.05$; Figure2B) whereas those of *Arc*, *Dusp1*, *Dusp6* and *Cyr61* were not or only mildly induced by TBI (1.22 ± 0.20, 1.25 ± 0.13, 1.33 ± 0.39 and 1.72 ± 0.61 of sal-S, respectively, $p > 0.05$). EtOH pretreatment led to the significant downregulation of *Dusp5* induction (1.04 ± 0.27 of sal sham in eth-TBI samples; $p < 0.05$ vs sal-TBI; Fig. 3B) and showed a trend toward decreasing also *Dusp1*, *Dusp6* and *Cyr61*.

Next, we considered chemokines and neuroinflammatory molecules and other activity-dependent transcription factors. This included for instance Ccl chemokine family members such as *Ccl2* known to be repressed by ATF3 (Gey et al., 2016). TBI caused strong upregulation of *Ccl2* (9.71 ± 8.35 of sal-S, $p < 0.001$; Fig. 3C) and *Il6* (2.21 ± 0.10 of sal-S, $p < 0.001$; Fig. 3C), but only weakly, at this time point, of *Ccl5* (1.34 ± 0.20 of sal-S, $p > 0.05$; Fig. 3C), or *Mmp9* (1.26 ± 0.10 of sal-S, $p > 0.05$; Fig. 3C). On the contrary, *C3* showed only a trend toward being downregulated in sal-TBI samples (0.73 ± 0.06 of sal-S, $p > 0.05$; Fig. 3C). In eth-TBI samples, levels of mRNA for *Ccl2*, *Ccl5* and *C3* were actually increased compared to sal-TBI or sham (29.14 ± 13.88, 3.73 ± 0.88, 3.01 ± 1.00 of sal-S, respectively; $p < 0.05$, Fig. 3C). On the other hand, *Il6* induction was unaffected by EtOH (2.25 ± 0.59 of sal-S, $p > 0.05$ vs sal-TBI; Fig. 3C) and levels of *Mmp9* (0.73 ± 0.03 of sal-S, $p < 0.05$; Fig. 3C) were actually decreased by EtOH.

Taken together, these data confirm the specific effect of EtOH in preventing TBI-induced upregulation of a distinct set of activity-regulated effector genes.

3.3. EtOH pretreatment has a prolonged impact on hippocampal activity pattern and prevents hippocampal cell loss

In order to verify if the observed effects of EtOH on the trauma-induced gene induction pattern were long-term and corresponded to consequences on the integrity of hippocampal function, we measured the density of neurons in CA1 and in dentate gyrus (DG) at 7 days post injury in sal-S and eth-S mice and in sal-TBI and eth-TBI mice. For this, we assessed numbers of NeuN$^+$ and c-Fos$^+$ neurons in these areas (Fig. 4).

Notably, the moderate closed TBI protocol resulted in a small, albeit statistically significant, loss of neurons specifically in DG ($F_{(2,52)} = 10.4$, $p = 0.0002$; post-hoc: 107.5 ± 12.5 NeuN$^+$/10^4 μm^2 in sal-TBI vs 127.5 ± 16.3 NeuN$^+$/10^4 μm^2 in sal-S; $p < 0.01$; Fig. 4A,B), but not in CA1 ($F_{(2,53)} = 0.1$, $p = 0.8$; post-hoc: 68.9 ± 3.9 NeuN$^+$/10^4 μm^2 in sal-TBI vs 70.2 ± 8.4 NeuN$^+$/10^4 μm^2 in sal-S; $p > 0.05$; Fig. 4D,E). EtOH pretreatment, which impinged on the TBI-induced transcriptional program (see Figs. 1, 2 and 3), resulted in normal neuronal counts in the DG after TBI (128.3 ± 21.1 NeuN$^+$/10^4 μm^2 in eth-TBI vs 127.5 ± 16.3 NeuN$^+$/10^4 μm^2 in sal-S, $p > 0.05$; Fig. 4A, B).

The number of c-Fos$^+$ neurons in mice subjected to TBI 7 days before was significantly different across treatment groups both in DG and CA1 ($F_{(2,31)} = 13.7$, $p < 0.0001$; $F_{(2,41)} = 175.5$, $p < 0.0001$). Post-hoc analysis revealed higher numbers of c-Fos$^+$ cells both in DG (52.4 ± 3.2 c-Fos$^+$/10^4 μm^2; $p < 0.01$ Fig. 4A, C) and CA1 (61.2 ± 4.4 c-fos$^+$/10^4 μm^2; $p < 0.01$; Fig. 4D,F) of sal-TBI compared to sal-S (27.22 ± 0.31 c-fos$^+$/10^4 μm^2 and 22.7 ± 3.4 c-fos$^+$/10^4 μm^2, respectively; Fig. 4C,F) mice. No difference was found at 7 dpi in sal-S or eth-S mice. Acute EtOH administration before TBI, however, resulted in reduced numbers of c-Fos$^+$ neurons at 7 dpi both in DG (37.4 ± 4.5 c-fos$^+$/10^4 μm^2, $p < 0.05$ vs sal-TBI; Fig. 4A, C) and CA1 (24.5 ± 1.4 c-fos$^+$/10^4 μm^2, $p < 0.05$ vs sal-TBI; Fig. 4D, F).

Thus, EtOH pretreatment reduced long term consequences of TBI such neuronal cell loss and induction of TFs associated with propagation of neuronal activity.

3.4. Administration of EtOH after TBI has a limited effect on the TBI-activated transcriptional program

We have demonstrated that EtOH pre-administration is able to downregulate a large gene set of the TBI-induced transcriptional program. In order to exploit this effect for therapeutic purposes, however, EtOH should prove effective when administered after the occurrence of the trauma. Therefore, we compared the gene induction (at the 3 h timepoint) in the hippocampus of mice treated with the same dose of EtOH (5 g/kg) either 30 min before (pre-eth-TBI) or 20 min after TBI (post-eth-TBI).

For control, we administered saline either 30 min before or 20 min after TBI. Since these two groups displayed the same effect across all genes tested, they were grouped for analysis. Strikingly, the different timings (pre- or post-TBI) of EtOH delivery differentially affected gene transcription. The TBI-induced upregulation of *Atf3*, *Egr3*, *FosB* and

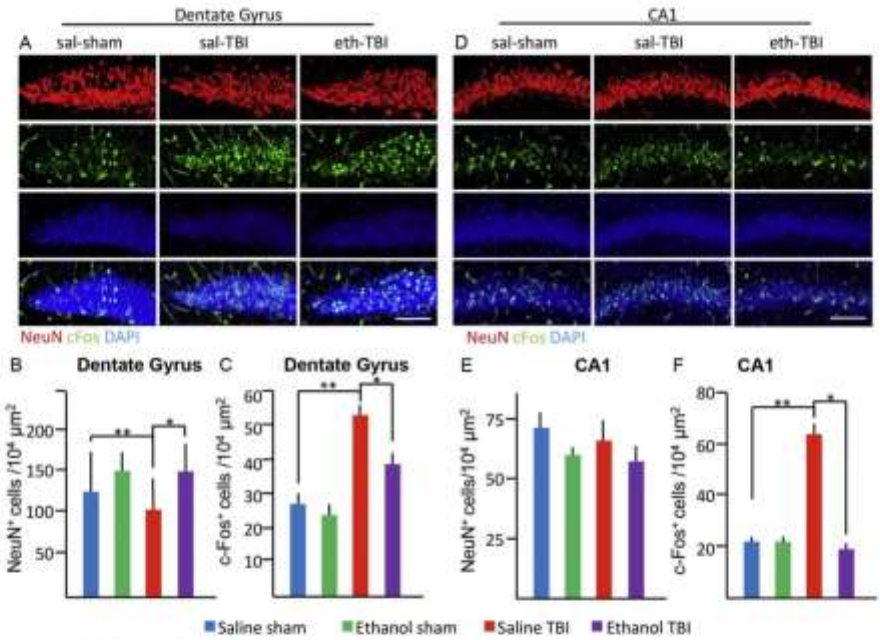

Fig. 4. Ethanol pretreatment abolishes the loss of DG neurons and the chronic upregulation of c-Fos at 7 dpi.
A,B) TBI results in a small but statistically significant reduced neuronal density in DG which is prevented by ethanol pretreatment.
A,C) The number of c-Fos$^+$ neurons is significantly higher in the DG in sal-TBI than in sham but it is reduced by ethanol pretreatment.
D,E) TBI does not affect the density of NeuN$^+$ in CA1.
D,F) Density of c-fos$^+$ cells is increased in the CA1 of sal-TBI mice compared to sal-sham but this effect is reversed by ethanol pretreatment. Scalebar 50 µm. (* ≤ 0.05, ** ≤ 0.01, *** ≤ 0.001).

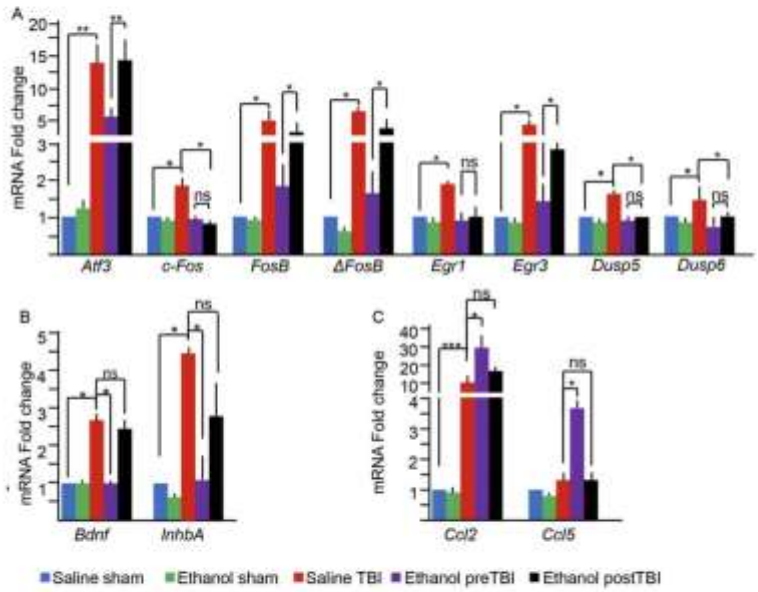

Fig. 5. Ethanol administration after TBI largely ineffective on TBI-induced transcriptional changes.
A) Administration of ethanol 20 min after TBI no longer decreased the induction of *Atf3*, *Egr3*, *FosB* and *ΔFosB* ($p > 0.05$ vs pre-eth-TBI) whereas the induction of *Egr1*, *c-Fos*, *Dusp5* and *Dusp6* were still markedly decreased
B, C) Induction of effector genes *Bdnf*, *InhbA* (B) and *Ccl2*, *Ccl5* (C) were no longer affected by ethanol when administered after TBI. (* ≤ 0.05, ** ≤ 0.01, *** ≤ 0.001).

ΔFosB was no longer decreased by EtOH when administered after TBI (*Atf3*: 14.50 ± 7.81 in post-eth-TBI vs 13.83 ± 8.59 in sal-TBI, $p > 0.05$; *FosB*: 3.37 ± 0.85 vs 5.07 ± 1.96, $p > 0.05$; *ΔFosB* 3.93 ± 0.56 vs 6.33 ± 3.12, $p > 0.05$; *Egr3*: 2.90 ± 0.65 vs 4.49 ± 1.09, $p > 0.05$; Fig. 5A). In contrast, the induction of *c-Fos*, *Dusp5* and *Dusp6* was strongly reduced (*c-Fos*: 0.86 ± 0.20 vs 1.86 ± 0.54, $p < 0.05$; *Dusp5* 1.07 ± 0.20 vs 1.67 ± 0.39, $p < 0.05$; *Dusp6* 0.99 ± 0.20 vs 1.33 ± 0.39; $p < 0.05$; Fig. 5A).

Thus, a subset of genes was still downregulated when EtOH was administered after TBI, whereas a distinct subset became insensitive to EtOH administration. We then examined if the induction of *Bdnf* and *InhbA* was EtOH-dependent or -independent. We found both genes to be no longer affected by EtOH when this is administered after TBI (*Bdnf*: 2.49 ± 0.50 vs 2.62 ± 0.57, $p > 0.05$; *InhbA*: 2.94 ± 0.53 vs 4.40 ± 2.19, $p > 0.05$; Fig. 5B). Likewise, the upregulation of *Ccl2* and *Ccl5* observed in eth-TBI vs sal-TBI samples is no longer detected when EtOH is administered after the TBI (14.3 ± 3.5 and 1.21 ± 0.32 of sal-S, respectively; $p > 0.05$ vs sal-TBI; Fig. 5C).

3.5. EtOH fails to downregulate the transcriptional responses in severe TBI

The effect of EtOH on TBI prognosis may be dependent on the severity of the trauma itself. Therefore, we compared the effect of EtOH on the transcriptional response in a moderate TBI (see Fig. 2 above) to a severe trauma. In case of severe trauma, a 3 cm weight-drop blunt TBI, corresponding to an increase in kinetic energy of 33.3 mJ (66.6 mJ in the 2-cm model vs 99.9 mJ in the 3-cm model) was employed. Overall survival was lower in severe TBI than in moderate TBI (4/6 [67%] in severe sal-TBI, 4/5 [80%] in severe eth-TBI).

The transcriptional pattern was comparable in the severe sal-TBI and in the moderate sal-TBI: severe sal-TBI resulted in the marked elevation of mRNA levels of *Atf3* (13.6 ± 12.1 of sal-Sham, $p < 0.05$; Fig. 6A), *c-Fos* (2.8 ± 1.5 of sal-S, $p < 0.05$), *FosB* (10.4 ± 5.2of sal-S, $p < 0.05$; Fig. 6A), *Gadd45b* (2.5 ± 1.2 of sal-S, $p < 0.05$; Fig. 6A) and *Gadd45g* (2.0 ± 0.6 of sal-S, $p < 0.05$; Fig. 6A). When compared to the moderate sal-TBI, the upregulation of IEG in severe-TBI was statistically significant only for *FosB* ($p = 0.04$) although a trend toward higher levels of expression was detected for *c-Fos and for Atf3* (both $p = 0.1$).

On the contralateral hippocampus, we observed a slight elevation of *Atf3*, *FosB* and *Gadd45g* (2.6 ± 1.6, 3.4 ± 2.7 and 1.7 ± 0.4 of sal-S, respectively, $p < 0.05$; Fig. 1B) whereas mRNA abundance of all other IEGs was not induced. When compared to contralateral moderate-TBI IEG pattern, a significant elevation of *Atf3* was detected ($p = 0.03$), whereas no difference was found in the other IEG (including, for example, *c-Fos*, *FosB* and *Gadd45b*).

Interestingly, now the same dose of EtOH that significantly reduced IEG induction in moderate TBI (Fig. 1A) was completely ineffective in severe TBI. In fact, now levels of *Atf3* (17.5 ± 12.5), *c-Fos* (2.6 ± 1.2), *FosB* (9.2 ± 7.6) but also *Gadd45b* and *Gadd45g* were comparable in sal-TBI and eth-TBI (Fig. 6A). Likewise, EtOH pretreatment did neither prevent *Atf3* and *FosB* induction in the contralateral hippocampus (Supplementary Fig. 2) nor modulate *Bdnf* and *InhbA* expression (Fig. 6B). Thus, EtOH's potential to modulate TBI associated gene expression appears to be only effective within a certain TBI intensity range and is blunted once TBI severity is too high.

4. Discussion

Our data suggest that EtOH intoxication may have protective effects in TBI at behavioral and histological level. Furthermore, these effects are correlated with a distinct TBI associated modulation of an early transcriptional response connected to propagation of neuronal activity. We narrowed down the impact of ethanol on modulating TBI inflicted processes and demonstrated the importance of pre-TBI alcohol administration and to moderate, but not to severe TBI.

Our data suggest that EtOH intoxication at the time shortly before trauma is potentially protective, although this effect is restricted to a high-dose of EtOH. The protective effect appears already at the earliest time points assessed, suggesting that the main effect is on dampening acute pathogenic pathways which contribute to the onset of neurological deficits and set the stage for pathogenic evolution over the next few hours or days. These findings are in agreement with clinical studies suggesting a possible beneficial interaction (Salim et al., 2009; Berry et al., 2011; Brennan et al., 2015) and with some (Janis et al., 1998; Kelly et al., 1997) but not all (Vaagenes et al., 2015) experimental data. While the effect in clinical cohorts may have been relatively small because of the large variability of clinical presentations of TBI (e.g., contusive vs concussive, with or without bone fracture), experimental conditions such as species differences (rat vs mice) and different models of TBI (open vs blunt) may affect EtOH action by modifying its own kinetics and the pathogenic events unfolding (e.g., the presence of

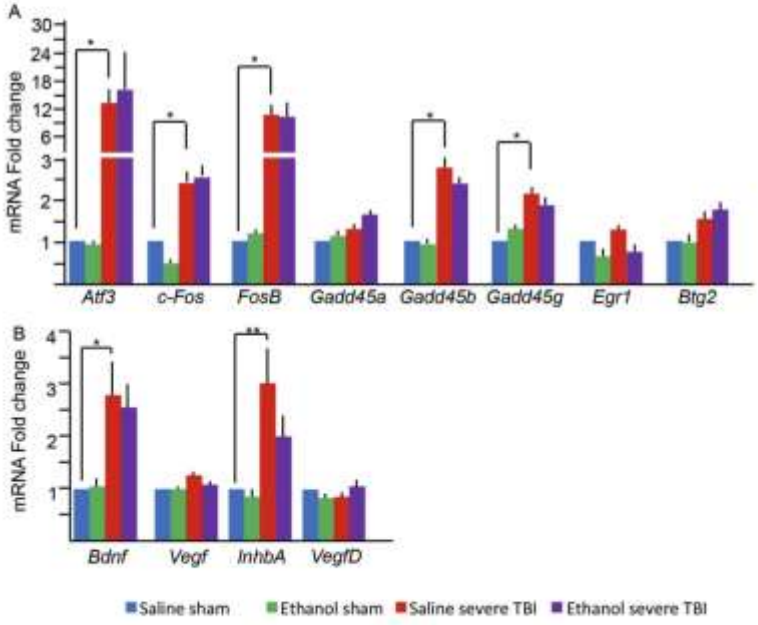

Fig. 6. Ethanol failed to decrease the transcriptional responses to severe TBI.
A) Severe sal-TBI resulted in the marked upregulation of *Atf3*, *c-Fos*, *FosB*, *Gadd45b* and *Gadd45g*. The transcriptional response of *Atf3*, *c-Fos* and *FosB* were not affected by ethanol administration (at the same dose administered in the moderate TBI model).
B) Severe sal-TBI causes the upregulation of *Bdnf* and *InhbA*. However, this response was not modulated by ethanol pretreatment. (* ≤ 0.05, ** ≤ 0.01, *** ≤ 0.001).

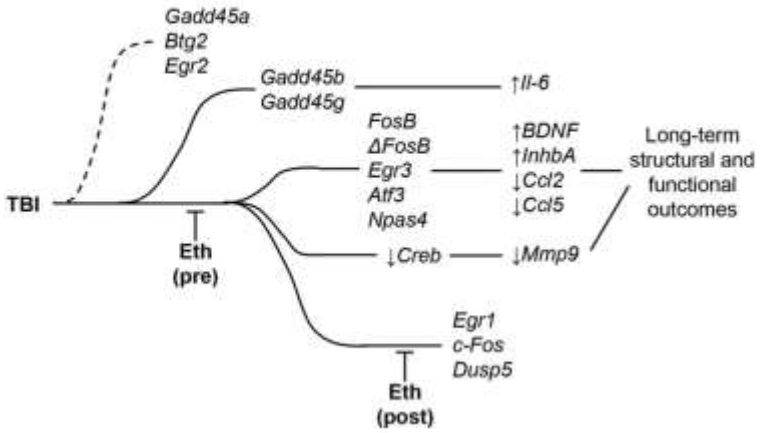

Fig. 7. Effect of ethanol on TBI-induced transcriptional response was dependent on the subset of genes and on the time of administration. Pre-administration of ethanol successfully downregulated a large set of transcriptional responses and led to enhanced structural and functional integrity of hippocampus at 7 dpi.

macroscopic hematomas; Chandrasekar et al., 2017). Despite some intrinsic experimental restrictions required by ethical reasons (pre-administration of opioids, binge administration *vs* self-administration), the beneficial effect of EtOH, observed in clinical and experimental conditions, provides an entry point to the understanding of acute cascades in TBI.

The early transcriptional response to TBI is not only the direct consequence of signaling cascades (Wang et al., 2014) but also a staging event of the processes unfolding in the following hours or days (Samal et al., 2015). To this respect, the interaction of TBI and EtOH reveals a hierarchy of gene induction characterized by sensitivity to TBI, and to EtOH sensitivity and schedule of administration (Fig. 7). When evaluated at 3 h, a set of genes (*Gadd45a, Srf, Btg2, Egr2)* are not modified by TBI at all and are not affected by EtOH, implying that this set is not involved in pathogenic events explored here. On the other hand, the epigenetic regulators *Gadd45b* and *Gadd45g* were upregulated by TBI but were insensitive to EtOH. Whereas, the latter may be due to the redundant pathways triggering *Gadd45b* and *Gadd45g* expression (neuronal depolarization, BDNF, TGF-β; Grassi et al., 2017), their persistent activation may be relevant not only to direct neuroprotective effects (related to large scale control of activity-regulated transcription, Grassi et al., 2017) but also to the regulation of the neuroinflammatory cascade. In fact, their gene target *Il6* (Kigar et al., 2015; Shin et al., 2012) is unaffected by EtOH. It remains to be understood if the persistent upregulation of *Gadd45b* and *Gadd45g and Il-6* is a necessary prerequisite for EtOH effects.

The largest group of IEGs is activated by TBI and markedly, although in some cases not completely, downregulated by EtOH pre-administration. EtOH reduces (although to variable extent, cfr. *Atf-3* and *Egr-3*) the transcription of *c-Fos, FosB, ΔFosB, Egr3, Atf3, Npas4*, which are known to depend on excitation-activated Erk signaling cascade (Wang et al., 2014; Flavell and Greenberg, 2008). Many IEGs investigated in this study are well-established surrogates to label neuronally and synaptically activated neurons (Flavell and Greenberg, 2008). Thus, it is conceivable that EtOH administration pre-TBI interferes with a signaling cascade triggered by neuronal excitation and leading to transcriptional regulation. EtOH is recognized to be either a potentiator of GABAR currents (Hanchar et al., 2005; Kumar et al., 2009; Botta et al., 2014) or an antagonist of NMDAR (Criswell et al., 2004; He et al., 2013), and therefore exerts an overall suppressive action on neuronal excitation. Thus, it is likely that EtOH directly impinges on propagation of neuronal activity inducing signaling cascades at the neurotransmitter receptor level. Subsequently, activity of downstream signaling effectors including MAP kinases known to activate IEGs might be inhibited.

Despite the fact that IEGs are classically correlated with proliferation and neuroprotection (Zhang et al., 2002; Flavell and Greenberg, 2008), their functional targets and the involvement in regulating neuronal cellular biology is only partially understood. In fact, both protective and detrimental effects have been associated with IEG induction: reduced IEG induction is associated with preservation of neuronal integrity in epilepsy models (Lösing et al., 2017) and in the retina (Oshitari et al., 2002). Thus, ethanol-induced downregulation of IEG may contribute directly to the observed ethanol-related neuroprotection.

Although the transcriptional programs regulated by activity-induced transcription factors are broad (Samal et al., 2015), we have shown that several effector genes are effectively downregulated by ethanol pretreatment. In particular, *Bdnf* transcription is strongly reduced by ethanol (Fig. 3), and excess BDNF has been linked to excitotoxic cell death in trauma (Gill et al., 2013). Furthermore, ethanol pretreatment prevents the elevation of the *Dusp* mRNA levels, which are involved in the homeostatic shut-down of Erk signaling. In fact, once their transcription is induced by the Erk signaling pathway, the accumulation of the Dusp phosphatases results in the dephosphorylation of Erk itself (Kidger et al., 2017). The induction of *Dusp5* and *Dusp6* remains sensitive to EtOH even when administered after TBI, suggesting that the feedback loop on Erk signaling may remain sensitive to the intervention delivered after TBI. Notably, persistent shut-down of Erk signaling has been reported after TBI (Atkins et al., 2009), since activity-dependent neuroprotection may contribute to the survival of neurons after TBI (Ikonomidou et al., 2000). Prevention of DUSP accumulation may further contribute to ethanol-induced neuroprotection after trauma.

Finally, ethanol decreased the TBI-induced elevation of *Atf3*. Atf3 plays multiple roles in neuroprotection and neuroregeneration (Gey et al., 2016) but it has been shown to downregulate injury-induced neuroinflammation (Wang et al., 2012). In fact, ethanol administration resulted in the actual elevation of chemokines (e.g. Ccl2) which are normally repressed by ATF3 (Gey et al., 2016). The interaction of ethanol with TBI are complex and rather than suppressing inflammation, ethanol appears to polarize the neuroinflammatory response toward a pro-survival phenotype (Chandrasekar et al., 2017; Goodman et al., 2013; Wang et al., 2013), although this may not happen in every model (Teng et al., 2015; Katada et al., 2009).

Notably, only a smaller subset of the IEGs (*Egr1, c-Fos*) remained sensitive to EtOH administered after the trauma, suggesting that the majority of the transcriptional responses are activated in a very narrow time-window at the instance of trauma and EtOH must be present at that moment to impact them significantly. In line with this, NMDAR are

activated in a time-restricted manner after trauma (Biegon et al., 2004) similar to our findings on EtOH administration. Furthermore, similar to our data on EtOH, NMDA receptor blockers convey neuroprotective effects only if administered in a narrow time window while application at later stages were detrimental (Ikonomidou et al., 2000).

As a limitation of the present study, it must be stressed that, despite the careful match in the dose of ethanol administered to eth-S and eth-TBI mice, the BAL measured at 3 h were significantly higher in the latter than in the former. We hypothesize that a significant slow-down of ethanol metabolism may take place in mice undergoing TBI. In fact, TBI per se can affect visceral blood flow (Yuan et al., 1990) and liver metabolic enzymes expression (Ma et al., 2017). The details of the pharmacokinetic of ethanol under TBI conditions are therefore worth to be further investigated.

In conclusion, our data show that when EtOH intoxication is present at the moment right before trauma, it significantly decreases the trauma-induced transcriptional responses of hippocampal neurons. However, the buffering capacity of EtOH may be limited in parametric space of insult severity and timing of administration, limiting its translational potential.

Supplementary data to this article can be found online at https://doi.org/10.1016/j.expneurol.2017.12.017.

Acknowledgement

The work by FR and BK has been supported by the Deutsche Forschungs Gemeinschaft (DFG) as part of the Collaborative Research Center 1149 "Danger Response, Disturbance Factors and Regenerative Potential after Acute Trauma". FR is also supported by the ERANET-NEURON initiative "External Insults to the Nervous System" as part of the MICRONET consortium and by the Baustein Program of Ulm University. BK is supported by an Ulm University-Bundeswehr Krankenhaus Ulm research initiative. The work performed by DM is supported by DFG grants SFB1158 and FOR2325. DM is a member of the Excellence Cluster *CellNetworks* at Heidelberg University.

References

Ahlgren, H., Bas-Orth, C., Freitag, H.E., Hellwig, A., Ottersen, O.P., Bading, H., 2014 Apr 4. The nuclear calcium signaling target, activating transcription factor 3 (ATF3), protects against dendrotoxicity and facilitates the recovery of synaptic transmission after an excitotoxic insult. J. Biol. Chem. 289 (14), 9970–9982.

Aitken, C.M., Palu, M.C., Alonso OF, Bramlett, H.M., Dietrich, W.D., 2009 Aug 7. Deficits in ERK and CREB activation in the hippocampus after traumatic brain injury. Neurosci. Lett. 459 (2), 52–56.

Berry, C., Ley, E.J., Margulies, D.R., Mirocha, J., Bukur, M., Malinoski, D., Salim, A., 2011 Oct. Correlating the blood alcohol concentration with outcome after traumatic brain injury: too much is not a bad thing. Am. Surg. 77 (10), 1416–1419.

Biegon, A., Fry, P.A., Paden, C.M., Alexandrovich, A., Tsenter, J., Shohami, E., 2004 Apr 6. Dynamic changes in N-methyl-D-aspartate receptors after closed head injury in mice: implications for treatment of neurological and cognitive deficits. Proc. Natl. Acad. Sci. U. S. A. 101 (14), 5117–5122.

Botta, P., Zucca, A., Valenzuela, C.F., 2014 Feb 6. Acute ethanol exposure inhibits silencing of cerebellar Golgi cell firing induced by granule cell axon input. Front. Integr. Neurosci. 8, 10.

Brennan, J.H., Bernard, S., Cameron, P.A., Rosenfeld, J.V., Mitra, B., 2015 Sep. Ethanol and isolated traumatic brain injury. J. Clin. Neurosci. 22 (9), 1375–1381.

Chamoun, R., Suki, D., Gopinath, S.P., Goodman, J.C., Robertson, C., 2010 Sep. Role of extracellular glutamate measured by cerebral microdialysis in severe traumatic brain injury. J. Neurosurg. 113 (3), 564–570.

Chandrasekar, A., Heuvel, F.O., Palmer, A., Linkus, B., Ludolph, A.C., Boeckers, T.M., Relja, B., Huber-Lang, M., Roselli, F., 2017 Oct. Acute ethanol administration results in a protective cytokine and neuroinflammatory profile in traumatic brain injury. Int. Immunopharmacol. 51, 66–75.

Cho, J.S., Shin, S.D., Lee, E.J., Song, K.J., Noh, H., Kim, Y.J., Lee, S.C., Park, J.O., Kim, S.C., Hwang, S.S., 2016 Jun. Alcohol intake and reduced mortality in patients with traumatic brain injury. Alcohol. Clin. Exp. Res. 40 (6), 1290–1294.

Corbett, B.F., You, J.C., Zhang, X., Pyfer, M.S., Tosi, U., Iascone, D.M., Petrof, I., Hazra, A., Chi, Fu, Stephens, G.S., Ashok, A.A., Aschmies, S., Zhao, L., Nestler, E.J., Chin, J., 2017 Jul 11. ΔFosB regulates gene expression and cognitive dysfunction in a mouse model of Alzheimer's disease. Cell Rep. 20 (2), 344–355.

Criswell, H.E., Ming, Z., Griffith, B.L., Breese, G.R., 2003 Jun. Comparison of effect of ethanol on N-methyl-D-aspartate- and GABA-gated currents from acutely dissociated neurons: absence of regional differences in sensitivity to ethanol. J. Pharmacol. Exp. Ther. 304 (1), 192–199.

Criswell, H.E., Ming, Z., Pleasant, N., Griffith, B.L., Mueller, R.A., Breese, G.R., 2004 Jul 23. Macrokinetic analysis of blockade of NMDA-gated currents by substituted alcohols, alkanes and ethers. Brain Res. 1015 (1–2), 107–113.

Cummings, P., Rivara, F.P., Olson, C.M., Smith, K.M., 2006 Jun. Changes in traffic crash mortality rates attributed to use of alcohol, or lack of a seat belt, air bag, motorcycle helmet, or bicycle helmet, United States, 1982–2001. Inj. Prev. 12 (3), 148–154.

Czigner, A., Mihály, A., Farkas, O., Büki, A., Krisztin-Péva, B., Dobó, E., Barzó, P., 2004 Aug. Dynamics and regional distribution of c-fos protein expression in rat brain after a closed head injury. Int. J. Mol. Med. 14 (2), 247–252.

Dunnett, C.R., McGuire, J.L., DePasquale, E.A., Gardner, A.E., Floyd, C.L., McCullumsmith, R.E., 2017 Jan 15. Glutamate neurotransmission in rodent models of traumatic brain injury. J. Neurotrauma 34 (2), 263–272.

Dutcher, S.A., Underwood, B.D., Walker, P.B., Diaz, F.G., Michael, D.B., 1999 Apr. Patterns of immediate early gene mRNA expression following rodent and human traumatic brain injury. Neurol. Res. 21 (3), 234–242.

Flavell, S.W., Greenberg, M.E., 2008. Signaling mechanisms linking neuronal activity to gene expression and plasticity of the nervous system. Annu. Rev. Neurosci. 31, 563–590.

Flierl, M.A., Stahel, P.F., Beauchamp, K.M., Morgan, S.J., Smith, W.R., Shohami, E., 2009. Mouse closed head injury model induced by a weight-drop device. Nat. Protoc. 4 (9), 1328–1337.

Folkersma, H., Foster Dingley, J.C., van Berckel, B.N., Rozemuller, A., Boellaard, R., Huisman, M.C., Lammertsma, A.A., Vandertop, W.P., Molthoff, C.F., 2011 Jan 14. Increased cerebral (R)-[(11) C]PK11195 uptake and glutamate release in a rat model of traumatic brain injury: a longitudinal pilot study. J. Neuroinflammation 8, 67.

Gey, M., Wanner, R., Schilling, C., Pedro, M.T., Sinske, D., Knöll, B., 2016 Aug. Atf3 mutant mice show reduced axon regeneration and impaired regeneration-associated gene induction after peripheral nerve injury. Open Biol. 6 (8).

Gill, R., Chang, P.K., Prenosil, G.A., Deane, E.C., McKinney, R.A., 2013 Dec. Blocking brain-derived neurotrophic factor inhibits injury-induced hyperexcitability of hippocampal CA3 neurons. Eur. J. Neurosci. 38 (11), 3554–3566.

Giza, C.C., Prins, M.L., Hovda, D.A., Herschman, H.R., Feldman, J.D., 2002 Apr. Genes preferentially induced by depolarization after concussive brain injury: effects of age and injury severity. J. Neurotrauma 19 (4), 387–402.

Goodman, M.D., Makley, A.T., Campion, E.M., Friend, L.A., Lentsch, A.B., Pritts, T.A., 2013 Oct. Preinjury alcohol exposure attenuates the neuroinflammatory response to traumatic brain injury. J. Surg. Res. 184 (2), 1053–1058.

Grassi, D., Franz, H., Verzali, R., Bovio, P., Heidrich, S., Dehghanian, F., Lagunas, N., Belzung, C., Krieglstein, K., Vogel, T., 2017 Apr. Neuronal activity, TGFβ-signaling and unpredictable chronic stress modulate transcription of Gadd45 family members and DNA methylation in the hippocampus. Cereb. Cortex 21, 1–16.

Hanchar, H.J., Dodson, P.D., Olsen, R.W., Otis, T.S., Wallner, M., 2005 Mar. Alcohol-induced motor impairment caused by increased extrasynaptic GABA(A) receptor activity. Nat. Neurosci. 8 (3), 339–345.

Hardingham, G.E., Bading, H., 2010 Oct. Synaptic versus extrasynaptic NMDA receptor signalling: implications for neurodegenerative disorders. Nat. Rev. Neurosci. 11 (10), 682–696.

He, Q., Titley, H., Grasselli, G., Piochon, C., Hansel, C., 2013 Mar. Ethanol affects NMDA receptor signaling at climbing fiber-Purkinje cell synapses in mice and impairs cerebellar LTD. J. Neurophysiol. 109 (5), 1333–1342. http://dx.doi.org/10.1152/jn.00350.2012. **(Epub 2012 Dec 5. PubMed PMID: 23221414; PubMed Central PMCID: PMC36028301).**

Hinzman, J.M., Wilson, J.A., Mazzeo, A.T., Bullock, M.R., Hartings, J.A., 2016 Oct 1. Excitotoxicity and metabolic crisis are associated with spreading depolarizations in severe traumatic brain injury patients. J. Neurotrauma 33 (19), 1775–1783.

Honkaniemi, J., Sharp, F.R., 1999 Jun. Prolonged expression of zinc finger immediate-early gene mRNAs and decreased protein synthesis following kainic acid induced seizures. Eur. J. Neurosci. 11 (1), 10–17.

Hu, B., Liu, C., Bramlett, H., Sick, T.J., Alonso OF, Chen, S., Dietrich, W.D., 2004 Aug. Changes in trkB-ERK1/2-CREB/Elk-1 pathways in hippocampal mossy fiber organization after traumatic brain injury. J. Cereb. Blood Flow Metab. 24 (8), 934–943.

Ikonomidou, C., Stefovska, V., Turski, L., 2000 Nov 7. Neuronal death enhanced by N-methyl-D-aspartate antagonists. Proc. Natl. Acad. Sci. U. S. A. 97 (23), 12885–12890.

Janis, L.S., Hoane, M.R., Conde, D., Falop, Z., Stein, D.G., 1998 Feb. Acute ethanol administration reduces the cognitive deficits associated with traumatic brain injury in rats. J. Neurotrauma 15 (2), 105–115.

Joseph, B., Khalil, M., Pandit, V., Kulvatunyou, N., Zangbar, B., O'Keeffe, T., Asif, A., Tang, A., Green, D.J., Gries, L., Friese, R.S., Rhee, P., 2015 Feb. Adverse effects of admission blood alcohol on long-term cognitive function in patients with traumatic brain injury. J. Trauma Acute Care Surg. 78 (2), 403–408.

Karelina, K., Gaier, K.R., Prabhu, M., Wenger, V., Corrigan, T.E., Weil, Z.M., 2017 Feb. Binge ethanol in adulthood exacerbates negative outcomes following juvenile traumatic brain injury. Brain Behav. Immun. 60, 304–311.

Katada, R., Nishitani, Y., Hosmou, O., Okazaki, S., Houkin, K., Matsumoto, H., 2009 Nov. Prior ethanol injection promotes brain edema after traumatic brain injury. J. Neurotrauma 26 (11), 2015–2025.

Kelly, D.F., Lee, S.M., Pinanoeg, P.A., Hovda, D.A., 1997 May. Paradoxical effects of acute ethanolism in experimental brain injury. J. Neurosurg. 86 (5), 876–882.

Kidger, A.M., Rushworth, L.K., Stellzig, J., Davidson, J., Bryant, C.J., Bayley, C., Caddye, E., Rogers, T., Keyse, S.M., Caunt, C.J., 2017 Jan 17. Dual-specificity phosphatase 5 controls the localized inhibition, propagation, and transforming potential of ERK signaling. Proc. Natl. Acad. Sci. U. S. A. 114 (3), E317–E326.

Kigar, S.L., Chang, L., Auger, A.P., 2015 May. Gadd45b is an epigenetic regulator of juvenile social behavior and alters local pro-inflammatory cytokine production in the rodent amygdala. Brain Behav. Immun. 46, 60–69.

Kumar, S., Porcu, P., Werner, D.F., Matthews, D.B., Diaz-Granados, J.L., Helfand, R.S., Morrow, A.L., 2009 Sep. The role of GABA(A) receptors in the acute and chronic effects of ethanol: a decade of progress. Psychopharmacology 205 (4), 529–564.

Li, L., Yun, S.H., Keblesh, J., Trommer, B.L., Xiong, H., Radulovic, J., Tourtellotte, W.G., 2007 May. Egr3, a synaptic activity regulated transcription factor that is essential for learning and memory. Mol. Cell. Neurosci. 35 (1), 76–88.

Löscher, P., Nitucad, C.E., Harrer, M., Reckendorf, C.M.Z., Schatz, T., Simke, D., Lerche, H., Maljevic, S., Kröll, B., 2017 Jul 17. SRF modulates seizure occurrence, activity induced gene transcription and hippocampal circuit reorganization in the mouse pilocarpine epilepsy model. Mol. Brain 10 (1), 30.

Luong, T.N., Carlisle, H.J., Southwell, A., Patterson, P.H., 2011 Mar 10. Assessment of motor balance and coordination in mice using the balance beam. J. Vis. Exp. 49,

Ma, J., Wang, J., Cheng, J., Xiao, W., Fan, K., Gu, J., Yu, B., Yin, G., Wu, J., Ren, J., Hou, J., Jiang, Y., Tan, Y., Jin, W., 2017 Jan. Impacts of blast-induced traumatic brain injury on expressions of hepatic cytochrome P450 1A2, 2B1, 2D1, and 3A2 in rats. Cell. Mol. Neurobiol. 37 (1), 111–120,

Mauceri, D., Freitag, H.E., Oliveira, A.M., Bengtson, C.P., Bading, H., 2011 Jul 14. Nuclear calcium-VEGFD signaling controls maintenance of dendrite arborization necessary for memory formation. Neuron 71 (1), 117–130.

Mellström, B., Sahún, I., Ruiz-Nuño, A., Murtra, P., Gomez-Villafuertes, R., Savignac, M., Oliveros, J.C., Gonzalez, P., Kastanauskaite, A., Knafo, S., Zhuo, M., Higuera-Matas, A., Errington, M.L., Maldonado, R., DeFelipe, J., Jefferys, J.G., Bliss, T.V., Dierssen, M., Naranjo, J.R., 2014 Mar. DREAM controls the on/off switch of specific activity-dependent transcription pathways. Mol. Cell. Biol. 34 (5), 877–887.

Morris, T.A., Jafari, N., DeLorenzo, R.J., 2000 Jun 23. Chronic DeltaFosB expression and increased AP-1 transcription factor binding are associated with the long term plasticity changes in epilepsy. Brain Res. Mol. Brain Res. 79 (1–2), 138–149.

Natale, J.E., Ahmed, F., Cernak, I., Stoica, B., Faden, A.I., 2003 Oct. Gene expression profile changes are commonly modulated across models and species after traumatic brain injury. J. Neurotrauma 20 (10), 907–927.

Nomaru, H., Sakumi, K., Katogi, A., Ohnishi, Y.N., Kajitani, K., Tsuchimoto, D., Nemler, E.J., Nakabeppu, Y., 2014 Aug. FosB gene products contribute to excitotoxic microglial activation by regulating the expression of complement C5a receptors in microglia. Glia 62 (8), 1284–1298.

Oshitari, T., Dezawa, M., Okada, S., Takano, M., Negishi, H., Horie, H., Sawada, H., Tokuhisa, T., Adachi-Usami, E., 2002 Jul. The role of c-fos in cell death and regeneration of retinal ganglion cells. Invest. Ophthalmol. Vis. Sci. 43 (7), 2442–2449.

Pandit, V., Patel, N., Rhee, P., Kulvatunyou, N., Aziz, H., Green, D.J., O'Keeffe, T., Zangbar, B., Tang, A., Gries, L., Friese, R.S., Joseph, B., 2014 Aug. Effect of alcohol in traumatic brain injury: is it really protective? J. Surg. Res. 190 (2), 634–639.

Raj, R., Skrifvars, M.B., Kivisaari, R., Hernesniemi, J., Lappalainen, J., Siironen, J., 2015 Jan 15. Acute alcohol intoxication and long-term outcome in patients with traumatic brain injury. J. Neurotrauma 32 (2), 95–100,

Raj, R., Mikkonen, E.D., Siironen, J., Hernesniemi, J., Lappalainen, J., Skrifvars, M.B., 2016 Jun. Alcohol and mortality after moderate to severe traumatic brain injury: a meta-analysis of observational studies. J. Neurosurg. 124 (6), 1684–1692.

Ramanan, N., Shen, Y., Sarsfield, S., Lemberger, T., Schütz, G., Linden, D.J., Ginty, D.D.S.R.F., 2005 Jun. Mediates activity-induced gene expression and synaptic plasticity but not neuronal viability. Nat. Neurosci. 8 (6), 759–767,

Rawat, V., Gours, W., Piecharzyk, M., D'Mello, S.R., 2016 Mar. c-Fos protects neurons through a noncanonical mechanism involving HDAC3 interaction: identification of a 21-amino acid fragment with neuroprotective activity. Mol. Neurobiol. 53 (2), 1165–1180.

Relja, B., Henrich, D., Wetzel, G., Sander, A.L., Jakob, H., Marzi, I., Lehnert, M., 2013 Apr. Effects of acute ethanol gavage on intestinal integrity after hemorrhage/resuscitation. Scand. J. Gastroenterol. 48 (4), 448–458,

Renaudineau, S., Poucet, B., Laroche, S., Davis, S., Save, E., 2009 Jul 14. Impaired long-term stability of CA1 place cell representation in mice lacking the transcription factor zif268/egr1. Proc. Natl. Acad. Sci. U. S. A. 106 (28), 11771–11775.

Salim, A., Teixeira, P., Ley, E.J., DuBose, J., Inaba, K., Margulies, D.R., 2009 Oct. Serum ethanol levels: predictor of survival after severe traumatic brain injury. J. Trauma 67 (4), 697–703,

Samal, B.B., Waites, C.K., Almeida-Suhett, C., Li, Z., Marini, A.M., Samal, N.R., Elkahloun, A., Braga, M.F., Eiden, L.E., 2015 Oct. Acute response of the hippocampal transcriptome following mild traumatic brain injury after controlled cortical impact in the rat. J. Mol. Neurosci. 57 (2), 282–303.

Sato, S., Kawauchi, S., Okuda, W., Nishidate, I., Nawashiro, H., Tsumatori, G., 2014 Jan 8. Real-time optical diagnosis of the rat brain exposed to a laser-induced shock wave: observation of spreading depolarization, vasoconstriction and hypoxemia-oligemia. PLoS One 9 (1), e82891.

Savola, O., Niemelä, O., Hillbom, M., 2005 Jul-Aug. Alcohol intake and the pattern of trauma in young adults and working aged people admitted after trauma. Alcohol Alcohol. 40 (4), 269–273.

Shin, G.T., Lee, H.J., Kim, H., 2012 Nov. GADD45γ regulates TNF-α and IL-6 synthesis in THP-1 cells. Inflamm. Res. 61 (11), 1195–1202. http://dx.doi.org/10.1007/s00011-012-0515-x. **(Epub 2012 Jul 1. PubMed PMID: 22752116).**

Teng, S.X., Katz, P.S., Maxi, J.K., Mayeux, J.P., Gilpin, N.W., Molina, P.E., 2015 Mar. Alcohol exposure after mild focal traumatic brain injury impairs neurological recovery and exacerbates localized neuroinflammation. Brain Behav. Immun. 45, 145–156.

Vaagenes, I.C., Tsai, S.Y., Ton, S.T., Husak, V.A., McGuire, S.O., O'Brien, T.E., Kartje, G.L., 2015 Mar 13. Binge ethanol prior to traumatic brain injury worsens sensorimotor functional recovery in rats. PLoS One 10 (3), e0120356,

Wagner, N., Franz, N., Dieteren, S., Perl, M., Möra, K., Marzi, I., Relja, B., 2017 Sep. Acute alcohol binge deteriorates metabolic and respiratory compensation capability after blunt chest trauma followed by hemorrhagic shock-a new research model. Alcohol. Clin. Exp. Res. 41 (9), 1559–1567.

Wang, L., Deng, S., Lu, Y., Zhang, Y., Yang, L., Guan, Y., Jiang, H., Li, H., 2012 Sep 18. Increased inflammation and brain injury after transient focal cerebral ischemia in activating transcription factor 3 knockout mice. Neuroscience 220, 100–108.

Wang, Y., Chou, D.Y., Ding, J.Y., Fredrickson, V., Peng, C., Schafer, S., Guthikonda, M., Kreipke, C., Rafols, J.A., Ding, Y., 2013 Feb. Reduction of brain edema and expression of aquaporins with acute ethanol treatment after traumatic brain injury. J. Neurosurg. 118 (2), 390–396,

Wang, Y., Hameed, M.Q., Rakhade, S.N., Iglesias, A.H., Muller, P.A., Mou, D.L., Rozenberg, A., 2014 Aug 20. Hippocampal immediate early gene transcription in the rat fluid percussion traumatic brain injury model. Neuroreport 25 (12), 954–959,

Weber, J.T., 2012 Apr 12. Altered calcium signaling following traumatic brain injury. Front. Pharmacol. 3, 60.

Weber, J.T., Rzigalinski, B.A., Ellis, E.F., 2001 Jan 19. Traumatic injury of cortical neurons causes changes in intracellular calcium stores and capacitative calcium influx. J. Biol. Chem. 276 (3), 1800–1807.

Yuan, X.Q., Wade, C.E., Prough, D.S., DeWitt, D.S., 1990 Fall. Traumatic brain injury creates biphasic systemic hemodynamic and organ blood flow responses in rats. J. Neurotrauma 7 (3), 141–153.

Yuzwalo, N., Kamada, T., Kajitani, K., Nomaru, H., Katogi, A., Ohnishi, Y.H., Ohnishi, Y.N., Takase, K., Sakumi, K., Shigeto, H., Nakabeppu, Y., 2013 Apr. fosB-null mice display impaired adult hippocampal neurogenesis and spontaneous epilepsy with depressive behavior. Neuropsychopharmacology 38 (5), 895–906.

Zhang, J., Zhang, D., McQuade, J.S., Behbehani, M., Tsien, J.Z., Xu, M., 2002 Apr. C-fos regulates neuronal excitability and survival. Nat. Genet. 30 (4), 416–420.

Zhang, S.J., Zou, M., Lu, L., Lau, D., Ditzel, D.A., Delucinge-Vivier, C., Aso, Y., Descombes, P., Bading, H., 2009 Aug. Nuclear calcium signaling controls expression of a large gene pool: identification of a gene program for acquired neuroprotection induced by synaptic activity. PLoS Genet. 5 (8), e1000604.

Zhang, S.J., Buchthal, B., Lau, D., Hayer, S., Dick, O., Schwaninger, M., Veltkamp, R., Zou, M., Weiss, U., Bading, H., 2011 Mar 30. A signaling cascade of nuclear calcium-CREB-ATF3 activated by synaptic NMDA receptors defines a gene repression module that protects against extrasynaptic NMDA receptor-induced neuronal cell death and ischemic brain damage. J. Neurosci. 31 (13), 4978–4990,

Zhang, X.Y., CG, Gu, JW, Gu, Zhang, J.H., Zhu, H., Zhang, Y.C., Cheng, J.M., Li, Y.M., Yang, T., 2014 Nov 7. Analysis of key genes and modules during the courses of traumatic brain injury with microarray technology. Genet. Mol. Res. 13 (4), 9220–9228.

Zimprich, A., Garrett, L., Deussing, J.M., Wotjak, C.T., Fuchs, H., Gailus-Durner, V., de Angelis, M.H., Wurst, W., Hölter, S.M.A., 2014 Apr 15. Robust and reliable non-invasive test for stress responsivity in mice. Front. Behav. Neurosci. 8, 125.

6.3 The neuroprotective effect of ethanol intoxication in TBI is associated with the suppression of ErbB signaling in PV positive interneurons

Akila Chandrasekar[a], Florian olde Heuvel[a], Martin Wepler[b], Rida Rehman[a], Annette Palmer[c], Alberto Catanese[d], Birgit Linkus[a], Albert Ludolph[a], Tobias Boeckers[d], Markus Huber-Lang[c], Peter Radermacher[b], Francesco Roselli[a,d]

a) Dept. of Neurology, Ulm University, Germany

b) Institute of Anesthesiological Pathophysiology and Process Engineering, University Ulm, Germany

c) Institute of Clinical and Experimental Trauma-Immunology, Ulm University, Germany

d) Dept. of Anatomy and Cell Biology, Ulm University, School of Medicine, Germany

Accepted: 18 May 2018

Published in: Journal of Neurotrauma. 1 November 2018. 35(22): 2718-2735

doi: https://doi.org/10.1089/neu.2017.5270

JOURNAL OF NEUROTRAUMA 35:2718–2735 (November 15, 2018)

DOI: 10.1089/neu.2017.5270

The Neuroprotective Effect of Ethanol Intoxication in Traumatic Brain Injury Is Associated with the Suppression of ErbB Signaling in Parvalbumin-Positive Interneurons

Akila Chandrasekar,[1] Florian olde Heuvel,[1] Martin Wepler,[2] Rida Rehman,[1] Annette Palmer,[3] Alberto Catanese,[4] Birgit Linkus,[1] Albert Ludolph,[1] Tobias Boeckers,[4] Markus Huber-Lang,[3] Peter Radermacher,[2] and Francesco Roselli[1,4]

Abstract

Ethanol intoxication (EI) is a frequent comorbidity of traumatic brain injury (TBI), but the impact of EI on TBI pathogenic cascades and prognosis is unclear. Although clinical evidence suggests that EI may have neuroprotective effects, experimental support is, to date, inconclusive. We aimed at elucidating the impact of EI on TBI-associated neurological deficits, signaling pathways, and pathogenic cascades in order to identify new modifiers of TBI pathophysiology. We have shown that ethanol administration (5 g/kg) before trauma enhances behavioral recovery in a weight-drop TBI model. Neuronal survival in the injured somatosensory cortex was also enhanced by EI. We have used phospho–receptor tyrosine kinase (RTK) arrays to screen the impact of ethanol on TBI-induced activation of RTK in somatosensory cortex, identifying ErbB2/ErbB3 among the RTKs activated by TBI and suppressed by ethanol. Phosphorylation of ErbB2/3/4 RTKs were upregulated in vGlut2$^+$ excitatory synapses in the injured cortex, including excitatory synapses located on parvalbumin (PV)-positive interneurons. Administration of selective ErbB inhibitors was able to recapitulate, to a significant extent, the neuroprotective effects of ethanol both in sensorimotor performance and structural integrity. Further, suppression of PV interneurons in somatosensory cortex before TBI, by engineered receptors with orthogonal pharmacology, could mimic the beneficial effects of ErbB inhibitors. Thus, we have shown that EI interferes with TBI-induced pathogenic cascades at multiple levels, with one prominent pathway, involving ErbB-dependent modulation of PV interneurons.

Keywords: chemogenetics; ethanol intoxication; inhibitory interneurons; traumatic brain injury; tyrosine kinase receptors

Introduction

BRAIN TRAUMA IS A FREQUENT CAUSE OF INJURY IN civilian and military populations, with 577 per 100,000 cases per year reported in the United States (between 2002 and 2006) and even larger numbers in the developing world.[1,2] Moderate-to-severe traumatic brain injury (TBI) accounts for 10–30% of the overall incidence, but results, nevertheless, in 17.6 per 100,000 deaths per year in the United States alone.[1,3] It is also estimated that 3.2–5.3 million patients live with long-term disability related to TBI in the United States.[4] Overall survival in cases of severe TBI has changed very little in the last 20–30 years.[5] Epidemiological evidence can be used to identify modifiers and modulators of TBI prognosis in humans, alleviating the pitfalls of target identification in rodent models.

Clinical data have shown that ethanol intoxication (EI) is a potential modifier of TBI outcome. EI is detected in up to 55% patients admitted for TBI, with the great majority of patients displaying a binge-drinking pattern (i.e., not being chronic alcoholics).[3,6] Surprisingly, positive blood-alcohol level (BAL) has been associated with a better outcome of TBI,[7–12] although not in all studies.[13,14] In particular, Berry and colleagues reported BAL >230 mg/dL as being strongly associated with reduced mortality in moderate-to-severe TBI.[10] Likewise, patients with positive BAL showed a faster recovery of neurocognitive functions,[15] although other studies found detrimental or no effect.[16,17]

Interaction between EI and TBI has been investigated in experimental models utilizing different TBI models and different schedules of ethanol administration: ethanol administration before a fluid percussion injury[18] or three-dose ethanol administration before and

[1]Department of Neurology, [2]Institute of Anesthesiological Pathophysiology and Process Engineering, [3]Institute of Clinical and Experimental Trauma-Immunology, and [4]Department of Anatomy and Cell Biology, Ulm University, Ulm, Germany.

after controlled cortical impact (in rats)[19] worsened sensorimotor recovery, whereas single-dose ethanol administration soon after blunt TBI[12] or before blunt TBI,[20] contusive TBI,[21] or controlled cortical injury[22] lead to faster recovery. Thus, EI may provide context-dependent beneficial effects in TBI, offering an entry point to understanding board- or subtype-specific targets of intervention.

Mechanistic understanding of EI influence on TBI is limited: EI at the instance of trauma modulates the neuroinflammatory cascade, reducing production of proinflammatory cytokines and enhancing secretion of interleukin (IL)-13,[20,23] although it is also reported to increase brain edema.[24] Nevertheless, EtOH pharmacological spectrum of activities include antagonistic effects on N-methyl-D-aspartate receptor (NMDAR)[25] and agonistic effects on gamma-aminobutyric acid (GABA) receptor,[26] suggesting that EI may affect multiple, distinct sets of biological functions in neurons, astrocytes, and immune cells (such as synaptic plasticity, proliferation, and inflammation) at once.

At the molecular level, these functions are mediated and orchestrated (although not exclusively) by a set of receptor tyrosine kinases (RTKs), including, among many, the ErbB family and Trk family receptors (involved in synaptic plasticity and astrocyte proliferation),[27–29] Axl/Dtk/Metk receptors (affecting microglia physiology),[30] and EphA and EphB family receptors (modulating astrocyte responses).[31] Because distinct sets of RTKs control different biological responses and structures (synaptic plasticity, astroglial responses, and neurovascular unit),[28,31–34] monitoring the activation status of such receptors make it possible to probe the ongoing cellular responses elicited by TBI and the combination of EI and TBI. In particular, activation of the ErbB family RTKs provides an entry point to the excitation/inhibition balance in the affected cortex: In fact, ErbB family members are expressed on inhibitory interneurons,[35–37] where they control the strength of excitatory synapses.[27,38] Among the inhibitory interneurons, ErbB receptors are prominent regulators of parvalbumin-positive (PV) Interneurons[39,40] and thus provide an entry point to the effects of EI and TBI on perisomatic inhibition and cortical excitability.[41]

Therefore, we monitored the impact of EI on behavioral and histological consequences of TBI and exploited an array of antibodies directed against phosphorylated RTKs to identify the pattern of RTK activation in TBI and how this was influenced by EI. Because of the highly dynamic nature of phosphorylation events, this approach provided a more direct sampling of the ongoing signaling compared to gene-transcription profiling. In addition, because RTKs are targeted by a growing number of small molecules approved for human use (e.g., see a previous work[42]), they provide opportunities for drug repurposing in TBI.

We have demonstrated that EI accelerates neurological recovery and ameliorates the histological damage caused by TBI. The RTK array analysis revealed that EI prevented the TBI-induced phosphorylation of several RTKs and, in particular, the ErbB family. We have demonstrated that phosphorylated ErbB family members are localized in vesicular glutamate transporter 2 (vGlut2) synapses on inhibitory neurons, and that neuroprotective effects of EI can be partially recapitulated by pharmacological modulation of ErbB or by chemogenetic control of PV interneurons.

Methods

Animals, ethanol administration, and traumatic brain injury model

The experiments described were approved by the local veterinary and animal experimentation service under the license n.1222 and successive integration. B6 mice were bred locally (Ulm University, Ulm, Germany) under standard husbandry conditions (24°C, 60–80% humidity, 14/10 light/dark cycle, with *ad libitum* access to food and water). B6/PV-Cre mice were a kind gift of Pico Caroni (FMI, Basel, Switzerland) and were bred locally (Ulm University) under the same conditions. Experimental data are reported from a total of 194 mice from an overall cohort of 224 mice (with 30 mice experiencing acute mortality or meeting termination criteria, see below). Experimental groups and mice allocations for each group with respective readouts are summarized in Supplementary Table 1 (see online supplementary material at http://www.liebertpub.com). For behavioral and histological analysis of EI/TBI interactions, the experimental design included four groups: 1) control mice administered with saline and subject to sham surgery (sal-S; $n=3$); 2) control mice administered with high-dose ethanol (5 g/kg) diluted in saline and subject to sham surgery (eth-S; $n=3$); 3) mice pre-treated with saline before TBI (sal-TBI; $n=8$); and 4) mice pre-treated with high-dose ethanol (5 g/kg) diluted in saline before TBI (eth-TBI; $n=6$). Ethanol solution (400 μL of ethanol solution, 5 g/kg in 32% [v/v] in saline or saline alone), diluted in saline was administered by oral gavage 30 min before the procedure.[43] Wild-type male mice 80–90 days of age were subject to closed weight-drop TBI after administration of buprenorphine (0.1 mg/kg by subcutaneous injection) and put under sevoflurane anesthesia (2.5% in 97.5% O_2). Scalp skin was incised on the midline to expose the skull. Animals were then manually positioned in the weight-drop apparatus, as previously described, with the impactor site localized at the center of the right parietal bone. TBI was delivered by a 333-g impactor free-falling from a 2-cm distance.[43]

Immediately after the experimental TBI, animals were administered 100% O_2 and were monitored for apnea time. After spontaneous breathing was restored, scalp skin of anesthetized mice was stitched with Prolene 6.0 surgical thread and animals were transferred to a warmed recovery cage (single-housed) with *ad libitum* access to food and water. Additional doses of buprenorphine were administered every 12 h for the following 24 h post-injury. For sham-surgery, mice were subject to the same procedures and treatments (anesthesia, skin opening and closure, handling, and positioning in the TBI apparatus), but no trauma was delivered.

To avoid unnecessary suffering of mice, their general state was checked regularly using a score sheet developed for TBI determining fixed termination criteria. Effort was made to minimize animal suffering and reduce the number of necessary animals.

Phospho–receptor tyrosine kinase screening

For the screening of RTK activation pattern, a single time point (3 h) was considered and four experimental groups were included: 1) saline-sham ($n=8$); 2) ethanol-sham ($n=5$); 3) saline-TBI ($n=7$); and 4) ethanol-TBI ($n=5$). Mice were sacrificed 3 h after TBI (or sham surgery) by cervical dislocation and the brain was quickly dissected in ice-cold phosphate-buffered saline (PBS). Cortex samples 1.5–2.0 mm in diameter were dissected from the parietal lobe (somatosensory area) and snap-frozen. In order to obtain cortical protein extracts, cortical samples were thawed in homogenization buffer (1 × Lysis Buffer; CST; 20 of mM Tris-HCl [pH 7.5], 150 mM of NaCl, 1mM of Na_2 EDTA (ethylenediaminetetraacetic acid), 1 mM of ethylene glycol tetraacetic acid, 1% Triton, 2.5 mM of sodium pyrophosphate, 1 mM of β-glycerophosphate, 1 mM of Na_3VO_4, and 1 μg/mL of leupeptin) containing phosphatase (1 tablet per 10 mL of lysis buffer) and protease (1 tablet per 50 mL of lysis buffer) inhibitor (Roche cOmplete tablets; Sigma-Aldrich, Taufkirchen, Germany) cocktail and homogenized with 20 strokes of Dounce apparatus. Tissue homogenates were then cleared by centrifugation (10,000 *g*, 10 min) and assayed for protein concentration with the Bradford protein assay.

Phospho-RTK activation screening was based on a nitrocellulose-membrane sandwich immunoassay and was performed according to

the manufacturer's instructions (R&D Systems, Minneapolis, MN). Briefly, nitrocellulose membrane spotted with the anti-RTK antibody were blocked in array buffer 1 for 1 h at room temperature (RT), before being incubated with 500 μg of tissue homogenates diluted in 1.5 mL of Array buffer 1 for 24 h at 4°C. Thereafter, membranes were quickly rinsed in sterile water and washed 3 × 10 min in wash buffer. Membranes were then incubated with the anti-phospho-tyrosine horseradish peroxidase (HRP) detection antibody, diluted to 1 × Array Buffer 2, for 2 h at RT. Membranes were then washed again as before and detection of the HRP was performed by adding to each membrane 1 mL of the Chemi Reagent Mix and imaged using the chemiDOC MP Imaging System from Bio-Rad (Hercules, CA).

Array images were then quantified using ImageJ (NIH, Bethesda, MD). A fixed-size region of interest (ROI) was drawn on each antibody spot and the integrated median gray value was obtained, together with a value for the local background. Each experimental run contained at least two saline-sham samples, and values for each spot are expressed as percentage of the saline-sham reference.

Drugs and drug administration

The ErbB2 inhibitor, Lapatinib (Selleck chemicals, Munich, Germany), the ErbB inhibitor, AG825 (Tocris, Bristol, UK), the broad-spectrum TK inhibitor, LDN-211904 (Merck, Darmstadt, Germany), and the platelet-derived growth factor (PDGF) inhibitor, CP-673451 (Selleck Chemicals, Munich, Germany), were commercially available. Each drug was dissolved in a minimal volume of dimethyl sulfoxide and diluted in vehicle (containing 5% PEG-400, 5% Tween-80, and 90% saline) before administration. Mice were administered with each drug in a volume of 400 μL of vehicle by oral gavage. The experimental design included 1) mice administered with vehicle undergoing sham-surgery (veh-S; $n = 4$), 2) mice pre-treated with ethanol (5 g/kg) diluted in vehicle and undergoing sham surgery (eth-S; $n = 3$), 3) mice administered with vehicle undergoing TBI (veh-TBI; $n = 5$), 4) mice pre-treated with ethanol and undergoing TBI (eth-TBI; $n = 4$), and 5) mice pre-treated with specific inhibitors undergoing TBI. For ErbB inhibitors Lapatinib and AG825, two treatment doses were considered: 10 mg/kg ($n = 6$ and $n = 5$, respectively) and 50 mg/kg ($n = 4$ and $n = 4$, respectively). For LDN-211904 ($n = 4$) and CP-673451 ($n = 4$), only one dose (10 mg/kg) was considered. In pre-treated mice, all drugs (or vehicle alone) were administered 30 min before TBI. In addition to the four groups cited above, for Lapatinib and AG825 one more group was analyzed: mice treated with the specific inhibitor 30 min after TBI ($n = 4$ and $n = 4$, respectively). In this group, only one dose (50 mg/kg) was administered. Of note, administration of ethanol diluted in saline or saline alone did not produce a significantly different effect on behavioral or histological readouts than ethanol diluted in PEG400-Tween80-saline vehicle or of vehicle alone.

Behavioral and neurological score assessment

Overall neurological impairment was evaluated using the composite Neurological Severity Score (NSS), as described by Flierl and colleagues.[41] At 3 h post-injury, 24 h post-injury, 2 days post-injury (dpi), 3 dpi, 5 dpi, and 7 dpi, assessment of motor (muscle status, abnormal movement), sensory (visual, tactile, and proprioceptive), reflex, and balance abilities were tested. Animals are awarded 1 point for failure to perform a task, such that scores ranged from 0 to 10, increasing with severity of dysfunction. The Arena Escape test, part of NSS evaluation, was performed putting the animals into a circular, brightly-lit area whose wall included a narrow opening leading to the dark compartment. The time required to enter the dark compartment was measured and averaged over three attempts. The Beam Walk test was performed as previously reported: Mice were habituated to walking over a suspended wooden beam, from an open platform to a dark compartment, and the test was then repeated at 2 and 7 dpi.[44] Time required to reach the dark box was measured.

Immunostaining, confocal imaging, and image analysis

For evaluation of ErbB family members' phosphorylation by immunostaining, mice treated with either 1) saline (sal-S; $n = 3$) or 2) ethanol (eth-S; $n = 3$) were subject to sham surgery, and independent groups of 3) saline pre-treated (sal-TBI; $n = 5$) and 4) ethanol pre-treated (eth-TBI; $n = 4$) mice underwent the TBI procedure (as indicated above). In order to further evaluate the phosphorylation of ErbB2 after the administration of ErbB-specific inhibitors: AG825 and Lapatinib, the following groups were considered: 1) mice treated with vehicle and undergoing sham surgery (veh-S, $n = 3$), 2) mice treated with vehicle and undergoing TBI (veh-TBI, $n = 3$), 3) mice treated with AG825 inhibitor and undergoing TBI ($n = 3$), and 4) mice treated with Lapatinib and undergoing TBI ($n = 3$). Mice were perfusion-fixed (25 mL of ice-cold PBS followed by 50 mL of ice-cold 4% paraformaldehyde [PFA] in PBS) after 3 h or 7 days. Brains were dissected and stored in PFA (4% in PBS) for 18 h at 4°C, before being washed in PBS, cryoprotected in 30% sucrose in PBS, and embedded in optimum cutting temperature compound (TissueTek; Sakura Finetek USA, Torrance, CA). Sections were cut in cryostat at 40-μm thickness. Immunostaining was performed as previously reported.[46] Briefly, free-floating brain sections spanning the trauma site were blocked in bovine serum albumin 3%+ donkey serum 3%+ Triton 0.3% in PBS for 2 h at 24°C and incubated with primary antibody in blocking buffer for 40 h at 4°C.

The following primary antibodies were used: rabbit anti-phosphorylated-ErbB2 (pErbB2; 1:200, #2243; Cell Signaling Technology [CST], Danvers, MA), rabbit anti-phosphorylated-ErbB3 (pErbB3; 1:1000, #2842; CST), phosphorylated ErbB4 (pErbB4; 1:400, ab109273; Abcam, Cambridge, MA), mouse anti-vGlut1 (1:500, #135311; Synaptic Systems, Brussels, Belgium), guinea pig anti-vGlut2 (1:500, #135404; Synaptic Systems), mouse anti-Synaptotagmin-2 (1:200, ab154035; Abcam), and goat anti-PV (1:1000, PVG-214; Swant, Bellizona, Switzerland).

For detection of phospho-ErbB2 and phospho-ErbB3 and phospho-ErbB4, the tyramide signal amplification protocol was used (Alexa Fluor-488 Tyramide SuperBoost kit, B40922; Thermo Fisher Scientific, Waltham, MA), and the manufacturer's instructions were modified according to free-floating staining. Briefly, sections were washed 3 × 10 min in PBS at RT and incubated for 60 min with poly-HRP–conjugated secondary antibody. After washing (3 × 30 min in PBS at RT), sections were incubated in tyramide working solution (100 × tyramide stock solution, 100 × H_2O_2 solution, and 1 × reaction buffer) for 10 min, the tyramide working solution was stopped by adding the sections in stop reagent. After washing (3 × 30 min in PBS at RT), brain sections were incubated with opportune secondary antibodies (Alexa-conjugated donkey antimouse, antirabbit, anti–guinea pig) diluted 1:500 together with the nuclear stain TOPRO-3 (Invitrogen, Carlsbad, CA) 1:1000 for 2 h at RT and mounted using FluoroGold mounting medium. For assessment of neuronal loss, the following groups were considered: 1) mice administered with vehicle and undergoing sham surgery (veh-S; $n = 3$), 2) mice administered with ethanol (eth-S; $n = 3$, 5 g/kg, diluted in vehicle) undergoing sham surgery, 3) mice administered with vehicle undergoing TBI (veh-TBI; $n = 5$), 4) mice administered with ethanol undergoing TBI (eth-TBI; $n = 4$), 5) mice administered with AG825 or Lapatinib ($n = 5$ and $n = 6$, respectively), and 6) mice administered with LDN or CP ($n = 4$ and $n = 4$, respectively). Mice were sacrificed at 7 dpi by perfusion/fixation, and brain tissue was then processed for immunostaining as reported above. Immunostaining was performed with mouse anti–neuronal nuclei (NeuN; 1:100,

MAB377; Millipore, Billerica, MA) with the same experimental protocol detailed above.

Confocal images were acquired using an LSM-700 (Carl Zeiss AG, Jena, Germany) inverted microscope, fitted with a 20× air or 40× oil objective. All images were acquired in 12-bit format and imaging parameters were set in order to obtain signal for the immunostained antigen >150 while avoiding saturation in high-intensity neurons. For neuronal density measurements, ROIs corresponding to the trauma site and spanning the surrounding regions for at least 1500 μm were acquired with 20× objective in tile-scan mode, with optical section thickness set at 1 μm. NeuN$^+$ were counted in ROIs located in the primary injury site (on the axis of the injury site; Supplementary Fig. 1) (see online supplementary material at http://www.liebertpub.com) and in the penumbral zone (located at a fixed distance of 400 μm from the axis of the injury site; Supplementary Fig. 1) (see online supplementary material at http://www.liebertpub.com). Multiple brain sections spanning the injury site were imaged, and the ones with the largest extent of injury (measured in the latero-lateral axis) were considered as a reference for the evaluation of the injury size.

For phospho-RTK quantification, images were acquired with 40× objective with optical thickness set at 500 nm and using the tile-scan mode to acquire composite pictures spanning the primary injury site and the penumbra. Confocal image stacks composed of 10 optical sections were collapsed in maximum-intensity projection using the ImageJ software suite (NIH). For overall pErbB2, pErbB3, and pErbB4 levels, two fixed-size rectangular ROIs were located symmetrically on each side of the axis of the injury site and the mean gray value was computed.

For analysis of pErbB2 colocalization with synaptic markers, single optical sections acquired with the 40×/oil objective were considered and each channel was acquired independently to prevent fluorescence cross-bleed. Each synaptic marker was evaluated independently against pErbB2 (the following co-immunostainings were performed: pErbB2/vGlut1, pErbB2/vGlut2, and pErbB2/Syt2). Multi-channel images were processed in ImageJ (NIH); ROIs for synaptic analysis were located at 40–50 μm from the axis of the injury site. pErbB2 fluorescence images from veh-TBI samples were thresholded to allow a binary classification and the colocalization of pErbB2$^+$ synapses and vGlut1, vGlut2, or Synaptotagmin was visually evaluated by listing the number of pErbB$^+$ synapses also displaying >10 pixels positive for each synaptic marker considered. A minimum of 150 synapses for each marker were evaluated (from three replicates) and the percentage of pErbB2+/vGlut1$^+$, pErbB2+/vGlut2$^+$, and pErbB2+/Syt2$^+$ synapses (over the total number of pErbB2$^+$ in the considered ROIs) was computed.

Intracerebral injection of adeno-associated virus and chemogenetic agonist administration

For the study of PV activation or inhibition by chemogenetics, and the eventual additive effect of ethanol, PV-Cre mice were injected with adeno-associated virus (AAV)9 expressing either activator pharmacologically selective actuator module (PSAM) or inhibitor PSAM. For both the former and the latter (independently), the following experimental design was considered: 1) mice injected with saline and subject to sham surgery (sal-actPSAM-S and sal-inhPSAM-S, both $n=3$), 2) mice injected with pharmacologically selective effector molecule (PSEM) and subject to sham surgery (PSEM-actPSAM-S and PSEM-inhPSAM-S, both $n=3$), 3) mice injected with saline and subject to TBI (sal-actPSAM-TBI and sal-inhPSAM-TBI, both $n=4$), 4) mice injected with PSEM and subject to TBI (PSEM-actPSAM-TBI and PSEM-inhPSAM-TBI, both $n=5$), 5) mice injected with PSEM, administered ethanol and subject to TBI (eth-PSEM-actPSAM-TBI and eth-PSEM-inhPSAM-TBI, both $n=4$), and 6) mice administered with ethanol alone and subject to TBI (eth-actPSAM-TBI and eth-inhPSAM-TBI, both $n=3$).

Intracerebral injection of AAV vector was performed at the age of P30–P40 as previously reported.[47] Briefly, mice were pretreated with buprenorphine (0.01 mg/kg; Reckitt Beckiser Healthcare, Berkshire, UK) and meloxicam (1.0 mg/kg; Böhringer Ingelheim, Biberach an der Riß, Germany) before being put into a stereotaxic frame (Bilaney Consultants GmbH, Düsseldorf, Germany) under continuous isoflurane anesthesia (4% in O_2 at 800 mL/min). Skin scalp was incised on the midline to expose the skull. Using a hand-held micro drill, a burr hole was drilled at the coordinates (x = +2.0, y = −2.0), corresponding to the primary somatosensory cortex. AAV9 vectors, encoding floxed PSAM-carrying AAV9 (excitation, pAAV(9)-pCAG-flox-PSAM(Leu41Phe,Tyr116Phe)5HT3-WPRE; inhibition, pAAV(9)-cbaflox-PSAM(Leu141Phe,Tyr116Phe)GlyR-WPRE was obtained from Vector Biolabs (Malvern, PA) at the titer of 9*10 viral genomes/mL. Next, 200–500 nL of viral suspension were injected at z = −0.4/0.7 using a pulled-glass capillary connected to a Picospritzer microfluidic device.

Injection was performed with 10-msec pulses over 10 min and the capillary was kept in place for 10 more minutes before being withdrawn.[13,48] Scalp skin was stitched with Prolene 7.0 surgical threads and animals were transferred for recovery in single cages with facilitated access to water and food. Animals were monitored for eventual neurological impairment for the following 72 h and were administered additional doses of buprenorphine, if needed. TBI procedure was performed 30–40 days after viral injection. No increase in mortality or morbidity was observed in mice intracranially injected in comparison to mice,which were subject to TBI, but were never subject to microdrilling and viral injection (corresponding to the saline-TBI or vehicle-TBI mice used as controls in behavioral and pharmacological experiments). The PSEM308 agonist (obtained from Apex Scientific Inc., Stony Brook, NY)[48] was administered as previously reported[47] at the dose of 5 g/kg 20–30 min before the TBI procedure by intraperitoneal injection (diluted in sterile saline at 20 mg/mL). Administration of ethanol was performed as reported above (oral gavage, diluted in saline, 5 g/kg).

Blood gas analysis

For the evaluation of hypoxemia and hypercapnia, which may result from the interaction of ethanol intoxication and TBI, blood gas analysis was performed. Three experimental groups were considered: 1) ethanol administered, sham TBI ($n=3$); 2) saline-pretreated and TBI ($n=3$); and 3) ethanol-pretreated, TBI ($n=4$). Baseline reference values for PaO_2 and $PaCO_2$ were obtained from Schwarzkopf and colleagues.[49] Briefly, 50 μL of arterial blood was drawn from the abdominal aorta in calcium-heparin–containing syringes. Blood gas tensions were measured using a Radiometer ABL 800® blood gas analyzer.

Blood glial fibrillary acidic protein assay

For glial fibrillary acidic protein (GFAP) blood measurements, the following experimental groups were considered: 1) mice administered with saline undergoing sham surgery ($n=3$), 2) mice administered with ethanol (5 g/kg) and undergoing sham surgery ($n=3$), 3) mice administered with saline undergoing TBI ($n=4$), and 4) mice administered ethanol undergoing TBI ($n=4$). Whole blood was taken by puncture of the right ventricle and transferred into sterile plasma EDTA microtubes (Kabe Labortechnik, Nuembrecht-Elsenroth, Germany). After centrifugation at 800g for 10 min at 4°C, the supernatant was taken and centrifuged at 13,000g for 2 min at 4°C. Plasma samples were analyzed by commercially available enzyme-linked immunosorbent assay specified for mouse GFAP, according to the manufacturer's instructions (LSBio, Seattle, WA). Colorimetric detection was made at a wavelength of 450 nm using a plate reader (Tecan Sunrise Plate Reader; Tecan, Crailsheim, Germany).

(a proxy of the severity of parenchymal damage caused by TBI in human and murine models) at the 3-h time point: Plasma GFAP was strongly elevated in both TBI groups compared to sham mice, but were not significantly affected by ethanol (1.25 ± 0.32 ng/mL in sal-TBI vs. 1.17 ± 0.42 ng/mL in eth-TBI, as compared to 0.058 ± 0.004 and 0.058 ± 0.013 ng/mL in sal-S and eth-S groups, respectively; $p > 0.05$ for sal-TBI vs. eth-TBI; Fig. 1E).[29,30]

Taken together, these data show that sensorimotor abilities were significantly conserved after trauma in ethanol-treated TBI mice compared to sal-TBI, suggesting an acute neuroprotective effect of ethanol.

Screening receptor tyrosine kinase activation identifies multiple signaling cascades activated by traumatic brain injury and affected by ethanol

In order to gain mechanistic insights on the neuroprotective effect of EI in TBI, we set out to screen the phosphorylation level (in other words, the activation status) of 38 different RTKs representing multiple functional pathways (including neuronal, glial, vascular, and inflammatory responses) and endowed with high translational potential. To achieve this aim, we sampled the trauma site from mice treated with saline or ethanol which underwent TBI or sham surgery. Whole-cortex protein extracts were then probed for RTK phosphorylation using nitrocellulose antibody arrays.

For four phospho-RTK (EphA7, EphA8, EphB2, and EphB4) absolute levels were below the detection limit and could not be analyzed. Two-way ANOVA revealed a statistically significant difference between treatment groups ($F_{(3,21)} = 15.25$; $p < 0.0001$) and a significant interaction between TBI and EI ($F_{(102,714)} = 3.005$; $p < 0.0001$). Post-hoc analysis (35 groups, six comparisons per group) revealed that Sal-TBI caused a statistically significant upregulation of the phosphorylation levels of nine RTKs (ErbB2, $p = 0.011$; ErbB3, $p = 0.001$; FGFR1, $p = 0.0004$; FGFR3, $p = 0.0311$; hepatocyte growth factor receptor [HGFR]/c-Met, $p < 0.0001$; MSP-R, $p = 0.022$; EphA2, $p < 0.0001$; EphA3, $p < 0.0001$; EphA6, $p = 0.0204$) and the downregulation of one RTK (IGF-R1) when compared to sham samples which had not reached statistical significance after multiple-comparisons correction.

Ethanol displayed a mainly negative effect on TBI-activated RTK, although not all activated RTK were equally downregulated by EI (Fig. 2A,B). When sal-TBI and eth-TBI groups were compared post-hoc, EI caused a statistically significant downregulation of nine RTKs: ErbB2 (154 ± 15% in sal-TBI vs. 73 ± 26% in eth-TBI; $p = 0.0003$), ErbB3 (166 ± 19% in sal-TBI vs. 67 ± 20% in eth-TBI; $p < 0.0001$), fibroblast growth factor receptor 1 (FGFR1; 170 ± 31% in sal-TBI vs. 75 ± 21% in eth-TBI; $p = 0.001$). Other RTKs whose activation was significantly reduced by ethanol include PDGF-Rb (138 ± 16% in sal-TBI vs. 67 ± 21% in eth-TBI; $p = 0.0029$), Flt-3 (135 ± 49% in sal-TBI vs. 71 ± 34% in eth-TBI; $p = 0.0088$), EphA2 (190 ± 72% in sal-TBI vs. 137 ± 51% in eth-TBI; $p = 0.04$), MSP-R (150 ± 109 in sal-TBI vs. 93 ± 85% in eth-TBI; $p = 0.0237$), EphA3 (although with large variations: 209 ± 103% in sal-TBI vs. 152 ± 33% in eth-TBI; $p = 0.0243$), and EphA6 and EphB1 (EphA6, 152 ± 33% in sal-TBI vs. 75 ± 19% in eth-TBI; $p = 0.0011$; EphB1, 138 ± 22% in sal-TBI vs. 64 ± 11% in eth-TBI; $p = 0.0041$). Additionally, some RTKs were not affected by ethanol, such as HGFR/c-Met (269 ± 151% in sal-TBI vs. 255 ± 121% in eth-TBI; $p > 0.05$) and FGFR3 (147 ± 35% in sal-TBI vs. 108 ± 35% in eth-TBI; $p > 0.05$).

Taken together, these data suggest that the effect of ethanol in TBI is multi-faceted and involves the modulation of multiple signaling cascades unfolding in possibly multiple cellular subpopulations.

ErbB2, ErbB3, and ErbB4 phosphorylation is upregulated by traumatic brain injury and it is downregulated by concomitant ethanol intoxication

Among the multiple RTKs modulated by TBI and ethanol, we decided to analyze in further detail the effect of TBI and ethanol intoxication on ErbB2/3/4 activation and signaling, because of their high expression in the cerebral cortex and because of their translational value given that these receptors can be targeted with U.S. Food and Drug Administration (FDA)-approved small molecules.[42,52,53] First, we sought to validate the screening results and identify the cellular sources of the phosphorylated RTKs by immunostaining of brain sections (sampling the trauma site) from sal-sham, eth-sham, sal-TBI, or eth-TBI mice (perfused 3 h after TBI) for phosphorylated ErbB2 (pY1221/1222), phosphorylated ErbB3 (pY1289), and phosphorylated ErbB4 (pY1284).

At 3 h post-injury, pErbB2, pErbB3, and pErbB4 immunofluorescence levels were strongly increased in the site of injury in sal-TBI mice compared to sal-sham control cortical samples and nearby cortices (371 ± 68%, 422 ± 73%, and 321 ± 57% of baseline, respectively; $p < 0.01$; Fig. 3A–F). Notably, whereas eth-sham did not display significantly lower levels of pErbB2, eth-TBI mice showed a significant reduction in pErbB2 fluorescence intensity (204 ± 47% of sal-sham; $p < 0.05$ vs. sal-sham and vs. sal-TBI; Fig. 3A,B). Likewise, ethanol pre-treatment resulted in the blunting of TBI-induced upregulation of pErbB3 and pErbB4 (249 ± 51% and 203 ± 48.9% of baseline, respectively; $p < 0.01$ sal-sham and vs. sal-TBI; Fig. 3C–F). Thus, immunostaining data validated the antibody array findings and demonstrated the suppressive effects of ethanol on ErbB family activation after TBI.

pErbB2 and pErbB3 (and, to a lesser extent, pErbB4) displayed a strikingly punctuate pattern, reminiscent of synaptic localizations in the areas proximal to the injury site and in the penumbra. pErbB4 also displayed immunolocalization in cell bodies and proximal dendrites of a subset of neurons. In fact, when cortical samples were co-immunostained for pErbB2 together with the excitatory presynaptic markers vGlut1 and vGlut2, pERbB2 puncta colocalized almost exclusively with $vGlut2^+$ puncta (93 ± 4%) and very little with vGlut1 (3 ± 2%) and never with the marker of inhibitory synapses, Synaptotagmin-2 (Fig. 3G,H).

Acute administration of ErbB2 inhibitors mimics ethanol effect on traumatic brain injury behavioral outcome.

We further investigated the importance ethanol-induced suppression of RTK, particularly of ErbB- signaling in TBI. More accurately, we explored whether specific RTK inhibitors could recapitulate EI-associated improved behavioral outcomes. Because the pharmacokinetics of ErbB inhibitors have not been studied in the context of TBI (Lapatinib penetration of the brain has been previously assessed, although in a condition in which no central nervous system [CNS] insult was delivered),[54] we verified that pre-administration of 50 mg/kg of the ErbB inhibitors, AG825 and Lapatinib (or vehicle), could affect pErbB2 levels in the cortex after TBI. Mice were sacrificed 3 h after trauma and pErbB2 immunofluorescence levels were assessed: Whereas in sal-TBI we detected a significant increase in ErbB2 phosphorylation in $vGlut2^+$ synapses (Sal-TBI 354 ± 60% vs. sal-s; $p < 0.01$ vs. sham), TBI-induced

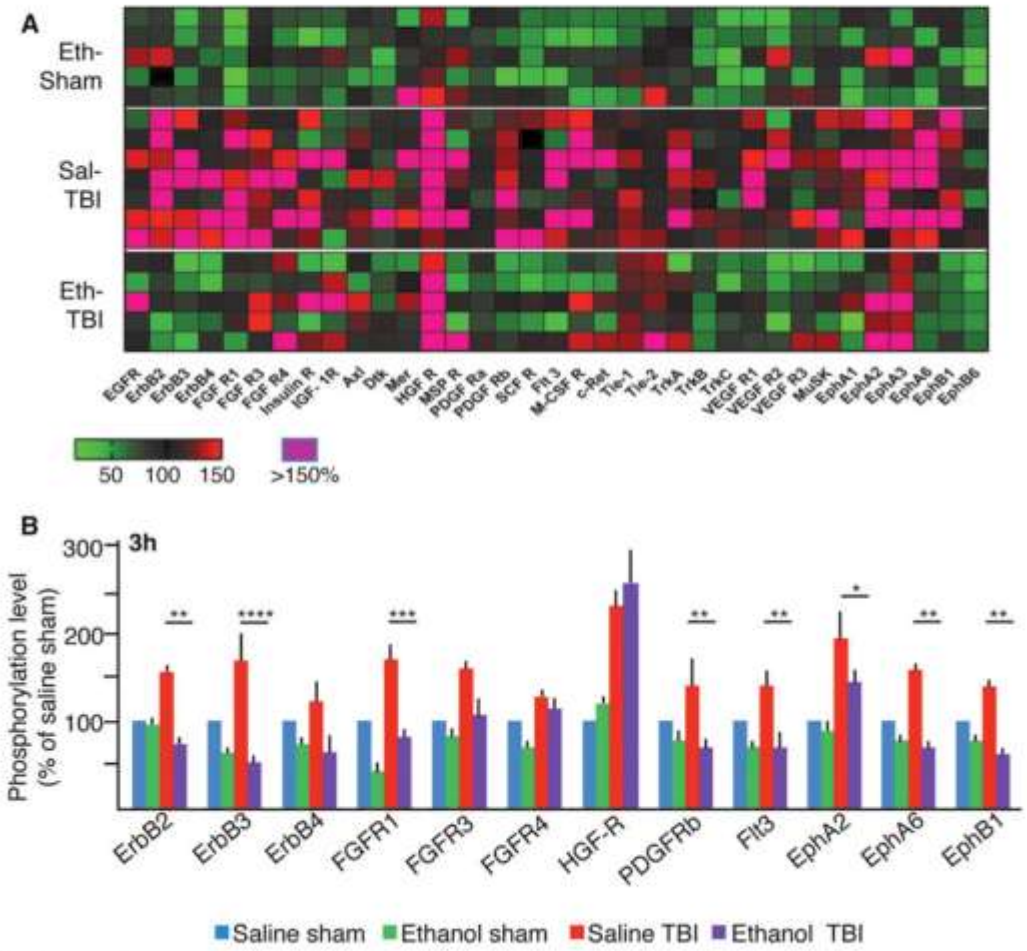

FIG. 2. Phosphorylation of multiple RTKs after TBI and their modulation by ethanol. (**A**) Heatmap depicts the relative phosphorylation level of 38 RTKs measured in samples from eth-S ($n=5$), sal-TBI ($n=7$), and eth-TBI ($n=5$), using sal-S ($n=8$) as baseline. TBI induces a significant increase in phosphorylation of 11 RTKs (ErbB2, ErbB3, FRFG1, FGFR3, FGFR4, HGF-R/c-Met, PDGFR-β, Flt3, EphA2, EphA6, and EphB1) at the 3-h time point. Ethanol pre-treatment decreases phosphorylation of ErbB2, ErbB3, FGFR1, PDGFRb, flt3, Epha6, and EphB1, but not of FGFR2 and 3, HGFR, and EphA6. (**B**) Quantification of a subset of RTK phosphorylation after TBI. In whole-cortex protein extract; TBI upregulates ErbB2, ErbB3, and FGFR1, whereas ethanol pretreatment prevents upregulation (ErbB2, $p=0.0003$; ErbB3, $p<0.0001$; FGFR1, $p=0.001$; Flt3, $p=0.0088$; EphA6, $p=0.0011$; EphB1, $p=0.0041$). Statistical analysis by two-way ANOVA with Tukey's post-hoc test. For clarity, only statistical significance for comparisons between sal-TBI and eth-TBI are graphically depicted. ANOVA, analysis of variance; RTK, receptor tyrosine kinase; TBI, traumatic brain injury. Color image is available online at www.liebertpub.com/neu

pErbB2 increase was strongly limited by pre-treatment with AG825 50 mg/kg (AG825-TBI 162 ± 46% of sal-S; $p<0.01$ vs. TBI; Supplementary Fig. 2) (see online supplementary material at http://www.liebertpub.com) or Lapatinib 50 mg/kg (Lapatinib-TBI 153 ± 65% of sal-S; $p<0.01$ vs. TBI; Supplementary Fig. 2) (see online supplementary material at http://www.liebertpub.com).

Thereafter, distinct groups of mice were administered ErbB2 inhibitors (AG825 50 mg/kg or Lapatinib 50 mg/kg) a PDGF receptor (PDGFR) inhibitor (CP-673451, 10 mg/kg) or the broad RTK inhibitor (LDN-211904, 10 mg/kg), in a single administration before TBI, and assessed for their performance in sensorimotor and behavioral tests. We also considered two groups of mice treated with a lower dose (10 mg/kg) of either Lapatinib or AG825. For comparison, independent groups of mice were pre-treated with ethanol diluted in vehicle or with vehicle alone and subject to sham surgery or to TBI. No difference in performance in any test was detected between veh-S and eth-S mice, which were comparable to saline pre-treated mice (cfr. Fig. 1).

When assessed in the Beam Walk test, mice treated with 50 mg/kg of AG825 or Lapatinib performed significantly better than vehicle-treated TBI mice and comparable to eth-TBI mice (at 2 dpi, 10.1 ± 2.7 and 12.6 ± 2.4 sec, respectively, as compared to 30.9 ± 7.8 sec in veh-

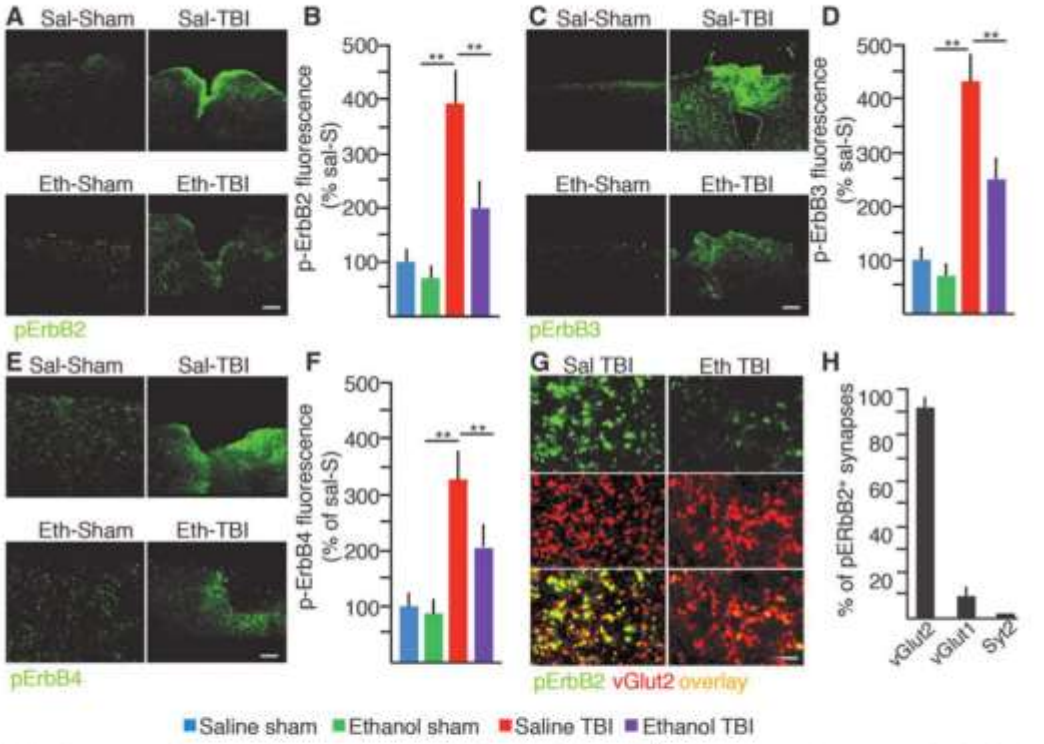

FIG. 3. Suppression of TBI-induced phosphorylation of ErbB2 and ErbB3 in vGlut2$^+$ excitatory synapses by ethanol. (**A** and **B**) Levels of phosphorylated ERbB2 were increased 3 h after TBI. Immunofluorescence intensity for pErbB2 was increased to 371 ± 68% of sal-S ($n = 4$; $p < 0.01$) in sal-TBI mice ($n = 5$), whereas ethanol pretreatment resulted in reduced elevation of pERbB2 levels ($n = 4$; $p < 0.01$ vs. sal-TBI and vs. sal-S and eth-S) after TBI (eth-TBI). Scale bar, 50 μm. (**C** and **D**) Levels of phosphorylated ErbB3 were increased after TBI. Immunofluorescence intensity for pErbB3 significantly increased compared to sal-S ($p < 0.01$) at 3 h in sal-TBI mice ($n = 4$), whereas ethanol pretreatment (eth-TBI, $n = 4$) resulted in reduced elevation of pERbB2 levels ($p < 0.01$ vs. sal-TBI and vs. sal-S) after TBI. Scale bar, 50 μm. (**E** and **F**) Increased levels of phosphorylated ErbB4 was noted after TBI. Immunofluorescence intensity for pErbB4 was significantly increased ($n = 4$; $p < 0.01$) at 3 h in sal-TBI mice, whereas ethanol pretreatment results in the reduced elevation of pERbB4 levels ($n = 4$; $p < 0.01$ vs. sal-TBI and vs. sham) after TBI. Scale bar, 50 μm. (**G** and **H**) ERbB2 phosphorylated at vGlut2$^+$ synapses after TBI. At 3 h post-injury (sal-TBI, $n = 3$), 93 ± 4% of pERbB2 clusters colocalized with vGlut2 whereas only 3 ± 2% colocalized with vGlut1 and never with inhibitory synapses synaptotagmin-2$^+$. Statistical analysis by two-way ANOVA. Scale bar 2μm. ANOVA, analysis of variance; TBI, traumatic brain injury; vGlut, vesicular glutamate transporter. Color image is available online at www.liebertpub.com/neu

TBI and 14.3 ± 2.8 sec in eth-TBI mice; $p < 0.001$ vs. veh-TBI for both compounds; ethanol was diluted in vehicle for proper comparison; Fig. 4A). The effect of ErbB inhibitors was still detectable when a 10-mg/kg dose was administered, with trends toward dose-dependent effects (although for AG825 the strong trend did not reach statistical significance; at 2 dpi, 15.1 ± 2.3 and 17.3 ± 3.4 sec and $p = 0.071$ for AG825 10 vs. 50 mg; $p < 0.05$ for Lapatinib 10 vs. 50 mg; Fig. 4A). The broad-selectivity RTK inhibitor, LDN-211904, also produced a significant improvement in performance (8.6 ± 3.4 sec; $p < 0.01$ vs. veh-TBI; Fig. 5A) whereas the PDGFR-selective drug, CP-673451, did not affect significantly the performance (at 2 dpi, 22.0 ± 6.5 sec; $p > 0.05$ vs. veh-TBI; Fig. 4A). At 7dpi, eth-TBI as well as mice treated with either dose of Lapatinib, AG825, or LDN were similar in performance to sal-S or eth-S mice, whereas sal-TBI was still significantly slower (Fig. 4B).

Likewise, performance in the Arena Escape test was significantly modified by RTK inhibitors. Both 10- and 50-mg/kg AG825- and Lapatinib-treated mice performed significantly better than vehicle-treated ones after TBI (at 2 dpi, 9.1 ± 2.4 and 6.4 ± 1.1 sec for AG825 and 11.3 ± 1.3 and 7.5 ± 1.6 sec, respectively, vs. 17.2 ± 2.4sec; $p < 0.05$; Fig. 4C) and comparably to the ethanol-treated ones (7.4 ± 2.2 sec, $p > 0.05$ when compared to AG825 and Lapatinib). Likewise, mice pretreated with the broad-selectivity RTK inhibitors were comparable to veh-S, eth-S, or eth-TBI mice (6.1 ± 2.4 sec; $p > 0.05$ when compared to veh-S or eth-S or eth-TBI), whereas mice pretreated with the PDGFR inhibitor performed comparably to the veh-TBI mice (20.0 ± 6.5 sec; $p > 0.05$ vs. veh-TBI; Fig. 4C). Like in the Beam Walk, in the Arena Escape tests the improved performance of mice acutely treated with AG825 or Lapatinib was still detectable at 7 dpi (Fig. 4D).

To explore the translational potential of ErbB inhibitors as therapeutic agents for acute TBI, we administered a single dose of 50 mg/kg of Lapatinib (an FDA-approved drug, is known to be able to penetrate the brain parenchyma)[55] or of the alternative ErbB

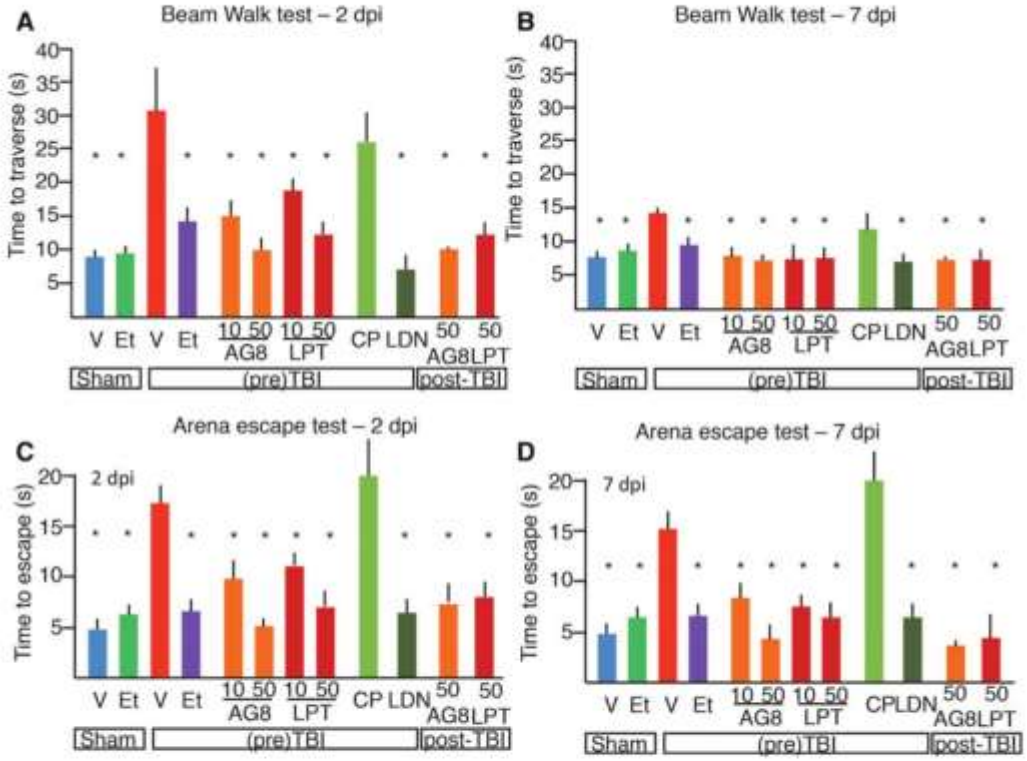

FIG. 4. Improvement in behavioral outcome by administration of ErbB inhibitors before or after TBI. (**A** and **B**) Treatment with ErbB inhibitor AG825 or Lapatinib before or after TBI resulted in improved recovery in the Beam Walk test. To demonstrate whether selective RTK inhibition may recapitulate EI effect, mice were administered with either 10 or 50 mg/kg of the ErbB2-specitic inhibitor, Lapatinib ($n=6$ and $n=4$, respectively), or of the pan-ErbB inhibitor, AG825 ($n=5$ and $n=4$, respectively), 30 min before TBI. Mice treated with 10 mg/kg of AG825 or Lapatinib performed significantly better than vehicle-treated TBI mice at 2 dpi ($p<0.001$ vs. veh-TBI for both compounds). Mice administered with 50 mg/kg of AG825 or Lapatinib mice showed a trend toward better performance than mice administered with a 10-mg/kg dose ($p<0.05$ for Lapatinib 10 vs. 50 mg). Administration of the broad-selectivity RTK inhibitor, LDN-211904 (10 mg/kg; $n=4$), also produced a significant improvement in performance ($p<0.01$ vs. veh-TBI) whereas the PDGFR-selective drug, CP-673451 (10 mg/kg; $n=4$) did not affect significantly performance ($p>0.05$ vs. veh-TBI). Administration of AG825 or Lapatinib (50 mg/kg; $n=4$ and $n=4$, respectively) 30 min after TBI resulted in a significant improvement in performance at 2 dpi ($p<0.05$ vs. veh-TBI). At 7 dpi, eth-TBI as well as mice treated with either dose of Lapatinib, AG825, or LDN were similar in performance to sal-S or eth-S mice, whereas sal-TBI were still significantly slower. Statistical analysis by one-way ANOVA with Bonferroni post-hoc test. (**C** and **D**) Performance in the Arena Escape test was significantly improved in mice pretreated with AG825 (10 or 50 mg/kg; $n=5$ and $n=4$, respectively), Lapatinib (10 or 50 mg/kg; $n=6$ and $n=4$, respectively) or LDN-211904 (10 mg/kg; $n=4$). At 2 dpi, AG825, Lapatinib, 10 or 50 mg/kg, and LDN-211904 pre-treated mice performed significantly better than veh-TBI mice ($p<0.05$). Mice pre-treated with the PDGFR inhibitor (10 mg/kg; $n=3$) performed comparable to veh-TBI mice. At 7 dpi, mice treated with ethanol, Lapatinib, AG825, or LDN-211904 displayed a comparable performance and were significantly better than vehicle-treated TBI mice. Notably, mice treated with either 50 mg/kg of AG825 or 50 mg/kg of Lapatinib ($n=4$ and $n=4$, respectively) 30 min after TBI displayed a significant improvement in performance compared to sal-TBI ($p<0.05$). This beneficial effect was persistent at 7 dpi. Statistical analysis by one-way ANOVA with Bonferroni post-hoc test. For clarity, statistical significance indicated graphically is corresponding to the comparison each treatment group with veh-TBI. ANOVA, analysis of variance; dpi, days post-injury; EI, ethanol intoxication; RTK, receptor tyrosine kinase; TBI, traumatic brain injury. Color image is available online at www.liebertpub.com/neu

inhibitor, AG825, 30 min after TBI. Performance of mice in the Beam Walk and Arena Escape tests was evaluated at 2 and 7 dpi. Interestingly, mice treated with either ErbB inhibitor post-TBI displayed a significantly improved performance in both tests (for the Beam Walk, 10.1 ± 0.6 and 12.5 ± 2.3 sec at 2 dpi; for the Arena Escape, 6.2 ± 2.2 and 8.4 ± 1.9 sec for AG825 and Lapatinib, respectively, at 2 dpi; $p<0.05$ compared to sal-TBI). The beneficial effect was persistent at 7 dpi.

Traumatic brain injury–induced neuronal loss is prevented by ethanol intoxication and ErbB inhibitors

We then explored the structural counterparts of the reduced behavioral disturbances observed in ethanol-pretreated TBI mice. To this aim, we measured the density of NeuN-positive cells in the injury area ("core," defined by the longitudinal axis of the injury site in coronal sections) and in the penumbra (Supplementary Fig. 1

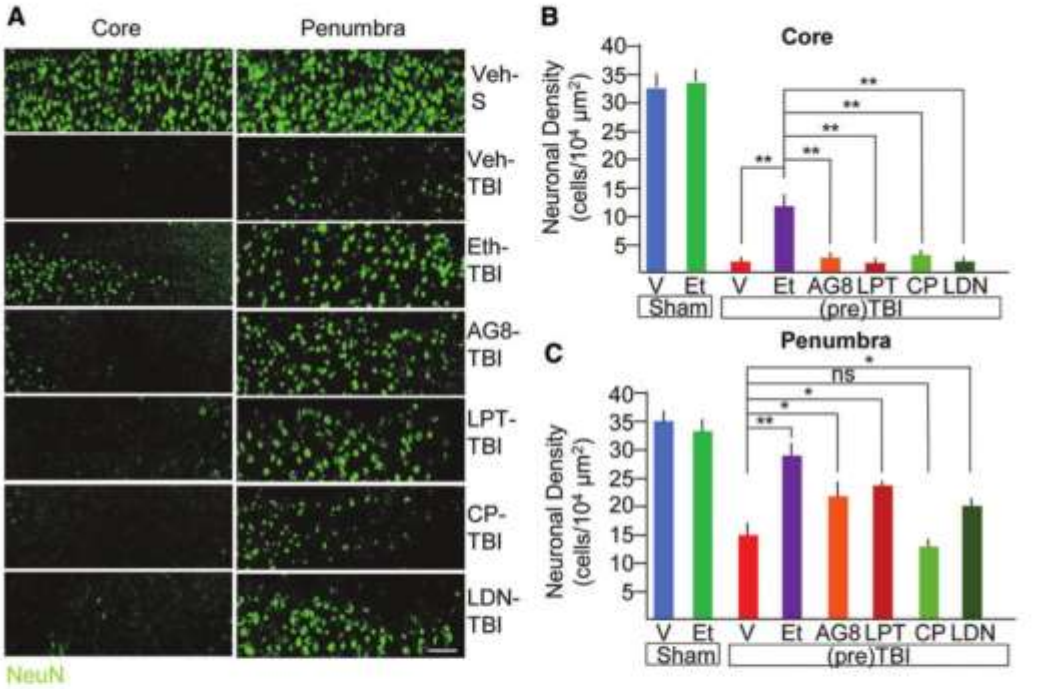

FIG. 5. Ethanol pre-treatment and ErbB inhibitors treatment reduces neuronal loss after TBI. (**A–C**) At 7 dpi, mice administered with vehicle alone ($n=3$) or ethanol ($n=3$) in vehicle that underwent sham surgery displayed a comparable density of NeuN$^+$ cells in the "core" and in the "penumbra" ROI. Veh-TBI ($n=6$) displayed an almost complete loss of NeuN$^+$ cells in the core as compared to veh-S ($p<0.001$) and a significant decrease of NeuN$^+$ in penumbra ($p<0.001$). Ethanol pretreatment (eth-TBI; $n=4$) resulted in a larger population of NeuN$^+$ cells at the injury site ($p<0.01$) and in the penumbra ($p<0.01$; vs. both veh-S and veh-TBI). Administration of ErbB inhibitors (10 mg/kg; $n=6$ and $n=5$ for Lapatinib and AG825) or of broad-spectrum RTK inhibitor LDN-211904 (10 mg/kg; $n=4$) did not affect NeuN$^+$ cells in the core ($p>0.05$ vs. veh-TBI), but significantly preserved it in the penumbra (as compared to veh-TBI, $p<0.05$). Administration of the PDGFR inhibitor (10 mg/kg; $n=4$) did not affect the number of NeuN$^+$ cells in the core ($p>0.05$) or in the penumbra ($p>0.05$). Statistical analysis by one-way ANOVA with Bonferroni post-hoc test .Scale bar 20μm. ANOVA, analysis of variance; NeuN, neuronal nuclei; ROI, region of interest; RTK, receptor tyrosine kinase; TBI, traumatic brain injury. Color image is available online at www.liebertpub.com/neu

(see online supplementary material at http://www.liebertpub.com); see Methods). As control, mice undergoing sham surgery were administered either vehicle (5% PEG400/5% Tween80/90% Saline) alone (veh-S) or ethanol diluted in vehicle (eth-S). In sham mice, ethanol administration *per se* did not affect the density of NeuN-positive cells (33.4 ± 3.1 vs. $34.9\pm2.2/10^4$ μm^2 NeuN$^+$ cells in veh-S and eth-S, respectively, $p>0.05$; Fig. 4A). On the other hand, 7 days after TBI, cortical samples from veh-TBI mice displayed a primary injury site largely devoid of NeuN$^+$ cells ($2.3\pm0.9/10^4$ μm^2 NeuN$^+$ cells as compared to $33.4\pm3.1/10^4$ μm^2 in veh-S mice; $p<0.001$; Fig. 4A,B) whereas a significant decrease was observed in the penumbral area ($15.6\pm1.1/10^4$ μm^2 vs. $35.5\pm2.5/10^4$ μm^2 in veh-S and vs. $34.4\pm2.1/10^4$ μm^2 in eth-S mice; $p<0.001$; Fig. 4B,C). Notably, ethanol (diluted in vehicle) pre-treated TBI mice displayed a significantly larger population of surviving NeuN$^+$ neurons in the injury site ($11.3\pm1.3/10^4$ μm^2; $p<0.01$) and a strong preservation of NeuN$^+$ neurons in the penumbra ($27.1\pm1.9/10^4$ μm^2; $p<0.01$ vs. both veh-S and veh-TBI; Fig. 4B,C), further supporting the view of neuroprotective effects of acute ethanol in TBI.

Because our findings had shown that EI results in a significant suppression of TBI-induced ErbB phosphorylation and we have shown that ErbB inhibitors partially recapitulate EI effect, we set out to verify whether selective inhibition of ErbB signaling could be sufficient to partially recapitulate EI effect on neuronal survival. To this aim, mice were administered either with two structurally distinct ErbB inhibitors (Lapatinib, 10 mg/kg and AG825 10mg/kg; because both 50 and 10 mg/kg proved effective in behavioral tests, we selected the lowest dose to ensure specificity) or with a PDGFR inhibitor (CP-673451, 10 mg/kg) or with a broad-spectrum RTK inhibitor (including EphR within its selectivity spectrum, LDN-211904, 10 mg/kg). All drugs were administered in a single dose before the TBI and mice were then sacrificed after 7 days for the evaluation of the neuronal survival.[56] Single-dose administration of either drug did not affect apnea time and acute or overall survival (not shown), and all drugs were well tolerated. Although ErbB inhibitors did not affect NeuN$^+$ cells in the core (2.3 ± 0.9 and $1.5\pm0.3/10^4$ μm^2 for AG825 and Lapatinib, respectively; $p>0.05$ vs. veh-TBI), they significantly preserved neuronal density in the penumbra (21.3 ± 3.2 and $23.3\pm4.7/10^4$ μm^2 for AG825 and Lapatinib, as compared to $10.6\pm5.1/10^4$ μm^2 in veh-TBI; $p<0.05$; Fig. 4A,C), albeit to a lesser extent than what obtained with ethanol. In fact, the broad-spectrum RTK also caused a significant increase in surviving NeuN$^+$ cells in the penumbra ($19.9\pm3.2/10^4$ μm^2;

$p < 0.05$ vs. veh-TBI), whereas administration of the PDGFR inhibitor was much less effective ($13.5 \pm 4.5/10^4$ μm^2; $p < 0.05$). Neither of them, however, helped with preservation of $NeuN^+$ cells in the core (2.9 ± 2.4 and $1.9 \pm 0.2/10^4$ μm^2; $p > 0.05$; Fig. 4A,C).

Traumatic brain injury–induced increase in pErbB2 excitatory synapses on parvalbumin interneurons is prevented by ethanol intoxication

ErbB receptors are expressed mainly in inhibitory neurons (in the cortex),[35–37] including PV interneurons, where they control the strength of excitatory inputs[38,40] and, in turn, the level of perisomatic inhibition and principal neurons firing.[39,41] We therefore elected to investigate whether ErbB2 phosphorylation in excitatory synapses on PV interneurons was upregulated by TBI and affected by ethanol. PV interneurons were identified by immunostaining for PV, and the subpopulation within a 500-μm ROI centered on the injury site and restricted to layers I–IV was considered. On each PV interneuron, the fraction of vGlut2 $ErbB2^+$ synapses over the total $vGlut2^+$ was counted. The fraction of $vGlut2^+$ $ErbB2^+$ was comparatively low in sal-S and eth-S ($8 \pm 5\%$ and $5 \pm 4\%$ of all $vGlut2^+$ were $pErbB2^+$). However, in sal-TBI mice, $57 \pm 21\%$ of $vGlu2^+$ on PV interneurons was $pErbB2^+$. Notably, in eth-TBI samples, the fraction of $vGlut2^+$ $ErbB2^+$ synapses on PV interneurons was significantly lower than in sal-TBI samples ($34 \pm 18\%$; $p < 0.05$ vs. sal-TBI; Fig. 6A,B). Thus, TBI results in ErbB phosphorylation in excitatory synapses on PV interneurons, an effect prevented by concomitant EI. Given that EI and TBI reciprocally regulate PV excitatory input, we reasoned that TBI-induced increase in PV activation and perisomatic inhibition may have pathogenic effects, which would be prevented by EI. We therefore set out to manipulate directly PV firing in TBI, to verify whether suppression of PV firing may recapitulate EI effect.

Chemogenetic inhibition of parvalbumin interneurons partially mimics but does not fully preclude ethanol intoxication–associated neuroprotection

We injected AAV9 encoding either cation- or anion-permeable engineered ion channels with orthogonal pharmacology (PSAM, either excitatory or inhibitory) in the somatosensory cortex of PV-Cre mice.[48] Mice were then injected 30 min before further procedures with either saline alone or the orthogonal agonist (pharmacologically selective effector module, PSEM308) and subjected to either sham surgery or TBI. Mice were sacrificed at 7 dpi. The density of $NeuN^+$ cells at 7 dpi both in the core and in the penumbra of the TBI-induced lesion was used as a readout. In sham-operated mice, whether administered with saline or PSEM and expressing either excitatory or inhibitory PSAM, $NeuN^+$ cell density was comparable at 7 dpi (32.4 ± 4.4, 33.4 ± 2.9, 31.9 ± 6.5, and 34.2 ± 4.8 $NeuN^+$ cells/10^4 μm^2; $p > 0.05$; Fig. 6C–E). In saline pre-treated mice (sal-actPSAM-TBI or sal-inhPSAM-TBI, only saline but no PSEM administered), irrespective of PSAM expression, TBI resulted in almost complete loss of $NeuN^+$ cells in the core lesion (2.3 ± 1.4 and 1.9 ± 1.1 $NeuN^+$ cells/10^4 μm^2 in saline-treated mice expressing either actPSAM or inhPSAM; $p < 0.05$ vs. sal-S samples; Fig. 6D,E) and a significant loss of neurons in the penumbral zone (20.1 ± 3.3 and 19.4 ± 4.4 $NeuN^+$ cells/10^4 μm^2, $p < 0,05$ vs. sal-s samples; Fig. 6D,E). However, when PV interneurons were activated in mice undergoing TBI (PSEM-actPSAM-TBI), the number of $NeuN^+$ cells in the core was not affected (3.1 ± 1.4 $NeuN^+$ cells/10^4 μm^2), but an increased loss of neurons in the penumbra was observed (10.5 ± 2.7 $NeuN^+$ cells/10^4 μm^2; $p < 0.05$ vs. sal-actPSAM-TBI; Fig. 6D). On the other hand, inhibiting PV interneurons (PSEM-inhPSAM-TBI) produced a significantly higher number of $NeuN^+$ cells in the core (8.2 ± 3.1; $p < 0.05$ vs. sal-TBI) and a larger preservation of $NeuN^+$ cells in the penumbra (24.4 ± 3.2 $NeuN^+$ cells/10^4 μm^2; $p < 0.05$ vs. sal-inhPSAM-TBI). Thus, acute inhibition of PV firing resulted in reduced long-term principal neurons vulnerability whereas activation of PV firing increased neuronal loss.

We than reasoned that if reducing excitation of PV interneurons was the major mechanism of EI-associated neuroprotection and suppressing PV firing would preclude any further beneficial effect of EI. We therefore administered ethanol (5 g/kg) together with PSEM in PV-Cre mice expressing the inhibitory PSAM and compared the loss of neurons to that observed in PSEM-only administered mice. Although EI did not improve neuronal survival in the core lesion when applied together with the chemogenetic inhibition of PV interneurons (9.3 ± 1.4 cells/10^4 μm^2; $p > 0.05$ vs. PSEM alone or EI alone), EI exerted an additional beneficial effect on the preservation of neurons in the penumbra (28.4 ± 1.1 cells/10^4 μm^2; $p < 0.05$ vs. sal-TBI and vs. PSEM-TBI; Fig. 6E), with PSEM + EI being comparable to EI alone (29.5 ± 2.2 cells/10^4 μm^2, $p > 0.05$

FIG. 6. pErbB phosphorylation involves excitatory synapses on PV interneurons and chemogenetic suppression of PV interneurons reduces neuronal loss after TBI. (**A** and **B**) pErbB activation in excitatory synapses on PV interneurons is reduced by ethanol pretreatment. In sal-TBI mice, a significantly larger fraction of $vGlut2^+$ synapses was $pErbB2^+$ compared to sal-S and eth-S; in eth-TBI samples, however, the fraction of $vGlut2^+$ $ErbB2^+$ synapses on PV interneurons were significantly lower than in sal-TBI samples ($p < 0.05$, sal-TBI vs. eth-TBI). Scale bar, 4 μm. (**C–E**) Enhancement of PV interneuron activity reduced neuronal survival. All PV-Cre mice were injected with the AAV9 for PSAM expression. In sham-operated mice (sal-actPSAM-S, $n = 3$; PSEM-actPSAM-S, $n = 3$; sal-inhPSAM-S, $n = 3$; PSEM-inhPSAM-S, $n = 3$), $NeuN^+$ cells counts were comparable at 7 dpi ($p > 0.05$; panels C–E) and were comparable to saline-treated, naïve mice (C). Sal-TBI (sal-actPSAM-TBI, $n = 4$; sal-inhPSAM-TBI, $n = 4$) resulted in the almost complete loss of $NeuN^+$ cells in the core lesion ($p < 0.05$ vs. sham samples) and a significant decrease in the penumbra ($p < 0.05$). Activation of PV interneurons firing (PSEM-actPSAM-TBI; $n = 5$) did not affect the number of $NeuN^+$ cells in the core (D), but worsened the loss of $NeuN^+$ immunoreactivity in the penumbra ($p < 0.05$ vs. sal-actPSAM-TBI; panel D). Conversely, inhibiting PV interneurons (PSEM-inhPSAM-TBI; $n = 5$) resulted in a higher number of $NeuN^+$ cells in the core (E) and significantly higher $NeuN^+$ cells in the penumbra ($p < 0.05$ vs. sal-inhPSAM-TBI; panel E). Coadministration of ethanol and PV inhibition (eth-PSEM-inhPSAM-TBI; $n = 4$) did not increase neuronal survival further in the core lesion ($p > 0.05$ vs. PSEM alone; panel E), but further enhanced the preservation of neurons in the penumbra ($p < 0.05$ vs. sal-actPSAM-TBI and vs. PSEM-inhPSAM-TBI; panel E) to a level comparable to eth-inhPSAM-TBI mice ($n = 3$). Reciprocally, application of ethanol together with PV activation (eth-PSEM-actPSAM-TBI; $n = 4$) did not increase the number of NeuN in the core, but increased neuronal preservation in the penumbra ($p < 0.05$ vs. PSEM-actPSAM-TBI; panel D), whereas both values remained lower than eth-actPSAM-TBI mice ($n = 3$). Statistical analysis by one-way ANOVA with Bonferroni's post-hoc test. Scale bar, 200 μm. ANOVA, analysis of variance; dpi, days post-injury; NeuN, neuronal nuclei; ns, not significant; PV, parvalbumin; RTK, receptor tyrosine kinase; TBI, traumatic brain injury; vGlut, vesicular glutamate transporter. Color image is available online at www.liebertpub.com/neu

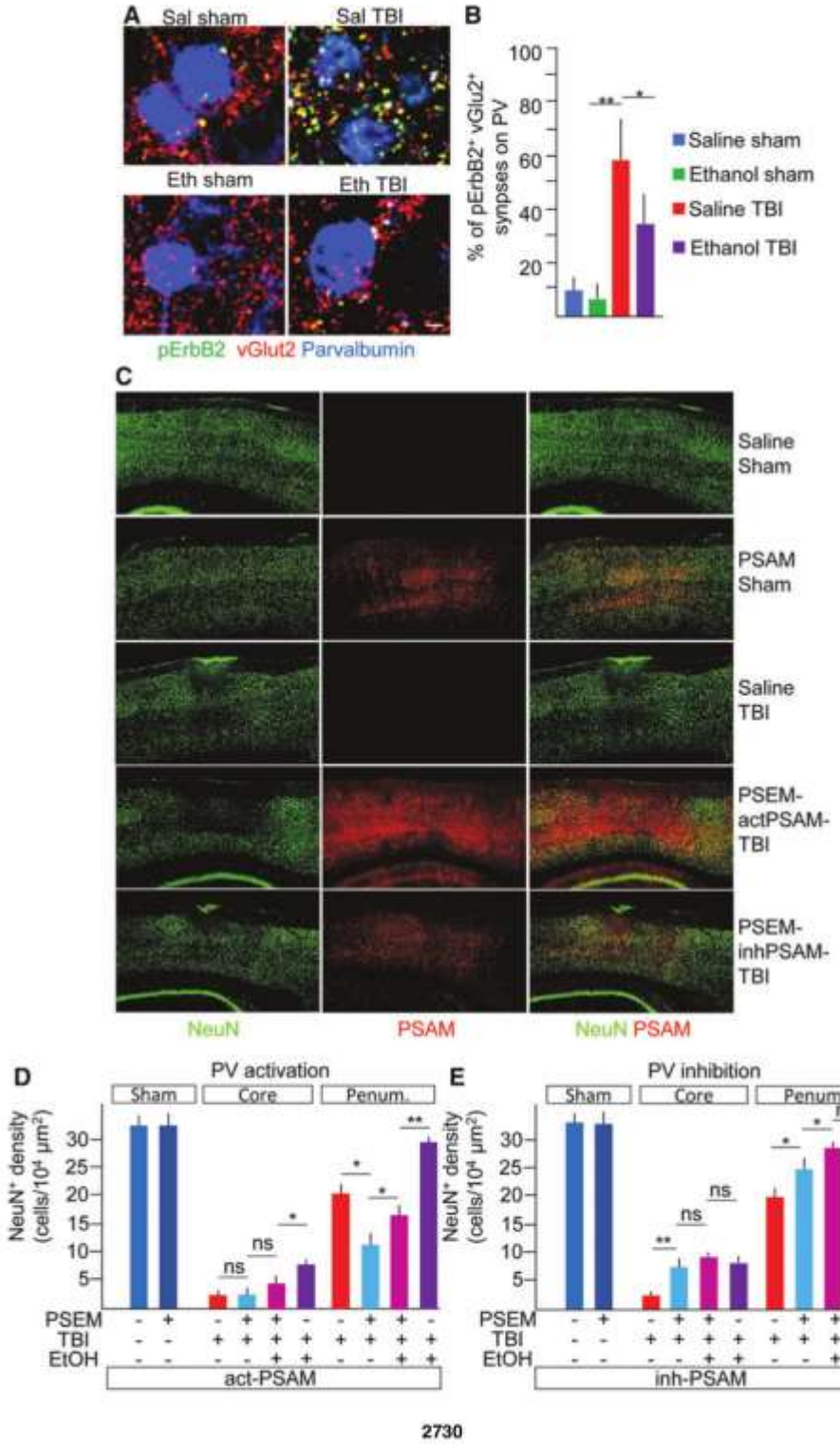

2730

vs. PSEM + EI; Fig. 6E). Likewise, when ethanol was pre-administered to mice in which PV firing was enhanced, it did not enhance survival in the core of the lesion compared to chemogenetics only (4.1 ± 1.7 cells/10^4 μm^2; $p > 0.05$ vs. PSEM) and the PSEM + EI group showed fewer cells than EI alone (7.9 ± 1.2 cells/10^4 μm^2). Conversely, the addition of EI to the chemogenetic activation of PV interneurons increased neuronal survival compared to chemogenetic only (17.6 ± 2.4 cells/10^4 μm^2 vs. 10.5 ± 2.7 $NeuN^+$ cells/10^4 μm^2; $p < 0.05$; Fig. 6), although did not reach the level of preservation produced by EI alone (27.8 ± 3.4 $NeuN^+$ cells/10^4 μm^2). Taken together, these data indicate that inhibition of PV interneurons does not preclude EI effects, but chemogenetic activation of PV strongly decreases EI-associated neuroprotection.

Ethanol intoxication does not reduce overall survival upon traumatic brain injury

Finally, we retrospectively investigated whether EI had a significant effect on the overall survival of experimental mice to TBI. In the sal-TBI and veh-TBI groups, a total of 52 mice underwent TBI procedure and 11 died either during the procedure or met the pre-specified criteria for euthanization (21.2%). In eth-TBI groups, a total of 45 mice underwent TBI, with 12 fatal outcomes (26.7%). When all animals treated with inhibitors were grouped together, 7 fatalities were observed out of 48 which underwent TBI (14.6%). The χ^2 value was 1.067, with $p = 0.58$. Therefore, neither ethanol administration nor RTK inhibitors caused a significant increase in overall mortality after TBI.

Discussion

Here, we have shown that ethanol pre-treatment, resulting in a BAL comparable to the one that was found to be highly correlated with protective effects on TBI patients (>230 mg/dL),[10] results in enhanced recovery of sensorimotor skills and in reduced neuronal loss in cortex after blunt TBI, supporting the hypothesis of neuroprotective effects of ethanol observed in clinical series. Lower doses of ethanol were not explored, because we have previously reported that the dose of 1 g/kg does not provide protective effects on sensorimotor performance.

We have investigated the involved mechanisms exploiting as an entry point the pattern of phosphorylation of multiple RTK after TBI. Activation of RTK may be a physiological, protective response set in motion by the trauma itself (and therefore, in agreement with the classical antiapoptotic role of RTK, play a protective role in TBI). Under this viewpoint, EI-associated downregulation of activation of several RTKs may reveal that EI may limit the initial damage and prevent the activation of the protective response in the first place. Given that ethanol has powerful GABAergic activities[26] and it is an NMDAR antagonist,[25] it may prevent excitation-related damage[7] and limit excitation-related RTK activation (such as the phosphorylation of ErbB[58] or FGFR and EphB phosphorylation).[31,57] On the other hand, in the CNS, RTK may be involved in maladaptive responses to trauma, which may be directly pathogenic. In fact, activation of PDGFR has been linked to increased permeability of the blood–brain barrier (BBB) after trauma, and the PDGFR inhibitor, Imatinib, has been shown to reduce edema and reduce cognitive dysfunctions.[33] Further, activation of the RTK EphA2 has been linked to increased BBB dysfunction and neuronal loss in a stroke model.[58] Thus, although the RTK activation pattern reveals the breadth of EI impact on TBI-associated signaling events, the specific role of each RTK (and associated cascades) in EI-associated neuroprotection should be investigated in a case-by-case manner. Of note, some cascades endowed with pathogenic potential are not modulated by EI: Tie-2 phosphorylation, which is linked to reduced permeability of endothelial barriers, is not significantly modified by ethanol pretreatment.[34] Likewise, HGFR signaling is strongly activated by TBI, but not affected by EI. The role of HGFR in TBI has never been explored before, but its involvement in enhancing NMDAR[59] may suggest a potential involvement.

Notably, several of the TBI-activated RTKs are also involved (although not exclusively) in the regulation of synaptic events: EphB signaling can potentiate NMDAR currents[60] and may therefore enhance glutamate toxicity in the acute phase of TBI. Activation of other RTKs, such as FGFR1 and the ErbB family, is known to control protein clustering at inhibitory synapses[61,62] and excitatory inputs on interneurons,[28] respectively. Thus, our RTK screening reveals that EI may affect strongly events unfolding at the synaptic level after trauma and may identify new targets for intervention at this level.

Focusing on the ErbB receptor family, we have shown that TBI induces the phosphorylation of ErbB receptors in excitatory synapses and that specific inhibitors of ErbB are able to recapitulate a significant fraction of EI-associated neuroprotection. ErbB family expression pattern has been originally reported to include pyramidal cells as well as inhibitory interneurons. However, recent data obtained by *in situ* hybridization and reporter expression based on ErbB4 endogenous promoter[35–38] as well as cell-specific knockout experiments[40] have demonstrated that ErbB4 expression is restricted in the cortex only to inhibitory interneurons (although ErbB4 is expressed in several non-GABAergic subpopulations in subcortical structures) and that ErbB4 is dispensable for the function of excitatory synapses between pyramidal neurons.[36] Although data on the expression of ERbB2 and ErbB3 are not as detailed, ErBB family members signal either as ERbB4 homodimers or as heterodimers of ErbB4, ErbB3, and Erbb2,[63] and therefore their expression is predicted to be comparable. Thus, we show that TBI induces the phosphorylation of ErbB in excitatory synapses on inhibitory interneurons. Among inhibitory interneurons, ErbB expression in PV interneurons has been shown to be highly relevant for the control of the function of these cells in normal cortex[39,40] and under pathological conditions.[64,65]

The effect of EI on ErbB and PV activation may appear paradoxical, considering the GABAergic action of ethanol. However, ErbB phosphorylation on interneurons has been shown to be homeostatically regulated: Reduced cortical excitation leads to the decrease in ErbB phosphorylation in PV interneurons, depotentiation and de-stabilization of excitatory synapses, and, ultimately, reduced PV activation.[27,66] Reciprocally, activation of ErbB results in the insertion of α-amino-3-hydroxy-5-methyl-4-isoxazolepropionic acid receptor (AMPAR) and increase excitation to inhibitory interneurons,[27] although the ratio between AMPAR and NMDAR may change significantly.[38] Thus, after TBI-associated depolarization, upregulation of ErbB in excitatory synapses on PV interneurons may result in upregulation of perisomatic inhibition, whereas concomitant EI may prevent it and leave PV interneurons at their basal state of excitatory input. We speculate that upregulation of ErbB phosphorylation may be a homeostatic event triggered by TBI-triggered excitation and may lead to increased PV excitation after TBI. In fact, ErbB receptors are activated by the extracellular domain of several isoforms of neuregulins (Nrg). Immature Nrg are transmembrane proteins (widely expressed in principal neurons)[67] whose extracellular N-terminal

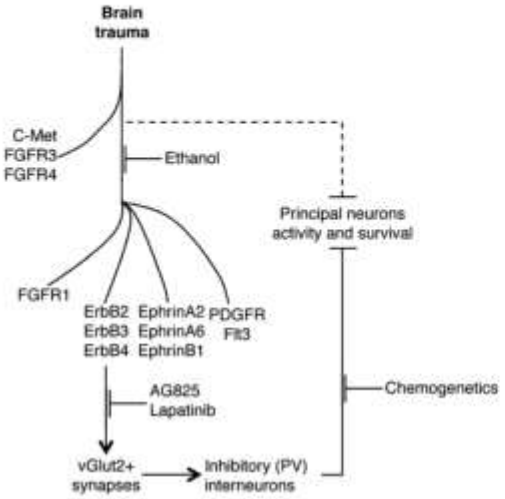

FIG. 7. ErbB-mediated the effect of ethanol on inhibitory microcircuitry after TBI. Ethanol pre-treatment results in suppression of the activation of multiple RTKs by TBI. In particular, TBI-induced activation of ErbB phosphorylation in vGlut2$^+$ synapses on PV interneurons is suppressed by ethanol. Loss of excitation attributed to excess inhibition may increase the vulnerability of neurons to TBI-induced neurotoxic cascades; and by suppressing PV-mediated perisomatic inhibition, ethanol may enhance neuronal survival. This effect is recapitulated by either direct ErbB inhibition or by direct suppression of PV firing by chemogenetics. FGFR1, fibroblast growth factor receptor 1; PDGFR, platelet-derived growth factor receptor; PV, parvalbumin; RTK, receptor tyrosine kinase; TBI, traumatic brain injury; vGlut, vesicular glutamate transporter.

domain is released upon activity-dependent proteolysis[68] and activates ErbB family receptor signaling.[28] Nrg1 has been shown to act directly on ErbB receptors localized on interneurons to enhance the release of GABA.[67,69] In fact, seizure activity strongly enhances activation of the Neuregulin1/ErbB signaling unit,[70] whereas deletion of ErbB4 in PV interneurons increases seizures susceptibility.[67] On the other hand, administration of soluble Nrg1 rapidly upregulates excitatory inputs in PV interneurons through ErbB4 signaling.[27]

If excitatory input to PV is upregulated as a consequence of TBI, and prevented by EI, downregulation of PV firing would mimic, at least partially, EI effects. Our chemogenetic manipulation of PV firing, in fact, demonstrates that whereas increasing PV firing is detrimental, decreasing it results in an improved neuronal survival. This result may apparently contradict the current model of hyperexcitability and excitotoxicity-induced neuronal death in TBI.[71] Although a number of neurons may be directly killed by an excitotoxic mechanism at the instance of trauma, it must be noted that cortical neurons subject to TBI develop a hyperexcitable phenotype several weeks after trauma.[71,72] On the other hand, recordings of sensory-evoked responses in multiple TBI models have revealed that cortical neurons are largely hypoactive[68] and do not respond to sensory stimulation in agreement with increased inhibition.[73–75] This effect has been hypothesized to contribute to the generation of TBI-associated acute neurological deficits.[75] Thus, cortical neurons may be actually hypoactive soon after trauma, an effect that may be related to increased inhibition (in fact, activation of PV interneurons have been shown to be sufficient to completely shutting down the firing of principal cells).[41]

Although the mechanisms linking neuronal hypoactivity to cell death in TBI require further elucidation, the current evidence is in agreement with the view that preventing neuronal silencing by either preventing ErbB upregulation (as in the case of EI) or reducing perisomatic inhibition (as in the case of chemogenetic inhibition of PV interneurons) may contribute to neuroprotection (Fig. 7). In fact, neuronal activity has been shown to increase resilience of neurons to several toxic agents and to neurodegenerative processes through activity-controlled neuroprotective transcriptional programs[36,76–79] and silencing neurons renders them more sensitive to the degenerative processes (Fig. 6).[46]

Nevertheless, the neuroprotective mechanisms of EI may extend beyond the limitation of post-TBI inhibition. In fact, chemogenetic suppression of PV interneurons does not preclude EI effects and EI enhances neuronal survival even in the case of strong activation of PV interneurons. Given that ethanol is both a GABA agonist[26,51] as well as an NMDAR antagonist,[25] EI-associated neuroprotection may include direct decrease of excitability at the instance of trauma, reduced excitotoxicity through glutamate receptor inhibition, as well as modulatory effects on the neuroimmunological response.[20]

Intriguingly, blockade of ErbB2 signaling by trastuzumab enhances peripheral nerve regeneration after acute or chronic damage.[80] However, the mechanism involved requires the interaction between Neuroligin expressed on axons and ErBB2 and epidermal growth factor receptor (EGFR) expressed on Schwann cells, whose interactions control Schwann cell dedifferentiation after injury and may therefore be independent of potential effects in the CNS.[80] Nevertheless, in polytrauma patients suffering from central and peripheral nervous system injuries, targeting of ErbB signaling would be highly attractive for the delivery of a double benefit.

The present work has been performed, in agreement with ethical guidelines for animal experimentation, providing the animals with the best supportive care and with the opportune measures to prevent unnecessary pain. This has required the administration of O_2 during the procedure and the treatment of animals with buprenorphine. Although these conditions are not comparable to those experienced by human patients after TBI, we have provided evidence showing that the combination of ethanol and buprenorphine did not result in additional respiratory suppression and $PaCO_2$ levels were comparable in ethanol and saline pre-treated animals. In addition, administration of O_2 has been shown to have neuroprotective effects in a TBI + hemorrhagic shock model.[81] Although administration of O_2 may have affected the disease process examined in our model, it must be stressed that neuroprotection was observed with hypoxemia lasting for no less than 2 h, whereas our animals were returned to ambient air within 15 min of the trauma. Further, any protective effect of O_2 would have been balanced across groups, given that PaO_2 was comparable across treatment groups.

We have identified a previously unrecognized strong effect of TBI on ethanol metabolism leading to distinct pharmacokinetics in eth-TBI versus eth-S, which resulted in significantly higher levels of ethanol assessed 3 h (but not 15 min after TBI). Given that the kinetics of the BAL are different in terms of metabolism, they could not be matched by increasing the dose administered to the eth-S group. In addition, administration of doses larger than 5 g/kg (32% ethanol [v/v]) may be against ethically acceptable practices for animal experimentations given that they may cause mucosal

damage or unacceptably high mortality rates. TBI has been previously shown to affect liver biochemistry and gene expression,[82,83] which may affect drug metabolism[84]; in addition, TBI decreases perfusion of the liver (and of other abdominal organs).[85] These factors may contribute to the altered pharmacokinetics of ethanol in TBI and may contribute to accounting for the increased BAL values. Thus, the difference in BAL obtained by administering the same ethanol dose in eth-S and eth-TBI mice should be considered a limitation of the present study (and further investigations of TBI-induced changes in pharmacokinetics are warranted). However, it is noteworthy that for no RTKs, the effect of eth-S and eth-TBI was qualitatively divergent (i.e., eth-S and eth-TBI either showed both to decrease RTK [such as for ErbB2, ErbB3, FGFR1, Flt3, and PDGFR] activation or to have no or limited effect on RTK activation [like for HGFR, FGFR3, and EphA2]), and there is no evidence suggesting that higher levels of ethanol found in eth-TBI mice may have a radically different or opposite effect on RTK than those observed in eth-S mice. Therefore, the difference in BAL between eth-S and eth-TBI does not negate the main conclusions of the article. Given that patients with very high BAL have been reported on,[86] and in clinical series ethanol has been reported to be protective for the groups with the highest BAL,[10] the effect of high-dose ethanol on TBI remains relevant for clinical and translational investigations.

The translational potential of our finding is supported by the identification of Lapatinib (an FDA-approved drug for the treatment of breast cancer) as a potential neuroprotective agent when administered before but, most important, also after the trauma. Lapatinib pharmacokinetics have been described and partial, dose-dependent penetration of the brain has been shown in murine models.[54,87] Penetration of brain parenchyma has been shown to be enhanced when the BBB is disrupted,[88] suggesting that it may reach therapeutically relevant concentrations in murine and human brains after TBI. We have supported the Lapatinib data with a second ErbB inhibitor, AG825. Although AG825 has been previously used *in vivo*,[89–91] currently no pharmacokinetics data about AG825 penetration of the BBB are available.

In conclusion, our data provide support to the clinical evidence of a neuroprotective effect of high-dose ethanol in TBI, showing a mechanistic effect targeting multiple signaling cascades, including, importantly, RTK signaling, controlling the activity and plasticity of inhibitory interneurons. Direct modulation of the pathways that control inhibitory microcircuits may therefore offer a new approach for understanding and targeting TBI pathogenic pathways.

Acknowledgments

This work has been supported by the Deutsche Forschungsgemeinschaft as part of the Collaborative Research Center 1149 "Danger Response, Disturbance Factors and Regenerative Potential after Acute Trauma." F.R. and R.R. are also supported by the ERANET-NEURON initiative "External Insults to the Nervous System" as part of the MICRONET consortium and by the Baustein program of the Medical Faculty of Ulm University.

Author Disclosure Statement

No competing financial interests exist.

References

1. Coronado, V.G., Xu, L., Basavaraju, S.V., McGuire, L.C., Wald, M.M., Faul, M.D., Guzman, B.R., and Hemphill, J.D.; Centers for Disease Control and Prevention (CDC). (2011). Surveillance for traumatic brain injury-related deaths—United States, 1997-2007. MMWR Surveill. Summ. 60, 1–32.
2. Bruns, J., and Hauser, W.A. (2003). The epidemiology of traumatic brain injury: a review. Epilepsia 44, Suppl. 10, 2–10.
3. Leo P. and McCrea M. (2016). Epidemiology, in: *Translational Research in Traumatic Brain Injury*. D. Laskowitz and G. Grant (eds). CRC Press/Taylor and Francis Group: Boca Raton, FL, chapter 1.
4. Zaloshnja, E., Miller T., Langlois J.A., and Selassie, A. W. (2005). Prevalence of long-term disability from traumatic brain injury in the civilian population of the United States. J. Head Trauma Rehabil. 23, 394–400.
5. Stein, C.S., Georgoff, P., Meghan, S., Mizra, K., and Sonnad, S.S. (2010). 150 years of treating severe traumatic brain injury: a systematic review of progress in mortality. J. Neurotrauma 27, 1343–1353.
6. Savola, O., Niemelä, O., and Hillbom, M. (2005). Alcohol intake and the pattern of trauma in young adults and working aged people admitted after trauma. Alcohol Alcohol 40, 269–273.
7. Brennan, J.H., Bernard, S., Cameron, P.A., Rosenfeld, J.V., and Mitra, B. (2015). Ethanol and isolated traumatic brain injury. J. Clin. Neurosci. 22, 1375–1381.
8. Raj, R., Skrifvars, M.B., Kivisaari, R., Hernesniemi, J., Lappalainen, J., and Siironen, J. (2015). Acute alcohol intoxication and long-term outcome in patients with traumatic brain injury. J. Neurotrauma 32, 95–100.
9. Raj, R., Mikkonen, E.D., Siironen, J., Hernesniemi, J., Lappalainen, J., and Skrifvars, M.B. (2016). Alcohol and mortality after moderate to severe traumatic brain injury: a meta-analysis of observational studies. J. Neurosurg. 124, 1684–1692.
10. Berry, C., Ley, E.J., Margulies, D.R., Mirocha, J., Bukur, M., Malinoski, D., and Salim, A. (2011). Correlating the blood alcohol concentration with outcome after traumatic brain injury: too much is not a bad thing. Am. Surg. 77, 1416–1419.
11. Salim, A., Teixeira, P., Ley, E.J., DuBose, J., Inaba, K., and Margulies, D.R. (2009). Serum ethanol levels: predictor of survival after severe traumatic brain injury. J. Trauma 67, 697–703.
12. Wang, T., Chou, D.Y., Ding, J.Y., Fredrickson, V., Peng, C., Schafer, S., Guthikonda, M., Kreipke, C., Rafols, J.A., and Ding, Y. (2013). Reduction of brain edema and expression of aquaporins with acute ethanol treatment after traumatic brain injury. J. Neurosurg. 118, 390–396.
13. Joseph, B., Khalil, M., Pandit, V., Kulvatunyou, N., Zangbar, B., O'Keeffe, T., Asif, A., Tang, A., Green, D.J., Gries, L., Friese, R.S., and Rhee, P. (2015). Adverse effects of admission blood alcohol on long-term cognitive function in patients with traumatic brain injury. J. Trauma Acute Care Surg. 78, 403–408.
14. Pandit, V., Patel, N., Rhee, P., Kulvatunyou, N., Aziz, H., Green, D.J., O'Keeffe, T., Zangbar, B., Tang, A., Gries, L., Friese, R.S., and Joseph, B. (2014). Effect of alcohol in traumatic brain injury: is it really protective? J. Surg. Res. 190, 634–639.
15. Lange, R.T., Iverson, G.L., and Franzen, M.D. (2008). Effects of day-of-injury alcohol intoxication on neuropsychological outcome in the acute recovery period following traumatic brain injury. Arch. Clin. Neuropsychol. 23, 809–822.
16. Schutte, C., and Hanks, R. (2010). Impact of the presence of alcohol at the time of injury on acute and one-year cognitive and functional recovery after traumatic brain injury. Int. J. Neurosci. 120, 551–556.
17. Kaplan, C.P., and Corrigan, J.D. (1992). Effect of blood alcohol level on recovery from severe closed head injury. Brain Inj. 6, 337–349.
18. Wu, W., Tian, R., Hao, S., Xu, F., Mao, X., and Liu, B. (2014). A pre-injury high ethanol intake in rats promotes brain edema following traumatic brain injury. Br. J. Neurosurg. 28, 739–745.
19. Vaagenes, I.C., Tsai, S.Y., Ton, S.T., Husak, V.A., McGuire, S.O., O'Brien, T.E., and Kartje, G.L. (2015). Binge ethanol prior to traumatic brain injury worsens sensorimotor functional recovery in rats. PloS One, 10, e0120356.
20. Chandrasekar, A., Heuvel, F.O., Palmer, A., Linkus, B., Ludolph, A.C., Boeckers, T.M., Relja, B., Huber-Lang, M., and Roselli, F. (2017). Acute ethanol administration results in a protective cytokine and neuroinflammatory profile in traumatic brain injury. Int. Immunopharmacol. 51, 66–75.
21. Kelly, D.F., Lee, S.M., Pinanong, P.A., and Hovda, D.A. (1997). Paradoxical effects of acute ethanolism in experimental brain injury. J. Neurosurg. 86, 876–882.

22. Janis, L.S., Hoane, M.R., Conde, D., Fulop, Z., and Stein, D.G. (1998). Acute ethanol administration reduces the cognitive deficits associated with traumatic brain injury in rats. J. Neurotrauma 15, 105–115.
23. Goodman, M.D., Makley, A.T., Campion, E.M., Friend, L.A., Lentsch, A.B., and Pritts, T.A. (2013). Preinjury alcohol exposure attenuates the neuroinflammatory response to traumatic brain injury. J. Surg. Res. 184, 1053–1058.
24. Katada, R., Nishitani, Y., Honmou, O., Mizuo, K., Okazaki, S., Tateda, K., Watanabe, S., and Matsumoto, H. (2012). Expression of aquaporin-4 augments cytotoxic brain edema after traumatic brain injury during acute ethanol exposure. Am. J. Pathol. 180, 17–23.
25. Criswell, H.E., Ming, Z., Pleasant, N., Griffith, B.L., Mueller, R.A., and Breese, G.R. (2004). Macrokinetic analysis of blockade of NMDA-gated currents by substituted alcohols, alkanes and ethers. Brain Res. 1015, 107–113.
26. Kumar, S., Porcu, P., Werner, D.F., Matthews, D.B., Diaz-Granados, J.L., Helfand, R.S., and Morrow, A.L. (2009). The role of GABA(A) receptors in the acute and chronic effects of ethanol: a decade of progress. Psychopharmacology (Berl.) 205, 529–564.
27. Sun, Y., Ikrar, T., Davis, M.F., Gong, N., Zheng, X., Luo, Z.D., Lai, C., Mei, L., Holmes, T.C., Gandhi, S.P., and Xu, X. (2016). Neuregulin-1/ErbB4 signaling regulates visual cortical plasticity. Neuron. 92, 160–173.
28. Mei, L., and Nave, K.A. (2014). Neuregulin-ERBB signaling in the nervous system and neuropsychiatric diseases. Neuron 83, 27–49.
29. Gupta, V.K., You, Y., Gupta, V.B., Klistorner, A., and Graham, S.L. (2013). TrkB receptor signalling: implications in neurodegenerative, psychiatric and proliferative disorders. Int. J. Mol. Sci. 14, 10122–10142.
30. Fourgeaud, L., Través, P.G., Tufail, Y., Leal-Bailey, H., Lew, E.D., Burrola, P.G., Callaway, P., Zagórska, A., Rothlin, C.V., Nimmerjahn, A., and Lemke, G. (2016). TAM receptors regulate multiple features of microglial physiology. Nature 532, 240–244.
31. Sheffler-Collins, S.I., and Dalva, M.B. (2012). EphBs: an integral link between synaptic function and synaptopathies. Trends Neurosci. 35, 293–304.
32. Guillemot, F., and Zimmer, C. (2011). From cradle to grave: the multiple roles of fibroblast growth factors in neural development. Neuron 71, 574–588.
33. Su, E.J., Fredriksson, L., Kanzawa, M., Moore, S., Folestad, E., Stevenson, T.K., Nilsson, I., Sashindranath, M., Schielke, G.P., Warnock, M., Ragsdale, M., Mann, K., Lawrence, A.L., Medcalf, R.L., Eriksson, U., Murphy, G.G., and Lawrence, D.A. (2015). Imatinib treatment reduces brain injury in a murine model of traumatic brain injury. Front. Cell. Neurosci 9, 385.
34. Gurnik, S., Devraj, K., Macas, J., Yamaji, M., Starke, J., Scholz, A., Sommer, K., Di Tacchio, M., Vutukuri, R., Beck, H., Mittelbronn, M., Foerch, C., Pfeilschifter, W., Liebner, S., Peters, K.G., Plate, K.H., and Reiss, Y. (2016). Angiopoietin-2-induced blood-brain barrier compromise and increased stroke size are rescued by VE-PTP-dependent restoration of Tie2 signaling. Acta Neuropathol. 31, 753–773.
35. Bean, J.C., Lin, T.W., Sathyamurthy, A., Liu, F., Yin, D.M., Xiong, W.C., and Mei, L. (2014). Genetic labeling reveals novel cellular targets of schizophrenia susceptibility gene: distribution of GABA and non-GABA ErbB4-positive cells in adult mouse brain. J. Neurosci. 34, 13549–13566.
36. Fazzari, P., Paternain, A.V., Valiente, M., Pla, R., Luján, R., Lloyd, K., Lerma, J., Marín, O., and Rico, B. (2010). Control of cortical GABA circuitry development by Nrg1 and ErbB4 signalling. Nature 464, 1376–1380.
37. Neddens, J., Fish, K.N., Tricoire, L., Vullhorst, D., Shamir, A., Chung, W., Lewis, D.A., McBain, C.J., and Buonanno, A. (2011). Conserved interneuron-specific ErbB4 expression in frontal cortex of rodents, monkeys, and humans: implications for schizophrenia. Biol. Psychiatry 70, 636–645.
38. Vullhorst, D., Mitchell, R.M., Keating, C., Roychowdhury, S., Karavanova, I., Tao-Cheng, J.H., and Buonanno, A. (2015). A negative feedback loop controls NMDA receptor function in cortical interneurons via neuregulin 2/ErbB4 signalling. Nat. Commun. 6, 7222.
39. Wen, L., Lu, Y.S., Zhu, X.H., Li, X.M., Woo, R.S., Chen, Y.J., Yin, D.M., Lai, C., Terry, A.V., Vazdarjanova, A., and Xiong, W.C. (2010). Neuregulin 1 regulates pyramidal neuron activity via ErbB4 in parvalbumin-positive interneurons. Proc. Natl. Acad Sci. U. S. A. 107, 1211–1216.
40. Yin, D.M., Sun, X.D., Bean, J.C., Lin, T.W., Sathyamurthy, A., Xiong, W.C., Gao, T.M., Chen, Y.J., and Mei, L. (2013). Regulation of spine formation by ErbB4 in PV-positive interneurons. J. Neurosci. 33, 19295–19303.
41. Atallah, B.V., Bruns, W., Carandini, M., and Scanziani, M. (2012). Parvalbumin-expressing interneurons linearly transform cortical responses to visual stimuli. Neuron 73, 159–170.
42. Jacobs, N., Seeboeck, R., Hofmann, E., and Eger, A. (2017). ErbB family signalling: a paradigm for oncogene addiction and personalized oncology. Cancers (Basel) 9, E33.
43. Flierl, M.A., Stahel, P.F., Beauchamp, K.M., Morgan, S.J., Smith, W.R., and Shohami, E. (2009). Mouse closed head injury model induced by a weight-drop device. Nat. Protoc.4, 1328–1337.
44. Luong, T.N., Carlisle, H.J., Southwell, A., and Patterson, P.H. (2011). Assessment of motor balance and coordination in mice using the balance beam. J. Vis. Exp. 10, 2376.
45. Zimprich, A., Garrett, L., Deussing, J.M., Wotjak, C.T., Fuchs, H., Gailus-Durner, V., de Angelis, M.H., Wurst, W., and Hölter, S.M. (2014). A robust and reliable non-invasive test for stress responsivity in mice. Front. Behav. Neurosci. 8, 125.
46. Saxena, S., Roselli, F., Singh, K., Leptien, K., Julien, J.P., Gros-Louis, F., and Caroni, P. (2013). Neuroprotection through excitability and mTOR required in ALS motoneurons to delay disease and extend survival. Neuron 80, 80–96.
47. Karunakaran, S., Chowdhury, A., Donato, F., Quairiaux, C., Michel, C.M., and Caroni, P. (2016). PV plasticity sustained through D1/5 dopamine signaling required for long-term memory consolidation. Nat. Neurosci. 19, 454–464.
48. Magnus, C.J., Lee, P.H., Atasoy, D., Su, H.H., Looger, L.L., and Sternson, S.M. (2011). Chemical and genetic engineering of selective ion channel-ligand interactions. Science 333, 1292–1296.
49. Schwarzkopf, T.M., Horn, T., Lang, D., and Klein, J. (2013). Blood gases and energy metabolites in mouse blood before and after cerebral ischemia: the effects of anesthetics. Exp. Biol. Med. (Maywood) 238, 84–89.
50. Papa, L., Brophy, G.M., Welch, R.D., Lewis, L.M., Braga, C.F., Tan, C.N., Ameli, N.J., Lopez, M.A., Haeussler, C.A., Mendez-Giordano, D.I, Silvestri, S., Giordano, P., Weber, K.D., Hill-Pryor, C., and Hack, D.C. (2016). Time course and diagnostic accuracy of glial and neuronal blood biomarkers GFAP and UCH-L1 in a large cohort of trauma patients with and without mild traumatic brain injury. JAMA Neurol. 73, 551–560.
51. Huang, X.J., Glushakova, O., Mondello, S., Van, K., Hayes, R.L., and Lyeth, B.G. (2015). Acute temporal profiles of serum levels of UCH-L1 and GFAP and relationships to neuronal and astroglial pathology following traumatic brain injury in rats. J. Neurotrauma 32, 1179–1189.
52. Gerecke, K.M., Wyss, J.M., Karavanova, I., Buonanno, A., and Carroll, S.L. (2001). ErbB transmembrane tyrosine kinase receptors are differentially expressed throughout the adult rat central nervous system. J. Comp. Neurol. 433, 86–100.
53. Thompson, M., Lauderdale, S., Webster, M.J., Chong, V.Z., McClintock, B., Saunders, R., and Weickert, C.S. (2007). Widespread expression of ErbB2, ErbB3 and ErbB4 in non-human primate brain. Brain Res. 30, 95–109.
54. Polli, J.W., Humphreys, J.E., Harmon, K.A., Castellino, S., O'Mara, M.J., Olson, K.L., John-Williams, L.S., Koch, K.M., and Serabjit-Singh, C.J. (2008). The role of efflux and uptake transporters in [N-(3-chloro-4-[(3-fluorobenzyl)oxy]phenyl]-6-[5-({[2-(methylsulfonyl) ethyl]amino}methyl)-2-furyl]-4-quinazolinamine (GW572016, lapatinib) disposition and drug interactions. Drug Metab. Dispos. 36, 695–701.
55. Hudachek, S.F., and Gustafson, D.L. (2013). Physiologically based pharmacokinetic model of lapatinib developed in mice and scaled to humans. J. Pharmacokinet. Pharmacodyn. 40, 157–176.
56. Qiao, L., Choi, S., Case, A., Gainer, T.G., Seyb, K., Glicksman, M.A., Lo, D.C., Stein, R.L., and Cuny, G.D. (2009). Structure-activity relationship study of EphB3 receptor tyrosine kinase inhibitors. Bioorg. Med. Chem. Lett. 19, 6122–6126.
57. Flajolet, M., Wang, Z., Futter, M., Shen, W., Nuangchamnong, N., Bendor, J., Wallach, I., Nairn, A.C., Surmeier, D.J., and Greengard, P. (2008). FGF acts as a co-transmitter through adenosine A(2A) receptor to regulate synaptic plasticity. Nat. Neurosci. 11, 1402–1409.
58. Thundyil, J., Manzanero, S., Pavlovski, D., Cully, T.R., Lok, K.Z., Widiapradja, A., Chunduri, P., Jo, D.G., Naruse, C., Asano, M., Launikonis, B.S., Sobey, C.G., Coulthard, M.G., and Arumugam, T.V.

(2013). Evidence that the EphA2 receptor exacerbates ischemic brain injury. PloS One 8, e53528.
59. Akimoto, M., Baba, A., Ikeda-Matsuo, Y., Yamada, M.K., Itamura, R., Nishiyama, N., Ikegaya, Y., and Matsuki, N. (2004). Hepatocyte growth factor as an enhancer of NMDA currents and synaptic plasticity in the hippocampus. Neuroscience 128, 155–162.
60. Nolt, M.J., Lin, Y., Hruska, M., Murphy, J., Sheffler-Colins, S.I., Kayser, M.S., Passer, J., Bennett, M.V., Zukin, R.S., and Dalva, M.B. (2011). EphB controls NMDA receptor function and synaptic targeting in a subunit-specific manner. Neuroscience 31, 5353–5364.
61. Kriebel, M., Metzger, J., Trinks, S., Chugh, D., Harvey, R.J., Harvey, K., and Volkmer, H. (2011). The cell adhesion molecule neurofascin stabilizes axo-axonic GABAergic terminals at the axon initial segment. J. Biol. Chem. 286, 24385–24393.
62. Wuchter, J., Beuter, S., Treindl, F., Herrmann, T., Zeck, G., Templin, M.F., and Volkmer, H. (2012). A comprehensive small interfering RNA screen identifies signaling pathways required for gephyrin clustering. J. Neurosci. 32, 14821–14834.
63. Mei, L., and Xiong, W.C. (2008). Neuregulin 1 in neural development, synaptic plasticity and schizophrenia. Nat. Rev. Neurosci. 9, 437–452.
64. Guan, Y.F., Wu, C.Y., Fang, Y.Y., Zeng, Y.N., Luo, Z.Y., Li, S.J., Li, X.W., Zhu, X.H., Mei, L., and Gao, T.M. (2015). Neuregulin 1 protects against ischemic brain injury via ErbB4 receptors by increasing GABAergic transmission. Neuroscience 307, 151–159.
65. Zhang, H., Zhang, L., Zhou, D., He, X., Wang, D., Pan, H., Zhang, X., Mei, Y., Qian, Q., Zheng, T., Jones, F.E., and Sun, B. (2017). Ablating ErbB4 in PV neurons attenuates synaptic and cognitive deficits in an animal model of Alzheimer's disease. Neurobiol. Dis. 106, 171–180.
66. Lu, Y., Sun, X.D., Hou, F.Q., Bi, L.L., Yin, D.M., Liu, F., Chen, Y.J., Bean, J.C., Jiao, H.F., Liu, X., Li, B.M., Xiong, W.C., Gao, T.M., and Mei, L. (2014). Maintenance of GABAergic activity by neuregulin 1-ErbB4 in amygdala for fear memory. Neuron 84, 835–846.
67. Tamura, H., Kawata, M., Hamaguchi, S., Ishikawa, Y., and Shiosaka, S. (2012). Processing of neuregulin-1 by neuropsin regulates GABAergic neuron to control neural plasticity of the mouse hippocampus. J. Neurosci. 32, 12657–12672.
68. Iwakura, Y., Wang, R., Inamura, N., Araki, K., Higashiyama, S., Takei, N., and Nawa H. (2017). Glutamate-dependent ectodomain shedding of neuregulin-1 type II precursors in rat forebrain neurons. PLoS One 12, e0174780.
69. Woo, R.S., Li, X.M., Tao, Y., Carpenter-Hyland, E., Huang, Y.Z., Weber, J., Neiswender, H., Dong, X.P., Wu, J., Gassmann, M., Lai, C., Xiong, W.C., Gao, T.M., and Mei, L. (2007). Neuregulin-1 enhances depolarization-induced GABA release. Neuron 54, 599–610.
70. Tan, G.H., Liu, Y.Y., Hu, X.L., Yin, D.M., Mei, L., and Xiong, Z.Q. (2011). Neuregulin 1 represses limbic epileptogenesis through ErbB4 in parvalbumin-expressing interneurons. Nat. Neurosci. 15, 258–266.
71. Carron, S.F., Alwis, D.S., and Rajan, R. (2016). Traumatic brain injury and neuronal functionality changes in sensory cortex. Front. Syst. Neurosci. 10, 47.
72. Alwis, D.S., Yan, E.B., Morganti-Kossmann, M.C., and Rajan, R. (2012). Sensory cortex underpinnings of traumatic brain injury deficits. PLoS One 7, e52169.
73. Johnstone, V.P., Yan, E.B., Alwi,. D.S., and Rajan, R. (2013). Cortical hypoexcitation defines neuronal responses in the immediate aftermath of traumatic brain injury. PloS One 8, e63454.
74. Allitt, B.J., Iva, P., Yan, E.B., and Rajan, R. (2016). Hypo-excitation across all cortical laminae defines intermediate stages of cortical neuronal dysfunction in diffuse traumatic brain injury. Neuroscience 334, 290–308.
75. Johnstone, V.P., Shultz, S.R., Yan, E.B., O'Brien, T.J., and Rajan, R. (2014). The acute phase of mild traumatic brain injury is characterized by a distance-dependent neuronal hypoactivity. J. Neurotrauma 31, 1881–1895.
76. Bading, H. (2013). Nuclear calcium signalling in the regulation of brain function. Nat. Rev. Neurosci. 14, 593–608.
77. Roselli, F., and Caroni, P. (2015). From intrinsic firing properties to selective neuronal vulnerability in neurodegenerative diseases. Neuron 85, 901–910.
78. Zhang, S.J., Buchthal, B., Lau, D., Hayer, S., Dick, O., Schwaninger, M., Veltkamp, R., Zou, M., Weiss, U., and Bading, H. (2011). A signaling cascade of nuclear calcium-CREB-ATF3 activated by synaptic NMDA receptors defines a gene repression module that protects against extrasynaptic NMDA receptor-induced neuronal cell death and ischemic brain damage. J. Neurosci. 31, 4978–4990.
79. Zhang, S.J., Zou, M., Lu, L., Lau, D., Ditzel, D.A., Delucinge-Vivier, C., Aso, Y., Descombes, P., and Bading, H. (2009). Nuclear calcium signaling controls expression of a large gene pool: identification of a gene program for acquired neuroprotection induced by synaptic activity. PLoS Genet 5, e1000604.
80. Hendry, J.M., Alvarez-Veronesi, M.C., Placheta, E., Zhang, J.J., Gordon, T., and Borschel, G.H. (2016). ErbB2 blockade with Herceptin (trastuzumab) enhances peripheral nerve regeneration after repair of acute or chronic peripheral nerve injury. Ann. Neurol. 80, 112–126.
81. Boerboom, A., Dion, V., Chariot, A., and Franzen, R. (2017). Molecular mechanisms involved in Schwann cell plasticity. Front. Mol. Neurosci. 10, 38.
82. Blasiole, B., Bayr, H., Vagni, V.A., Janesko-Feldman, K., Cheikhi, A., Wisniewski, S.R., Long, J.B., Atkins, J., Kagan, V., and Kochanek, P.M. (2013). Effect of hyperoxia on resuscitation of experimental combined traumatic brain injury and hemorrhagic shock in mice. Anesthesiology 118, 649–663.
83. Kalsotra, A., Turman, C.M., Dash, P.K., and Strobel, H.W. (2003). Differential effects of traumatic brain injury on the cytochrome p450 system: a perspective into hepatic and renal drug metabolism. J. Neurotrauma 20, 1339–1350.
84. Nizamutdinov, D., DeMorrow, S., McMillin, M., Kain, J., Mukherjee, S., Zeitouni, S., Frampton, G., Bricker, P.C., Hurst, J., and Shapiro, L.A. (2017). Hepatic alterations are accompanied by changes to bile acid transporter-expressing neurons in the hypothalamus after traumatic brain injury. Sci. Rep. 7, 40112.
85. Boucher, B.A., and Hanes, S.D. (1998). Pharmacokinetic alterations after severe head injury. Clinical relevance. Clin. Pharmacokinet. 35, 209–221.
86. Yuan, X.Q., Wade, C.E., Prough, D.S., and DeWitt, D.S. (1990). Traumatic brain injury creates biphasic systemic hemodynamic and organ blood flow responses in rats. J. Neurotrauma 7, 141–153.
87. Afshar, M., Netzer, G., Salisbury-Afshar, E., Murthi, S., and Smith, G.S. (2016). Injured patients with very high blood alcohol concentrations. Injury 47, 83–88.
88. Polli, J.W., Humphreys, J.E., Harmon, K.A., Castellino, S., O'mara, M.J., Olson, K.L., John-Williams, L.S., Koch, K.M., and Serabjit-Singh, C.J. (2008). The role of efflux and uptake transporters in N-[3-chloro-4-[(3-fluorobenzyl) oxy] phenyl]-6-[5-([[2-(methylsulfonyl) ethyl] amino] methyl)-2-furyl]-4-quinazolinamine (GW572016, lapatinib) disposition and drug interactions. Drug Metab. Dispos. 36, 695–701.
89. Morikawa, A., Peereboom, D.M., Thorsheim, H.R., Samala, R., Balyan, R., Murphy, C.G., Lockman, P.R., Simmons, A., Weil, R.J., Tabar, V., and Steeg, P.S. (2014). Capecitabine and lapatinib uptake in surgically resected brain metastases from metastatic breast cancer patients: a prospective study. Neuro-oncology 17, 289–295.
90. Sysa-Shah, P., Tocchetti, C.G., Gupta, M., Rainer, P.P., Shen, X., Kang, B.H., Belmonte, F., Li, J., Xu, Y., Guo, X., and Bedja, D. (2015). Bidirectional cross-regulation between ErbB2 and β-adrenergic signalling pathways. Cardiovasc. Res. 109, 358–373.
91. Kedrin, D., Wyckoff, J., Boimel, P.J., Coniglio, S.J., Hynes, N.E., Arteaga, C.L., and Segall, J.E. (2009). ERBB1 and ERBB2 have distinct functions in tumor cell invasion and intravasation. Clin. Cancer Res. 15, 3733–3739.

Address correspondence to:
Francesco Roselli, MD, PhD
Department of Neurology
Department of Anatomy and Cell Biology
Ulm University
Center for Biomedical Research (ZBMF)
Helmholtzstrasse 8/1 (R1.44)
89081 Ulm
Germany

E-mail: francesco.roselli@uni-ulm.de

6.4 Parvalbumin interneurons shape neuronal vulnerability in blunt TBI

Akila Chandrasekar[a], Florian olde Heuvel[a], Lilla Tar[a], Anna M. Hagenston[b], Annette Palmer[c], Birgit Linkus[a], Albert C. Ludolph[a], Markus Huber-Lang[c], Tobias Boeckers[d], Hilmar Bading[b], Francesco Roselli[a,c,e]

a) Dept. of Neurology, Ulm University, Germany

b) Dept. of Neurobiology, IZN, Heidelberg University, Germany

c) Institute of Clinical and Experimental Trauma-Immunology, Ulm University, Germany

d) Dept. of Anatomy and Cell Biology, Ulm University, School of Medicine, Germany

e) Neurozentrum, Ulm University, Germany

Accepted: 17 May 2018

Published in: Cerebral Cortex. 30 June 2018. 1-15

doi: https://doi.org/10.1093/cercor/bhy139

Title: **Parvalbumin interneurons shape neuronal vulnerability in blunt TBI**

Authors: Akila Chandrasekar[1], Florian olde Heuvel[1], Lilla Tar[1], Anna M. Hagenston[2], Annette Palmer[3], Birgit Linkus[1], Albert C. Ludolph[1], Markus Huber-Lang[3], Tobias Boeckers[4], Hilmar Bading[2], Francesco Roselli[1,3,5]

Affiliation:
1. Department of Neurology, Ulm University, Ulm-DE
2. Department of Neurobiology- IZN, Heidelberg University, Heidelberg-DE
3. Institute of Clinical and Experimental Trauma-Immunology, Ulm University, Ulm-DE
4. Department of Anatomy and Cell Biology, Ulm University, Ulm-DE
5. Neurozentrum- Ulm University, Ulm-DE

Correspondence: Francesco Roselli, MD, PhD

Dept. of Neurology-Ulm University

Center for Biomedical Research (ZBF)

Helmholtzstrasse 8/2(R1.44)-89081 Ulm-DE

Key words: Traumatic brain injury, parvalbumin interneurons, chemogenetics, nuclear calcium

Summary

Excessive excitation has been hypothesized to subsume a significant part of the acute damage occurring after Traumatic Brain Injury (TBI). However, reduced neuronal excitability, loss of neuronal firing and a disturbed excitation/inhibition balance have been detected. Parvalbumin (PV) interneurons are major regulators of perisomatic inhibition, principal neurons firing and overall cortical excitability. However, their role in acute TBI pathogenic cascades is unclear. We exploited the chemogenetic PSAM/PSEM control of PV-Cre^{+} neurons and the DREADDs control of principal neurons in a blunt model of TBI to explore the role of inhibition in shaping neuronal vulnerability to TBI. We demonstrated that inactivation of PV interneurons at the instance or soon after trauma enhances survival of principal neurons and reduces gliosis at 7dpi whereas, activation of PV interneurons decreased neuronal survival. The protective effect of PV inactivation was suppressed by expressing the nuclear calcium buffer PV-NLS in principal neurons, implying an activity-dependent neuroprotective signal. In fact, protective effects were obtained by increasing the excitability of principal neurons directly using DREADDs. Thus, we show that sustaining neuronal excitation in the early phases of TBI may reduce neuronal vulnerability by increasing activity-dependent survival, while excess activation of perisomatic inhibition is detrimental to neuronal integrity.

Introduction

The acute phase of concussive and contusive Traumatic Brain Injury (TBI) is characterized by pathogenic cascades linked to the physical damage of neurons and their uncontrolled excitation. Axonal stretching, membrane damage and neuronal depolarization (triggered by the physical forces of the trauma) are known to cause glutamate release and/or failure in glutamate re-uptake system (Kaur and Sharma, 2017). Elevated levels of glutamate in the extracellular space causes supraphysiological activation of glutamate receptors, which includes extrasynaptic N-methyl-D-aspartate (NMDA) receptors that are link to cell death pathways (Hardingham et al., 2002; Hardingham and Bading, 2010; Pohl et al., 1999; Wroge et al., 2012; Hinzman et al., 2015; Samson et al., 2016). Toxic NMDA receptor signaling leads to calcium (Ca^{2+}) overload, followed by a loss of structural integrity, mitochondrial dysfunction and metabolic disturbances, culminating in bioenergetics failure and neuronal loss (Weber, 2012; Hinzman et al., 2015; Sun et al., 2017; Bading, 2017).

Despite the excitotoxic primary injury mechanisms, several lines of evidence suggest that reduced excitation may play a role in the pathophysiology of acute TBI: spreading depolarizations (pathophysiological features that closely follow TBI) have been reported to shift the excitation/inhibition balance towards increased inhibition (Sawant-Pokam et al., 2017). Neuronal responses to synaptic stimulation and sensory inputs are suppressed for several days after TBI (Johnstone et al., 2013; Johnstone et al., 2014; Allitt et al., 2016) and neuronal metabolism is decreased in the affected cortex (Dietrich et al., 1994). Interestingly, glutamatergic antagonists seem to be protective only in the very early phases of TBI and become detrimental to neuronal survival later (Pohl et al., 1999), suggesting that excitation-dependent neuroprotective signals may play a role in determining the vulnerability of neurons to TBI. Indeed, neuronal activity has been shown to increase resistance to oxidative stress and reduce vulnerability to apoptosis (Papadia et al., 2008; Zhang et al., 2007; 2009; Leveille et al., 2010; Hardingham and Bading, 2010). Thus, both excessive glutamatergic drive (excitotoxicity) and insufficient neuronal excitation may modulate the sensitivity of neurons to TBI-associated pathogenic cascades (as in other neurodegenerative conditions; Roselli and Caroni, 2015).

The net neuronal firing is determined not only by intrinsic properties, but is strongly influenced by the activity of glutamatergic synapses (together with the activation of non-synaptic glutamatergic receptors), as well as by the inhibitory inputs (Isaacson and Scanziani, 2011). GABAergic interneurons provide a homeostatic regulation of firing of excitatory neurons and shape the propagation of excitation in space and time (Wilent and Contreras, 2005; Haider et al., 2013). Although selective loss of GABAergic subpopulations has been shown to take place in the chronic phase of TBI (Cantu et al., 2015), the functional role of inhibitory interneurons in acute TBI is yet to be fully elucidated.

Parvalbumin-positive (PV) interneurons constitute a subset of the cortical GABAergic population integrated in the local microcircuitry and providing perisomatic inhibition both in feedback and feed-forward architectures (Hu et al., 2014). PV interneurons regulate the overall output of the principal neurons (Defelipe et al., 1999; Cardin et al., 2009; Donato et al., 2013; Donato et al., 2015). In fact, strong activation of PV interneurons is sufficient to shut-down the firing of principal neurons (Atallah et al., 2012) and to curb pathological excitatory drive (Khoshkoo et al., 2017). Although PV interneurons appear to be affected by TBI (Vascak et al., 2017) and their derangement may contribute to the delayed-onset of post-traumatic hyperexcitability (Hsieh et al., 2017), their role in the acute phase after TBI remain unexplored. Is perisomatic inhibition a fundamental force in preventing excess excitation and excitotoxicity, or do PV interneurons instead exacerbate cortical silencing and neuronal vulnerability? Do PV interneurons represent an entry point to modulate the biological response of principal neurons to traumatic injury? To investigate these issues at a functional level, acute time-resolved manipulations of PV activity in vivo is necessary.

To these ends, we exploited a set of AAV-delivered tools, including engineered ion channels with orthogonal pharmacology (Pharmacologically Selective Activation Module [PSAM] and Pharmacologically Selective Effector Module [PSEM]; Magnus et al., 2011) and Designer Receptors Exclusively Activated by Designer Drug (DREADDs; Roth, 2016) to control PV interneuron and principal neuron firing within discrete time windows in TBI. We have revealed that modulation of PV firing bidirectionally modulates the acute response of principal neurons, their

long-term viability and TBI-associated astrogliosis. Furthermore, we have demonstrated that neuroprotection of principal neurons through PV manipulation requires nuclear Ca^{2+} signals that are known to activate a neuroprotective gene program (Zhang et al., 2009). Taken together, our findings imply that early restoration of neuronal firing through microcircuit manipulation provides an innovative route to neuroprotection in TBI.

Materials and Methods

Mouse lines: All experiments and procedures were approved by the local animal experimentation committee under the license no. 1222. B6;129P2-Pvalbtm1(cre)Arbr/J (henceforth PV-Cre) were a kind gift of Pico Caroni. PV-Cre mice were bred into homozygosity and maintained under standard husbandry conditions (24°C, 40-60% humidity, 14/10h light/dark cycle, unlimited access to water and food).

Viral vectors and chemogenetic agonists: AAV9 mediating the expression of Pharmacologically Selective Activation Modules (PSAM) (previously described; Magnus et al., 2011; Saxena et al., 2013) were obtained from Vector Biolabs (Malvern-PA, US) at the titre of $9*10^{12}$ viral genomes/ml using the following constructs: pAAV-pCAG-flox-PSAM(Leu41Phe, Tyr116Phe)5HT3-WPRE and pAAV-cbaflox-PSAM(Leu141Phe, Tyr116Phe) GlyR-WPRE, encoding the cation-permeable (activator PSAM, henceforth actPSAM) and the anion-permeable (inhibitory PSAM, henceforth inhPSAM) channels. AAV8 mediating the expression of the activating DREADD (pAAV-CaMKIIa-hM3D(Gq)-mCherry, corresponding to the plasmid #50476) were obtained from AddGene viral service. AAV2 mediating the expression of pAAV-flex-taCasp3-TEVp (previously reported; Yang et al., 2013) were obtained from the University of North Carolina (UNC) Vector Core facility. AAV2 mediating the expression of rAAV-GFP/Cre were obtained from University of North Carolina (UNC) Vector Core facility. pAAV-hSyn-PV-NLS-mC, which drives the expression of Parvalbumin-NLS-mCherry (PV-NLS-mCherry) under control of the human synapsin promoter, was constructed by PCR-amplifying the PV-NLS-mCherry coding sequence from pAAV-CMV-PV-NLS-mCherry (Schlumm et al., 2013) and then subcloning it into a pAAV-hSyn expression plasmid. AAV1/2 particles were prepared as described previously (Zhang et al., 2007).

Since AAV2, AAV8 and AAV9 have been reported to have a similar neuronal infectivity in the cerebral cortex (Aschauer et al., 2013) and the viral suspensions were injected at high titer (in order to saturate the injection volume), the choice of the AAV pseudotype was due solely to the availability of high-quality, validated batches of viral vectors from different sources.

The PSAM agonist PSEM308 was obtained from Apex Scientific Inc. (Stony Brook-NY, US) and was administered by intraperitoneal injection (i.p.) at the dose of 5 µg/g (dissolved in sterile saline) 30 min before TBI. The DREADD agonist Clozapine-N-Oxide (CNO) was purchased from Tocris (Wiesbaden-Nordenstadt, Germany) and administered i.p. at the dose of 5 µg/g (dissolved in sterile saline) 30 min before TBI.

Intracerebral injection of viruses: Intracortical injection of AAVs was performed in mice at the age of P30-P35 as previously reported (Karunakaran et al., 2016). Mice undergoing surgery were administered buprenorphine (0.05 mg/kg; Reckitt Beckshire Healthcare, Beckshire, UK) and meloxicam (1.0 mg/kg; Böhringer Ingelheim, Biberach an der Riß, Germany) 20 min before the procedure. After administration, mice were put under continuous isoflurane anesthesia (4% isoflurane in 96% O_2) and positioned into a stereotactic frame. The scalp was incised at the midline and a burr hole was drilled (using a hand micro-drill) at the coordinates x=+2.0, y=-2.0, corresponding to the somatosensory cortex. 200 to 500 nl of the viral suspension (mixed with an equal volume of 1% Fast green solution) was injected using a pulled glass capillary, connected to a Picospritzer microfluidic device, over a span of 10 min. The capillary was kept in place for another 10 min to prevent backflow of the virus. The burr hole was left open to allow the bone to heal and the skin was sutured using a Prolene 7.0 surgical thread. After surgery, the animals were transferred to a recovery cage with a warmed surface and *ad libitum* access to food and water. Animals were administered additional doses of buprenorphine for the following 72 hours and monitored for eventual neurological impairment.

Experimental traumatic brain injury procedure and experimental groups: TBI was induced in mice by a modified closed, blunt weight-drop model (previously reported Flierl et al., 2009). Animals were pre-administered buprenorphine (0.1 mg/kg by subcutaneous injection) and put under sevoflurane anesthesia (5% sevoflurane in 95% O_2). The scalp skin was incised on the midline to expose the skull and the animals were positioned in the weight drop apparatus in which the head was secured to a holding frame. Using the three-axis mobile platform

in the apparatus, the impactor was positioned to the coordinates of the injection site (x=+2.0; y=-2.0, z=0.0). TBI was delivered by a weight of 120 g dropping from a height of 40cm. A mechanical stop prevented a skull displacement (by the impactor) larger than 1.5 mm, in order to limit brain damage. Apnea time was monitored after TBI. Mice were administered 100% O_2 until normal breathing was restored. The scalp skin was sutured using the Prolene 6.0 surgical thread and the mice were transferred to a recovery cage (single-housed) with *ad libitum* access to food and water (Supplementary Figure 1A). Additional doses of buprenorphine were administered every 12h for the following 24h after TBI. To reduce the suffering of the mice, their general state was checked using a score sheet (based on the NSS score, Flierl et al, 2009) to instate opportune measures or to euthanize the mice. Effort was made to minimize animal suffering and reduce the number of mice used.

For mice injected with the AAV9-PSAM/PSEM chemogenetics, 6 experimental groups were established: saline sham (mice with intracerebral injection of inhPSAM or actPSAM virus but injected with saline before undergoing sham surgery, henceforth sal-S), inhPSAM/PSEM sham (mice with intracerebral injection of the inhPSAM virus and injected with PSEM agonist before undergoing sham surgery, henceforth inh-S), actPSAM sham (mice with intracerebral injection of actPSAM virus but injected with PSEM agonist before undergoing sham surgery, henceforth act-S), saline TBI (mice with intracerebral injection of inhPSAM or actPSAM virus but injected with saline before undergoing TBI, henceforth sal-TBI), inhPSAM/PSEM TBI (mice with intracerebral injection of inhPSAM virus and injected with PSEM agonist before undergoing TBI, henceforth inh-TBI) and actPSAM/PSEM TBI (mice with intracerebral injection of actPSAM virus but injected with PSEM agonist before undergoing TBI, henceforth act-TBI). In order to establish if PV inactivation after TBI was effective, 6 experimental groups were established (Supplementary Figure 1B): saline sham (mice with intracerebral injection of inhPSAM virus but injected with saline before undergoing sham surgery, henceforth sal-S), inhPSAM/PSEM sham (mice with intracerebral injection of the inhPSAM virus and injected with PSEM agonist before undergoing sham surgery, henceforth inh-S), saline TBI (mice with intracerebral injection of inhPSAM virus but injected with saline before

undergoing TBI, henceforth sal-TBI), inhPSAM/PSEM TBI acute (pre) agonist administration (mice with intracerebral injection of inhPSAM virus and injected with PSEM agonist before undergoing TBI, henceforth inh-TBI), inhPSAM/PSEM TBI acute (post) agonist administration (mice with intracerebral injection of inhPSAM virus and injected with PSEM agonist 30min after TBI and 8h after TBI, such that the inhibition of PV interneurons was maintained for a total of 24h, henceforth inh-24h-TBI) and inhPSAM/PSEM TBI sub-acute agonist administration (mice with intracerebral injection of inhPSAM virus and injected with PSEM agonist starting 2dpi up to 4dpi (two doses daily), such that the inhibition of PV interneurons was maintained for a total of 72h, henceforth inh-72h-TBI). The experiment in which the PV interneurons were ablated had 4 groups: GFP sham (intracerebral injection of AAV2-GFP and sham surgery, henceforth GFP-S), ablation sham (intracerebral injection of AAV2-Caspase 3 and sham surgery, henceforth abl-S), GFP TBI (intracerebral injection of AAV2-GFP and TBI, henceforth GFP-TBI) and ablation TBI (intracerebral injection of AAV2-Caspase 3 and TBI, henceforth abl-TBI). The chemogenetic stimulation (AAV8-DREADD(Gq), CaMKIIa promoter) of ipsi or contralateral principal neurons was explored with an experimental design including 7 groups: mice expressing the DREADD(Gq) expressed on the ipsilateral side but saline injection before sham surgery (henceforth Gq-sal-S), mice expressing the DREADD(Gq), injected with CNO but subject to sham surgery (henceforth Gq-CNO-S), mice expressing the DREADD(Gq) expressed on the ipsilateral side but saline injection before TBI (henceforth Gq-sal-TBI), mice expressing DREADD(Gq) virus on the ipsilateral side and administered the Clozapine-N-Oxide agonist before TBI (henceforth Gq-CNO-TBI), mice expressing DREADD(Gq) virus on the ipsilateral side, administered CNO, subject to sham surgery but for which the contralateral cortex was assessed (henceforth Gq-contra-CNO-S), mice injected with DREADD(Gq) virus on the ipsilateral side, injected with saline before TBI delivered on the contralateral side (henceforth Gq-contra-sal-TBI), mice expressing DREADD Gq virus on the ipsilateral side and administered CNO before TBI on the contralateral side (henceforth Gq-contra-CNO-TBI).

Mice injected with the AAV1/2-PV-NLS-mCherry virus along with the inhPSAM inhibitor virus were divided in 3 groups: injected with PV-NLS-mCherry and inhPSAM viruses, subject to sham surgery; injected with PV-NLS-

mCherry and inhPSAM viruses but administered saline before TBI and injected with PV-NLS-mCherry and inhPSAM viruses and administered PSEM agonist before TBI (Supplementary Figure 2).

Immunostaining: For immunostaining, mice were intracardially perfused. Animals were terminally anesthetized with ketamine/ xylazine and fixed (25 ml ice-cold PBS followed by 50 ml 4% PFA in PBS, pH 7.4) at 3h or 7 dpi. The brain was carefully extracted and post fixed in 4% PFA for 18h and thereafter washed in PBS and cryoprotected in 30% sucrose in PBS. Cryoprotected brains were embedded in OCT (TissueTek, Sakura). 40 µm thick free-floating sections, spanning the injection/TBI site (identified by fast green) were cut in a cryostat, collected in PBS and immunostaining was done based on the following protocol: sections were blocked in a blocking buffer (3% BSA, 0.3% Triton in PBS) for 2h at 24°C on a rotary shaker. Following blocking an appropriate mix of primary antibodies (chicken anti-GFP, 1:000, Abcam; goat anti-Parvalbumin, 1:1000, Swant; rabbit anti-phosphorylated S6 (Ser235/236) 1:200, Cell Signaling Technology; mouse anti-NeuN, 1:100, Millipore; rabbit anti-c-Fos, 1:500, Santa Cruz Biotechnologies; mouse anti-RFP, 1:500, cell Biolabs; rabbit anti-cleaved caspase 3, 1:400, Cell Signalling Technology; mouse anti-GFAP, 1:400, Sigma; rabbit anti-GFAP, 1:500, Abcam or fluorescently-conjugated Bungarotoxin, BTX-555, 1:500, Thermo Fisher) were diluted in blocking buffer and incubated for 48h at 4°C. Sections were then washed in PBS for 3*30 min and incubated in the appropriate mix of secondary antibodies (Alexa-conjugated donkey anti-mouse, donkey anti-goat, donkey anti-rabbit, donkey anti-chicken, 1:500, Invitrogen), together with, whenever appropriate, the DNA dye TOPRO-3 (1:1000, Invitrogen), diluted in blocking buffer for 2h at 24°C. After further washing the sections for 3*30min in PBS, the sections were mounted on coverslips and onto the slides using FluoroGold Plus (Invitrogen).

Confocal imaging and image analysis: Confocal images were acquired using an LSM-700 (Carl Zeiss AG) inverted microscope, fitted with a 20x air or 40x oil objective. Tile-scans of 5x3 were acquired to cover the full span of the injury site and the full cortical thickness. The images were acquired in a 12-bit format. Imaging parameters

(laser power, photomultiplier voltage, digital gain and offset) were established with the goal of preventing saturation in target structures while obtaining a lowest signal intensity of at least 150 (in arbitrary units). Imaging parameters were kept constant across different specimens.

For pS6 fluorescence intensity analysis, confocal stacks composed of 10 optical sections (acquired at the same depth in the tissue section) were collapsed in maximum-intensity projections using the ImageJ software. Neurons were identified based on their morphology, size and positive immunostaining for the neuronal marker (NeuN). A target region of 40,000 μm^2 was considered for each section, spanning the cortical layer II-III and centered on the axis of the injury site. Regions of Interest (ROIs) encompassing the cellular soma (excluding the nucleus) were manually drawn for each neuron in the target region and the integrated average fluorescence intensity was logged. A minimum of 300 neurons (layer II-III) from 3 distinct tissue sections from each of 3-5 mice were quantified. The intensity of pS6 in PV interneurons was also measured separately. The median fluorescence intensity of pS6 was computed.

For the counting of c-Fos^+ neurons, confocal stacks of 10-12 optical sections were collapsed in maximum intensity projections in ImageJ and a threshold was set for the resulting images, to establish a reproducible criterion to distinguish c-Fos^+ neurons from c-Fos^- neurons. A ROI ($2.5*10^6$ μm^2) was then traced in layer II-III and the number of c-Fos^+ cells were counted. The number of c-Fos^+ PV interneurons were also separately counted.

For the measurement of $NeuN^+$ cells, 5x3 composite tile-scans of confocal stacks were acquired with the 20x objective to image the injury site and the surrounding penumbral and perilesional areas. Confocal stacks of 5-6 optical sections (at the same depth) were collapsed in maximum-intensity projections in ImageJ. Multiple ROIs were considered: the “lesion core” (76,000 μm^2) ROI was positioned centered on the axis of the injury site and two “penumbral” (48,000 μm^2) ROIs were located at 400 µm from the lesion axis, bilaterally, in correspondence of the layer II-III (Supplementary Figure 3A). A third ROI was considered for the experiment with the NLS-PV-mCherry AAV2; this ROI (76,000 μm^2) was located 700 µm away from the lesion axis (Supplementary Figure 3B).

In these ROIs, the number of $NeuN^+$ cells (or of $mCherry^+$ or GFP^+ cells) were manually counted. At least 3-5 tissue sections were analyzed from each of 3-6 mice per experimental group.

Statistics: Statistical analysis was performed with the GraphPad Prism software suite. Neuronal counts and fluorescence intensities were compared by one-way ANOVA with Tukey correction for multiple comparisons. The whiskers in the box and whiskers plot were set between 10 and 90 percentiles. For the fluorescence intensity of pS6 in PV interneurons and the number of $cFOS^+$ cells in PV interneurons, non-parametric t-test with Mann-Whitney correction was performed to compare the two groups (sham vs TBI). Non-parametric t-test with Mann-Whitney correction was also used to compare the number of PV interneurons in mice injected with AAV2 GFP vs AAV2 Caspase 3. The values for the neuronal counts are reported as mean±SD. For the fluorescence intensities the median values and the interquartile range are reported. Statistical significance was set at $p<0.05$.

Results

PV interneurons modulate the acute response of principal neurons to TBI.

First, we explored the recruitment of PV interneurons in the early stages after blunt TBI. To this end, PV interneurons were genetically labelled (to prevent identification biases due to the state- and subpopulation-specific variations in parvalbumin expression; Donato et al., 2013) by injecting PV-Cre mice with an inhPSAM (tagged with GFP) or actPSAM (tagged with BTX binding site) viruses (Supplementary Figure 4A). One month after injection, we verified by double immunostaining for PV and for the corresponding tag (GFP or BTX) that 92% of PV^+ neurons were GFP^+ (or BTX^+) and that 100% of GFP^+ (or BTX^+) neurons were PV^+, confirming the precise targeting of the PV population (Supplementary Figure 4B). We verified that, at the 3h time point and in correspondence of the injury site, PV^+ cells displayed significantly higher levels of the neuronal activity marker (Knight et al., 2012) phosphorylated-S6 (pS6; median fluorescence intensity : 1340, interquartile range 1215-2015 in sal-TBI vs 679 with an interquartile range 615-796 in sal-S, $p<0.0001$) compared to sham-operated mice (Supplementary Figure 5A-B). Likewise, the number of $c\text{-}Fos^+$ PV interneurons was significantly higher in TBI mice than in sham mice (18±3 cells/$2.2*10^5$ μm^2 in sal-TBI vs 7±2 cells/$2.2*10^5$ μm^2 in sal-S, $p<0.0001$; Supplementary Figure 5D,F), suggesting the recruitment of these interneurons by the cortical trauma. Recruitment of PV interneurons did not differ, in terms of median pS6 and in the number of $c\text{-}Fos^+$ cells, from that of non-PV neurons: in non-PV neurons, TBI induced a similar increase in pS6 (median fluorescence intensity 1483, interquartile range of 1108-1997 in sal-TBI vs 756 with an interquartile range 652-1021 in sal-S, $p<0.0001$; Supplementary Figure 5A,C) as well as in the fraction of $c\text{-}Fos^+$ neurons (for non-PV neurons, 18±3 cells/$2.2*10^5$ μm^2 in sal-TBI vs 57±5 cells/$2.2*10^5$ μm^2 in sal-S, $p<0.0001$; Supplementary Figure 4E,F). Likewise, the increase in $c\text{-}Fos^+$ cells in TBI vs sham was 257±22% in PV neurons and 311±32% in non-PV neurons ($p=0.34$).

We then functionally explored the impact of PV interneurons on the biological response of principal neurons to TBI. To this end, we used PSAM/PSEM chemogenetics (Magnus et al., 2011) to either activate or inhibit PV

interneurons at the time of TBI. Thereafter, we monitored the impact of activation or inhibition of PV interneurons on the acute response of cortical neurons to TBI. More specifically, PV-Cre mice were injected (30 days before the TBI) with AAV mediating either actPSAM or inhPSAM expression; 30 min before the procedure, mice were administered either the PSEM agonist (or saline) and then underwent either TBI (act-TBI, inh-TBI or sal-TBI, respectively) or sham surgery (act-S, inh-S and sal-S, respectively (Supplementary Figure 1A, 2A). We focused on three readouts: the levels of the activity marker pS6, the induction of c-Fos and the level of the autophagy marker LC3A in the overall neuronal ($NeuN^+$) population (composed largely of principal neurons, Supplementary Figure 6A-C) 3h post-TBI.

One-way ANOVA revealed a significant difference among the groups in pS6 levels ($F_{(5,3318)}$=209, p<0.0001). The number of neurons counted in each case were as follows: sal-S= 451, inh-S= 427, act-S= 495, sal-TBI= 1276, inh-TBI= 798 and act-TBI= 822. In sham-treated mice, chemogenetic activation of PV interneurons resulted in the anticipated decrease of pS6 levels (median fluorescence intensity of 702 with an interquartile range of 480-1041 in act-S mice compared to a median fluorescence intensity of 925.9 with an interquartile range of 682-1345 in sal-S mice, p<0.01; Figure 1A-B), whereas, PV inactivation caused the predicted increase in pS6 levels (median fluorescence intensity of 1105 with an interquartile range of 887-1546 in inh-S mice compared to a median fluorescence intensity of 926 with an interquartile range of 682-1345 sal-S mice, p<0.01; Figure 1A-B), confirming the proper functioning of the chemogenetic system. In TBI-treated mice, a significant increase in pS6 levels in cortical neurons subjected to sal-TBI compared to sal-S was observed (median fluorescence intensity of 1565 with an interquartile range of 1209-1976 in sal-TBI mice compared to a median fluorescence intensity of 926 with an interquartile range of 682-1345 sal-S mice, p<0.0001; Figure 1A-B). Interestingly, the TBI-evoked upregulation of pS6 was strongly modulated by PV interneurons: inactivation of PV interneurons (by inhPSAM/PSEM) resulted in a further increase in pS6 levels (median fluorescence intensity of 1839 with an interquartile range of 1509-2458 in inh-TBI mice compared to a median fluorescence intensity of 1564.7 with an interquartile range of 1209-1976 in sal-TBI mice, p<0.0001). Notably, chemogenetic activation of PV

interneurons caused a massive decrease in TBI-induced pS6 upregulation (median fluorescence intensity of 969 with an interquartile range of 764-1321 in act-TBI mice compared to a median fluorescence intensity of 1565 with an interquartile range of 1209-1976 in sal-TBI mice, $p<0.0001$; Figure 1A-B).

To confirm the changes in neuronal activation detected using pS6 immunochemistry, we evaluated the expression of the activity-dependent immediate-early gene c-Fos. In sham mice, once again the number of c-Fos$^+$ neurons were increased by PV inactivation and decreased by PV activation, as anticipated (inh-S vs sal-S, $p<0.05$ and act-S vs sal-S, $p<0.01$). At 3h post-injury, sal-TBI mice showed a strong increase in c-Fos$^+$ neurons in the affected cortex ($F_{(5,53)}=111$, $p<0.0001$, 35±5 cells/$2.2*10^5\mu m^2$ in sal-S vs 101±12 cells/$2.2*10^5\mu m^2$ in sal-TBI mice; $p<0.0001$, Figure 1C-D), in agreement with previous reports (Chandrasekar et al., 2018). Activation of PV interneurons at the time of trauma caused a massive decrease in c-Fos$^+$ cells 3h after injury (55±6 cells/$2.2*10^5\mu m^2$ in act-TBI, $p<0.0001$ vs sal-TBI; Figure 1C-D) down to baseline values ($p>0.05$ vs sal-S; Figure 1C-D). On the other hand, inactivation of PV interneuron by inhPSAM significantly increased the number of c-Fos$^+$ neurons after TBI (129±22 cells/$2.2*10^5\mu m^2$ in inh-TBI vs sal-TBI, $p<0.0001$; Figure 1C-D).

Finally, we investigated the impact of activation/inhibition of PV interneurons on the autophagy level in principal neurons by measuring the accumulation of LC3A$^+$ aggregates. At 3h post-injury there was a significant difference in LC3A levels for the different groups ($F_{(5,2765)}=283$, $p<0.0001$). In sham mice, chemogenetic activation or inactivation of PV interneurons did not affect LC3A burden (median fluorescence intensity of 740 with an interquartile range of 548-880 in inh-S mice compared to a median fluorescence intensity of 725 with an interquartile range of 578-870 in sal-S mice, $p>0.05$; and median fluorescence intensity of 675 with an interquartile range of 546-860 in act-S mice compared to a median fluorescence intensity of 725 with an interquartile range of 578-870 in sal-S mice; Figure 1E-F). Importantly, in saline-treated mice, TBI resulted in the significant elevation of LC3A levels in a population of principal neurons as compared to sal-S controls (median fluorescence intensity of 1250 with an interquartile range of 1024-1579 in sal-TBI; $p<0.0001$ vs sal-sham; Figure 1E-F). Interestingly, inactivation of PV interneurons strongly downregulated LC3A induction (median

fluorescence intensity of 693 with an interquartile range of 461-931 in inh-TBI mice; $p<0.0001$ vs sal-TBI; Figure 1E-F) whereas stimulation of PV firing did not result in a further elevation of LC3A levels (median fluorescence intensity of 1296 with an interquartile range of 1118-1546 in act-TBI mice, $p>0.05$ vs sal-TBI; Figure 1E-F).

Notably, virtually all cells (>95%) displaying the elevation of p-S6 and LC3A levels or positive for c-Fos were also $NeuN^+$, implying that the observed responses are specifically occurring in neurons (Supplementary Figure 5A-F).

Taken together, these findings show that PV interneurons strongly modulate neuronal activity in acute TBI and significantly affect proteostasis in principal neurons after trauma.

Activity of PV interneurons modulate neuronal survival and gliotic reaction in TBI.

We then investigated if the effects of PV firing at the time of TBI resulted in long-term effects on neuronal vulnerability and survival. To this end, we measured the density of $NeuN^+$ cells at 7dpi both in the core and in the penumbra of the TBI-induced lesion (as compared to sham-operated mice). The core and penumbra were defined as depicted in Supplementary Figure 3A. Differences between the groups (Supplementary Figure 2B) were noted both in the core ($F_{(5,53)}= 10,05$, $p<0.0001$) and in the penumbra ($F_{(5,53)}= 225$, $p<0.0001$). No effect on $NeuN^+$ density was observed after PV activation or inactivation in mice undergoing sham surgery (core: 29±2, 29±1 and 27±1 $NeuN^+$ cells/10^4 μm^2 in sal-S, inh-S and act-S, respectively, $p>0.05$; Figure 2A; penumbra: 32±3, 29±2 and 29±2 $NeuN^+$ cells/10^4 μm^2 in sal-S, inh-S and act-S respectively, $p>0.05$).

In saline-pretreated mice, irrespective of the PSAM expression, TBI resulted in an almost complete loss of $NeuN^+$ cells in the lesion core (2±1 $NeuN^+$ cells/10^4 μm^2 in sal-TBI, $p<0.0001$ vs sal-S; Figure 2A-C) and a significant cell loss in the penumbral ROI (14±1 $NeuN^+$ cells/10^4 μm^2 vs 29±2 in sal-S $p<0.0001$; Figure 2A-C). Activation of PV firing at the time of TBI did not significantly affect the number of $NeuN^+$ cells in the core (1±0.3 $NeuN^+$ cells/10^4 μm^2 in act-TBI vs sal-TBI, $p>0.05$; Figure 2A-C) but, surprisingly, it caused a significant worsening of neuronal loss in the penumbra (11±1 $NeuN^+$ cells/10^4 μm^2; $p=0.005$ in act-TBI vs sal-TBI; Figure 2A-C). Conversely, the inactivation of PV interneurons at the time of trauma resulted in improved long-term (7 dpi) preservation of

NeuN$^+$ cells in the core (8±1 NeuN$^+$ cells/10^4 µm^2 in inh-TBI, p<0.0001 vs sal-TBI; Figure 2A-C) as well as in the penumbra (22±1 NeuN$^+$ cells/10^4 µm^2 in inh-TBI; p<0.0001 vs sal-TBI; Figure 2A-C).

We assessed the effect of acute PV activation/inactivation on astrogliosis, as an independent measure of tissue damage, by monitoring the extent of GFAP immunostaining at 7dpi. We found significant differences in the expression of GFAP between the groups ($F_{(5,54)}$=257, p<0.001). Neither activation nor inactivation of PV interneurons affected GFAP$^+$ astrocytes in sham-surgery mice (i.e., in act-S or inh-S mice, which were comparable to sal-S). However, in mice administered with saline and subject to TBI, a significant increase in the surface area occupied by GFAP$^+$ cells were detected in the injury site (ROI area=6.3*10^4 µm^2, 31±1% of the total area in sal-TBI vs 5±0.4% in sal-S, p<0.0001; Figure 2D-E). Notably, inactivating PV interneurons firing at the time of trauma resulted in a significantly lesser area occupied by GFAP$^+$ cells in the injury site at 7dpi (9±0.5% in inh-TBI, p<0.0001 vs sal-TBI and p>0.05 vs sal-S; Figure 2D-E). Conversely, activation of PV interneurons resulted in a significant increase in the GFAP$^+$ volume when compared to sal-TBI (65±2% in act-TBI, p<0.0001 vs sal-TBI; Figure 2D-E).

Thus, these results show that acute manipulation of PV interneurons at the time of trauma determine the extent of neuronal loss and astrogliosis caused by blunt TBI. Since we had inactivated PV interneurons at the time of trauma, we investigated further the time constraints of the neuroprotective role of PV interneurons by inactivating them with PSEM injections administered at different time points (Supplementary Figure 1B, refer to the methods section) relative to TBI: 30 min before TBI (acute-pre), 30 min and 8h after TBI (acute-post), or 48h to 96h after TBI (sub-acute). The density of NeuN$^+$ neurons was assessed at 7 dpi.

At 7 dpi, significant differences were seen in NeuN$^+$ cell density among the groups (Supplementary Figure 2C) both in the core ($F_{(5,52)}$= 851, p<0.0001; Figure 2F) and the penumbra ($F_{(5,52)}$= 254, p<0.0001; Figure 2F). As mentioned before, inhibition of PV interneurons per se (i.e., without trauma) affected neuronal vulnerability neither in the core nor the penumbra. Interestingly, inactivation of PV interneurons starting 30 min after TBI for

24h still had a protective effect comparable to pre-TBI PV inactivation; reduced neuronal loss was observed in the injured cortex both in the core (8±0.6 $NeuN^+$ cells/10^4 μm^2 in inh-24h-TBI vs 3±1 $NeuN^+$ cells/10^4 μm^2 in sal-TBI, $p<0.0001$, $p>0.05$ vs inh-TBI; Figure 2F-H) and the penumbra (22±2 $NeuN^+$ cells/10^4 μm^2 in inh-24h-TBI vs 14±2 $NeuN^+$ cells/10^4 μm^2 in sal-TBI, $p<0.0001$, $p>0.05$ vs inh-TBI; Figure 2F-H). On the other hand, inactivation of PV interneurons starting 48h after TBI could not recapitulate the protective effects of acute inactivation; inactivation of PV interneurons starting 48h after TBI resulted in levels of neuronal loss comparable to that observed in saline-treated TBI mice both in the core (4±1 $NeuN^+$ cells/10^4 μm^2 in inh-72h-TBI vs 3±1 $NeuN^+$ cells/10^4 μm^2 in sal-TBI, $p>0.05$, $p<0.0001$ vs inh-TBI; Figure 2F-H) and in the penumbra (12±1 $NeuN^+$ cells/10^4 μm^2 in inh-72h-TBI vs 14±2 $NeuN^+$ cells/10^4 μm^2 in sal-TBI, $p>0.05$, $p<0.0001$ vs inh-TBI; Figure 2F-H).

Taken together, these data show that acute inactivation of PV interneurons before or soon after TBI is sufficient to enhance long-term neuronal survival and reduce astrogliosis.

Pre-injury ablation of PV interneurons increases vulnerability of principal neurons to TBI

Short-term chemogenetic inhibition of PV interneurons results in a protective effect on neuronal survival in the penumbra of the injured cortex. To explore the effects of chronic loss of PV-mediated inhibition, we injected PV-Cre mice (at P30) with AAV2s encoding GFP (as a control) or a mutant Caspase 3 whose activation is controlled by the co-expression of Tobacco envelop virus protease (TEV) in Cre^+ cells, mutant Caspase-3 is expressed and activated by TEV, leading to the apoptosis of the infected cell (as reported by Yang et al., 2013). We verified at P60 that the ablation strategy displayed a 97% efficiency within the infected cortical area (in an area of $2.7*10^6$ μm^2, ablated mice had 2±1 PV^+ neurons compared to non-ablated mice, which had 90±5 PV^+ neurons, $p<0.0001$), while nearby areas exhibited normal numbers of PV^+ neurons (Figure 3A-B).

When the density of $NeuN^+$ cells were assessed at 7dpi, a significant difference in the number of $NeuN^+$ cells among groups (Supplementary Figure 2D) was detected both in the core ($F_{(3,27)}= 2116$, $p<0.0001$) and the penumbra ($F_{(3,27)}= 224$, $p<0.0001$). In abl-S mice, the loss of PV interneurons did not lead to a major loss of $NeuN^+$

cells (PV interneurons constitute only a small fraction of the total cortical neuronal population) compared to GFP-S mice (26.4±1.0 $NeuN^+$ cells/10^4 μm^2 in GFP-S vs 26±1 $NeuN^+$ cells/10^4 μm^2 in abl-S, p>0.05). Upon TBI, both GFP-TBI and abl-TBI mice displayed a significant loss of $NeuN^+$ cells in the core of the injury (3±0.7 $NeuN^+$ cells/10^4 μm^2 in GFP-TBI vs 26±1 $NeuN^+$ cells/10^4 μm^2 in GFP-S, p<0.0001, and 1±0.2 $NeuN^+$ cells/10^4 μm^2 in abl-TBI vs 26±1 $NeuN^+$ cells/10^4 μm^2 in abl-S, p<0.0001). This loss was, however, more extensive in the ablated group (3±1 $NeuN^+$ cells/$10^4\mu m^2$ in GFP-TBI vs 0.6±0.2 $NeuN^+$ cells/10^4 μm^2 in abl-TBI, p<0.0001). Furthermore, in the penumbral area, abl-TBI mice showed a much larger loss of neurons (15±1 $NeuN^+$ cells/10^4 μm^2 in GFP-TBI vs 10±1 $NeuN^+$ cells/10^4 μm^2 in abl-TBI; p<0.0001, as compared to 32±1 $NeuN^+$ cells/10^4 μm^2 in GFP-S and 30±4 $NeuN^+$ cells/10^4 μm^2 in abl-S; Figure 3C-D).

We also examined the effects of PV interneuron ablation on the astrocytic response. In addition to the enhanced vulnerability of neurons upon chronic PV ablation, a significant difference in $GFAP^+$ area was detected ($F_{(5,47)}$=182, p<0.0001). The glial response was significantly larger in the abl-TBI than in the gfp-TBI mice (ROI=6.3*10^4 μm^2, 52±2% of the total area in abl-TBI vs 35±1% in GFP-TBI, p<0.0001; Figure 3E). The $GFAP^+$ areas in both the TBI conditions were significantly larger than in their respective sham controls (p<0.0001).

Taken together, these data imply that, although short-term inhibition of PV interneurons may be beneficial, their chronic ablation strongly increases the vulnerability of principal neurons to TBI.

The effect of acute PV inactivation is mediated by nuclear Ca^{2+} signals in principal neurons.

Acute inactivation of inhibitory (PV^+) interneurons delivers significant neuroprotection in both the core and the penumbra of the TBI site (Figure 2). Since PV inactivation resulted in an increase in the activity-dependent markers c-Fos and pS6, we investigated if the neuroprotective effect was dependent on activity-regulated neuroprotective programs (Bading, 2013). We reasoned that if nuclear Ca^{2+} signals were required for PV-inactivation-associated neuroprotection, neurons expressing exogenous PV-NLS would show no enhanced survival upon PSEM-mediated inactivation of PV neurons. Therefore, we co-injected mice with inhPSAM and an

AAV2 driving the neuronal expression of PV-NLS-mCherry (Schlumm et al., 2013) to buffer nuclear Ca^{2+} and prevent the induction of neuroprotective transcriptional responses (Zhang et al., 2009; Figure 4B).

Expression of hSyn-PV-NLS-mCherry alone or together with the inhPSAM did not affect neuronal survival in sham-operated mice (not shown). One way ANOVA revealed a significant difference in the number of PV-NLS-mCherry$^+$ cells among the different groups (Supplementary Figure 2E) both in the core ($F_{(2,39)}$= 832, p<0.0001) and in the penumbra ($F_{(2,39)}$= 23, p<0.0001). In fact, mice expressing inhPSAM and PV-NLS-mCherry and administered with PSEM (PV inactivation and nuclear Ca^{2+} buffering) displayed a loss of PV-NLS-mCherry$^+$ neurons comparable to mice in which PV interneurons were not inhibited (expressing the inhPSAM but administered with saline). More specifically, in the core, there were 20±1 PV-NLS-mCherry$^+$ cells/10^4 µm^2 in the sham mice. For those animals receiving TBI, there were 2±0.5 PV-NLS-mCherry$^+$ cells/10^4 µm^2 in NLS-inh-sal-TBI vs 2±0.4 PV-NLS-mCherry$^+$ cells/10^4 µm^2 in NLS-inh-PSEM-TBI (p>0.05; p<0.0001 vs NLS-ihn-sal-S; Figure 4A, C). Likewise, the penumbra of the mice injected with the PV-NLS along with the inhPSAM also showed increased vulnerability to loss of neurons (12±1 PV-NLS-mCherry$^+$ cells/10^4 µm^2 in NLS-inh-sal-TBI vs 18±2 PV-NLS-mCherry$^+$ cells/10^4 µm^2 in NLS-inh-sal-S, p<0.0001 and 13±2 PV-NLS-mCherry$^+$ cells/10^4 µm^2 in NLS-inh-PSEM-TBI, p>0.05 vs NLS-inh-sal-TBI; Figure 4A,D). Of note, the number of PV-NLS-mCherry$^+$ cells in a third ROI (located further away from the core and not affected by TBI, Supplementary Figure 3B) was comparable in sham and TBI samples (8±2 PV-NLS-mCherry$^+$ cells/10^4 µm^2 in NLS-inh-sal-TBI vs 10±2 PV-NLS-mCherry$^+$ cells/10^4 µm^2 in NLS-inh-sal-S, p<0.0001 and 9±1 PV-NLS-mCherry$^+$ cells/10^4 µm^2 in NLS-inh-PSEM-TBI, p>0.05 vs NLS-inh-sal-TBI and NLS-inh-sal-S; Figure 4E), indicating a comparable infection rate in all mice. In addition, the density of inhPSAM$^+$ PV interneurons (measured in the third, not-affected ROI) was comparable in sham and TBI mice (20±5 GFP$^+$ cells/10^5 µm^2 in NLS-inh-sal-TBI vs 25±7 GFP$^+$ cells/10^5 µm^2 in NLS-inh-sal-S, p>0.05 and 23±6 GFP$^+$ cells/10^5 µm^2 in NLS-inh-PSEM-TBI, p>0.05 vs NLS-inh-sal-TBI and NLS-inh-sal-S, Figure 4E), underscoring the reproducibility of the AAV injection.

Thus, the inactivation of PV interneurons enhances the survival of neurons through an activity-dependent program requiring nuclear Ca^{2+} signals.

Direct chemogenetic activation of neuronal firing reduces vulnerability to TBI.

Since inactivation of PV interneurons was sufficient to enhance the activation of principal neurons (Figure 1), and provided neuroprotection following TBI through an activity-dependent neuroprotective mechanism involving nuclear Ca^{2+} signaling (Figure 4), we explored whether a direct manipulation of principal neuron firing may mimic the effect of PV inactivation. In addition, we explored if activity-dependent protective effect could be elicited by increasing the activity of excitatory inputs. To this end, we injected mice at P30 with an AAV8 mediating expression of the chemogenetic activator DREADD(Gq)-mCherry (under the CaMKIIa promoter) either in the side going to be subject to TBI (ipsilateral injection, Figure 5A) or in the opposite side (contralateral injection, Figure 5B). In the latter experiment, we aimed at exploiting the homotopic connectivity between the symmetrical somatosensory (SS) cortices (Chovsepian et al., 2017) to drive the activity of ipsilateral neurons (subject to TBI) by chemogenetically stimulating projection neurons in the contralateral cortex. Indeed, the expression of DREADD(Gq)-mCherry highlighted numerous $mCherry^{+}$ axons in the corpus callosum connecting the two hemispheres (Figure 5B) and providing input to all layers of the SS targeted by TBI (Figure 5A, B).

Mice subject to ipsilateral injection were administered saline or the DREADD cognate agonist, CNO (5mg/kg), 30 min before undergoing sham surgery (Gq-sal-S or Gq-CNO-S) or TBI (Gq-sal-TBI and Gq-CNO-TBI; Supplementary Figure 2F). Likewise, mice subjected to contralateral injection were administered CNO before sham surgery or TBI (Gq-contra-CNO-S and Gq-contra-CNO-TBI; note that saline-treated, contralateral injected mice subject to sham surgery were equivalent to Gq-sal-S and are therefore conflated in a single group). In sham-treated mice, the excitation of ipsilateral SS by activating DREADD(Gq) resulted in a significant increase in $c\text{-}Fos^{+}$ cells compared to Gq-sal-S mice (37±5 cells/$2.2*10^5 \mu m^2$ in Gq-sal-S vs 69±8 cells/$2.2*10^5 \mu m^2$ in Gq-CNO-S, $p<0.001$). Notably, activation of the contralateral SS also resulted in a significant increase, although with a trend towards

lower absolute values, in c-Fos$^+$ cells in the ipsilateral SS (49±7 cells/2.2*10^{5}µm^2 in Gq-contra-CNO-S vs Gq-CNO-S, p=0.2; Figure 5C,D). Thus, these results show that both ipsilateral and contralateral activation of principal neurons induce c-Fos expression. Next, we investigated the interaction between TBI and DREADD(Gq) activation on c-Fos induction. In Gq-sal-TBI mice, a significant increase in c-Fos$^+$ cells in the injured site was observed (Figure 5D, in agreement with what shown in Figure 1D). Notably, activation of ipsilateral DREADD(Gq) resulted in a further increase in the number of c-Fos$^+$ cells (104±12 cells/2.2*10^{5}µm^2 in Gq-sal-TBI vs 150±20 cells/2.2*10^{5}µm^2 in Gq-CNO-TBI; p<0.0001; figure 5D). On the other hand, activation of contralateral cortex resulted in a much smaller increase the number of c-Fos$^+$ cells compared to Gq-sal-TBI (115±9 cells/2.2*10^{5}µm^2 in Gq-contra-CNO-TBI, p=0.3827 vs Gq-sal-TBI, Figure 5C,D), suggesting that the efficiency with which the contralateral cortex is activated by the injured cortex is reduced in TBI.

When neuronal preservation was assessed at 7 dpi, we found that activation of DREADD(Gq) resulted in a minor increase in neuronal preservation in the core at 7 dpi (3±1 NeuN$^+$ cells/10^4 µm^2 in Gq-CN0-TBI vs 1±0.4 NeuN$^+$ cells/10^4 µm^2 in Gq-sal-TBI, p<0.0001; Figure 5E,F). However, the penumbra of the mice injected with the DREADD(Gq) showed a strong reduction in neuronal vulnerability, resulting in a pronounced preservation of neurons (27±3 NeuN$^+$ cells/10^{4}µm^2 in Gq-CNO-TBI vs 11±1 NeuN$^+$ cells/10^{4}µm^2 in Gq-sal-TBI, p<0.0001; Figure 5E,G). Thus, direct excitation of principal neurons could recapitulate the neuroprotective effect of PV inactivation. Notably, the neuroprotective effect of direct excitation of principal neurons was comparable to the one obtained by PV inactivation (p= 0.24; cfr. Figure 2B,C and Figure 5F,G).

When we investigated the effect of contralateral cortex activation on neuronal integrity at 7 dpi. One-way ANOVA revealed a significant difference of NeuN$^+$ cells between the four groups (Supplementary Figure 2F) both in the core ($F_{(3,32)}$= 22, p<0.0001) and in the penumbra ($F_{(3,32)}$= 83, p<0.0001). However, in contrast to the observation when principal neurons were directly (ipsilateral) activated, activation of the contralateral cortex produced no difference in the neuronal survival in the core (1±0.6 NeuN$^+$ cells/10^{4}µm^2 in Gq-sal-contra-TBI when compared to 1±0.4 NeuN$^+$ cells/10^{4}µm^2 in Gq-contra-CNO-TBI, p>0.05) and only a modest (although statistically

significant) increase in the number of neurons in the penumbra of the Gq-contra-CNO-TBI mice when compared to the Gq-contra-sal-TBI was observed (16±3 $NeuN^+$ cells/$10^4\mu m^2$ in Gq-contra-CNO-TBI, 12±2 $NeuN^+$ cells/$10^4\mu m^2$ in Gq-contra-sal-TBI when compared to $p<0.05$; Figure 5E-G) indicating that synaptic activity may produce a small but significant neuroprotective effect.

These findings show that activating neurons directly at the site of the TBI helps preserve neurons both in the core as well as the penumbra, and that this effect cannot be recapitulated by indirect activation of the neurons via afferents arising from the contralateral cortex.

Discussion

In the present work we have demonstrated that chemogenetic manipulation of cortical microcircuitry involving PV interneurons modulates neuronal loss in TBI. Acute inactivation of PV interneurons is sufficient to decrease autophagy, enhance protein synthesis and promote the survival of principal neurons; conversely, stimulation of PV firing results in the decreased viability of principal neurons and increases gliosis. Notably, chronic depletion of PV interneurons results in the reverse effect, leading to an increase in neuronal loss. Mechanistically, we show that the beneficial effect of early PV inactivation is prevented by buffering nuclear Ca^{2+}, suggesting that an activity-regulated nuclear Ca^{2+} signal is responsible for the activity-dependent neuroprotection. Thus, we provide evidence that i) interventions on cortical microcircuitry may modulate principal neurons vulnerability to TBI, and ii) maintaining excitation in acute TBI may exhibit protective effects (summarized in Supplementary Figure 7).

Interestingly, several reports have shown that spontaneous and evoked the activity in cortex appears to be suppressed in the acute phase (i.e., within a few minutes or hours) after TBI (Carron et al., 2016). In fact, 24h after trauma, cortical responses to sensory stimuli are significant reduced and principal neurons, particularly in the upper layers, are hypoexcitable (Johnstone et al., 2013). The suppression of stimulus-evoked cortical activity has been reported to be independent of the type of TBI model (Johnstone et al., 2014). The suppression of

cortical activity seems to affect infra- and supragranular principal neurons within the first 2 weeks after TBI (Allitt et al., 2016), well before hyperexcitability can be identified in the chronic phase (8 weeks after TBI; Allitt et al., 2017; Johnstone et al., 2013; Ding et al., 2011). Notably, persistent downregulation of neuronal firing has been recorded after the occurrence of Cortical Spreading Depression (CSD), a feature often associated with TBI (Hinzman et al., 2015). A significant decrease in action potential frequency together with an increase in the size of inhibitory post-synaptic potentials has also been described, ultimately resulting in a net shift of the excitation/inhibition balance toward increased inhibition (Sawant-Pokam et al., 2017). Notably, increasing inhibition by administering GABAergic drugs increases the occurrence of CSD in human patients (Hertle et al., 2012, 2016), suggesting that excess inhibition may be detrimental in this condition.

PV interneurons are powerful modulators of cortical excitability and might exert strong effects on cortical excitability in normal as well as in pathological conditions. In fact, strong activation of PV interneurons is sufficient to completely silence cortical areas (Atallah et al., 2012) whereas inactivation of PV interneurons is sufficient to increase the basal and evoked firing rate of principal neurons in the somatosensory cortex (Yang et al., 2017; Agetsuma et al., 2017). Likewise, PV interneurons are recruited early in epileptic discharges (Cammarota et al., 2013; Khoshkhoo et al., 2017) and activation of PV interneurons can block the propagation of pathological discharges (Trevelyan et al., 2006; Paz et al., 2013). Here we have demonstrated that PV interneurons offer an entry point to controlling cortical activity in the early phases after trauma. In fact, not only are PV interneurons recruited in TBI (as shown by elevation of pS6 and c-Fos in PV^{+} neurons), but their inactivation enhances, and their forced activation downregulates activity markers. In this way, the modulation of PV firing effectively modifies the biological response of principal neurons to TBI, decreasing the overall levels of the autophagic response. Although PV interneurons can effectively modulate the cortical response to TBI, their contribution to the cortical silencing that occurs after the trauma remains to be investigated. In this direction, we have recently found (Chandrasekar et al., unpublished data) that TBI upregulates the phosphorylation of ErbB RTK in excitatory synapses of PV interneurons, a condition associated with increased

excitation of PV interneurons (Sun et al., 2016) and an overall increase in GABAergic output (Lu et al., 2014). It is conceivable, therefore, that PV interneurons may actually be involved in the pathophysiological regulation of activity within microcircuits soon after trauma. These early events may affect principal neuronal survival at a critical junction within the first 24h after trauma. In fact, the effectiveness of PV inactivation disappears when treatment is given in a delayed manner (from 2 dpi). Interestingly, the amount of inhibition provided by PV interneurons seem to decrease after 24h (at least in a mild TBI trauma; Vascak et al., 2017) and progressive degeneration of PV interneurons may contribute to the chronic hyperexcitability of the injured cortex (Hsieh et al., 2017; Buritica´et al., 2009; although not in all models: Carron et al., 2016). Interestingly, loss of PV interneurons has been reported even in presence of preserved number of $NeuN^+$ neurons (Hsieh et al., 2017). Thus, the link between loss of PV interneurons after TBI, appearance of chronic hyperexcitability (2-4 weeks after TBI) and long-term loss of principal neurons remains to be verified.

Although early inactivation of PV interneurons may affect acute biology after TBI and enhance overall survival of neurons, permanent ablation of PV interneurons does not prove beneficial (and may actually increase the area of neuronal loss). Thus, the chronic hyperexcitability of principal neurons that is anticipated to occur (Martin et al., 2001) may enhance their vulnerability to the excitatory wave triggered by the trauma itself; on this basis, one may speculate that, although PV interneuron inactivation is beneficial after trauma, these cells may also be required for the control of acute epileptiform activity (Trevelyan et al., 2006; Khoshkhoo et al., 2017).

The neuroprotective effect of early PV inactivation can be recapitulated by direct activation of principal neurons with the unrelated DREADD(Gq) system (under the CaMKIIa promoter); in agreement with the pro-apoptotic effect of NMDAR antagonists in the subacute stage of TBI (Pohl et al., 1999) and with the neuroprotective effect of excitation observed in neurodegenerative conditions (Saxena et al., 2013; Roselli and Caroni, 2015), sustaining neuronal activity appears to be a viable option to deliver neuroprotection in TBI. In agreement with the limited response of cortical neurons subjected to trauma to synaptically-evoked stimulation (Johnstone et al., 2013),

the degree of c-Fos expression and the neuroprotective effect obtained through circuit activation (i.e., by activating contralateral, symmetrically-projecting projection neurons), was significantly smaller than that obtained by direct stimulation. Thus, the effects of synaptic excitation may be limited by the TBI itself (by injuring trans-callosal axons and/or by increasing the activity of local PV interneurons) and therefore be unable to sustain synaptic activity-dependent neuroprotective programs.

As an underlying mechanism, we show that the long-lasting effect of acute inactivation of PV interneurons is blocked by the expression of an engineered nuclear Ca^{2+} buffer (Schlumm et al., 2013), further confirming the excitation-dependent neuroprotective pathway. Indeed, synaptic activity and excitation-dependent transcriptional responses have been shown to generate a state of "acquired neuroprotection", which renders neurons less vulnerable to stressors while not affecting neuronal survival at baseline (Zhang et al., 2009). The build up of this "neuroprotective shield" is controlled by nuclear Ca^{2+} signaling (Bading, 2013) and involves the activation of the CREB/CBP transcription factor complex, as well as the IEG transcription factors, ATF-3 and Npas4, and the secreted proteins, inhibinβA and SerpinB2 (Zhang et al., 2009; Zhang et al., 2011; Ahlgren et al., 2014; Qiu et al., 2013; Bading 2013). Acquired neuroprotection attenuates excitotoxicity by mechanistically distinct processes, which includes inhibinβA-mediated reduction of toxic extrasynaptic NMDA receptor signaling (Lau et al., 2015), a shift in energy metabolism towards glycolysis ('Neuronal Warburg effect'; Bas-Orth et al., 2017), a decrease in mitochondrial Ca^{2+} load through Npas4 mediated suppression of the mitochondrial calcium uniporter (Mcu) (Qiu et al., 2013), and increased resilience to oxidative stress and oxygen radicals production (Papadia et al., 2008; Depp et al., 2017). The beneficial effects of promoting ongoing activity may affect additional readouts besides neuronal survival. For example, TBI causes acute and subacute dendritic degeneration and synaptic loss (Winston et al., 2013; Wang et al., 2016), whereas the synaptic activity- and nuclear Ca^{2+} -regulated factor, VEGF-D up-holds structural integrity of dendritic arbors (Mauceri et al., 2011), and suppression by nuclear Ca^{2+} of C1q, a synapse pruning factor (Simonetti et al., 2013) prevents spine loss (Mauceri et al., 2015).

Notably, the neuroprotective effect delivered by increasing neuronal activity, either directly or indirectly, appears to be more pronounced in the penumbra rather than in core. It is conceivable that neurons lost due to trauma physical forces or acute excitotoxicity (unfolding in seconds or minute after injury) are relatively insensitive to activity-dependent mechanisms, whereas neurons in the penumbra may be affected by pathogenic processes (taking place over hours or days), such as extrasynaptic glutamate receptor activation (Bading, 2017), neuroinflammation and oxidative stress, which may be effectively counteracted by excitation-activated transcriptional programs (Zhang et al., 2009; Zhang et al., 2011; Depp et al., 2017; Foerstner et al., 2018).

Thus, in a condition of acute excitotoxicity, maintaining an active synaptic network may enable the surviving neurons, in the core and possibly even more in the penumbra, to access a number of protective programs. In contrast, the shut-down of neuronal activity may render the surviving neurons more vulnerable to the unfavorable conditions generated by the trauma and by TBI primary injury.

Acknowledgement

This work has been supported by the Deutsche Forschungsgemeinschaft as part of the Collaborative Research Center 1149 “Danger Response, Disturbance Factors and Regenerative Potential after Acute Trauma” (SFB1149-B05). HB is supported by the Collaborative Research Center 1158 (SFB 1158-A05). FR is also supported by the ERANET-NEURON initiative “External Insults to the Nervous System” and BMBF as part of the MICRONET consortium (FKZ 01EW1705A), by the Synapsis Foundation and by the Baustein program of the Medical Faculty of Ulm University.

References

Agetsuma M, Hamm JP, Tao K, Fujisawa S, Yuste R. 2017. Parvalbumin-Positive Interneurons Regulate Neuronal Ensembles in Visual Cortex. Cereb Cortex. 6:1-15.

Ahlgren H, Bas-Orth C, Freitag HE, Hellwig A, Ottersen OP, Bading H. 2014. The nuclear calcium signaling target, activating transcription factor 3 (ATF3), protects against dendrotoxicity and facilitates the recovery of synaptic transmission after an excitotoxic insult. J Biol Chem. 289(14):9970-82.

Allitt BJ, Iva P, Yan EB, Rajan R. 2016. Hypo-excitation across all cortical laminae defines intermediate stages of cortical neuronal dysfunction in diffuse traumatic brain injury. Neuroscience. 334:290-308.

Allitt BJ, Johnstone VPA, Richards KL, Yan EB, Rajan R. 2017. Progesterone Sharpens Temporal Response Profiles of Sensory Cortical Neurons in Animals Exposed to Traumatic Brain Injury. Cell Transplant. 26(7):1202-1223.

Aschauer DF, Kreuz S, Rumpel S. 2013. Analysis of transduction efficiency, tropism and axonal transport of AAV serotypes 1, 2, 5, 6, 8 and 9 in the mouse brain. PLoS One. (9):e76310.

Atallah BV, Bruns W, Carandini M, Scanziani M. 2012. Parvalbumin-expressing interneurons linearly transform cortical responses to visual stimuli. Neuron. 73(1):159-70.

Bading H. 2013. Nuclear calcium signalling in the regulation of brain function. Nat Rev Neurosci. 14(9):593-608.

Bading, H. 2017. Therapeutic targeting of the pathological triad of extrasynaptic NMDA receptor signaling in neurodegenerations. J. Exp. Med. 214: 569-578.

Bas-Orth C, Tan YW, Lau D, Bading H. 2017. Synaptic Activity Drives a Genomic Program That Promotes a Neuronal Warburg Effect. J Biol Chem. 292(13):5183-5194.

Buriticá E, Villamil L, Guzmán F, Escobar MI, García-Cairasco N, Pimienta HJ. 2009. Changes in calcium-binding protein expression in human cortical contusion tissue. J Neurotrauma. 26(12):2145-55.

Cammarota M, Losi G, Chiavegato A, Zonta M, Carmignoto G. 2013. Fast spiking interneuron control of seizure propagation in a cortical slice model of focal epilepsy. J Physiol. 591(4):807-22.

Cardin JA, Carlén M, Meletis K, Knoblich U, Zhang F, Deisseroth K, Tsai LH, Moore CI. 2009. Driving fast-spiking cells induces gamma rhythm and controls sensory responses. Nature. 459(7247):663-7.

Carron SF, Alwis DS, Rajan R. 2016. Traumatic Brain Injury and Neuronal Functionality Changes in Sensory Cortex. Front Syst Neurosci. 10:47.

Cantu D, Walker K, Andresen L, Taylor-Weiner A, Hampton D, Tesco G, Dulla CG. 2015. Traumatic Brain Injury Increases Cortical Glutamate Network Activity by Compromising GABAergic Control. Cereb Cortex. 25(8):2306-20.

Chandrasekar A, Aksan B, Heuvel FO, Förstner P, Sinske D, Rehman R, Palmer A, Ludolph A, Huber-Lang M, Böckers T, Mauceri D, Knöll B, Roselli F. 2018. Neuroprotective effect of acute ethanol intoxication in TBI is associated to the hierarchical modulation of early transcriptional responses. Exp Neurol. 302:34-45.

Clarkson AN, Huang BS, Macisaac SE, Mody I, Carmichael ST. 2010. Reducing excessive GABA-mediated tonic inhibition promotes functional recovery after stroke. Nature. 468(7321):305-9.

Defelipe J, González-Albo MC, Del Río MR, Elston GN. 1999. Distribution and patterns of connectivity of interneurons containing calbindin, calretinin, and parvalbumin in visual areas of the occipital and temporal lobes of the macaque monkey. J Comp Neurol. 412(3):515-26.

Delestrée N, Manuel M, Iglesias C, Elbasiouny SM, Heckman CJ, Zytnicki D. 2014. Adult spinal motoneurones are not hyperexcitable in a mouse model of inherited amyotrophic lateral sclerosis. J Physiol. 592(7):1687-703.

Depp C, Bas-Orth C, Schroeder L, Hellwig A, Bading H. 2017. Synaptic Activity Protects Neurons Against Calcium-Mediated Oxidation and Contraction of Mitochondria During Excitotoxicity. Antioxid Redox Signal. doi: 10.1089/ars.2017.7092. [Epub ahead of print]

Ding MC, Wang Q, Lo EH, Stanley GB. 2011. Cortical excitation and inhibition following focal traumatic brain injury. J Neurosci. 31(40):14085-94.

Dietrich WD, Alonso O, Busto R, Ginsberg MD. 1994. Widespread metabolic depression and reduced somatosensory circuit activation following traumatic brain injury in rats. J Neurotrauma. 11(6):629-40.

Donato F, Rompani SB, Caroni P. 2013. Parvalbumin-expressing basket-cell network plasticity induced by experience regulates adult learning. Nature. 504(7479):272-6.

Donato F, Chowdhury A, Lahr M, Caroni P. 2015. Early- and late-born parvalbumin basket cell subpopulations exhibiting distinct regulation and roles in learning. Neuron. 85(4):770-86.

Farkas O, Povlishock JT. 2007. Cellular and subcellular change evoked by diffuse traumatic brain injury: a complex web of change extending far beyond focal damage. Prog Brain Res. 161:43-59.

Foerstner P, Rehman R, Anastasiadou S, Haffner-Luntzer M, Sinske D, Ignatius A, Roselli F, Knoell B. 2018. Neuroinflammation after traumatic brain injury (TBI) is enhanced in activating transcription factor 3 (ATF3) mutant mice. J Neurotrauma. doi: 10.1089/neu.2017.5593. [Epub ahead of print]

Johnstone VP, Yan EB, Alwis DS, Rajan R. 2013. Cortical hypoexcitation defines neuronal responses in the immediate aftermath of traumatic brain injury. PLoS One. 8(5):e63454.

Johnstone VP, Shultz SR, Yan EB, O'Brien TJ, Rajan R. 2014. The acute phase of mild traumatic brain injury is characterized by a distance-dependent neuronal hypoactivity. J Neurotrauma. 31(22):1881-95.

Haider B, Häusser M, Carandini M. 2013. Inhibition dominates sensory responses in the awake cortex. Nature. 493(7430):97-100.

Hardingham GE, Fukunaga Y, Bading H. 2002. Extrasynaptic NMDARs oppose synaptic NMDARs by triggering CREB shut-off and death pathways. *Nat Neurosci* 5: 405-415.

Hardingham GE, Bading H. 2010. Synaptic versus extrasynaptic NMDA receptor signalling: implications for neurodegenerative disorders. Nat Rev Neurosci. 11(10):682-96.

Hertle DN, Beynon C, Neumann JO, Santos E, Sánchez-Porras R, Unterberg AW, Sakowitz OW. 2016. Use of GABAergic sedatives after subarachnoid hemorrhage is associated with worse outcome-preliminary findings. J Clin Anesth. 35:118-122.

Hertle DN, Dreier JP, Woitzik J, Hartings JA, Bullock R, Okonkwo DO, Shutter LA, Vidgeon S, Strong AJ, Kowoll C, Dohmen C, Diedler J, Veltkamp R, Bruckner T, Unterberg AW, Sakowitz OW. 2012. Cooperative Study of Brain Injury Depolarizations (COSBID). Effect of analgesics and sedatives on the occurrence of spreading depolarizations accompanying acute brain injury. Brain. 135(Pt 8):2390-8.

Hinzman JM, DiNapoli VA, Mahoney EJ, Gerhardt GA, Hartings JA. 2015. Spreading depolarizations mediate excitotoxicity in the development of acute cortical lesions. Exp Neurol. 267:243-53.

Hsieh TH, Lee HHC, Hameed MQ, Pascual-Leone A, Hensch TK, Rotenberg A. 2017. Trajectory of Parvalbumin Cell Impairment and Loss of Cortical Inhibition in Traumatic Brain Injury. Cereb Cortex. 27(12):5509-5524.

Hu H, Gan J, Jonas P. 2014. Interneurons. Fast-spiking, parvalbumin^{+} GABAergic interneurons: from cellular design to microcircuit function. Science. 345(6196):1255263.

Isaacson JS, Scanziani M. 2011. How inhibition shapes cortical activity. Neuron. 72(2):231-43.

Kaur P, Sharma S. 2017. Recent Advances In Pathophysiology Of Traumatic Brain Injury. Curr Neuropharmacol. doi: 10.2174/1570159X15666170613083606. [Epub ahead of print]

Khoshkhoo S, Vogt D, Sohal VS. 2017. Dynamic, Cell-Type-Specific Roles for GABAergic Interneurons in a Mouse Model of Optogenetically Inducible Seizures. Neuron. 93(2):291-298.

Lau D, Bengtson CP, Buchthal B, Bading H. 2015. BDNF Reduces Toxic Extrasynaptic NMDA Receptor Signaling via Synaptic NMDA Receptors and Nuclear-Calcium-Induced Transcription of inhba/Activin A. Cell Rep. 12(8):1353-66.

Léveillé F, Papadia S, Fricker M, Bell KF, Soriano FX, Martel MA, Puddifoot C, Habel M, Wyllie DJ, Ikonomidou C, Tolkovsky AM, Hardingham GE. 2010. Suppression of the intrinsic apoptosis pathway by synaptic activity. J Neurosci. 30(7):2623-35.

Lu Y, Sun XD, Hou FQ, Bi LL, Yin DM, Liu F, Chen YJ, Bean JC, Jiao HF, Liu X, Li BM, Xiong WC, Gao TM, Mei L. 2014. Maintenance of GABAergic activity by neuregulin 1-ErbB4 in amygdala for fear memory. Neuron. 84(4):835-46.

Martin JL, Sloviter RS. 2001. Focal inhibitory interneuron loss and principal cell hyperexcitability in the rat hippocampus after microinjection of a neurotoxic conjugate of saporin and a peptidase-resistant analog of Substance P. J Comp Neurol. 436(2):127-52.

Mauceri D, Freitag HE, Oliveira AM, Bengtson CP, Bading H. 2011. Nuclear calcium-VEGFD signaling controls maintenance of dendrite arborization necessary for memory formation. Neuron 71: 117-130.

Mauceri D, Hagenston AM, Schramm K, Weiss U, Bading H. 2015. Nuclear Calcium Buffering Capacity Shapes Neuronal Architecture. J Biol Chem. 290(38):23039-49.

Papadia S, Soriano FX, Léveillé F, Martel MA, Dakin KA, Hansen HH, Kaindl A, Sifringer M, Fowler J, Stefovska V, McKenzie G, Craigon M, Corriveau R, Ghazal P, Horsburgh K, Yankner BA, Wyllie DJ, Ikonomidou C, Hardingham GE. 2008. Synaptic NMDA receptor activity boosts intrinsic antioxidant defenses. Nat Neurosci. 11(4):476-87.

Paz JT, Davidson TJ, Frechette ES, Delord B, Parada I, Peng K, Deisseroth K, Huguenard JR. 2013. Closed-loop optogenetic control of thalamus as a tool for interrupting seizures after cortical injury. Nat Neurosci. 16(1):64-70.

Pohl D, Bittigau P, Ishimaru MJ, Stadthaus D, Hübner C, Olney JW, Turski L, Ikonomidou C. 1999. N-Methyl-D-aspartate antagonists and apoptotic cell death triggered by head trauma in developing rat brain. Proc Natl Acad Sci U S A. 96(5):2508-13.

Qiu J, Tan YW, Hagenston AM, Martel MA, Kneisel N, Skehel PA, Wyllie DJ, Bading H, Hardingham GE. 2013. Mitochondrial calcium uniporter Mcu controls excitotoxicity and is transcriptionally repressed by neuroprotective nuclear calcium signals. Nat Commun. 4:2034.

Roth BL. 2016. DREADDs for Neuroscientists. Neuron. 89(4):683-94.

Samson AJ, Robertson G, Zagnoni M, Connolly CN. 2016. Neuronal networks provide rapid neuroprotection against spreading toxicity. Sci Rep. 6:33746.

Sawant-Pokam PM, Suryavanshi P, Mendez JM, Dudek FE, Brennan KC. 2017. Mechanisms of Neuronal Silencing After Cortical Spreading Depression. Cereb Cortex. 27(2):1311-1325.

Schlumm F, Mauceri D, Freitag HE, Bading H. 2013. Nuclear calcium signaling regulates nuclear export of a subset of class IIa histone deacetylases following synaptic activity. J Biol Chem. 288(12):8074-84.

Simonetti M, Hagenston AM, Vardeh D, Freitag HE, Mauceri D, Lu J, Satagopam VP, Schneider R, Costigan M, Bading H, Kuner R. 2013. Nuclear calcium signaling in spinal neurons drives a genomic program required for persistent inflammatory pain. Neuron 77: 43-57

Sun D, Chen X, Gu G, Wang J, Zhang J. 2017. Potential Roles of Mitochondria-Associated ER Membranes (MAMs) in Traumatic Brain Injury. Cell Mol Neurobiol. 37(8):1349-1357.

Sun Y, Ikrar T, Davis MF, Gong N, Zheng X, Luo ZD, Lai C, Mei L, Holmes TC, Gandhi SP, Xu X. 2016. Neuregulin-1/ErbB4 Signaling Regulates Visual Cortical Plasticity. Neuron. 92(1):160-173.

Trevelyan AJ, Sussillo D, Watson BO, Yuste R. 2006. Modular propagation of epileptiform activity: evidence for an inhibitory veto in neocortex. J Neurosci. 26(48):12447-55.

Yang CF, Chiang MC, Gray DC, Prabhakaran M, Alvarado M, Juntti SA, Unger EK, Wells JA, Shah NM. 2013. Sexually dimorphic neurons in the ventromedial hypothalamus govern mating in both sexes and aggression in males. Cell. 153(4):896-909.

Yang JW, Prouvot PH, Reyes-Puerta V, Stüttgen MC, Stroh A, Luhmann HJ. 2017. Optogenetic Modulation of a Minor Fraction of Parvalbumin-Positive Interneurons Specifically Affects Spatiotemporal Dynamics of Spontaneous and Sensory-Evoked Activity in Mouse Somatosensory Cortex in Vivo. Cereb Cortex. 27(12):5784-5803.

Vascak M, Jin X, Jacobs KM, Povlishock JT. 2017. Mild Traumatic Brain Injury Induces Structural and Functional Disconnection of Local Neocortical Inhibitory Networks via Parvalbumin Interneuron Diffuse Axonal Injury. Cereb Cortex. 4:1-20.

Wang CF, Zhao CC, Jiang G, Gu X, Feng JF, Jiang JY. 2016. The Role of Posttraumatic Hypothermia in Preventing Dendrite Degeneration and Spine Loss after Severe Traumatic Brain Injury. Sci Rep. 6:37063.

Weber JT. 2012. Altered calcium signaling following traumatic brain injury. Front Pharmacol. 3:60.

Wilent WB, Contreras D. 2005. Dynamics of excitation and inhibition underlying stimulus selectivity in rat somatosensory cortex. Nat Neurosci. 8(10):1364-70.

Winston CN, Chellappa D, Wilkins T, Barton DJ, Washington PM, Loane DJ, Zapple DN, Burns MP. 2013. Controlled cortical impact results in an extensive loss of dendritic spines that is not mediated by injury-induced amyloid-beta accumulation. J Neurotrauma. 30(23):1966-72.

Wroge CM, Hogins J, Eisenman L, Mennerick S. 2012. Synaptic NMDA receptors mediate hypoxic excitotoxic death. J Neurosci. 32(19):6732-42.

Zhang SJ, Steijaert MN, Lau D, Schütz G, Delucinge-Vivier C, Descombes P, Bading, H. 2007. Decoding NMDA receptor signaling: identification of genomic programs specifying neuronal survival and death. Neuron 53: 549-562.

Zhang SJ, Zou M, Lu L, Lau D, Ditzel DA, Delucinge-Vivier C, Aso Y, Descombes P, Bading H. 2009. Nuclear calcium signaling controls expression of a large gene pool: identification of a gene program for acquired neuroprotection induced by synaptic activity. PLoS Genet. 5(8):e1000604.

Zhang SJ, Buchthal B, Lau D, Hayer S, Dick O, Schwaninger M, Veltkamp R, Zou M, Weiss U, Bading H. 2011. A signaling cascade of nuclear calcium-CREB-ATF3 activated by synaptic NMDA receptors defines a gene repression module that protects against extrasynaptic NMDA receptor-induced neuronal cell death and ischemic brain damage. J Neurosci. 31(13):4978-90.

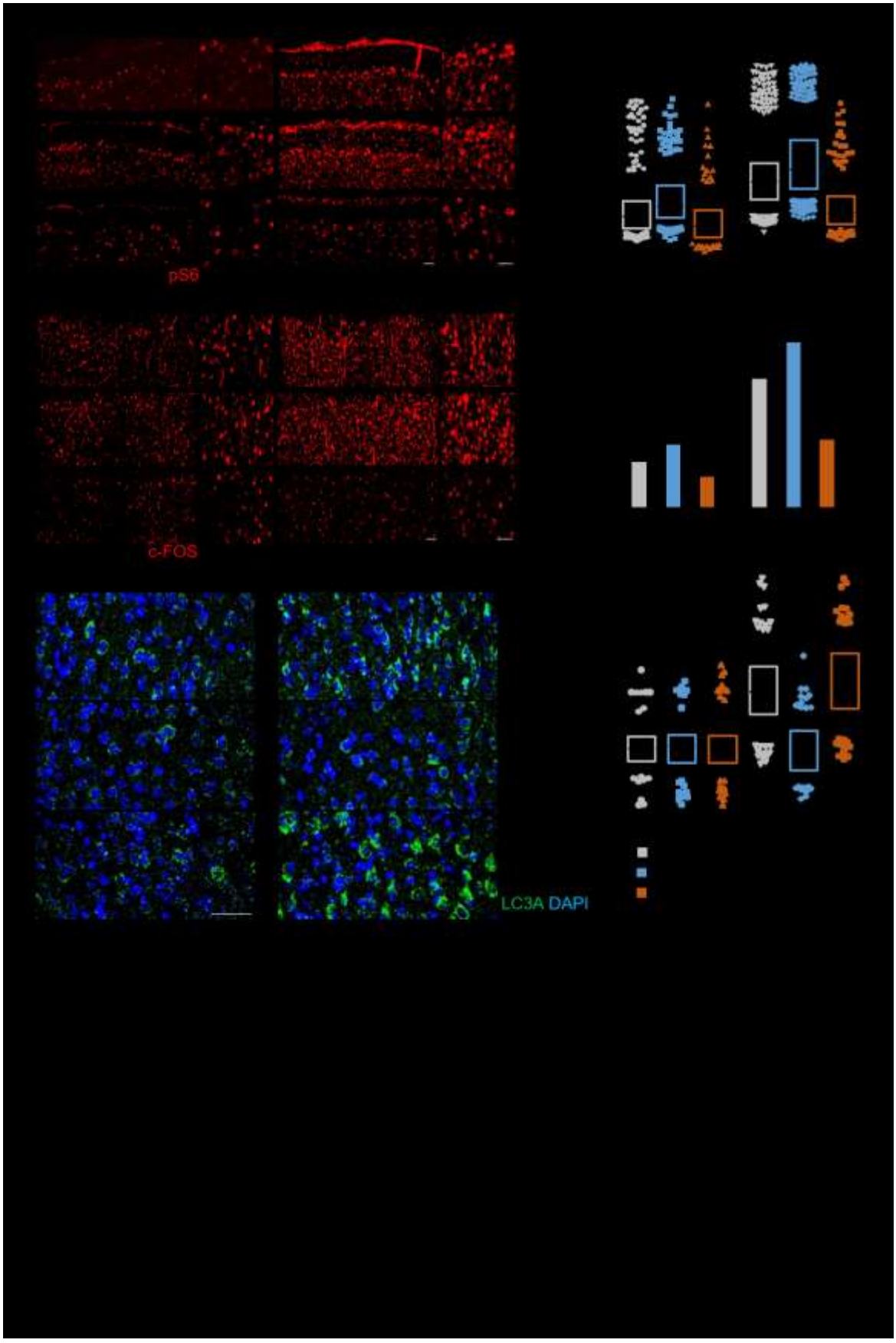
pS6
c-FOS
LC3A DAPI

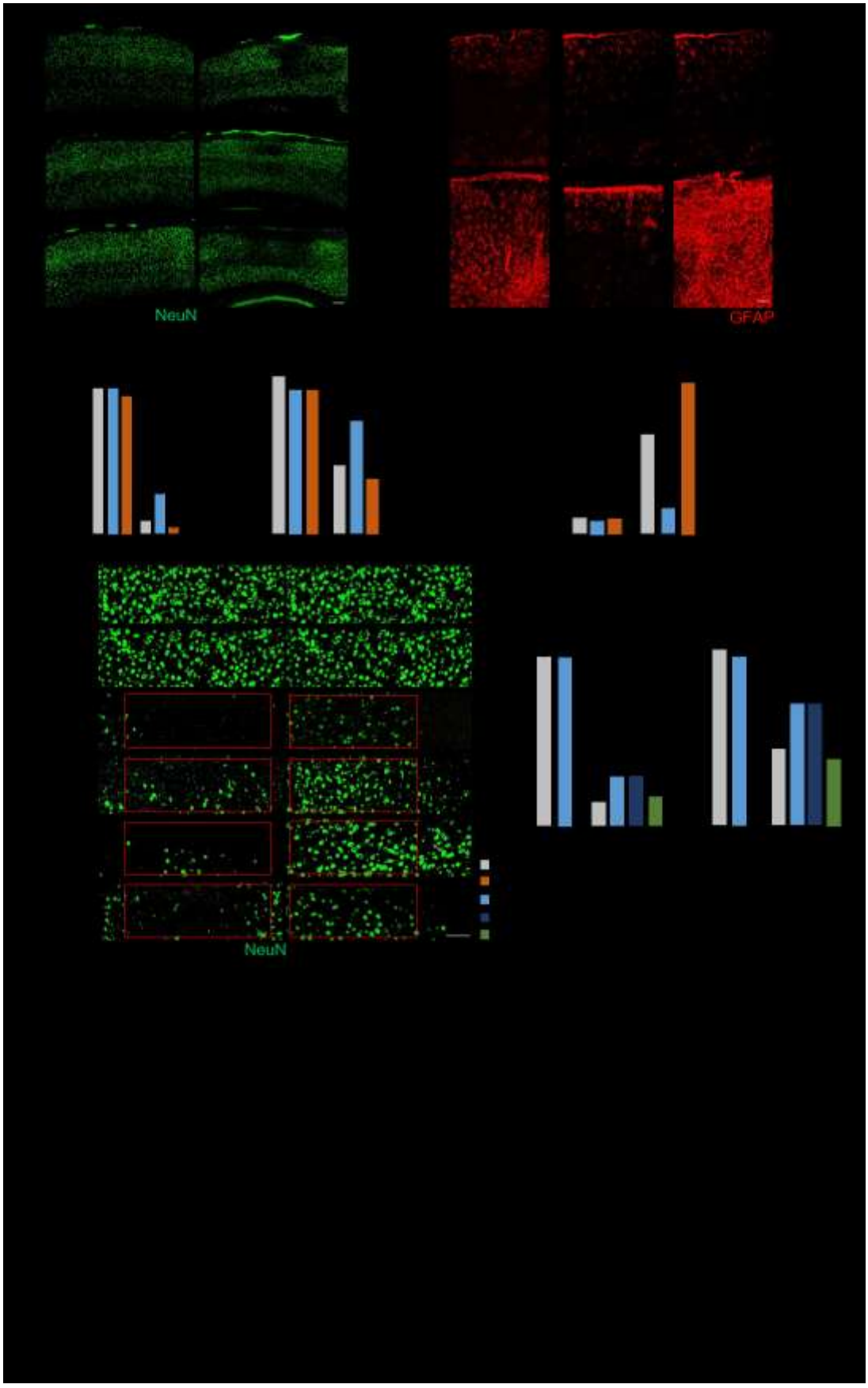
NeuN
GFAP
NeuN

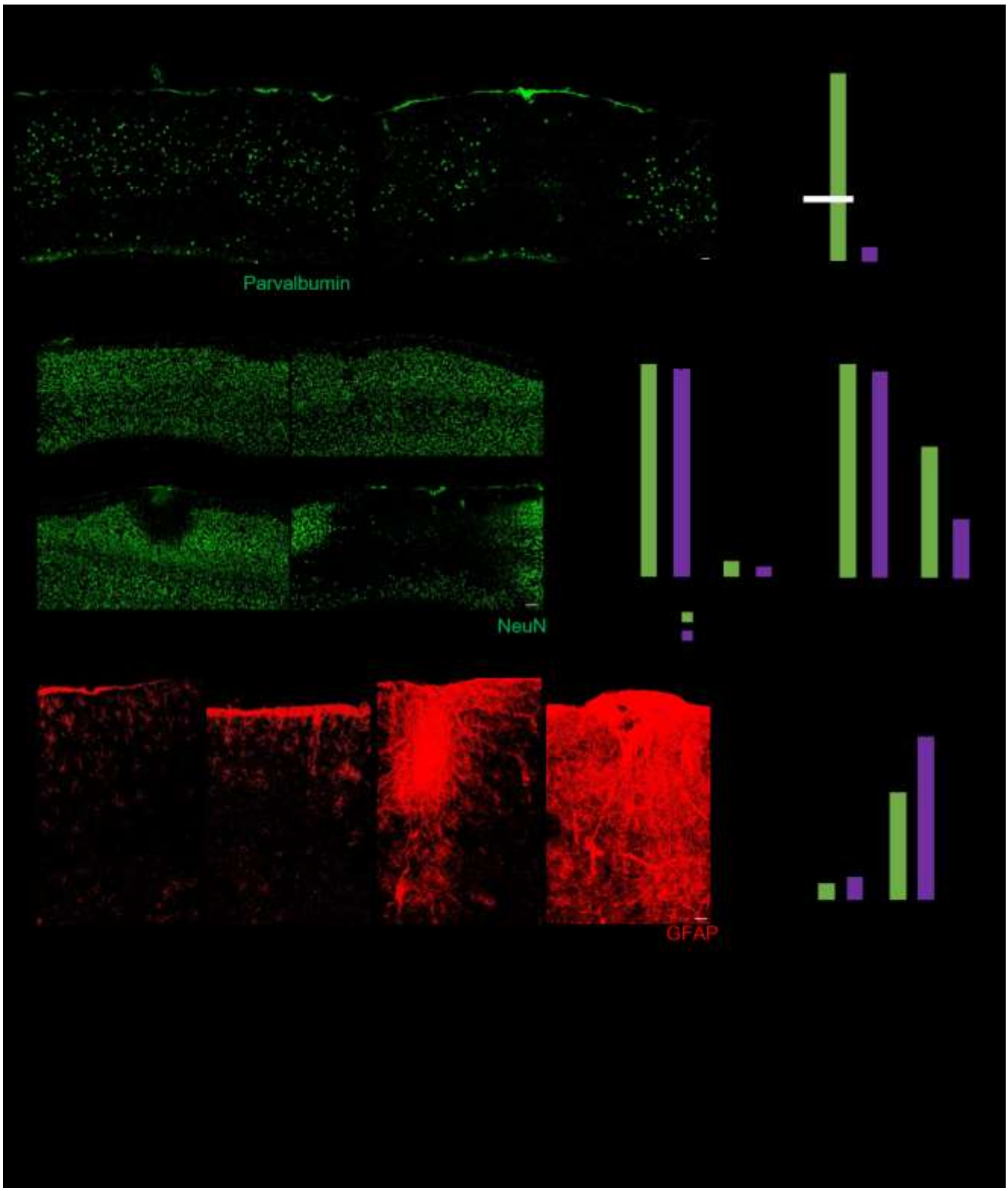
Parvalbumin
NeuN
GFAP

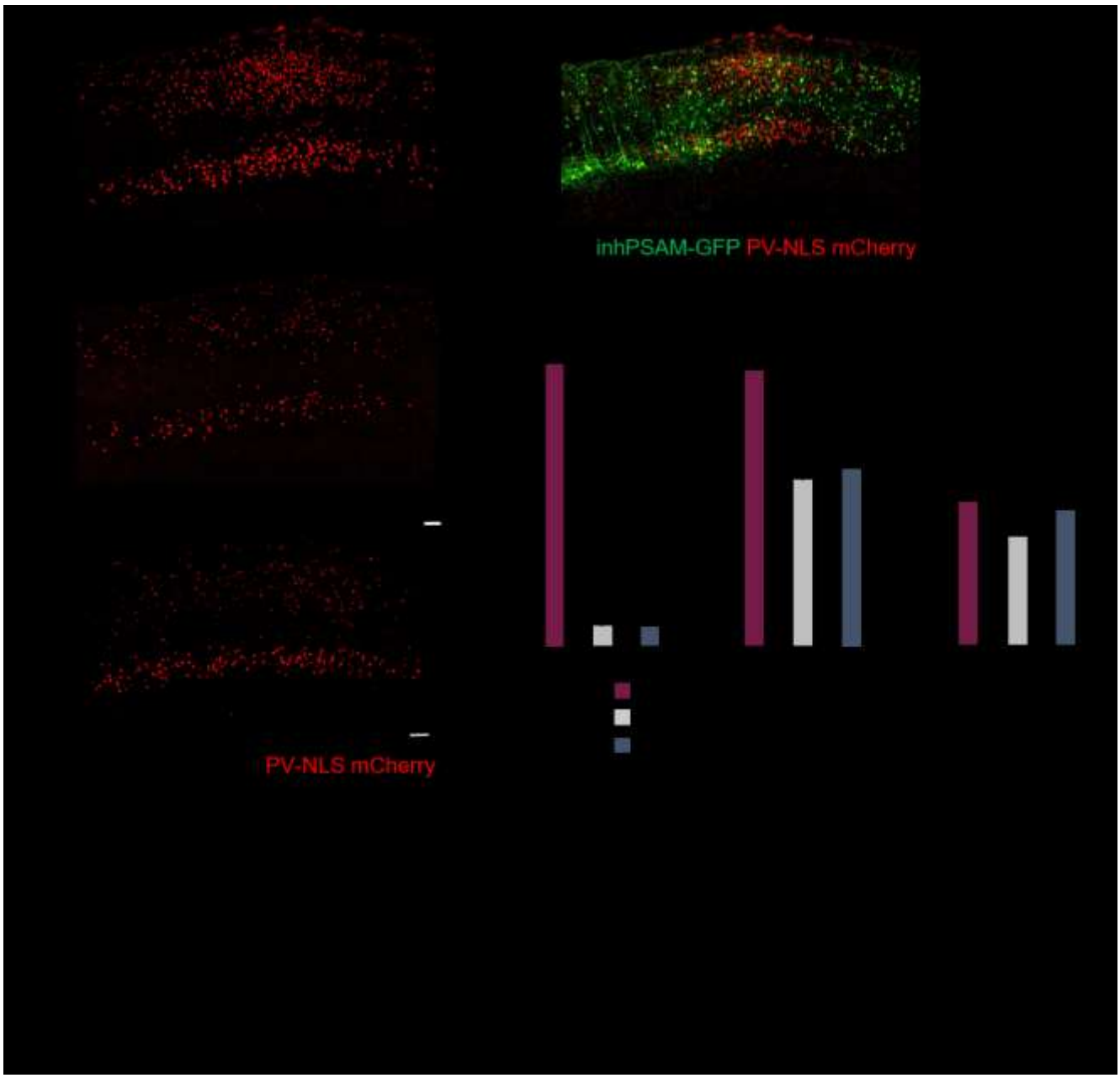
inhPSAM-GFP PV-NLS mCherry
PV-NLS mCherry

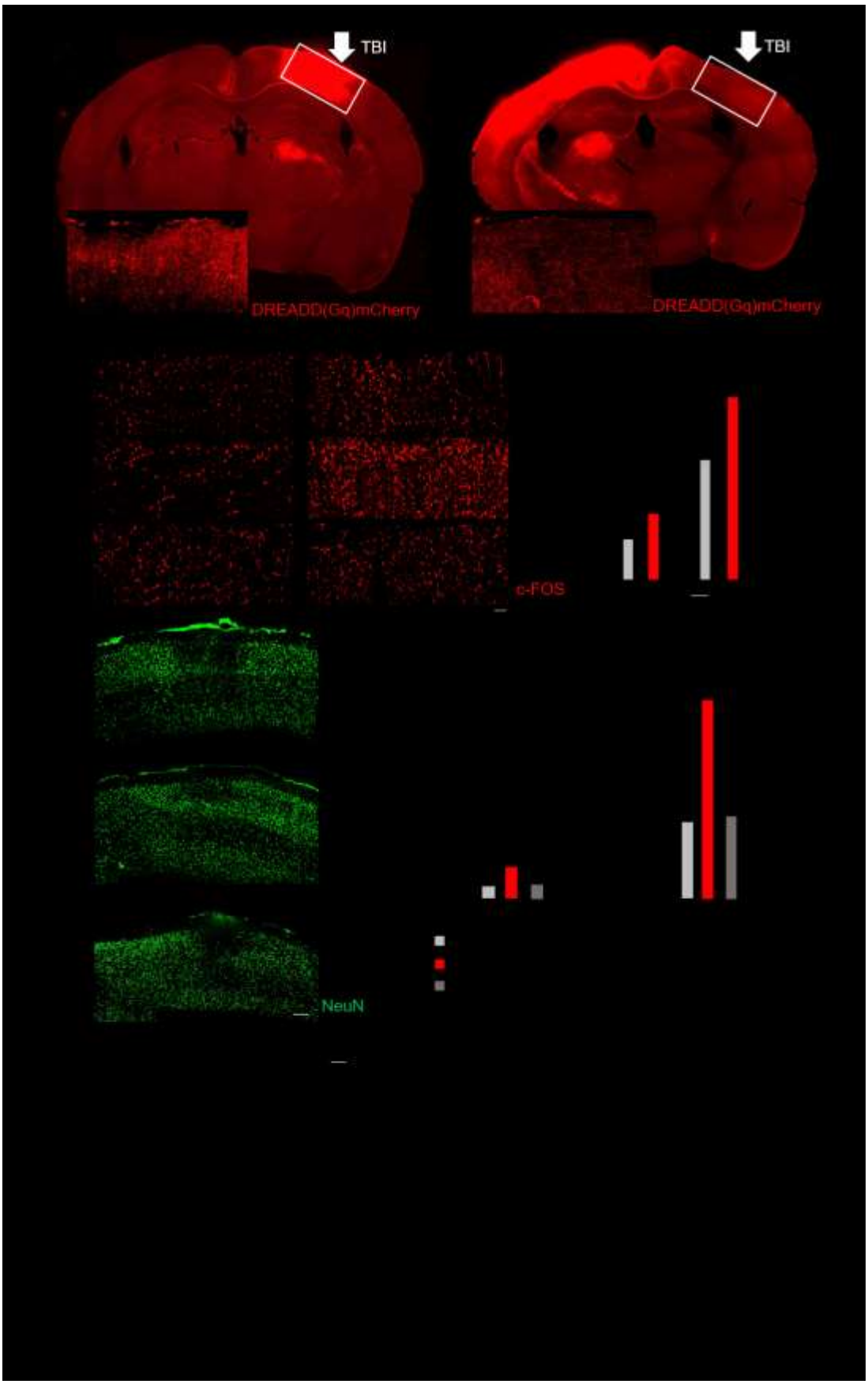
TBI
TBI
DREADD(Gq)mCherry
DREADD(Gq)mCherry
c-FOS
NeuN


Acute-pre agonist administration
Acute-post agonist administration
Sub-acute agonist administration

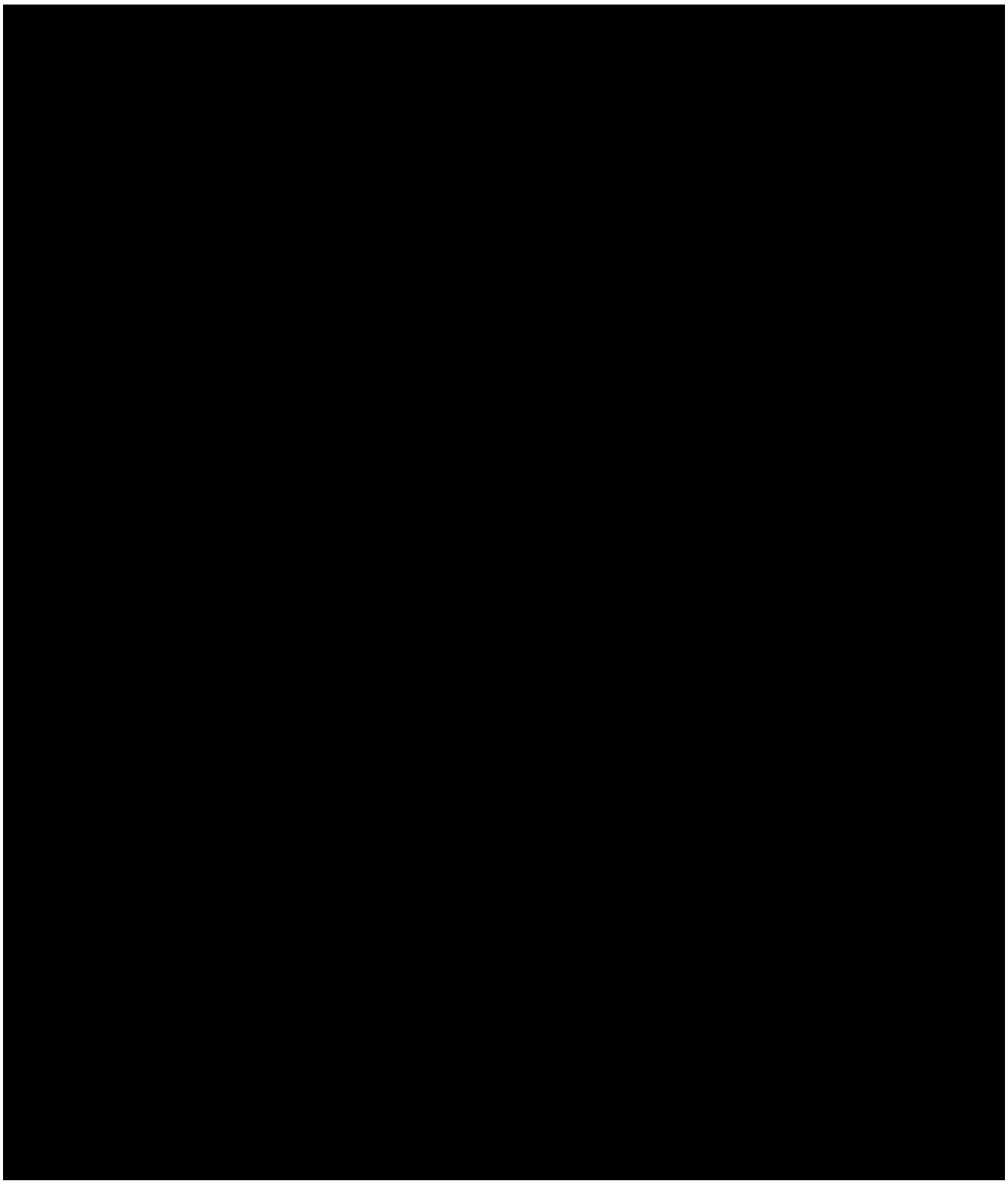

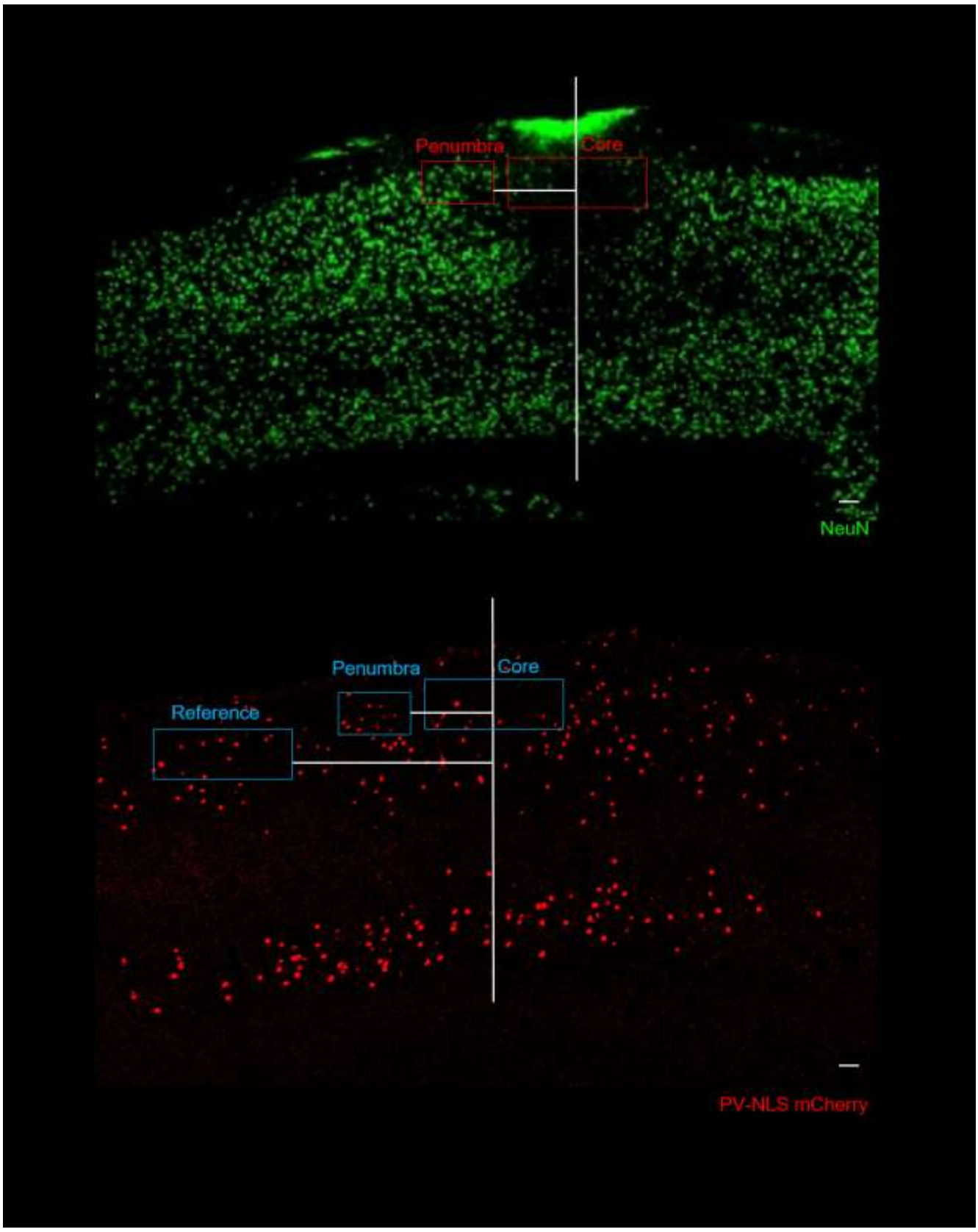
Penumbra
Core
NeuN
Penumbra
Core
Reference
PV-NLS mCherry

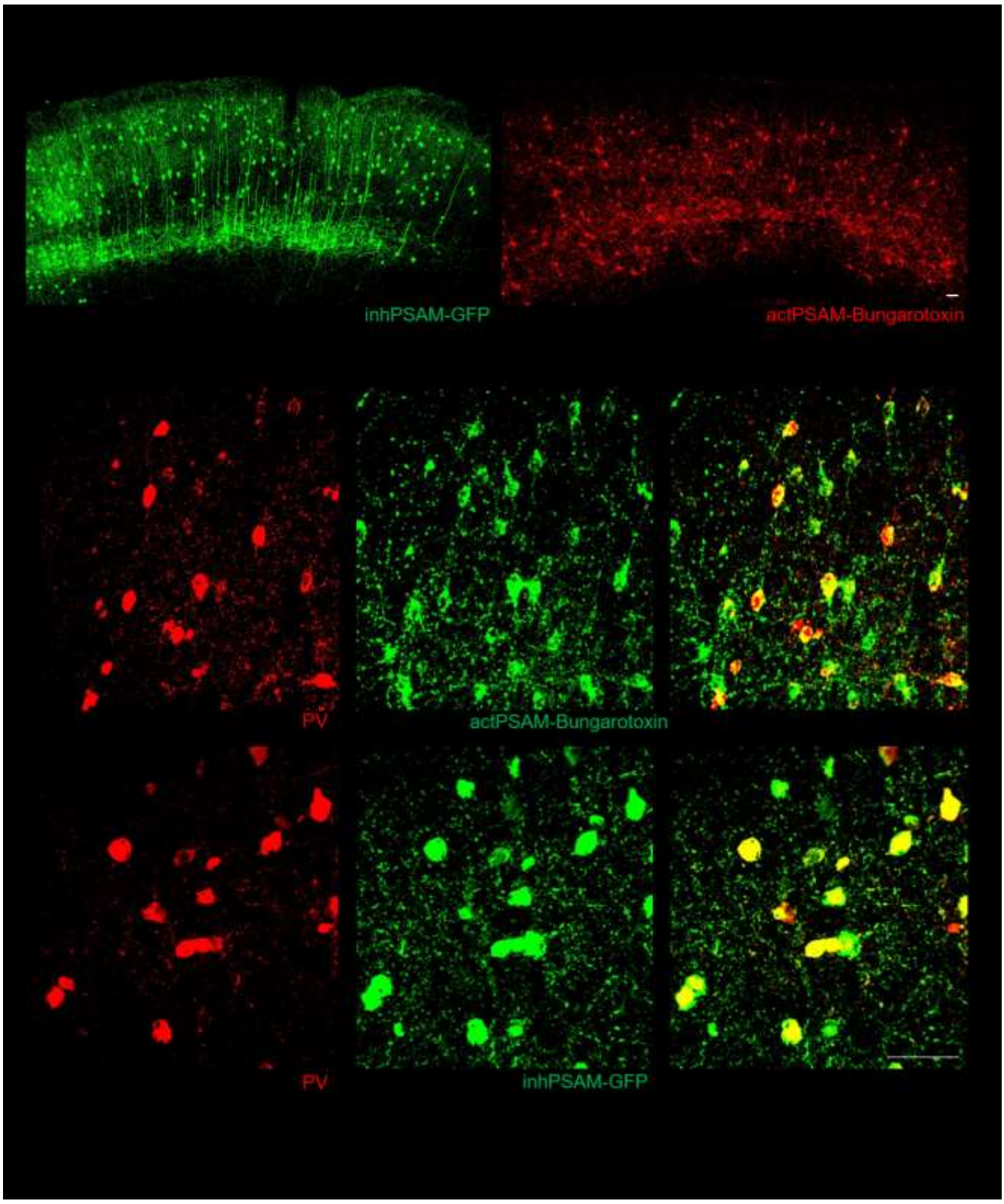
inhPSAM-GFP
actPSAM-Bungarotoxin
PV
actPSAM-Bungarotoxin
PV
inhPSAM-GFP

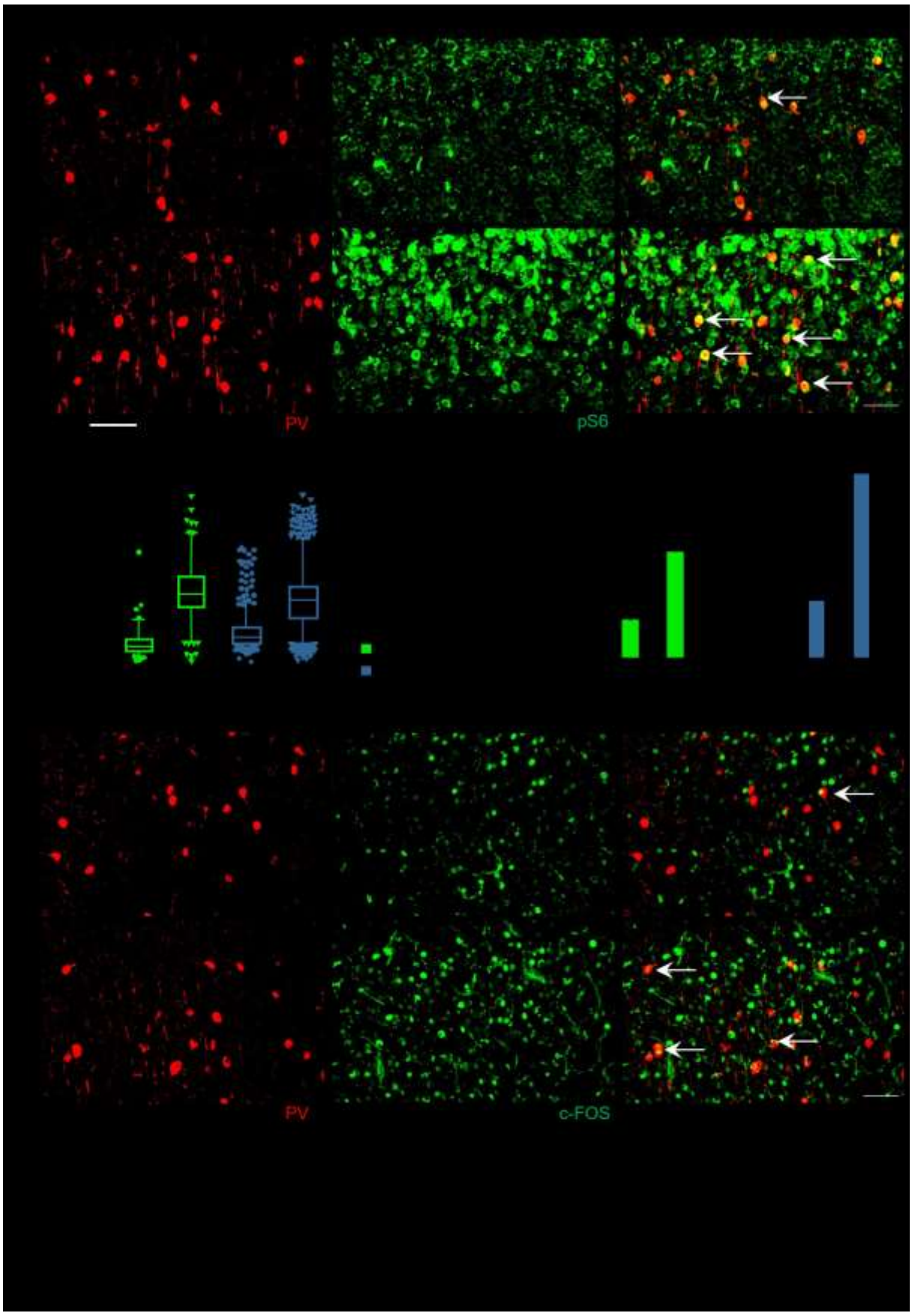
PV
pS6
PV
c-FOS

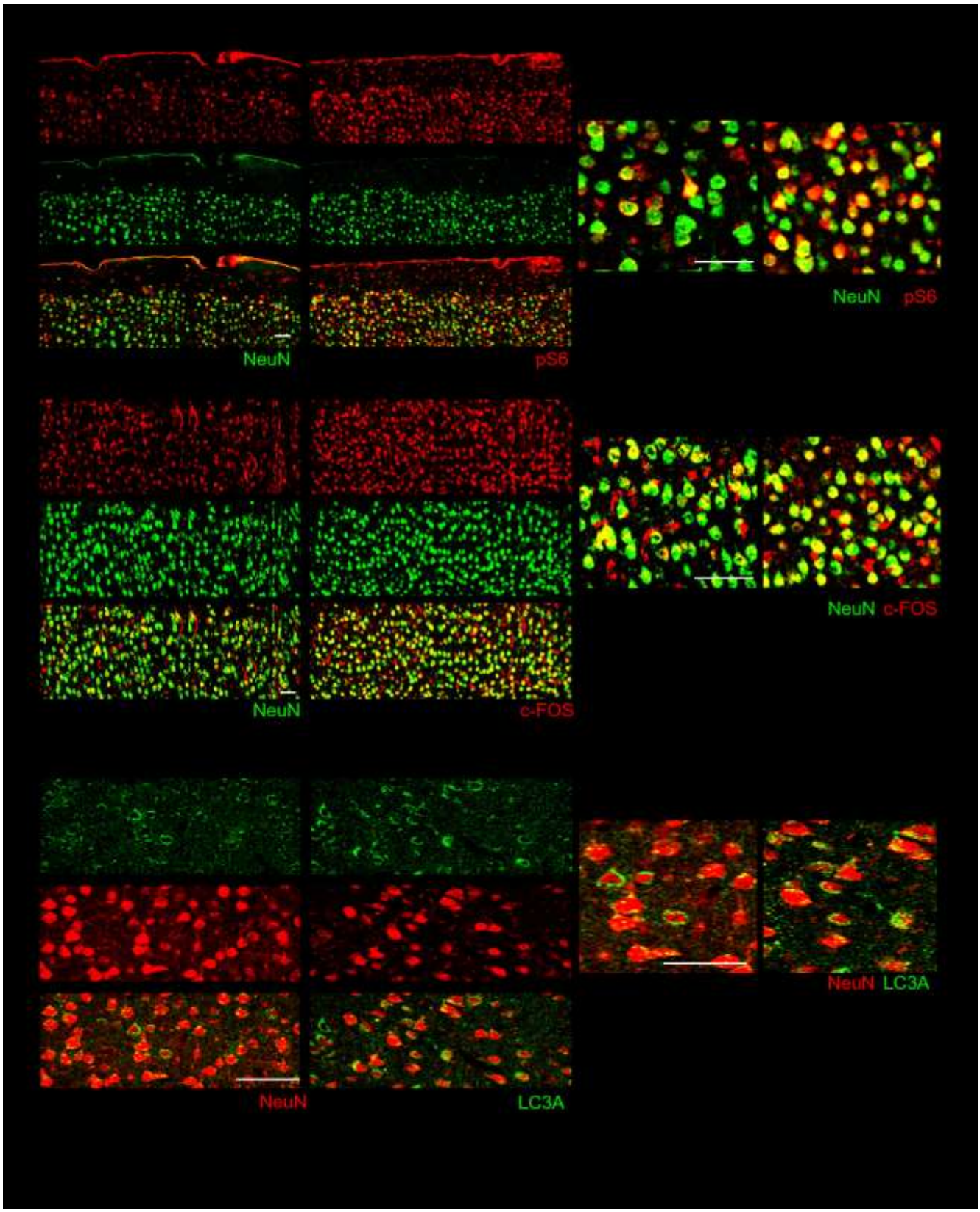
NeuN
pS6
NeuN pS6
NeuN
c-FOS
NeuN c-FOS
NeuN
LC3A
NeuN LC3A

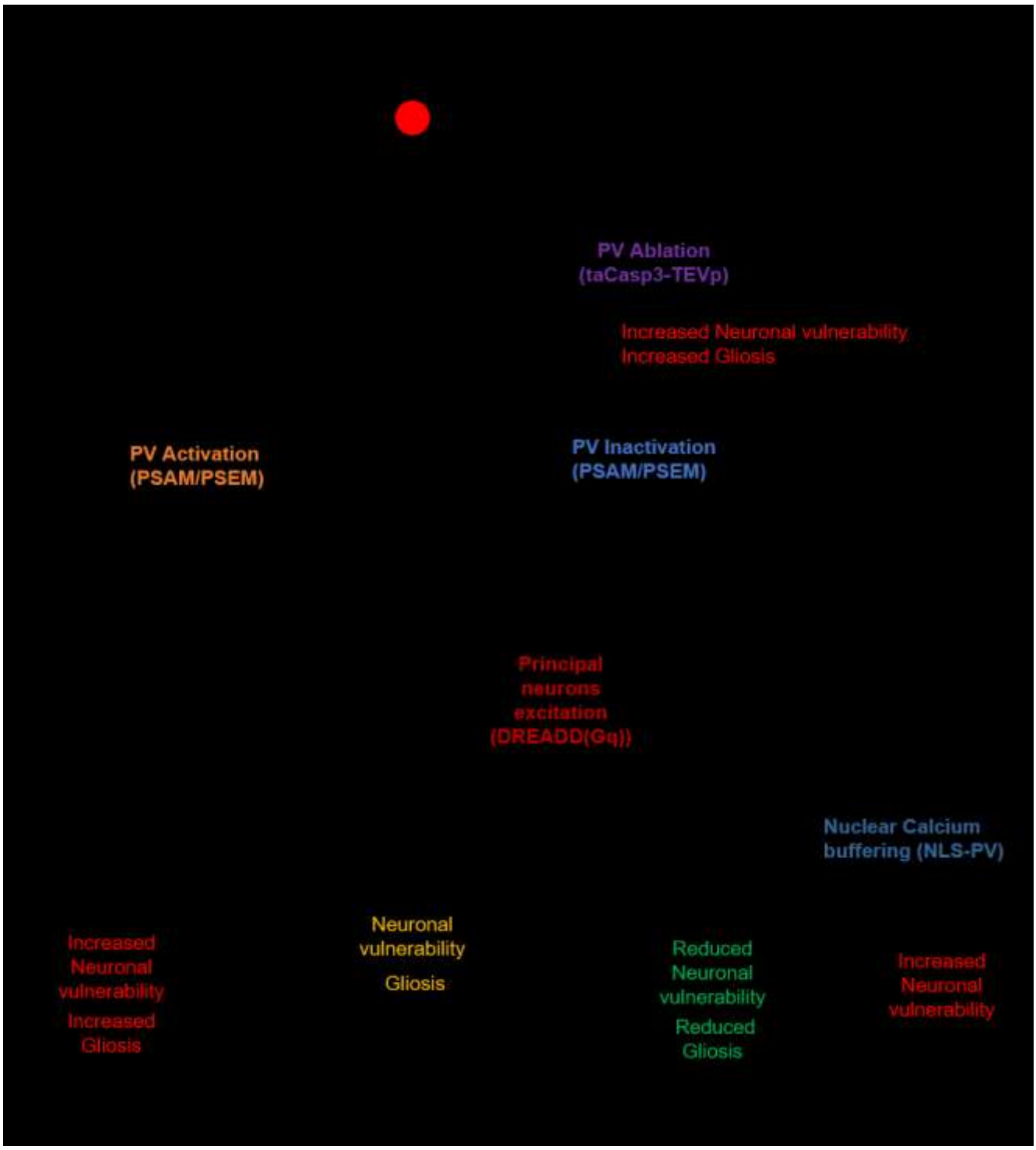
PV Ablation
(taCasp3-TEVp)
Increased Neuronal vulnerability
Increased Gliosis
PV Activation
(PSAM/PSEM)
PV Inactivation
(PSAM/PSEM)
Principal
neurons
excitation
(DREADD(Gq))
Nuclear Calcium
buffering (NLS-PV)
Increased
Neuronal
vulnerability
Increased
Gliosis
Neuronal
vulnerability
Gliosis
Reduced
Neuronal
vulnerability
Reduced
Gliosis
Increased
Neuronal
vulnerability

7 Discussion

In the present work, we have demonstrated that ethanol pre-treatment (resulting from a BAL that was comparable with protective effect on TBI patients [>230mg/dL], Berry et al 2011), resulted in enhanced recovery of sensorimotor skills and reducing neuronal vulnerability to TBI. This supports the clinical hypothesis that pre-ethanol intoxication is neuroprotective in TBI. Our findings also suggest that the modulation of the neuroinflammatory response and the early transcriptional response connected to the propagation of neuronal activity may be some of the many mechanisms of ethanol induced neuroprotection. We were also able to show that mechanistic targeting of signaling cascades, importantly RTK signaling, show that ethanol intoxication may strongly affect events unfolding at the synaptic level after trauma and thus pave the way for identification of new targets for intervention at this level. The translational potential of our finding is supported by the identification of Lapatinib (an FDA approved drug for breast cancer) as a potential neuroprotective agent when administered after trauma. Our results also show that apart from targeting RTK signaling which control the activity and plasticity of inhibitory interneurons, we could use chemogenetic tools to directly modulate the activity of the inhibitory microcircuits involving PV interneurons which modulate neuronal loss and gliosis in TBI.

7.1 Ethanol intoxication before TBI is neuroprotective

An aim of this work was to establish the effect of ethanol intoxication on TBI. Our data suggest that ethanol intoxication before injury is potentially protective both at a behavioral and histological level although this effect is restricted to a high-dose of ethanol. These findings are

in agreement with clinical studies suggesting a possible beneficial interaction (Salim et al., 2009; Berry et al., 2011; Brennan et al., 2015) and with some (Janis et al., 1998; Kelly et al., 1997) but not all (Vaagenes et al., 2015) experimental data.

The protective effect of ethanol already appears at the early time points assessed (starting 3h post injury) suggesting that ethanol works by dampening acute pathogenic pathways which contribute to the onset of neurological deficits, thus setting the stage for pathogenic evolution over the next hours or days after TBI.

While the effect of ethanol in TBI is controlled by many parameters including: the small clinical cohort (due to large variability in the clinical presentation of TBI), different species (rats vs mice) and different TBI models (open vs blunt) in an experimental setting and modification of its own kinetics due to the pathogenic effects unfolding after TBI (presence of macroscopic hematomas, Chandrasekar et al 2017), the beneficial effects of ethanol observed definitely provides an understanding into the acute cascades following injury.

7.2 Neuroinflammation after TBI is modulated by ethanol intoxication

The neuroprotective effect of ethanol intoxication on TBI suggests a modulation of the neuro-inflammatory response as shown by a shift in the cytokine pattern. Ethanol has immunosuppressive effects in experimental models and trauma patients as shown by the lower blood IL-6 and leukocyte counts (Griffenstein et al 2007, Wagner et al 2016, Relja et al 2016) which correlate with our finding of higher levels of Akt and Erk phosphorylation and loss of protein synthesis suppression.

In our study, a large cytokine panel helped us elucidate that ethanol exerts a suppressive effect on several but not all (exception TNF-α) inflammation related cytokines such as IL-6, MCP-1

and GM-CSF (Goodman et al 2013), to name a few, and at the same time increases intraparenchymal levels of IL-13 and M-CSF. The acute overall suppression of inflammatory cytokine levels suggests a stable decrease in the inflammatory response, which corresponds both to the improved neurological condition in ethanol-pretreated mice, and to the higher levels of Akt signaling and protein synthesis.

Although the overall neuroinflammatory effects of the cytokine patterns is influenced by the interaction of multiple players, IL-13 emerges as a striking cytokine in TBI which is strongly modulated by ethanol. It is know that ethanol can enhance IL-13 release under certain conditions (Bouchard et al 2012, Alonso et al 2012) which suggests that the observed peak in IL-13 could originate from the periphery or in the brain. IL-13 is a critical factor in inducing a protective/reparative phenotype in macrophages (Bosurgi et al 2017) and together with IL-4, is a key factor in inducing alternative polarization of microglia (Kiguchi et al 2017, Mori et al 2016, Dooley et al 2016). Furthermore, IL-13 can induce apoptosis in activated microglia (Yang et al 2002, Won et al 2013) and can have direct protective effects by inducing the secretion of BDNF in astrocytes (Brombacher et al 2017). Thus, the early peak in IL13 may be a critical instructive signal reducing early inflammation and therefore allowing for reduced neurological deterioration. These data suggest that the translational study of IL-13 in TBI is warranted.

Despite the short half-life of ethanol (Wilkinson et al 1980), the effects on cytokine patterns are long lasting and affect the extent of immune cells infiltration and microglial activation at 7 dpi, in agreement with the improvement in neurological function. Since ethanol is cleared within< 24 h, these long-lasting effects may be of consequence in early events of TBI neuro-inflammation that play a critical role in orienting the cascades that unfold in time.

7.3 TBI associated early transcriptional response helps modulate propagation of neuronal activity

Immediate early genes are classically correlated with proliferation and neuroprotection (Zhang et al., 2002, Flavell and Greenberg, 2008). This makes them interesting candidates of study for many pathological conditions including trauma.

The early transctiptional response to TBI is a staging event of the process which unfold in the following hours or days (Samal et al 2015). To study the interaction of TBI and ethanol we characterized a set of immediate early genes at 3h using RT PCR. This revealed that there is a hierarchy in the gene induction characterized by sensitivity to TBI, sensitivity to ethanol and the schedule of administration. The largest group of IEGs is activated by TBI and markedly, although in some cases not completely, downregulated by EtOH pre-administration. EtOH reduces (although to variable extent, cfr. Atf-3 and Egr-3) the transcription of c-Fos, FosB, ΔFosB, Egr3, Atf3, Npas4, which are known to depend on excitation-activated Erk signaling cascade (Wang et al., 2014; Flavell and Greenberg, 2008). Many of the IEGs investigating in this study are well-established in activating neurons which leads us to conceive that pre-administration of ethanol interferes with a signaling cascade triggered by neuronal excitation and leads to transcriptional regulation.

Ethanol is recognized to be either a potentiator of GABAR currents (Hanchar et al., 2005; Kumar et al., 2009; Botta et al., 2014) or an antagonist of NMDAR (Criswell et al., 2004; He et al., 2013), and therefore exerts an overall suppressive action on neuronal excitation. Thus, it is likely that EtOH directly impinges on propagation of neuronal activity inducing signaling cascades at the neurotransmitter receptor level. Subsequently, activity of downstream signaling effectors including MAP kinases known to activate IEGs might be inhibited.

Despite the correlation between IEGs and neuroprotection, their functional targets and involvement in the regulation of neuronal cell biology is poorly understood. In fact IEGs are associated both with protective and detrimental effects (Lösing et al 2017, Oshitari et al 2002). Thus, ethanol mediated downregulation of IEGs may contribute to the observed ethanol related neuroprotection after TBI.

In conclusion, our data shows that presence of ethanol at the moment before trauma significantly decreases the trauma induced transcriptional response in the hippocampal neurons and also reduces neuronal vulnerability to trauma in the dentate gyrus of the hippocampus. However, limitations of the buffering capacity of ethanol to the severity of injury and the timing of administration limits its translational potential.

7.4 ErBb inhibitors recapitulate ethanol intoxication associated neuroprotection

In the course of this study, we have investigated the involved mechanisms following TBI exploring the pattern of phosphorylation of multiple RTKs after TBI. RTKs are recruited in signaling pathways involved in growth and survival and are anti-apoptotic in nature. The activation of a panel of RTKs after trauma point to this physiological, protective response. Ethanol intoxication associated downregulation of several RTKs after TBI may point towards ethanol limiting the initial damage and preventing the activation of the protective response. Given that ethanol has powerful GABAergic activities (Fazzari et al 2010) and it is an NMDAR antagonist (Criswell et al 2004), it may also help prevent the excitation-related damage (Brennan et al 2015) and limit excitation related RTK activation (such as the phosphorylation of ErbB3 or FGFR and EphB phosphorylation, Neddens et al 2011, Huang et al 2015). On the

other hand, RTKs are also involved in pathogenic responses to trauma. Activation of PDGFR has been linked to increased permeability of the blood brain barrier (BBB) after trauma (Su et al 2015) and activation of EphA2 has been linked to increased BBB dysfunction and neuronal loss in a stroke model (Thundyil et al 2013). Taken together our results show that the RTK activation pattern helps reveal the impact of ethanol intoxication on TBI and the specific role of each RTK needs to be investigated further in a case-by-case manner.

Further we were able to identify that TBI induces phosphorylation of ErbB receptors in the excitatory synapses and specific inhibitors of ErbB were able to recapitulate a significant fraction of EI associated neuroprotection. ErbB family members signal either as ErbB4 homodimers or as heterodimers of ErbB4 and either ErbB3 or ErbB2 (Mei et al 2008) and thus their expression is predicted to be comparable. In this study, we were able to show that TBI induces phosphorylation of ErbB expression in the excitatory synapses of the inhibitory PV interneurons and this is highly relevant for the control of the functions of these cells in the normal cortex (Wen et al 2010, Yin et al 2013) and under pathological conditions (Guan et al 2015, Zhang et al 2017). ErbB phosphorylation on interneurons has been shown to be homeostatically regulated: Reduced cortical excitation leads to the decrease in ErbB phosphorylation in PV interneurons, depotentiation and de-stabilization of excitatory synapses, and, ultimately, reduced PV activation (Sun et al 2016, Lu et al 2014). We speculate that upregulation of ErbB phosphorylation may be a homeostatic event triggered by TBI-triggered excitation and may lead to increased PV excitation after TBI.

Intriguingly, blockade of ErbB2 signaling by trastuzumab enhances peripheral nerve regeneration after acute or chronic damage (Hendry et al 2016). Targeting ErbB signaling in polytrauma patients suffering from central and peripheral nervous system injuries, would be highly attractive for the delivery of a double benefit. The translational potential of our finding is

supported by the identification of Lapatinib (an FDA-approved drug for the treatment of breast cancer) as a potential neuroprotective agent when administered before but, most important, also after the trauma. Lapatinib pharmacokinetics have been described and partial, dose dependent penetration of the brain has been shown in murine models (Afshar et al 2016, Polli et al 2008). Penetration of brain parenchyma has been shown to be enhanced when the BBB is disrupted (Polli et al 2008), suggesting that it may reach therapeutically relevant concentrations in murine and human brains after TBI. We have supported the Lapatinib data with a second ErbB inhibitor, AG825.

ErbB family expression pattern has been originally reported to include pyramidal cells as well as inhibitory interneurons. If excitatory input to PV is upregulated as a consequence of TBI, and prevented by EI, downregulation of PV firing would mimic, at least partially, EI effects. To demonstrate the effect of PV firing on TBI, we used chemogenetic tools to manipulate the PV firing and we able to show that whereas increasing PV firing was detrimental, decreasing it resulted in improved neuronal survival. This result contradicts the current model of excitotoxicity-induced neuronal death in TBI (Carron et al 2016), however, it must be noted that cortical neurons subject to TBI develop hyperexcitable phenotypes several weeks after trauma (Carron et al 2016, Alwis et al 2012). On the other hand, recordings of sensory-evoked responses in multiple TBI models have revealed that cortical neurons are largely hypoactive (Iwakura et al 2017) and do not respond to sensory stimulation in agreement with increased inhibition (Johnstone et al 2013, Allitt et al 2016, Johnstone et al 2014). This effect has been hypothesized to contribute to the generation of TBI-associated acute neurological deficits (Johnstone et al 2014). Thus, cortical neurons may be actually hypoactive soon after trauma, an effect that may be related to increased inhibition (in fact, activation of PV interneurons have

been shown to be sufficient to completely shutting down the firing of principal cells, Atallah et al 2012).

In conclusion, our study shows that preventing neuronal silencing either by preventing ErbB upregulation (as in the case of EI) or reducing perisomatic inhibition (as in the case of chemogenetic inhibition of PV interneurons) my contribute to neuroprotection after TBI. The neuroprotective mechanisms of ethanol intoxication may extend beyond the limitation of post TBI inhibition. Chemogenetic suppression of PV interneurons does not preclude the effects of ethanol and in fact, ethanol intoxication enhances neuronal survival even in the case of strong activation of PV interneurons. Given that ethanol is both a GABA agonist (Kumar et al 2009, Huang et al 2015) as well as an NMDAR antagonist (Criswell et al 2004), EI-associated neuroprotection may include direct decrease of excitability at the instance of trauma, reduced excitotoxicity through glutamate receptor inhibition, as well as modulatory effects on the neuroimmunological response (Chandrasekar et al 2017).

7.5 Manipulation of cortical micro-circuitry using chemogenetics helps neuronal vulnerability to TBI

In this study, we explored more in detail the manipulation of the cortical microcircuitry involving PV interneurons and were able to show that an underlying mechanism of the modulation of neuronal loss after TBI was blockade of nuclear calcium.

PV interneurons are powerful modulators of cortical excitability. In fact, strong activation of PV interneurons is enough to completely silence cortical areas (Atallah et al 2012), whereas inactivation of PV interneurons increases the basal and evoked firing rate of principal neurons in the somatosensory cortex (Agetsuma et al 2017, Yang et al 2017). In this study we show

that modulation of neuronal activity through PV interneurons offers an entry point to controlling the cortical activity in the first phases after trauma. In fact, not only are PV interneurons recruited in TBI (as shown by elevation of pS6 and c-Fos in PV^+ neurons), but their inactivation enhances, and their forced activation downregulates activity markers. In this way, the modulation of PV firing effectively modifies the biological response of principal neurons to TBI, decreasing the overall levels of the autophagic response. Our previous finding that TBI upregulates the phosphorylation of ErbB in the excitatory synapses of PV interneurons shows that PV interneurons may actually be involved in the pathophysiological regulation of activity within the microcircuits soon after trauma.

The principal neuron survival can be enhanced by inhibition of PV interneurons within the first 24 hours after trauma. These effects disappear when the neurons are inhibited in a delyed manner (starting 2dpi). Interestingly, the amount of inhibition provided by PV interneurons seem to decrease after 24h (at least in a mild TBI trauma; Vascak et al. 2017) and progressive degeneration of PV interneurons may contribute to the chronic hyperexcitability of the injured cortex (Buriticá et al. 2009; Hsieh et al. 2017; although not in all models: Carron et al. 2016). Although early inactivation of PV interneurons enhance the overall survival of neurons, ablation of PV interneurons does not prove beneficial showing that the chronic hyperexcitability of neurons which is expected to occur (Martin and Sloviter 2001 may enhance their vulnerability to the excitatory wave triggered by trauma.

The neuroprotective effect of PV inactivation can be recapitulated by the direct activation of principal neurons. This is in agreement with the neuroprotective effects of excitation observed in neurodegenerative diseases (Saxena et al., 2013, Roselli and Caroni, 2015). As an underlying mechanism, we show that the effect of acute inactivation of PV interneurons is blocked by the expression of an engineered nuclear Ca^{2+} buffer (Schlumm et al 2013),

confirming the excitation dependent neuroprotective pathway. The neuroprotection after TBI is controlled by the nuclear Ca^{2+} and involves activation of IEG factors such as ATF-3 and Npas-4 and the secreted proteins inhibinβA and SerpinB2 (Zhang et al. 2009, 2011; Bading 2013; Qiu et al. 2013; Ahlgren et al. 2014).

In conclusion, increasing the neuronal activity of the principal neurons either directly or indirectly helps prevent loss of neurons after TBI and appears to have a more pronounced effect on the penumbra of the injury than the core.

7.6 Conclusion

Taken together, our data provides support to the clinical evidence of neuroprotective effect of high dose ethanol (Brennan et al 2015, Salime et al 2009) showing a mechanistic effect targeting the neuro-immune response, transcriptional response of IEGs, RTK signaling and controlling activity and plasticity of inhibitory interneurons. IL-13 emerges as a striking cytokine, from the panel, which is upregulated by TBI and modulated by ethanol but it warrants a translational study into the effect of IL-13 in TBI. Our data revealed a possible therapeutic intervention using Lapatinib (an FDA-approved drug for the treatment of breast cancer) as a possible neuroprotective agent when administered shortly after trauma. We were also able to show that controlling cortical activity using chemogenetic tools also modulates the neuronal loss in TBI. In fact, pathological decrease or increase in the firing properties of vulnerable neuronal subpopulations appears to be a shared phenotype of multiple neurodegenerative conditions (Roselli and Caroni, 2015). Further understanding into the signaling of RTKs following TBI and modulation of the pathways controlling the inhibitory microcircuits many offer new approaches for understanding and targeting TBI pathogenic pathways.

8 References

1) Afshar, M., Netzer, G., Salisbury-Afshar, E., Murthi, S., and Smith, G.S. (2016). Injured patients with very high blood alcohol concentrations. Injury 47, 83–88.

2) Agetsuma M, Hamm JP, Tao K, Fujisawa S, Yuste R. 2017. Parvalbumin-positive interneurons regulate neuronal ensembles in visual cortex. Cereb Cortex. 6:1–15.

3) Ahlgren, H., Bas-Orth, C., Freitag, H.E., Hellwig, A., Ottersen, O.P., Bading, H., 2014 Apr 4. The nuclear calcium signaling target, activating transcription factor 3 (ATF3), protects against dendrotoxicity and facilitates the recovery of synaptic transmission after an excitotoxic insult. J. Biol. Chem. 289 (14), 9970–9982.

4) Alder J, Fujioka W, Lifshitz J, Crockett DP, Thakker-Varia S. Lateral fluid percussion: model of traumatic brain injury in mice. *J Vis Exp*. 2011;(54):3063. Published 2011 Aug 22. doi:10.3791/3063

5) Allitt BJ, Iva P, Yan EB, Rajan R. 2016. Hypo-excitation across all cortical laminae defines intermediate stages of cortical neuronal dysfunction in diffuse traumatic brain injury. Neuroscience. 334:290–308.

6) Alonso, M., Gomez-Rial, J., Gude, f., et al. (2012). Influence of experimental alcohol administration on serum immunoglobulin levels: contrasting effects on IgE and other immunoglobulin classes. Int. J. Immunopathol. Pharmacol. 25:645–655.

7) Alwis, D.S., Yan, E.B., Morganti-Kossmann, M.C., and Rajan, R. (2012). Sensory cortex underpinnings of traumatic brain injury deficits. PLoS One 7, e52169.

8) Atallah, B.V., Bruns, W., Carandini, M., and Scanziani, M. (2012). Parvalbumin-expressing interneurons linearly transform cortical responses to visual stimuli. Neuron 73, 159–170.

9) Bading H. 2013. Nuclear calcium signalling in the regulation of brain function. Nat Rev Neurosci. 14(9):593–608.

10) Bading H. 2017. Therapeutic targeting of the pathological triad of extrasynaptic NMDA receptor signaling in neurodegenerations. J Exp Med. 214:569–578.

11) Bean, J.C., Lin, T.W., Sathyamurthy, A., Liu, F., Yin, D.M., Xiong, W.C., and Mei, L. (2014). Genetic labeling reveals novel cellular targets of schizophrenia susceptibility gene: distribution of GABA and non-GABA ErbB4-positive cells in adult mouse brain. J. Neurosci. 34, 13549–13566.

12) Berry, C., Ley, E.J., Margulies, D.R., Mirocha, J., Bukur, M., Malinoski, D., and Salim, A. (2011). Correlating the blood alcohol concentration with outcome after traumatic brain injury: too much is not a bad thing. Am. Surg. 77, 1416–1419.

13) Blume-Jensen, P., Hunter, T. (2001). Oncogenic kinase signalling. Nature. 411:355-365.

14) Brennan, J.H., Bernard, S., Cameron, P.A., Rosenfeld, J.V., and Mitra, B. (2015). Ethanol and isolated traumatic brain injury. J. Clin. Neurosci. 22, 1375–1381.

15) Bosurgi, L., Cao, Y.G., Cabeza-Cabrerizo, M., et al. (2017). Macrophage function in tissue repair and remodeling requires IL-4 or IL-13 with apoptotic cells. Science. http://dx.doi.org/10.1126/science.aai8132 (pii: eaai8132, Epub ahead of print).

16) Botta, P., Zucca, A., Valenzuela, C.F., 2014 Feb 6. Acute ethanol exposure inhibits silencing of cerebellar Golgi cell firing induced by granule cell axon input. Front. Integr. Neurosci. 8, 10.

17) Bouchard, J.C., Kim, J., Beal, D.R., et al. (2012). Acute oral ethanol exposure triggers asthma in cockroach allergen-sensitized mice, Am. J. Pathol. 181:845–857.

18) Brombacher, T.M., Nono, J.K., De Gouveia, K.S., et al. IL-13-mediated regulation of learning and memory, J. Immunol. 198 (2017) 2681–2688.

19) Bruns, J., and Hauser, W.A. (2003). The epidemiology of traumatic brain injury: a review. Epilepsia 44(S10), 2-10.

20) Buriticá E, Villamil L, Guzmán F, Escobar MI, García-Cairasco N, Pimienta HJ. 2009. Changes in calcium-binding protein expression in human cortical contusion tissue. J Neurotrauma. 26(12):2145–2155.

21) Cantu D, Walker K, Andresen L, Taylor-Weiner A, Hampton D, Tesco G, Dulla CG. 2015. Traumatic brain injury increases cortical glutamate network activity by compromising GABAergic control. Cereb Cortex. 25(8):2306–2320.

22) Cardin JA, Carlén M, Meletis K, Knoblich U, Zhang F, Deisseroth K, Tsai LH, Moore CI. 2009. Driving fast-spiking cells induces gamma rhythm and controls sensory responses. Nature. 459(7247):663–667.

23) Carron SF, Alwis DS and Rajan R (2016) Traumatic Brain Injury and Neuronal Functionality Changes in Sensory Cortex. Front. Syst. Neurosci. 10:47. doi: 10.3389/fnsys.2016.00047

24) Cernak I. Animal models of head trauma. *NeuroRx*. 2005;2(3):410-22.

25) Chamoun, R., Suki, D., Gopinath, S.P., Goodman, J.C., Robertson, C., 2010 Sep. Role of extracellular glutamate measured by cerebral microdialysis in severe traumatic brain injury. J. Neurosurg. 113 (3), 564–570.

26) Chandrasekar, A., Heuvel, F.O., Palmer, A., Linkus, B., Ludolph, A.C., Boeckers, T.M., Relja, B., Huber-Lang, M., Roselli, F., 2017 Oct. Acute ethanol administration results in a protective cytokine and neuroinflammatory profile in traumatic brain injury. Int. Immunopharmacol. 51, 66–75.

27) Chen Y, Constantini S, Trembovler V, Weinstock M, Shohami E. An experimental model of closed head injury in mice: pathophysiology, histopathology, and cognitive deficits. J Neurotrauma. 1996;13:557–568.

28) Chiu, C. C., Liao, Y. E., Yang, L. Y., Wang, J. Y., Tweedie, D., Karnati, H. K., Greig, N. H., Wang, J. Y. (2016). Neuroinflammation in animal models of traumatic brain injury. *Journal of neuroscience methods*, *272*, 38-49.

29) Cho, J.S., Shin, S.D., Lee, E.J., Song, K.J., Noh, H., Kim, Y.J., Lee, S.C., Park, J.O., Kim, S.C., Hwang, S.S., 2016 Jun. Alcohol intake and reduced mortality in patients with traumatic brain injury. Alcohol. Clin. Exp. Res. 40 (6), 1290–1294.

30) Corbett, B.F., You, J.C., Zhang, X., Pyfer, M.S., Tosi, U., Iascone, D.M., Petrof, I., Hazra, A., CH, Fu, Stephens, G.S., Ashok, A.A., Aschmies, S., Zhao, L., Nestler, E.J., Chin, J., 2017 Jul 11. ΔFosB regulates gene expression and cognitive dysfunction in a mouse model of Alzheimer's disease. Cell Rep. 20 (2), 344–355

31) Coronado, V.G., Xu, L., Basavaraju, S.V., McGuire, L.C., Wald, M.M., Faul, M.D., Guzman, B.R., and Hemphill, J.D.; Centers for Disease Control and Prevention (CDC). (2011). Surveillance for traumatic brain injury-related deaths--United States, 1997-2007. MMWR Surveill Summ. 60, 1-32.

32) Criswell, H.E., Ming, Z., Griffith, B.L., Breese, G.R., 2003 Jan. Comparison of effect of ethanol on N-methyl-D-aspartate- and GABA-gated currents from acutely dissociated neurons: absence of regional differences in sensitivity to ethanol. J. Pharmacol. Exp. Ther. 304 (1), 192–199.

33) Criswell, H.E., Ming, Z., Pleasant, N., Griffith, B.L., Mueller, R.A., Breese, G.R., 2004 Jul 23. Macrokinetic analysis of blockade of NMDA-gated currents by substituted alcohols, alkanes and ethers. Brain Res. 1015 (1–2), 107–113.

34) Cummings, P., F.P. Rivara, C.M. Olson, K.M. Smith, Changes in traffic crash mortality rates attributed to use of alcohol, or lack of a seat belt, air bag, motorcycle helmet, or bicycle helmet, United States, 1982–2001, Inj. Prev. 12 (2006) 148–154.

35) Czigner, A., Mihály, A., Farkas, O., Büki, A., Krisztin-Péva, B., Dobó, E., Barzó, P., 2004 Aug. Dynamics and regional distribution of c-fos protein expression in rat brain after a closed head injury. Int. J. Mol. Med. 14 (2), 247–252.

36) Defelipe J, González-Albo MC, Del Río MR, Elston GN. 1999. Distribution and patterns of connectivity of interneurons containing calbindin, calretinin, and parvalbumin in visual areas of the occipital and temporal lobes of the macaque monkey. J Comp Neurol. 412(3):515–526.

37) Dietrich WD, Alonso O, Busto R, Ginsberg MD. 1994. Widespread metabolic depression and reduced somatosensory circuit activation following traumatic brain injury in rats. J Neurotrauma. 11(6):629–640.

38) Dimou L, Gallo V. NG2-glia and their functions in the central nervous system. Glia. 2015; 63(8):1429-51.

39) Dooley, D., Lemmens, E., Vangansewinkel, T., et al. Cell-based delivery of interleukin-13 directs alternative activation of macrophages resulting in improved functional outcome after spinal cord injury, Stem Cell Rep. 7 (2016) 1099–1115.

40) Donato F, Rompani SB, Caroni P. 2013. Parvalbumin-expressing basket-cell network plasticity induced by experience regulates adult learning. Nature. 504(7479):272–276

41) Donato F, Chowdhury A, Lahr M, Caroni P. 2015. Early- and late-born parvalbumin basket cell subpopulations exhibiting distinct regulation and roles in learning. Neuron. 85(4): 770–786.

42) Dorsett,C.R.,McGuire,J.L.,DePasquale,E.A.,Gardner,A.E.,Floyd,C.L.,McCullumsmith, R.E., 2017 Jan 15. Glutamate neurotransmission in rodent models of traumatic brain injury. J. Neurotrauma 34 (2), 263–272.

43) Dutcher, S.A., Underwood, B.D., Walker, P.D., Diaz, F.G., Michael, D.B., 1999 Apr. Patterns of immediate early gene mRNA expression following rodent and human traumatic brain injury. Neurol. Res. 21 (3), 234–242.

44) Emamian ES (2012) AKT/GSK3 signaling pathway and schizophrenia. *Front. Mol. Neurosci*. **5**:33. doi: 10.3389/fnmol.2012.00033

45) Faul M, Xu L, Wald MM, Coronado VG (2010) Traumatic brain injury in the United States: emergency department visits, hospitalizations, and deaths. Atlanta: Centers for Disease Control and Prevention, National Center for Injury Prevention and Control.

46) Fazzari, P., Paternain, A.V., Valiente, M., Pla, R., Luja ´n, R., Lloyd, K., Lerma, J., Marı ´n, O., and Rico, B. (2010). Control of cortical GABA circuitry development by Nrg1 and ErbB4 signalling. Nature 464, 1376–1380.

47) Feeney DM, Boyeson MG, Linn RT, Murray HM, Dail WG. Responses to cortical injury: I. Methodology and local effects of contusions in the rat. Brain Res. 1981;211:67–77.

48)Flavell, S.W., Greenberg, M.E., 2008. Signaling mechanisms linking neuronal activity to gene expression and plasticity of the nervous system. Annu. Rev. Neurosci. 31, 563–590.

49)Flierl, M.A., Stahel, P.F., Beauchamp, K.M., Morgan, S.J., Smith, W.R., and Shohami, E. (2009). Mouse closed head injury model induced by a weight-drop device. Nat Protoc.4, 1328-1337.

50)Folkersma, H., Foster Dingley, J.C., van Berckel, B.N., Rozemuller, A., Boellaard, R., Huisman, M.C., Lammertsma, A.A., Vandertop, W.P., Molthoff, C.F., 2011 Jun 14. Increased cerebral (R)-[(11) C] PK11195 uptake and glutamate release in a rat model of traumatic brain injury: a longitudinal pilot study. J. Neuroinflammation 8, 67.

51)Fourgeaud, L., Trave ´s, P.G., Tufail, Y., Leal-Bailey, H., Lew, E.D., Burrola, P.G., Callaway, P., Zago ´rska, A., Rothlin, C.V., Nimmerjahn, A., and Lemke, G. (2016). TAM receptors regulate multiple features of microglial physiology. Nature 532, 240–244.

52)Fujikawa D. G. (2015). The role of excitotoxic programmed necrosis in acute brain injury. *Computational and structural biotechnology journal*, *13*, 212-21. doi:10.1016/j.csbj.2015.03.004

53)Garg, C., Seo, J.H., Ramachandran, J., Loh, J.M., Calderon, F., Contreras, J.E. (2018). Trovafloxacin attenuates neuroinflammation and improves outcome after traumatic brain injury in mice. J Neuroinflammation. 15:42

54) Gey, M., Wanner, R., Schilling, C., Pedro, M.T., Sinske, D., Knöll, B., 2016 Aug. Atf3 mutant mice show reduced axon regeneration and impaired regeneration-associated gene induction after peripheral nerve injury. Open Biol. 6 (8).

55) Giunta, B., Obregon, D., Velisetty, R., Sanberg, P. R., Borlongan, C. V., & Tan, J. (2012). The immunology of traumatic brain injury: a prime target for Alzheimer's disease prevention. *Journal of neuroinflammation*, *9*, 185. doi:10.1186/1742-2094-9-185

56) Giza, C.C., Prins, M.L., Hovda, D.A., Herschman, H.R., Feldman, J.D., 2002 Apr. Genes preferentially induced by depolarization after concussive brain injury: effects of age and injury severity. J. Neurotrauma 19 (4), 387–402.

57) Goodman, M.D., Makley, A.T., Campion, E.M., Friend, L.A., Lentsch, A.B., Pritts, T.A., 2013 Oct. Preinjury alcohol exposure attenuates the neuroinflammatory response to traumatic brain injury. J. Surg. Res. 184 (2), 1053–1058.

58) Greiffenstein, P., Mathis, K.W., Stouwe, C.V., Molina, P.E. (2007). Alcohol binge before trauma/hemorrhage impairs integrity of host defense mechanisms during recovery, Alcohol. Clin. Exp. Res. 31:704–715.

59) Grote, S., Böcker, W., Mutschler, W., Bouillion, B., and Lefering, R. (2011). Diagnostic value of the Glasgow Coma Scale for Traumatic Brain Injury in 18,002 Patients with Severe Multiple Injuries. J Neurotrauma. https://doi.org/10.1089/neu.2010.1433.

60) Guan, Y.F., Wu, C.Y., Fang, Y.Y., Zeng, Y.N., Luo, Z.Y., Li, S.J., Li, X.W., Zhu, X.H., Mei, L., and Gao, T.M. (2015). Neuregulin 1 protects against ischemic brain injury via ErbB4 receptors by increasing GABAergic transmission. Neuroscience 307, 151–159.

61) Guerriero, R. M., Giza, C. C., & Rotenberg, A. (2015). Glutamate and GABA imbalance following traumatic brain injury. *Current neurology and neuroscience reports*, *15*(5), 27.

62) Guillemot, F., and Zimmer, C. (2011). From cradle to grave: the multiple roles of fibroblast growth factors in neural development. Neuron 71, 574–588.

63) Gupta, V.K., You, Y., Gupta, V.B., Klistorner, A., and Graham, S.L. (2013). TrkB receptor signalling: implications in neurodegenerative, psychiatric and proliferative disorders. Int. J. Mol. Sci. 14, 10122– 10142.

64) Gurnik, S., Devraj, K., Macas, J., Yamaji, M., Starke, J., Scholz, A., Sommer, K., Di Tacchio, M., Vutukuri, R., Beck, H., Mittelbronn, M., Foerch, C., Pfeilschifter, W., Liebner, S., Peters, K.G., Plate, K.H., and Reiss, Y. (2016). Angiopoietin-2-induced blood-brain barrier compromise and increased stroke size are rescued by VE-PTPdependent restoration of Tie2 signaling. Acta Neuropathol. 31, 753– 773.

65) Gyoneva. S., Ransohoff. R.M. Inflammatory reaction after traumatic brain injury: therapeutic potential of targeting cell-cell communication by chemokines, Trends Pharmacol. Sci. 36 (2015) 471–480.

66) Haider B, Häusser M, Carandini M. 2013. Inhibition dominates sensory responses in the awake cortex. Nature. 493(7430): 97–100.

67) Hanchar, H.J., Dodson, P.D., Olsen, R.W., Otis, T.S., Wallner, M., 2005 Mar. Alcoholinduced motor impairment caused by increased extrasynaptic GABA(A) receptor activity. Nat. Neurosci. 8 (3), 339–345.

68) Hardingham GE, Fukunaga Y, Bading H. 2002. Extrasynaptic NMDARs oppose synaptic NMDARs by triggering CREB shutoff and death pathways. Nat Neurosci. 5:405–415.

69) Hardingham, G.E., Bading, H., 2010 Oct. Synaptic versus extrasynaptic NMDA receptor signalling: implications for neurodegenerative disorders. Nat. Rev. Neurosci. 11 (10), 682–696.

70) He, Q., Titley, H., Grasselli, G., Piochon, C., Hansel, C., 2013 Mar. Ethanol affects NMDA receptor signaling at climbing fiber-Purkinje cell synapses in mice and impairs cerebellar LTD. J. Neurophysiol. 109 (5), 1333–1342. http://dx.doi.org/10.1152/jn. 00350.2012. (Epub 2012 Dec 5. PubMed PMID: 23221414; PubMed Central PMCID: PMC3602830).

71) Hendry, J.M., Alvarez-Veronesi, M.C., Placheta, E., Zhang, J.J., Gordon, T., and Borschel, G.H. (2016). ErbB2 blockade with Herceptin (trastuzumab) enhances peripheral nerve regeneration after repair of acute or chronic peripheral nerve injury. Ann. Neurol. 80, 112–126.

72) Hernandez-Ontiveros, D. G., Tajiri, N., Acosta, S., Giunta, B., Tan, J., & Borlongan, C. V. (2013). Microglia activation as a biomarker for traumatic brain injury. *Frontiers in neurology*, *4*, 30. doi:10.3389/fneur.2013.00030

73) Hinzman JM, DiNapoli VA, Mahoney EJ, Gerhardt GA, Hartings JA. 2015. Spreading depolarizations mediate excitotoxicity in the development of acute cortical lesions. Exp Neurol. 267: 243–253.

74) Hinzman, J.M., Wilson, J.A., Mazzeo, A.T., Bullock, M.R., Hartings, J.A., 2016 Oct 1. Excitotoxicity and metabolic crisis are associated with spreading depolarizations in severe traumatic brain injury patients. J. Neurotrauma 33 (19), 1775–1783.

75) Holmin, S., Mathiesen, T., Shetye, J., Biberfeld, P. Intracerebral inflammatory response to experimental brain contusion, Acta Neurochir. 132 (1995) 110–119.

76) Honkaniemi, J., Sharp, F.R., 1999 Jan. Prolonged expression of zinc finger immediateearly gene mRNAs and decreased protein synthesis following kainic acid induced seizures. Eur. J. Neurosci. 11 (1), 10–17.

77) Hsieh, C. L., Kim, C. C., Ryba, B. E., Niemi, E. C., Bando, J. K., Locksley, R. M., Liu, J., Nakamura, M. C., Seaman, W. E. (2013). Traumatic brain injury induces macrophage subsets in the brain. *European journal of immunology*, *43*(8), 2010-22.

78) Hsieh TH, Lee HHC, Hameed MQ, Pascual-Leone A, Hensch TK, Rotenberg A. 2017. Trajectory of parvalbumin cell impairment and loss of cortical inhibition in traumatic brain injury. Cereb Cortex. 27(12):5509–5524.

79) Hu, B., Liu, C., Bramlett, H., Sick, T.J., Alonso OF, Chen, S., Dietrich, W.D., 2004 Aug. Changes in trkB-ERK1/2-CREB/Elk-1 pathways in hippocampal mossy fiber organization after traumatic brain injury. J. Cereb. Blood Flow Metab. 24 (8), 934–943.

80) Hu H, Gan J, Jonas P. 2014. Interneurons. Fast-spiking, parvalbumin+ GABAergic interneurons: from cellular design to microcircuit function. Science. 345(6196):1255263

81) Huang, X.J., Glushakova, O., Mondello, S., Van, K., Hayes, R.L., and Lyeth, B.G. (2015). Acute temporal profiles of serum levels of UCH-L1 and GFAP and relationships to neuronal and astroglial pathology following traumatic brain injury in rats. J. Neurotrauma 32, 1179–1189.

82) Hubbard, S. R., & Miller, W. T. (2007). Receptor tyrosine kinases: mechanisms of activation and signaling. *Current opinion in cell biology*, *19*(2), 117-23.

83) Isaacson JS, Scanziani M. 2011. How inhibition shapes cortical activity. Neuron. 72(2):231–243

84) Iwakura, Y., Wang, R., Inamura, N., Araki, K., Higashiyama, S., Takei, N., and Nawa H. (2017). Glutamate-dependent ectodomain shedding of neuregulin-1 type II precursors in rat forebrain neurons. PLoS One 12, e0174780.

85) Janis, L.S., Hoane, M.R., Conde, D., Fulop, Z., and Stein, D.G. (1998). Acute ethanol administration reduces the cognitive deficits associated with traumatic brain injury in rats. J. Neurotrauma 15, 105–115.

86) Johnson VE, Meaney DF, Cullen DK, Smith DH. Animal models of traumatic brain injury. *Handb Clin Neurol*. 2015; 127: 115-28.

87) Johnstone VP, Shultz SR, Yan EB, O'Brien TJ, Rajan R. 2014. The acute phase of mild traumatic brain injury is characterized by a distance-dependent neuronal hypoactivity. J Neurotrauma. 31(22):1881–1895.

88) Johnstone, V.P., Yan, E.B., Alwis, D.S., and Rajan, R. (2013). Cortical hypoexcitation defines neuronal responses in the immediate aftermath of traumatic brain injury. PloS One 8, e63454.

89) Joseph, B., Khalil, M., Pandit, V., Kulvatunyou, N., Zangbar, B., O'Keeffe, T., Asif, A., Tang, A., Green, D.J., Gries, L., Friese, R.S., Rhee, P., 2015 Feb. Adverse effects of admission blood alcohol on long-term cognitive function in patients with traumatic brain injury. J. Trauma Acute Care Surg. 78 (2), 403–408.

90) Joseph, B., Pandit, V., Aziz, H., Kulvatunyou, N., Zangbar, B., Green, D.J., Haider, A., Tang, A., O'Keeffe, T., Gries, L., Friese, R.S., and Rhee, P. (2015). Mild traumatic brain injury defined by Glasgow Coma Scale: Is it really mild? Brain Injury. 29, 11-16, DOI:10.3109/02699052.2014.945959

91) Kabadi SV, Hilton GD, Stoica BA, Zapple DN, Faden AI. Fluid-percussion-induced traumatic brain injury model in rats. *Nat Protoc*. 2010;5(9):1552-63.

92) Kabadi, S. V., & Faden, A. I. (2014). Neuroprotective strategies for traumatic brain injury: improving clinical translation. *International journal of molecular sciences*, *15*(1), 1216-36. doi:10.3390/ijms15011216

93)Kaplan, C.P., and Corrigan, J.D. (1992). Effect of blood alcohol level on recovery from severe closed head injury. Brain Inj. 6, 337–349.

94)Karelina, K., Gaier, K.R., Prabhu, M., Wenger, V., Corrigan, T.E., Weil, Z.M., 2017 Feb. Binge ethanol in adulthood exacerbates negative outcomes following juvenile traumatic brain injury. Brain Behav. Immun. 60, 304–311.

95)Katada, R., Nishitani, Y., Honmou, O., Okazaki, S., Houkin, K., Matsumoto, H., 2009 Nov. Prior ethanol injection promotes brain edema after traumatic brain injury. J. Neurotrauma 26 (11), 2015–2025.

96)Kaur P, Sharma S. 2017. Recent Advances in Pathophysiology of Traumatic Brain Injury. Curr Neuropharmacol. doi: 10.2174/1570159X15666170613083606.

97)Kelly, D.F., S.M. Lee, P.A. Pinanong, D.A. Hovda, Paradoxical effects of acute ethanolism in experimental brain injury, J. Neurosurg. 86 (1997) 876–882.

98)Khoshkhoo S, Vogt D, Sohal VS. 2017. Dynamic, cell-typespecific roles for gabaergic interneurons in a mouse model of optogenetically inducible seizures. Neuron. 93(2): 291–298.

99)Kiguchi, N., Sakaguchi, H., Kadowaki, Y., et al. Peripheral administration of interleukin-13 reverses inflammatory macrophage and tactile allodynia in mice with partial sciatic nerve ligation, J. Pharmacol. Sci. 133 (2017) 53–56.

100) Kumar, S., Porcu, P., Werner, D.F., Matthews, D.B., Diaz-Granados, J.L., Helfand, R.S., and Morrow, A.L. (2009). The role of GABA (A) receptors in the acute and chronic effects of ethanol: a decade of progress. Psychopharmacology (Berl.) 205, 529–564.

101) Kumar, A., Loane, D.J. (2012) Neuroinflammation after traumatic brain injury: Opportunities for therapeutic intervention. Brain Behav Immun. 26, 1191-1201.

102) Lange, R.T., Iverson, G.L., and Franzen, M.D. (2008). Effects of day of-injury alcohol intoxication on neuropsychological outcome in the acute recovery period following traumatic brain injury. Arch. Clin. Neuropsychol. 23, 809–822.

103) Lenzlinger, P.M., Morganti-Kossmann, MC., Laurer, H.L., McIntosh, T.K. The duality of the inflammatory response to traumatic brain injury. Mol Neurobiol (2001) 24: 169. https://doi.org/10.1385/MN:24:1-3:169.

104) Leo. P., M. McCrea, Epidemiology, in: D. Laskowitz, G. Grant (Eds.), Translational Research in Traumatic Brain Injury, CRC Press/Taylor and Francis Group, Boca Raton (FL), 2016(Chapter 1).

105) Léveillé F, Papadia S, Fricker M, Bell KF, Soriano FX, Martel MA, Puddifoot C, Habel M, Wyllie DJ, Ikonomidou C, et al. 2010. Suppression of the intrinsic apoptosis pathway by synaptic activity. J Neurosci. 30(7):2623–2635

106) Li, L., Yun, S.H., Keblesh, J., Trommer, B.L., Xiong, H., Radulovic, J., Tourtellotte, W.G., 2007 May. Egr3, a synaptic activity regulated transcription factor that is essential for learning and memory. Mol. Cell. Neurosci. 35 (1), 76–88.

107) Lösing,P.,Niturad,C.E.,Harrer,M.,Reckendorf,C.M.Z.,Schatz,T.,Sinske,D.,Lerche,H., Maljevic, S., Knöll, B., 2017 Jul 17. SRF modulates seizure occurrence, activity induced gene transcription and hippocampal circuit reorganization in the mouse pilocarpine epilepsy model. Mol. Brain 10 (1), 30.

108) Lu, Y., Sun, X.D., Hou, F.Q., Bi, L.L., Yin, D.M., Liu, F., Chen, Y.J., Bean, J.C., Jiao, H.F., Liu, X., Li, B.M., Xiong, W.C., Gao, T.M., and Mei, L. (2014). Maintenance of GABAergic activity by neuregulin 1ErbB4 in amygdala for fear memory. Neuron 84, 835–846.

109) Lu, C., Xia, J., Bin, W., Wu, Y., Liu, X., and Zhang, Y. Advances in diagnosis, treatments, and molecular mechanistic studies of traumatic brain injury. (2015). BioScience Trends. Volume 9, Issue 3, Pages 138-148.

110) Marciano, P.G., Eberwine, J.H., Ragupathi, R., Saatman, K.E., Meaney, D.F., McIntosh, T.K. (2002) Expression Profiling Following Traumatic Brain Injuy: A Review. Neurochem Res 27: 1147. https://doi.org/10.1023/A:1020973308941

111) Marmarou A, Foda MA, van den Brink W, Campbell J, Kita H, Demetriadou K. A new model of diffuse brain injury in rats. Part I: Pathophysiology and biomechanics. J Neurosurg. 1994 Feb; 80(2):291-300.

112) Martin JL, Sloviter RS. 2001. Focal inhibitory interneuron loss and principal cell hyperexcitability in the rat hippocampus after microinjection of a neurotoxic conjugate of saporin and a peptidase-resistant analog of Substance P. J Comp Neurol. 436(2):127–152.

113) Masel, B.E., and DeWitt, D.S. (2010). Traumatic Brain Injury: A disease process, not an event. Journal of Neurotrauma, 27:8, 1529-1540.

114) McKee, C.A., Lukens, J.R. emerging roles for the immune system in traumatic brain injury. Front. Immunol. 7 (2016) 556.

115) Menon, D. K., Schwab, K., Wright, D. W. & Maas, A. I. Position statement: definition of traumatic brain injury. Arch. Phys. Med. Rehabil. 91, 1637–1640 (2010).

116) Mei, L., and Nave, K.A. (2014). Neuregulin-ERBB signaling in the nervous system and neuropsychiatric diseases. Neuron 83, 27–49.

117) Mori, S., Maher, P., Conti, B. Neuroimmunology of the Interleukins 13 and 4, Brain Sci. 6 (2016) (pii: E18).

118) Morris, T.A., Jafari, N., DeLorenzo, R.J., 2000 Jun 23. Chronic DeltaFosB expression and increased AP-1 transcription factor binding are associated with the long term plasticity changes in epilepsy. Brain Res. Mol. Brain Res. 79 (1–2), 138–149.

119) Natale, J.E., Ahmed, F., Cernak, I., Stoica, B., Faden, A.I., 2003 Oct. Gene expression profile changes are commonly modulated across models and species after traumatic brain injury. J. Neurotrauma 20 (10), 907–927.

120) Neary, J. T. (2005). Protein kinase signaling cascades in CNS trauma. *IUBMB Life* 57, 711–718. doi: 10.1080/15216540500319143

121) Neddens, J., Fish, K.N., Tricoire, L., Vullhorst, D., Shamir, A., Chung, W., Lewis, D.A., McBain, C.J., and Buonanno, A. (2011). Conserved interneuron-specific ErbB4 expression in frontal cortex of rodents, monkeys, and humans: implications for schizophrenia. Biol. Psychiatry 70, 636–645.

122) Nomaru, H., Sakumi, K., Katogi, A., Ohnishi, Y.N., Kajitani, K., Tsuchimoto, D., Nestler, E.J., Nakabeppu, Y., 2014 Aug. Fosb gene products contribute to excitotoxic microglial activation by regulating the expression of complement C5a receptors in microglia. Glia 62 (8), 1284–1298.

123) Oshitari, T., Dezawa, M., Okada, S., Takano, M., Negishi, H., Horie, H., Sawada, H., Tokuhisa, T., Adachi-Usami, E., 2002 Jul. The role of c-fos in cell death and regeneration of retinal ganglion cells. Invest. Ophthalmol. Vis. Sci. 43 (7), 2442–2449.

124) Osier ND, Dixon CE. The Controlled Cortical Impact Model: Applications, Considerations for Researchers, and Future Directions. Front Neurol. 2016 (a);7:134. Published 2016 Aug 17. doi:10.3389/fneur.2016.00134

125) Osier N, Dixon CE. The Controlled Cortical Impact Model of Experimental Brain Trauma: Overview, Research Applications, and Protocol. Methods Mol Biol. 2016 (b);1462:177-92.

126) Pandit, V., N. Patel, P. Rhee, et al., Effect of alcohol in traumatic brain injury: is it really protective? J. Surg. Res. 190 (2014) 634–639.

127) Papadia S, Soriano FX, Léveillé F, Martel MA, Dakin KA, Hansen HH, Kaindl A, Sifringer M, Fowler J, Stefovska V, et al. 2008. Synaptic NMDA receptor activity boosts intrinsic antioxidant defenses. Nat Neurosci. 11(4):476–487.

128) Pohl D, Bittigau P, Ishimaru MJ, Stadthaus D, Hübner C, Olney JW, Turski L, Ikonomidou C. 1999. N-Methyl-D-aspartate antagonists and apoptotic cell death triggered by head trauma in developing rat brain. Proc Natl Acad Sci U S A. 96 (5):2508–2513.

129) Polli, J.W., Humphreys, J.E., Harmon, K.A., Castellino, S., O'Mara, M.J., Olson, K.L., John-Williams, L.S., Koch, K.M., and SerabjitSingh, C.J. (2008). The role of efflux and uptake transporters in [N-{3chloro-4-[(3-fluorobenzyl)oxy]phenyl}-6-[5-({[2-(methylsulfonyl) ethyl]amino}methyl)-2-furyl]-4-quinazolinamine (GW572016, lapatinib) disposition and drug interactions. Drug Metab. Dispos. 36, 695–701.

130) Prins, M., Greco, T., Alexander, D., & Giza, C. C. (2013). The pathophysiology of traumatic brain injury at a glance. Disease Models & Mechanisms, 6(6), 1307–1315. http://doi.org/10.1242/dmm.011585.

131) Qiu J, Tan YW, Hagenston AM, Martel MA, Kneisel N, Skehel PA, Wyllie DJ, Bading H, Hardingham GE. 2013. Mitochondrial calcium uniporter Mcu controls excitotoxicity and is transcriptionally repressed by neuroprotective nuclear calcium signals. Nat Commun. 4:2034.

132) Ramanan, N., Shen, Y., Sarsfield, S., Lemberger, T., Schütz, G., Linden, D.J., Ginty, D.D.S.R.F., 2005 Jun. Mediates activity-induced gene expression and synaptic plasticity but not neuronal viability. Nat. Neurosci. 8 (6), 759–767.

133) Raj, R., Skrifvars, M.B., Kivisaari, R., Hernesniemi, J., Lappalainen, J., and Siironen, J. (2015). Acute alcohol intoxication and long-term outcome in patients with traumatic brain injury. J. Neurotrauma 32, 95–100.

134) Raj, R., Mikkonen, E.D., Siironen, J., Hernesniemi, J., Lappalainen, J., and Skrifvars, M.B. (2016). Alcohol and mortality after moderate to severe traumatic brain injury: a meta-analysis of observational studies. J. Neurosurg. 124, 1684–1692.

135) Rawat, V., Goux, W., Piechaczyk, M., D'Mello, S.R., 2016 Mar. c-Fos protects neurons through a noncanonical mechanism involving HDAC3 interaction: identification of a 21-amino acid fragment with neuroprotective activity. Mol. Neurobiol. 53 (2), 1165–1180.

136) Relja, B., Omid, N., Schaible, A., et al. (2015). Pre- or post-treatment with ethanol and ethyl pyruvate results in distinct anti-inflammatory responses of human lung epithelial cells triggered by interleukin-6. Mol. Med. Rep. 12:2991–2998.

137) Relja, B., Menke, J., Wagner, N., et al. (2016a). Effects of positive blood alcohol concentration on outcome and systemic interleukin-6 in major trauma patients. Injury. 47: 640–645.

138) Relja, B., Omid, N., Wagner, N., et al. (2016b). Ethanol, ethyl and sodium pyruvate decrease the inflammatory responses of human lung epithelial cells via Akt and NF-κB in vitro but have a low impact on hepatocellular cells. Int. J. Mol. Med. 37:517–525.

139) Renaudineau, S., Poucet, B., Laroche, S., Davis, S., Save, E., 2009 Jul 14. Impaired longterm stability of CA1 place cell representation in mice lacking the transcription factor zif268/egr1. Proc. Natl. Acad. Sci. U. S. A. 106 (28), 11771–11775.

140) Reis, C., Wang, Y., Akyol, O., Ho, W.M., II, R.A.; Stier, G.; Martin, R.; Zhang, J.H. What's New in Traumatic Brain Injury: Update on Tracking, Monitoring and Treatment. Int. J. Mol. Sci. 2015, 16, 11903-11965.

141) Romine J, Gao X, Chen J. Controlled cortical impact model for traumatic brain injury. J Vis Exp. 2014;(90):e51781. Published 2014 Aug 5. doi:10.3791/51781

142) Roselli F, Caroni P. 2015. From intrinsic firing properties to selective neuronal vulnerability in neurodegenerative diseases. Neuron. 85:901–910.

143) Sahler, C. S., & Greenwald, B. D. (2012). Traumatic Brain Injury in Sports: A Review. Rehabilitation Research and Practice, 2012, 659652. http://doi.org/10.1155/2012/659652.

144) Salim, A., Teixeira, P., Ley, E.J., DuBose, J., Inaba, K., Margulies, D.R., 2009 Oct. Serum ethanol levels: predictor of survival after severe traumatic brain injury. J. Trauma 67 (4), 697–703.

145) Samal, B.B., Waites,C.K.,Almeida-Suhett, C.,Li, Z.,Marini,A.M.,Samal, N.R.,Elkahloun, A., Braga, M.F., Eiden, L.E., 2015 Oct. Acute response of the hippocampal transcriptome following mild traumatic brain injury after controlled cortical impact in the rat. J. Mol. Neurosci. 57 (2), 282–303.

146) Samson AJ, Robertson G, Zagnoni M, Connolly CN. 2016. Neuronal networks provide rapid neuroprotection against spreading toxicity. Sci Rep. 6:33746.

147) Sato,S.,Kawauchi,S.,Okuda,W.,Nishidate,I.,Nawashiro,H.,Tsumatori,G.,2014Jan8. Real-time optical diagnosis of the rat brain exposed to a laser-induced shock wave: observation of spreading depolarization, vasoconstriction and hypoxemia-oligemia. PLoS One 9 (1), e82891.

148) Savola, O., Niemelä, O., Hillbom, M., 2005 Jul-Aug. Alcohol intake and the pattern of trauma in young adults and working aged people admitted after trauma. Alcohol Alcohol. 40 (4), 269–273.

149) Sawant-Pokam PM, Suryavanshi P, Mendez JM, Dudek FE, Brennan KC. 2017. Mechanisms of neuronal silencing after cortical spreading depression. Cereb Cortex. 27(2): 1311–1325.

150) Saxena S, Roselli F, Singh K, Leptien K, Julien JP, Gros-Louis F, Caroni P. 2013. Neuroprotection through excitability and mTOR required in ALS motoneurons to delay disease and extend survival. Neuron. 80:80–96.

151) Schimmel, S. J., Acosta, S., & Lozano, D. (2017). Neuroinflammation in traumatic brain injury: A chronic response to an acute injury. *Brain circulation*, *3*(3), 135-142.

152) Schutte, C., and Hanks, R. (2010). Impact of the presence of alcohol at the time of injury on acute and one-year cognitive and functional recovery after traumatic brain injury. Int. J. Neurosci. 120, 551–556.

153) Shear DA., Xi-Chun May Lu, Rebecca Pedersen, Guo Wei, Zhiyong Chen, Angela Davis, Changping Yao, Jitendra Dave, and Frank C. Tortella. Severity Profile of Penetrating Ballistic-Like Brain Injury on Neurofunctional Outcome, Blood-Brain Barrier Permeability, and Brain Edema Formation. (2011) Journal of Neurotrauma. ahead of print http://doi.org/10.1089/neu.2011.1916

154) Sheffler-Collins, S.I., and Dalva, M.B. (2012). EphBs: an integral link between synaptic function and synaptopathies. Trends Neurosci. 35, 293–304.

155) Soares. H.D., Hicks. R.R., Smith. D., McIntosh. T.K. Inflammatory leukocytic recruitment and diffuse neuronal degeneration are separate pathological processes resulting from traumatic brain injury. J. Neurosci. 15 (1995) 8223–8233.

156) Stein, C.S., Georgoff, P., Meghan, S., Mizra, K., and Sonnad, S.S. (2010). 150 years of treating severe traumatic brain injury: a systematic review of progress in mortality. J Neurotrauma. 27, 1343-1353.

157) Su, E.J., Fredriksson, L., Kanzawa, M., Moore, S., Folestad, E., Stevenson, T.K., Nilsson, I., Sashindranath, M., Schielke, G.P., Warnock, M., Ragsdale, M., Mann, K.,

Lawrence, A.L., Medcalf, R.L., Eriksson, U., Murphy, G.G., and Lawrence, D.A. (2015). Imatinib treatment reduces brain injury in a murine model of traumatic brain injury. Front. Cell. Neurosci 9, 385.

158) Sun D, Chen X, Gu G, Wang J, Zhang J. 2017. Potential roles of mitochondria-associated ER membranes (MAMs) in traumatic brain injury. Cell Mol Neurobiol. 37(8):1349–1357.

159) Sun, Y., Ikrar, T., Davis, M.F., Gong, N., Zheng, X., Luo, Z.D., Lai, C., Mei, L., Holmes, T.C., Gandhi, S.P., and Xu, X. (2016). Neuregulin-1/ErbB4 signaling regulates visual cortical plasticity. Neuron. 92, 160–173

160) Teng, S.X., Katz, P.S., Maxi, J.K., Mayeux, J.P., Gilpin, N.W., Molina, P.E., 2015 Mar. Alcohol exposure after mild focal traumatic brain injury impairs neurological recovery and exacerbates localized neuroinflammation. Brain Behav. Immun. 45, 145–156.

161) Thundyil, J., Manzanero, S., Pavlovski, D., Cully, T.R., Lok, K.Z., Widiapradja, A., Chunduri, P., Jo, D.G., Naruse, C., Asano, M., Launikonis, B.S., Sobey, C.G., Coulthard, M.G., and Arumugam, T.V. (2013). Evidence that the EphA2 receptor exacerbates ischemic brain injury. PloS One 8, e53528.

162) Tien, H.C., L.N. Tremblay, S.B. Rizoli, et al., Association between alcohol and mortality in patients with severe traumatic head injury, Arch. Surg. 141 (2006) 1185–1191.

163) Vaagenes, I.C., Tsai,S.Y., Ton, S.T.,Husak, V.A., McGuire,S.O., O'Brien,T.E., Kartje,G.L., 2015 Mar 13. Binge ethanol prior to traumatic brain injury worsens sensorimotor functional recovery in rats. PLoS One 10 (3), e0120356.

164) Vascak M, Jin X, Jacobs KM, Povlishock JT. 2017. Mild traumatic brain injury induces structural and functional disconnection of local neocortical inhibitory networks via parvalbumin interneuron diffuse axonal injury. Cereb Cortex. 4:1–20.

165) Vullhorst, D., Mitchell, R.M., Keating, C., Roychowdhury, S., Karavanova, I., Tao-Cheng, J.H., and Buonanno, A. (2015). A negative feedback loop controls NMDA receptor function in cortical interneurons via neuregulin 2/ErbB4 signalling. Nat. Commun. 6, 7222.

166) Wagner, N., Akbarpour, A., Mörs, K., et al. (2016) Alcohol intoxication reduces systemic interleukin-6 levels and leukocyte counts after severe TBI compared with not intoxicated TBI patients. Shock. 46:261–269.

167) Wagner, N., Franz, N., Dieteren, S., Perl, M., Mörs, K., Marzi, I., Relja, B., 2017 Sep. Acute alcohol binge deteriorates metabolic and respiratory compensation capability after blunt chest trauma followed by hemorrhagic shock-a new research model. Alcohol. Clin. Exp. Res. 41 (9), 1559–1567.

168) Wang, L., Deng, S., Lu, Y., Zhang, Y., Yang, L., Guan, Y., Jiang, H., Li, H., 2012 Sep 18. Increased inflammation and brain injury after transient focal cerebral ischemia in activating transcription factor 3 knockout mice. Neuroscience 220, 100–108.

169) Wang, T., Chou, D.Y., Ding, J.Y., Fredrickson, V., Peng, C., Schafer, S., Guthikonda, M., Kreipke,C.,Rafols,J.A.,Ding,Y.,2013 Feb.Reduction of brain edema and expression of aquaporins with acute ethanol treatment after traumatic brain injury. J. Neurosurg. 118 (2), 390–396.

170) Wang, Y., Hameed, M.Q., Rakhade, S.N., Iglesias, A.H., Muller, P.A., Mou, D.L., Rotenberg, A., 2014 Aug 20. Hippocampal immediate early gene transcription in the rat fluid percussion traumatic brain injury model. Neuroreport 25 (12), 954–959.

171) Weber, J.T., Rzigalinski, B.A., Ellis, E.F., 2001 Jan 19. Traumatic injury of cortical neuronscauses changes in intracellular calcium stores and capacitative calcium influx. J. Biol. Chem. 276 (3), 1800–1807.

172) Weber, J.T., 2012 Apr 12. Altered calcium signaling following traumatic brain injury. Front. Pharmacol. 3, 60.

173) Wen, L., Lu, Y.S., Zhu, X.H., Li, X.M., Woo, R.S., Chen, Y.J., Yin, D.M., Lai, C., Terry, A.V., Vazdarjanova, A., and Xiong, W.C. (2010). Neuregulin 1 regulates pyramidal neuron activity via ErbB4 in parvalbumin-positive interneurons. Proc. Natl. Acad Sci. U. S. A. 107, 1211–1216.

174) Werner. C., Engelhard. K. Pathophysiology of traumatic brain injury, BJA: British Journal of Anaesthesia, Volume 99, Issue 1, 1 July 2007, Pages 4–9, https://doi.org/10.1093/bja/aem131

175) Whitfield, P.C., Pickard, J.D. (2000). Expression of immediate early genes c-Fos and c-Jun after head injury in man. Neurol Res. 22: 138-44.

176) Wilent WB, Contreras D. 2005. Dynamics of excitation and inhibition underlying stimulus selectivity in rat somatosensory cortex. Nat Neurosci. 8(10):1364–1370.

177) Williams AJ, Jed A., Xi-Chun MH., Lu, Michael L. Rolli, and Frank C. Tortella. Penetrating Ballistic-Like Brain Injury in the Rat: Differential Time Courses of Hemorrhage, Cell Death, Inflammation, and Remote Degeneration. (2006) Journal of Neurotrauma. ahead of print http://doi.org/10.1089/neu.2006.23.1828.

178) Wilkinson, P.K. Pharmacokinetics of ethanol: a review, Alcohol. Clin. Exp. Res. 4 (1980) 6–21.

179) Wojnarowicz MW, Fisher AM, Minaeva O and Goldstein LE (2017) Considerations for Experimental Animal Models of Concussion, Traumatic Brain Injury, and Chronic Traumatic Encephalopathy—These Matters Matter. Front. Neurol. 8:240. doi: 10.3389/fneur.2017.00240

180) Won, S.Y., Kim, S.R., Maeng, S., Jin, B.K. Interleukin-13/interleukin-4-induced oxidative stress contributes to death of prothrombinkringle-2 (pKr-2)-activated microglia, J. Neuroimmunol. 265 (2013) 36–42.

181) Woodcock T, Morganti-Kossmann MC. The role of markers of inflammation in traumatic brain injury. Front Neurol. 2013;4:18. Published 2013 Mar 4. doi:10.3389/fneur.2013.00018

182) Wroge CM, Hogins J, Eisenman L, Mennerick S. 2012. Synaptic NMDA receptors mediate hypoxic excitotoxic death. J Neurosci. 32(19):6732–6742.

183) Wu, W., Tian, R., Hao, S., Xu, F., Mao, X., and Liu, B. (2014). A preinjury high ethanol intake in rats promotes brain edema following traumatic brain injury. Br. J. Neurosurg. 28, 739–745.

184) Xiong Y, Mahmood A, Chopp M. Animal models of traumatic brain injury. Nat Rev Neurosci. 2013;14(2):128-42.

185) Xiong Y, Mahmood A, Chopp M. Current understanding of neuroinflammation after traumatic brain injury and cell-based therapeutic opportunities. *Chin J Traumatol*. 2018;21(3):137-151.

186) Yang, M.S., Park, E.J., Sohn, S., et al. Interleukin-13 and -4 induce death of activated microglia, Glia 38 (2002) 273–280.

187) Yang JW, Prouvot PH, Reyes-Puerta V, Stüttgen MC, Stroh A, Luhmann HJ. 2017. Optogenetic modulation of a minor fraction of parvalbumin-positive interneurons specifically affects spatiotemporal dynamics of spontaneous and sensoryevoked activity in mouse somatosensory cortex in vivo. Cereb Cortex. 27(12):5784–5803.

188) Yi, J.H., Hazell, A.S. (2006). Excitotoxic mechanisms and the role of astrocytic gulamate transporters in trumatic brain injury. Neurochem Int. 48:394-403.

189) Yutsudo, N., Kamada, T., Kajitani, K., Nomaru, H., Katogi, A., Ohnishi, Y.H., Ohnishi, Y.N., Takase, K., Sakumi, K., Shigeto, H., Nakabeppu, Y., 2013 Apr. fosB-null mice display impaired adult hippocampal neurogenesis and spontaneous epilepsy with depressive behavior. Neuropsychopharmacology 38 (5), 895–906.

190) Yin, D.M., Sun, X.D., Bean, J.C., Lin, T.W., Sathyamurthy, A., Xiong, W.C., Gao, T.M., Chen, Y.J., and Mei, L. (2013). Regulation of spine formation by ErbB4 in PV-positive interneurons. J. Neurosci. 33, 19295–19303.

191) Zaloshnja, E., Miller T., Langlois J. A., and Selassie, A. W. (2005). Prevalence of long-term disability from traumatic brain injury in the civilian population of the United States. The Journal of head trauma rehabilitation. 23, 394-400.

192) Zhang, J., Zhang, D., McQuade, J.S., Behbehani, M., Tsien, J.Z., Xu, M., 2002 Apr. C-fos regulates neuronal excitability and survival. Nat. Genet. 30 (4), 416–420.

193) Zhang SJ, Steijaert MN, Lau D, Schütz G, Delucinge-Vivier C, Descombes P, Bading H. 2007. Decoding NMDA receptor signaling: identification of genomic programs specifying neuronal survival and death. Neuron. 53:549–562.

194) Zhang SJ, Zou M, Lu L, Lau D, Ditzel DA, Delucinge-Vivier C, Aso Y, Descombes P, Bading H. 2009. Nuclear calcium signaling controls expression of a large gene pool: identification of a gene program for acquired neuroprotection induced by synaptic activity. PLoS Genet. 5(8):e1000604.

195) Zhang SJ, Buchthal B, Lau D, Hayer S, Dick O, Schwaninger M, Veltkamp R, Zou M, Weiss U, Bading H. 2011. A signaling cascade of nuclear calcium-CREB-ATF3 activated by synaptic NMDA receptors defines a gene repression module that protects against extrasynaptic NMDA receptor-induced neuronal cell death and ischemic brain damage. J Neurosci. 31(13):4978–4990.

196) Zhang, H., Zhang, L., Zhou, D., He, X., Wang, D., Pan, H., Zhang, X., Mei, Y., Qian, Q., Zheng, T., Jones, F.E., and Sun, B. (2017). Ablating ErbB4 in PV neurons attenuates synaptic and cognitive deficits in an animal model of Alzheimer's disease. Neurobiol. Dis. 106, 171–180.